A COMPARISON OF VARIOUS PROCEDURES ON SLOPE STABILITY

ALİ İHSAN ÇAKIR

February, 1986

BOĞAZIÇİ UNIVERSITY

To my parents,

Adnan and Nurten ÇAKIR.

A COMPARISON OF VARIOUS PROCEDURES ON SLOPE STABILITY

by

ALİ İHSAN ÇAKIR

B. Sc. in C.E., Sakarya D.M.M. Akademisi, 1980

Submitted to the Institute for Graduate Studies in Science and Engineering in Partial Fulfillment of the Requirements for the Degree of

Master of Science

of

Civil Engineering

BOĞAZİÇİ UNIVERSITY

February, 1986

ACKNOWLEDGEMENTS

I would like to express my sincere gratitude to my thesis supervisor Prof. Dr. H.Turan DURGUNOĞLU for his helpful suggestions, quidance and continuous interest throughout the course of my study.

I would wish to acknowledge my appreciation to those who have assisted me during the development of this study.

I am also indebted to all Boğaziçi University Computer Center personnel for making facilities available to me.

I am also grateful to Miss Gül Tuncel and Miss Ayşe Özen for their patience in typing the manuscript.

Istanbul, February 1986

Ali İhsan ÇAKIR

ABSTRACT

In this study, the effects of various procedures, Ordinary Method of Slices, Bishop's Modified Method, Spencer's Method, Janbu's Generalized Procedure of Slices and Wedge Method, on factor of safety for a practical problem taken from Alaybey Shipyard Construction are investigated. Soil profile used in the analyses is a sand fill on a soft clay foundation.

General slope stability considerations which are based for stability analyses, the slope stability charts and detailed stability analysis procedures are given in each subsequent section.

The computer programs developed for comparing the influences of the methods mentioned above on factor of safety are employed and the charts giving the differences between the factors of safety of various procedures are also developed. Additionally,the effects of these methods on minimum factor of safety are performed. For this purpose,the influences of the shear strengths parameters of the sand fill and the clay foundation on the factor of safety are investigated and the results are also given as the chart.

Stability of slopes during earthquakes is given in the last section. A typical soil profile taken from Alaybey Shipyard Construction with the earthquake forces and without considering these forces are analyzed using Wedge Method. For this purpose, a computer program is developed.

ÖZET

Bu çalışma, Alaybey Tersanesi'nin inşası sırasında karşılaşılan bir zemin profili ve dairesel olmayan bir şev kayma yüzeyi alınarak çeşitli metotların, basit dilimler metodu, Bishop Modifiye Metodu, Spencer Metod, Janbu genelleştirilmiş dilimler metodu ve Kama metotlarının, bu probleme uygulanması ve şev emniyet katsayısına etkilerinin araştırılması üzerine yapılmıştır. Stabilitesi incelenen zemin profili yumuşak bir kil temel zemini üzerine kum dolgudur.

Stabilite analizlerine esas teşkil eden genel şev stabilite kavramlarının yanısıra şev stabilite abakları ve stabilite analizleri ilgili bölümlerde detaylı olarak açıklanmıştır.

Yukarıda sözü edilen metotların şev emniyet katsayısına etkilerini mukayese etmek üzere geliştirilmiş bilgisayar programlarından yararlanılmış ve sonuçlar abaklar halinde verilmiştir. Ayrıca yine bu metotların minimum emniyet katsayısına etkileride incelenmiştir. Bu amaçla, kum dolgu ve yumuşak kil temel zeminin kayma mukavemetlerinin emniyet katsayılarına tesirleri incelenerek sonuçlar yine abaklar halinde verilmiştir.

Son bölümde deprem sırasında şevlerin stabilitesi verilmektedir. Alaybey Tersanesi'nin inşası sırasında karşılaşılan diğer bir tipik zemin profili örnek alınarak deprem kuvvetleri altında ve deprem kuvvetleri gözönüne alınmadan stabilitesi Kama metodu ile incelenmiştir. Bu amaçla bir bilgisayar programı geliştirilmiştir.

TABLE OF CONTENTS

LIST OF FIGURES

LIST OF TABLES

LIST OF SYMBOLS

Symbol	Meaning
α	length of the moment arm for the weight force (W) about a selected point (O); dimensionless parameter depending on the values of v,h,γ_e,H_e
A	dimensionless parameter
b	width of a slice
B	dimensionless parameter
c	cohesion in terms of total stresses
c'	cohesion in terms of effective stresses
c_b	cohesion at the elevation of the bottom of the slope
c_r	unit cohesive strength
c_m	mobilized cohesion
C_r	cohesive force
d	depth factor; dimensionless parameter depending on the values of c, γ_e, H_e
D	depth from the toe of the slope to the lowest point on the slip circle
E or E_j	total interslice normal force
E_o	horizontal force acting on the left of the first slice
E_n	horizontal force acting on the right of the last slice; resultant of the total horizontal forces on the section n

Symbol	Meaning
E_{n+1}	resultant of the total horizontal forces on the section n+1
$f(x)$	distributional relationship assumed for the side force inclinations
F	factor of safety
F_c	factor of safety with respect to cohesion
F_ϕ	factor of safety with respect to friction
F_s	factor of safety with respect to strength
Δ_g	distance between the location of the normal force and the center of the base of a slice
G	center of gravity of the sector
h	depth to the shear surface; height of an interslice boundary: average height of a slice; depth of foundation from which the failure surface passes
h_t	vertical distance between the line of thrust and the shear surface
H	slope height; depth corresponding to pore pressure
H_e	height of fill
H_f	depth of foundation
H_o	height at which the strength profile intersects zero
H_w	depth of water outside slope
H'_w	height of water within slope
k	seismic coefficient
k_α	dimensionless number depending on the values of α, ϕ and F
K	friction circle correction factors
l	length of a circular shear surface
Δl	length of the base of a particular slice
L	length of a plane shear surface

Symbol	Meaning
m	dimensionless stability coefficient
M_o	moment acting on the left of the first slice
M_n	moment acting on the right of the last slice
n	number of slices; dimensionless stability coefficient; number of unknowns
N	normal force acting on a segment of the shear surface, commonly the base of a slice; stability number
N_{cf} or N_o	stability number
P	the resultant normal and friction force on the shear surface
P_d	dimensionless number depending on the values of $\gamma, H, q, \gamma_\omega, H_\omega, \mu_q, \mu_\omega, \mu_t$
P_e	dimensionless number depending on the values of $\gamma, H, q, \gamma_\omega, H'_\omega, \mu_q, \mu'_\omega$
P_n	normal force
q	surcharge
Q	resultant of all side forces acting on a given slice
r	radial distance from the center point to a point an either a circular or log spiral shear surface; the radius of a circle
r_o	reference radius used to define a log spiral shear surface
r_u	pore pressure coefficient
R	radius of a circle
s	distance
s_u	undrained shear strength of a soil
S	shear force on the base of a slice
S_m	mobilized shear force
T	distance from the depth of sliding to the surface of the slope, measured normal to the surface of the slope

Symbol	Meaning
u	pore water pressure
W	weight of an entire soil mass bounded by an assumed shear surface and the slope surface; or, the weight of an individual slice
x	width of a slice
X	distance from the depth of sliding to the surface of seepage, measured normal to the surface of the slope; shear force between slices
X_o	vertical force acting on the left of the first slice
X_n	vertical force acting on the right of the last slice; vertical shear force on the section n
X_{n+1}	vertical shear force on the section n+1
v	rate of increase in foundation shear strength
y_s	y coordinate of a point on the shear surface
y_t	y coordinate of the line of thrust
z	depth of foundation from which the failure surface passes
z_c	depth of the tension crack
Z	resultant of all forces acting on an interslice boundary
α	angular measure
β	angular measure
γ	unit weight of soil
γ_e	unit weight of fill material
γ_w	unit weight of water
θ	angular measure
μ_q	surcharge correction factor
μ_t	tension crack correction factor

Symbol	Meaning
μ_ω	submergence correction factor
μ'_ω	seepage correction factor
λ	scaling factor for side force inclinations, used in the Morgenstern and Price procedure for slope stability analysis
$\lambda_{c\phi}$	dimensionless parameter used to describe a particular slope in terms of c, ϕ, γ and H.
$\lambda'_{c\phi}$	modified dimensionless parameter used in making stability analyses with pore pressures
σ or σ_n	normal stress on a selected plane
τ_a	average value of shear stress mobilized along a shear surface
ϕ	the angle of internal friction for a soil in terms of total stresses
ϕ_m	mobilized angle of internal friction

CHAPTER I
INTRODUCTION

Embankments are constructed for many different purposes including highways, railroads, dams, levees and stockpiles; in each instance the designer must check to see that the embankment has adequate factor of safety against stability. Stability failure occurs when an outer portion of an embankment slides downward and outward with respect to the remaining part of the embankment, generally along a fairly well defined slip surface.

A detailed investigation of slope stability includes a geological study; field observations, insitu testing, test borings, laboratory testing, and detailed slope stability calculations. The analysis can be performed using a computer or detailed hand calculations as described in subsequent sections. Slope stability charts may be used for preliminary studies or to check the final analysis.

In Chapter 2, the method of plane failure surfaces (Culmann, 1866), Circular Arc Method of Analysis, Friction Circle method, and Logarithmic Spiral method are discussed.

The slope stability charts which have been described in Chapter 3 assume simple slopes and uniform soil conditions. These

charts can be used to obtain reasonably accurate answers for most complex problems.

The procedures of slices are discussed in Chapter 4. These procedures are The Ordinary Method of Slices, Bishop's Procedure (1955), Bishop's Modified Procedure, Spencer's Procedure (1967), Janbu's Generalized Procedure of Slices (1968), Wedge Method, Morgenstern and Price's Procedure (1965,1967), Lowe and Karafiath's Procedure (1960). Every procedure has different assumptions in order to achieve statical determinancy.

In chapter 5,the different procedures for stability analysis of embankments on soft foundations are analyzed. The purpose of this chapter is to show the effects of the procedures which are The Ordinary Method of Slices, Bishop's Modified Procedure, Spencer's Procedure, Janbu's Generalized Procedure of Slices and Wedge Method on the calculated factors of safety for typical embankments on soft foundations. For this reason,the effects of the strength parameters of fill and foundation material on the factor of safety are also investigated. During these studies the computer programs SLOPE 22R, SLOPE 8R; SLOPE 9, and WEDGE 1 developed for comparison purposes are employed.

Moreover, the effect of foundation shear strength on minimum factor of safety calculated by different procedures as mentioned above is studied in Chapter 6. For this purpose, the computer program WEDGE 2 is also developed in this study.

Stability of slopes during Earthquakes is discussed in Chapter 7. An example problem taken from Alaybey Shipyard Construc-

tion is analyzed using the computer program WEDGE 3 in this chapter.

Consequently, in this study various slope stability procedures are given in details and a comparison of these methods on factor of safety for different soil characteristics and profiles is also given in each subsequent section.

CHAPTER 2

GENERAL SLOPE STABILITY CONSIDERATIONS

2.1 INTRODUCTION

The procedures given in Chapter 4 inclusive have broad applicability. Solutions by these methods can be obtained for embankments under wide ranges of conditions, but such solutions often require much time.

Solutions for simple cross sections of homogeneous soils, within which no seepage is occuring, may be obtained somewhat more easily and, once obtained, they may be made available in the form of relatively simple charts. A number of solutions that have been presented in the past in the form of equations or charts are mainly of academic interest, since they contain questionable assumptions and have no practical advantages over more logical methods. The highly mathematical treatments known as the Resal-Frontard method and the Jaky method fall into this category and thus are not discussed herein. Simple slope analyses based on plane failure surfaces, on circular failure surfaces, and on spiral failure surfaces are presented in this chapter.

2.2 STABILITY OF SLOPES IN SOILS WITH UNIFORM STRENGTH THROUGHOUT THE DEPTH OF THE SOIL LAYER, AND $\phi = 0$

At the present time, many different procedures of slope stability analyses are available which satisfy the conditions of static equilibrium to calculate the average value of shear strength required to prevent failure. These various procedures of analysis have different assumptions which are made to satisfy the particular conditions of equilibrium and to achieve statical determinancy. The well-known methods may be written as follows:

1. Plane Failure Surfaces
2. Circular Arc Method and $\phi = 0$ Analysis

2.2.1 Plane Failure Surfaces

Plane failure surfaces often occur when a soil deposit or embankment has a specific plane of weakness. Excavations into stratified deposits where the strata are dipping toward the excavation may fail along a plane parallel to the strata. Methods of analysis that consider blocks or wedges sliding along plane surfaces have been developed to analyze cases where there is a specific plane of weakness (Seed and Sultan, 1967). A plane failure surface is a simple failure mechanism. Such a plane failure surface analysed by Culmann (1886).

Consider the equilibrium of the triangular wedge formed by the assumed failure surface in Fig.2.1. The three forces considered are the weight of the wedge W, a cohesive force C_r, parallel to the potential sliding surface, and the resultant P, of the normal and frictional forces. The relationship of these forces is shown on the force polygon. The cohesive force C_r equals the required unit cohesive strength c_r times the length of

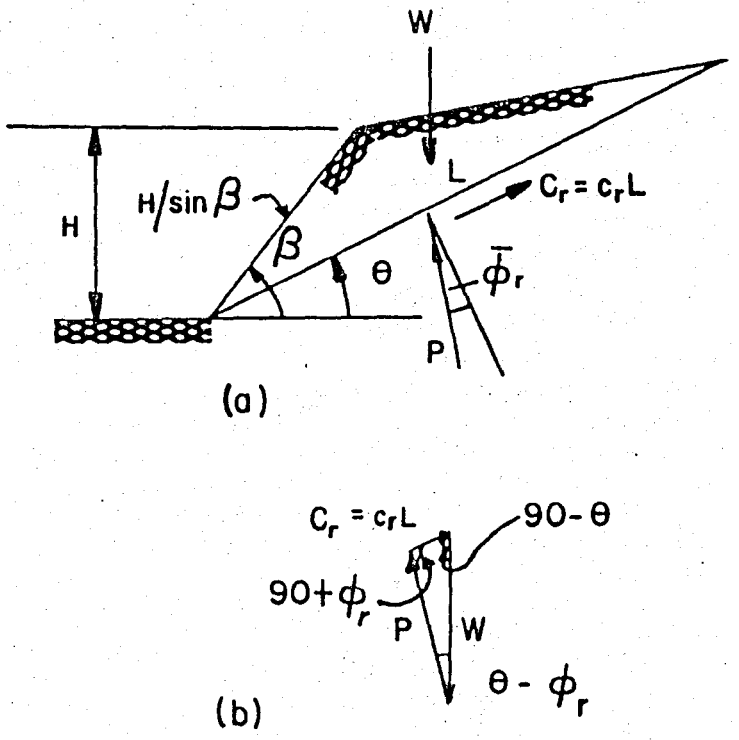

FIG.2.1 Slope Analysis Assuming a Plane Failure Surface

the potential failure surface L. The unit cohesion and friction angle are the values required for equilibrium and will be equal to or less than the available cohesion and friction. A safety factor with respect to cohesion, F_c , is defined as the ratio of available cohesion to required cohesion, and a factor of safety with respect to friction, F_ϕ, is defined as the ratio $\tan\phi$(available) to $\tan\phi_r$(required). If either safety factor is assumed to be 1, the other will be greater than 1 if the slope is stable. The factor of safety with respect to strength, F_s, or correct factor of safety for the assumed failure mechanism occurs when $F_c = F_\phi = F_s$. For a c-ϕ soil, F_s is determined by trial and error. A value of F_ϕ is assumed, and this establishes a value of ϕ_r. The value of F_c is then computed from the force polygon of Fig.2.1b and the definition of F_c. The procedure is then repeated until $F_c=F_\phi$. This safety factor represents the safety factor with respect to strength, F_s , for the assumed failure plane.

The critical plane can be established using the following procedure. From the force polygon of Fig. 2-1b,

$$\frac{C_r}{W} = \frac{\sin(\theta-\phi_r)}{\sin(90+\phi_r)} = \frac{\sin(\theta-\phi_r)}{\cos\phi_r} \qquad ...(2.1)$$

and, from Fig. 2-1a,

$$\frac{C_r}{W} = \frac{c_r L}{\frac{1}{2}\gamma L(H/\sin\beta)\sin(\beta-\theta)} \qquad ...(2.2)$$

Combining these expressions and solving for $c_r/\gamma H$ yields

$$\frac{c_r}{\gamma H} = \frac{\sin(\theta-\phi_r)\sin(\beta-\theta)}{2\cos\phi_r \sin\beta} \qquad ...(2.3)$$

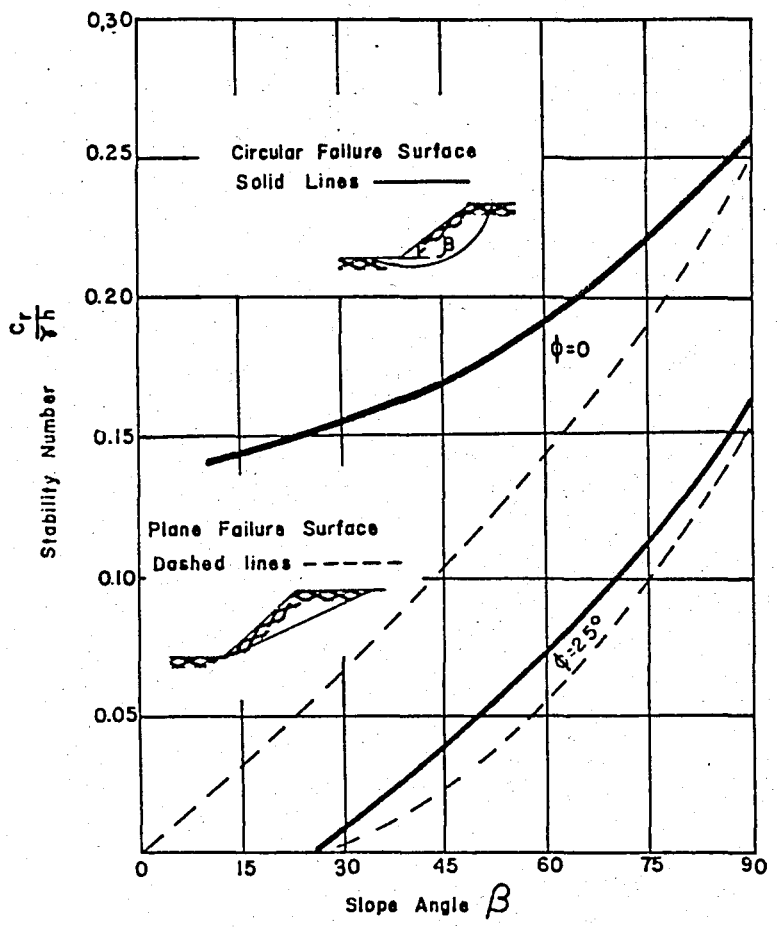

FIG 2.2 Comparison of Plane and Circular Failures

The critical failure plane(the one that will yield the lowest factor of safety) is defined by the value of θ that yields the maximum value of $c_r / \gamma H$. Differentiate Eq.2.3 with respect to θ and set equal to zero to find θ_c.

$$\theta_c = \frac{1}{2}(\beta+\phi_r) \qquad \ldots (2.4)$$

Substitution of this value into Eq.2.3 yields the maximum stability number for the slope.

$$\left(\frac{c_r}{\gamma H}\right)_{max} = \frac{1 - \cos(\beta-\phi_r)}{4\sin\beta\cos\phi_r} \qquad \ldots(2.5)$$

Equation 2.5 and the iterative procedure just explained can be used to find the safety factor with respect to strength F_s .

Equation 2.5 is the stability number for plane failure surfaces for c-ϕ soil. If ϕ= 0, Eq.2.5 reduces to

$$\left(\frac{c_r}{\gamma H}\right)_{max} = \frac{1 - \cos\beta}{4\sin\beta} = \frac{1}{4}\tan\frac{\alpha}{2} \qquad \ldots(2.6)$$

A plot of this function in Fig.2.2 shows that a plane failure surface is not the critical failure surface but approaches the results for circular failure surfaces at very steep slopes.

2.2.2 Circular Arc Method And ϕ= 0 Analysis

A more common problem is one in which the slope is of finite extent and in which failures occur on curved surfaces. The most widely used method of analysis of homogeneous, isotropic finite slopes is the Swedish method based on circular failure surfaces. It is believed that this method was first

used by K.E. Petterson in the study of the failure of a quay wall in Goeteborg in 1915 or 1916.

Numerous slope failures that had occurred along Swedish railroads led to the setting up of an elaborate program in that country in 1920 or earlier for the investigation of slope stability. This work was carried out by the Swedish Geotechnical Commission. From boring data the shapes of the failure surfaces of numerous slides were determined, and one of the main contributions of the program was the information that actual failure surfaces generally do not deviate greatly in shape from circle. This finding is the main justification of the method of analysis proposed by this commission; it was developed by W.Fellenius and others and is now widely used. In this method failure surfaces are assumed to be of clylindrical shape, and they appear on cross sections as circular arcs. There are many possible circular arcs through a cross section, and the location of the critical, or most dangerous , arc must usually be determined by methods of trial. Many procedures of stability analysis have been developed which utilize the several advantages afforded by such surfaces. The most important advantage of using circular surfaces is their significant simplification of the mechanics of stability analyses.

The average shear stress (τ_a) mobilized along the circular arc bpd shown in Fig.2.3 can be determined from the summation of moments about the center point (O). For a mass of soil in static equilibrium this sum must be zero. Thus,

$$\Sigma M_o = W a - \tau_a l r = 0 \qquad \ldots (2.7)$$

in which

W = the weight of the soil mass overlying bpd

a = the length of the moment arm of W about O

l = the length of the shear surface

r = the radius of the circle

By substituting $a = r \sin\alpha$

where α = the inclination of the shear surface at its intersection with the weight vector.

The average shear stress can be expressed as ,

$$\tau_a = \frac{W \sin\alpha}{l} \qquad \ldots (2.8)$$

This equation for the average value of shear stress required for equilibrium of a circular arc is free of any assumptions. Regardless of what method is used to determine the equilibrium of the sliding mass shown in Fig.2.3, the average shear stress must be the same as that given by Eq. 2.8 as long as static equilibrium is satisfied.

While the earliest procedures of stability analysis for circular shear surfaces assumed that the shearing resistance of the soil was due entirely to friction, in 1917, Hellan suggested that the shear strength of a clay could be treated entirely as a cohesion (Petterson, 1955; Bjerrum and Flodin, 1960). Combining this concept of the shear strength and the assumption of circular shear surfaces, Fellenius in 1918 proposed what is today commonly known as the "ϕ=0" method of stability analysis, a procedure which is widely used for analysis of short-term slope stability.

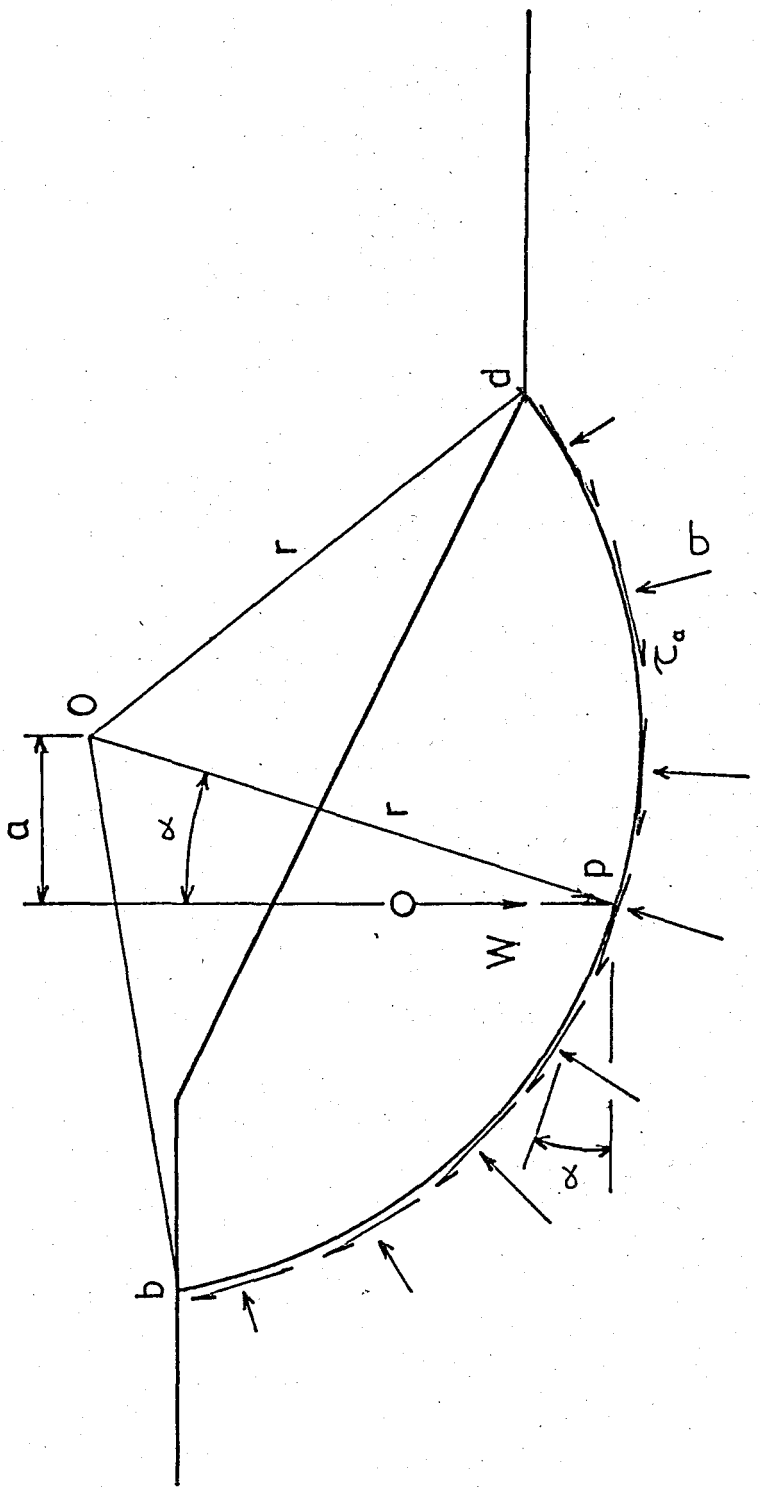

FIG.2.3 Stresses along a Circular Shear Surface

From an examination of actual slope failures in clay soils it was found that the slip surface was approximately cylindrical. In the $\phi=0$ Method which is also known as the Swedish Method a vertical section through the slope is drawn, and it is assumed that failure will take place along an arc of a circle. Several "slip circles" are drawn from different centres of rotation, and by a process of trial and error the slip circle giving the lowest factor of safety is found.

In many practical cases the clay soil in a cutting or embankment will behave as a purely cohesive material with "zero" angle of shearing resistance. The shearing resistance of the clay, if fully saturated , and hence the stability of the slope, will depend on the cohesion of the clay only. The stability analysis for such a case is described as a "$\phi=0$- analysis".

The principle of the method is illustrated in Fig.2.4. A slice of unit thickness of the slope is considered.

In the simplest case the cohesion c of the clay is assumed to be uniform throughout the material. The weight W of the sector is calculated, acting at G, the centre of gravity of the sector. Moments are taken about the centre of rotation O. The "disturbing moment" is $W \times x$. The "resisting moment" is the cohesion multiplied by the length l of the arc AB and the radius R,

i.e.,

$$c \times l \times R = c \times R^2 \times \theta \qquad \ldots (2.9)$$

If slipping is just about to take place the disturbing and resisting moments will be equal, i.e., disturbing moment= resisting moment

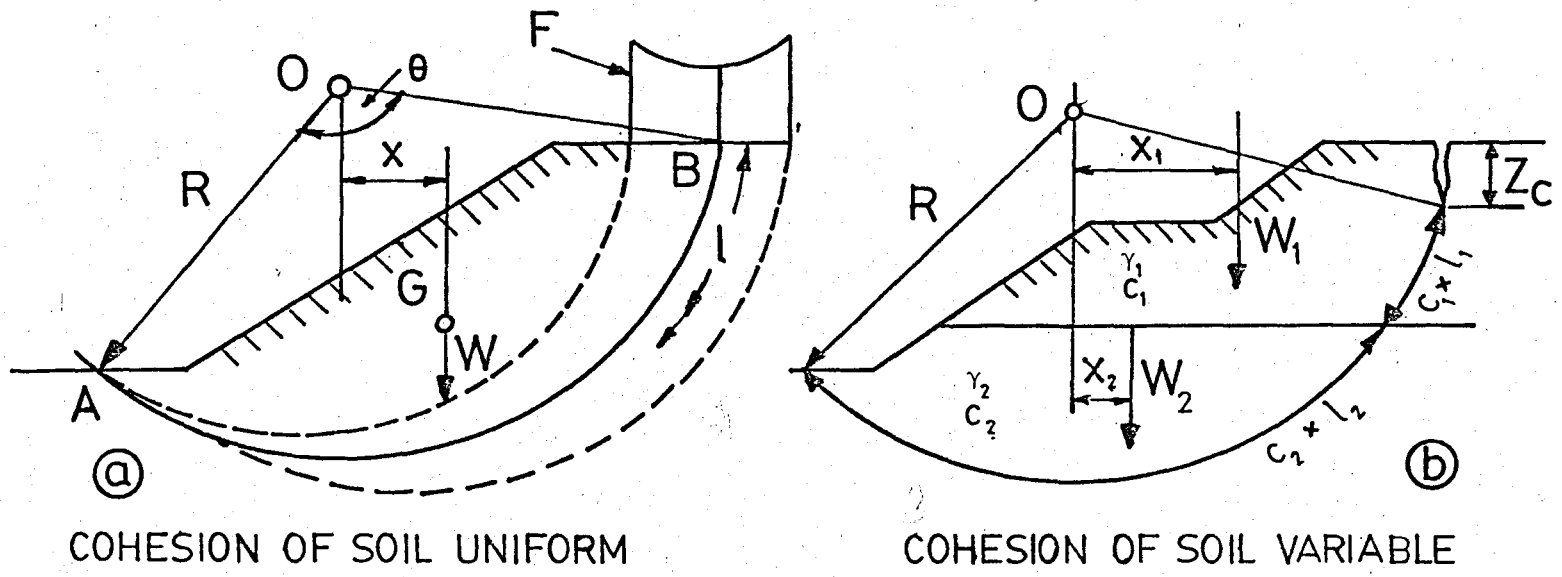

FIG.2.4 $\phi = 0$ Analysis of Slope Stability

$$W \times x = c \times l \times R = c \times R^2 \times \theta \qquad \ldots (2.10)$$

In order to have a margin of safety the resisting moment must be greater than the disturbing moment. The actual factor of safety is thus:

$$F = \frac{\text{resisting moment}}{\text{disturbing moment}} = \frac{c \times R^2 \times \theta}{W \times x} = \frac{c \times l \times R}{W \times x} \qquad \ldots (2.11)$$

Several possible slip circles have to be drawn in order to find the circle which results in the lowest factor of safety.

If the slope is not uniform and the cohesion of the clay varies, the sector is divided into suitable parallel vertical or horizontal strips. In case of failure a tension crack is likely to develop, and the length of the arc l resisting sliding will be measured from the bottom of the tension crack . The method of making the stability calculations is indicated in Fig.2.4b.

The disturbing moments are $\Sigma W \times x$ and the resisting moments are $R\Sigma c \times l$. The factor of safety is then calculated as before:

$$F = \frac{R.\Sigma c \times l}{\Sigma W \times x} \qquad \ldots (2.12)$$

The lowest factor of safety is again found by trial and error. An allowance should be made for the horizontal water pressure which would develop in the tension crack if it fills up with water. The moment of this lateral force about the centre of rotation of the slip circle causes an additional disturbing moment. The depth of the

tension crack in a purely cohesive soil is:

$$z_c = \frac{2c}{\gamma} \qquad \ldots (2.13)$$

Using a circular shear surface simplifies the $\phi=0$ procedure because the normal stresses all act through the center of the circle regardless of their distribution and consequently are eliminated from the equation for moments about the center point. In addition, the shear stresses all act at the same distance from the center of the circle and therefore their moment arm is constant and independent of their distribution. Thus, use of a circular shear surface, which is in itself an assumption, results in statical determinancy with respect to moment equilibrium and although the shear stress distribution is not known from the $\phi=0$ analysis procedure; the one unknown value of average shear stress may be calculated from the moment equilibrium equation.

2.2.3 The Factor of Safety

In many procedures for slope analyses, stability is measured in terms of an overall factor of safety with respect to shear strength. If the shear strength for the slope in Fig.2.3 is s_u, the factor of safety is defined by,

$$F = \frac{s_u}{\tau_a} \qquad \ldots (2.14)$$

which, upon substituting the expression for τ_a, gives the factor of safety for a particular circular shear surface in terms of known geometry and soil conditions:

$$F = \frac{s_u l}{W \sin\alpha} \qquad \ldots (2.15)$$

Because the critical shear surface is usually unkonwn, several trial surfaces must be analyzed until the minimum factor of safety for the slope is found.

The factor of safety expressed by Eq. 2.15 corresponds to the well-known ϕ=0 procedure of stability analysis and is free of any assumptions regarding the stress distributions along the failure surface. Although the factor of safety at any point along the shear surface bpd will be determined by the actual values of shear stress and shear strength at that point, the distribution of shear stresses cannot be determined by the ϕ= 0 method. Only when the factor of safety is unity the shear stresses are known, in which case they are implied to be equal to the corresponding shear strengths along the shear surface.

2.3 STABILITY OF SLOPES IN UNIFORM SOILS WITH $\phi \geq 0$

In this section Friction Circle Method and Logarithmic Sprial Method are discussed. These methods of stability analysis of slopes are particulary applicable to (c-ϕ) soils.

2.3.1 Friction Circle Method

A circular failure arc is drawn from a trial center in Fig.2.5. At the center a friction circle is drawn at a radius r sin ϕ_r such that all lines tangent to the friction circle and cutting the circular failure arc from the angle ϕ_r with the normal. These lines represent the direction of the combined normal and mobilized frictional forces distributed around the failure arc. The resultant normal and frictional force is assumed also to be tangent to the ϕ_r circle. Actually, the resultant is tangent to a slightly larger ϕ_r circle or radius Kr sin ϕ_r, where K is a factor greater than one. Values of K can be estimated from Fig.2.6. Note that the two

forces dP shown in Fig.2.5 intersect slightly outside the friction circle

The equilibrium of the circular wedge is analyzed by considering three vectors; the weight, W, a resultant cohesive force, C_r, and the resultant normal and friction force, P.

The weight vector is equal to the area of the wedge times the unit weight of the soil and acts through the centroid of the wedge.

The cohesive force C_r acts parallel to the chord of the failure arc and is equal to $c_r L_{chord}$. The force C_r is located a distance s from the center O, where

$$s = r \frac{L_{arc}}{L_{chord}} \qquad \ldots(2.16)$$

or a distance slightly greater than the radius r.

The intersection of the forces W and C_r establishes a point through which the third force, P, must act. The direction of P is established by drawing a line tangent to the adjusted ϕ circle from the intersection of W and C_r.

The weight of the wedge is known, but the magnitudes of P and C_r must be established by trial and error similar to the method illustrated in the preceding section for plane failure surfaces. If F_ϕ is assumed, the friction circle for ϕ_r equal to $\tan^{-1}(\tan\phi/F_\phi)$ can be drawn and the equilibrium triangle completed for the required cohesive force, C_r. The factor of safety with respect to cohesion $F_c = C/C_r$ is then compared with the assumed F_ϕ.

By plotting F_ϕ versus F_c, a new estimate for F_ϕ can be made and the process repeated until $F_c = F_\phi = F_s$.

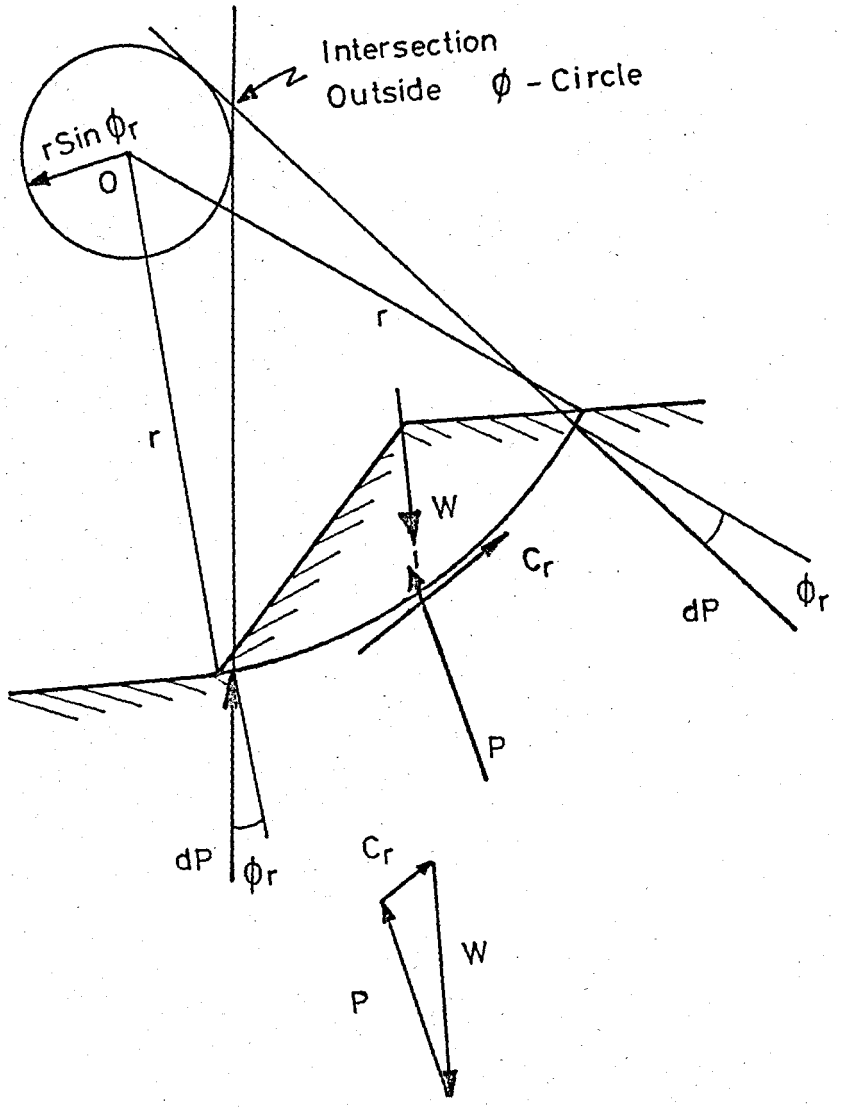

FIG.2.5 Friction Circle Method

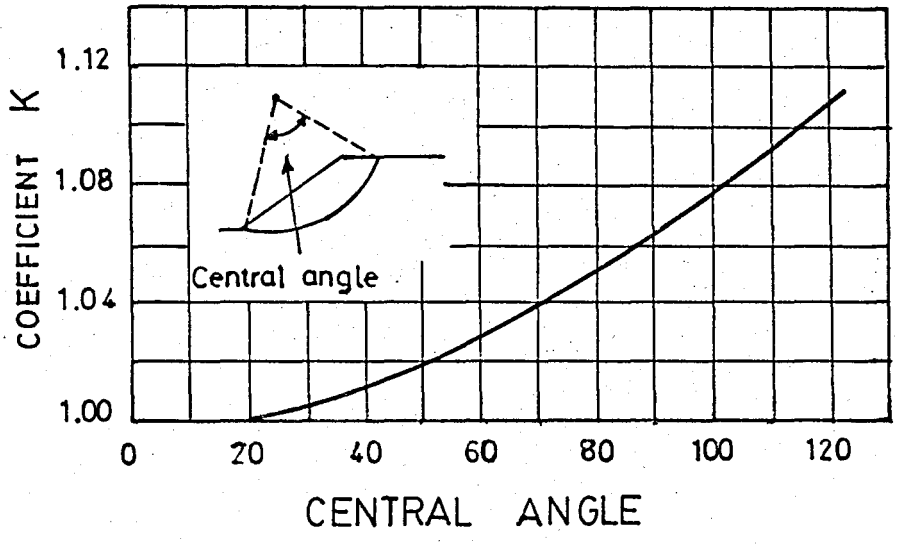

FIG.2.6 Friction Circle Correction Factors

Additional centers and arcs must be analyzed to determine the minimum factor of safety. The iterative procedure can be shortened somewhat by finding the critical circle as that which yields the minimum safety factor with respect to cohesion. Iteration to find F_s would then be required on the critical circle.

The friction circle method is primarily limited to homogeneous soils and a total stress analysis. The influence of pore pressure or boundary water forces can be included.

Stability numbers based on friction circle analyses are plotted in Fig.2.2 and compared with numbers based on a plane failure for $\phi=25^0$.

2.3.2 Logarithmic Spiral Method

When ϕ is not equal to zero, the assumption of a circular shear surface is insufficient to satisfy statical determinancy. In this case by assuming a logarithmic spiral surface the statical determinancy may be achieved. A logarithmic spiral surface has the following form.

$$r = r_o e^{\theta \tan\phi_m} \qquad \ldots (2.17)$$

where

r =the radial distance from the center point to a point on the spiral

r_o=the reference radius

θ=the angle between r and r_o

ϕ_m=the mobilized friction angle for the shear surface

In this method, all the resultants of the normal stresses (σ) and frictional components of shear strength ($\sigma \tan \phi_m$) pass through the center

point of the spiral. For this reason their contributions to the moments are zero. Consequently the moment equation will only involve the weight force and cohesive resistance of the soil.

By summation of moments about the center of the spiral, the average mobilized cohesion required for equilibrium may be calculated; however, since a value of ϕ_m must be assumed before a shear surface may be defined by Eq.2.17, the mobilized cohesion which is calculated may result in a different factor of safety with respect to cohesion than was assumed in calculating ϕ_m. Several trials must be made until a balanced factor of safety with respect to shear strength can be found which satisfies the relationship.

$$F = \frac{c}{c_m} = \frac{\tan\phi}{\tan\phi_m} \qquad \ldots (2.18)$$

It may be recalled that for a non-circular shear surface, like the log spiral, it was necessary to know the distribution of shear stresses along the surface in order to calculate moments about any point; however, by assuming that the factor of safety was constant along the log spiral surface the unknown shear stress distribution was replaced by the single unknown value of average shear stress. Nevertheless, because the normal stress distribution is not known for the log spiral shear surface, the available shear strength and distribution of shear stresses is indeterminant, as in the case of the $\phi = 0$ method

2.4 SUMMARY

There are several theories available for analyzing the stability of slopes, for example:

plane failure surfaces

circular failure surfaces

logarithmic spiral failure surfaces

In a homogeneous soil failure in shear along a plane surface may be assumed to take place in a surface such that the acting shear stresses are greater than the shear strength of the soil. The stability calculation is thus based on a shear plane. It should be mentioned that stability analyses of slopes on plane failure surfaces were studied by Coulomb.

One of the most commonly used type of failure surface in stability analyses of slopes is the circular failure surface. The circular is merely a conventional one in order to simplify mathematical computations involved in the stability analysis. Because of the early extensive studies of failures of slopes made by Swedish engineers , the circular failure surface is often referred to as the Swedish circle method.

A method based on the assumption that the failure surface is a logarithmic spiral was developed by Rendulic. The use of the logarithmic spiral is in some ways more inconvenient than the use of the circle as the failure surface, but satisfactory graphical procedures for the spiral method have been developed. The main advantage of the spiral method is that all intergranular forces with the obliquity ϕ_r (as shown in Fig.2.5) are directed toward the center of the spiral. Because of this condition the analysis is statically determinate without an assumption relative to the pressure distribution.

The friction-circle method of slope analysis is a convenient approach for both graphical and mathematical solutions. It is given this name because the characteristic assumption of the method refers to the ϕ circle.

When ϕ is not equal to zero, the assumption of a circular shear surface is insufficient to achieve statical determinancy. In this case assuming a logarithmic spiral surface satisfies the statical determinancy.

All the methods mentioned above are discussed and given in details in this chapter. Although some of these procedures are suitable for analyzing non-circular shear surfaces, others are restricted to circular surfaces. Examination of the mechanics of the various procedures of analysis shows that some of the earliest procedures developed are virtually identical to many of the recent techniques for analyzing non-circular shear surfaces.

CHAPTER 3
SLOPE STABILITY CHARTS

3.1 INTRODUCTION

The practising engineer and the designer frequently require a rapid means of estimating the factor of safety of a cut, an embankment, or a natural slope. A detailed analysis is often impracticable in the preliminary stages when a number of alternative schemes are under consideration. Stability charts are used in these circumstances. Stability charts provide perhaps the most convenient method of analysis for simple homogeneous slopes. However, charts are now available which make it possible to perform quite accurate analyses for many conditions. The stability of slopes can be analyzed quickly using the stability charts. Although the charts assume simple slopes and uniform soil conditions, they can be used to obtain reasonably accurate answers for most complex problems if irregular slopes are approximated by simple slopes, and average values of unit weight, cohesion, and friction angle are used. Charts which include the effects of surcharge, tension cracks, submergence, seepage, and increasing strength with depth allow a wide range of variables to be considered in the design of a slope by this method.

3.2 CHARTS FOR SOILS WITH CONSTANT STRENGTH, AND $\phi = 0$

Slopes that approximate simple sections of relatively uniform soil may be analyzed using the slope stability charts which were given by Taylor(1948) and Janbu (1968).

3.2.1 Taylor's Charts

Taylor (1948) has prepared two curves giving stability numbers whose solutions are valid only for the slopes that approximate simple sections of uniform soil. Three of the parameters, c_r, γ, and H, are combined into a dimensionless stability number, which is plotted as a function of the slope β for various values of ϕ_r.

Taylor proposed developed shear strength parameters c_r and ϕ_r in terms of c and ϕ,

where

c_r = the developed cohesion

ϕ_r = the developed friction angle

are defined respectively as:

$$c_r = \frac{c}{F} \qquad \ldots (3.1)$$

$$\tan\phi_r = \frac{\tan\phi}{F} \qquad \ldots (3.2)$$

The critical circle for steep slopes passes through the toe of the slope with the lowest point on the failure arc at the toe of the slope; this is shown by key sketch (A) in Fig. 3.1. This condition holds throughout zone A of this figure. In zone B the low point of the

critical circle is not at the toe of the slope, and three cases that will be considered are shown in key sketch (B). For small slope angles or small friction angles the critical circle may pass below rather than through the toe of the slope, as is shown in Case 2. For all ranges in which this case holds, stability numbers are given in the chart by dotted curves. Stability numbers for the most dangerous circles passing through the toe are given by solid lines in the chart both when there is and when there is not a more dangerous circle that passes below the toe; where a solid line does not appear in the chart the most dangerous circle passes below the toe, and the most dangerous circle through the toe does not have a perceptibly different stability number.

The case wherein the shearing strength is assumed constant is an important one, and it is represented in stability charts by a zero friction angle. For this case the critical circle passes below the toe for slopes with inclination of less than 53^0. Theoretically the critical slope for this case is at an infinite depth. In slopes encountered in practical problems, however, the depth to which the rupture may pass is usually limited by other underlying strong material. Thus the stability number for the zero-ϕ case is greatly dependent on the limiting value of the depth. To represent this condition the variable used is the ratio of depth of failure mass to height of slope; it is designated by D/H and is shown in Fig. 3.2.

For various values of D/H and for the zero-ϕ case the chart in Fig.3.2 supplements Fig.3.1. The coordinates used in Fig.3.2 allow a reasonably simple presentation of a number of items of practical information. As shown by the key sketches, circles passing below the toe are represented by full line curves and n values are represented by short dashed lines. Cases wherein there are loadings outside the toe,

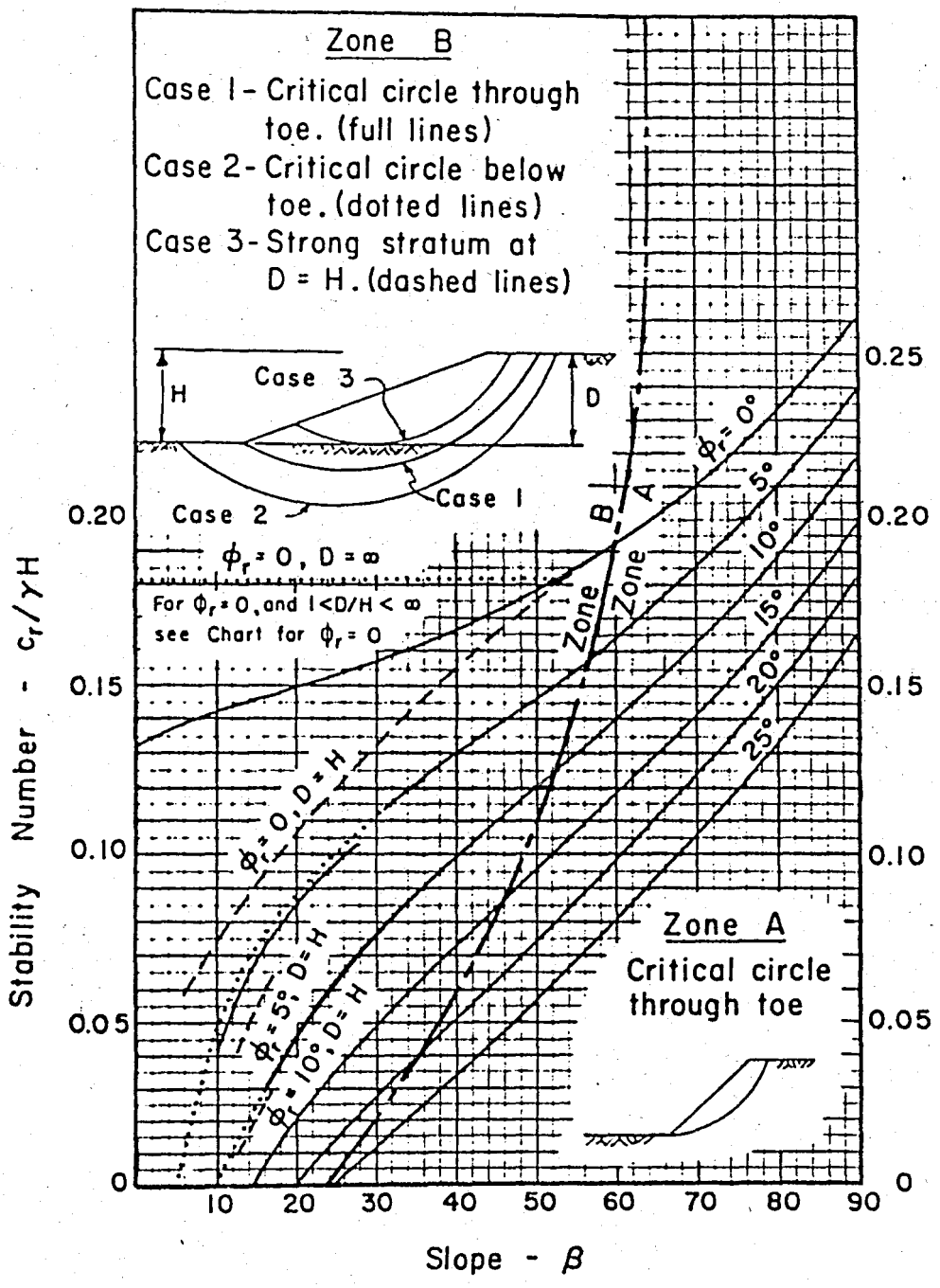

FIG.3.1 Stability Numbers for Homogeneous Simple Slopes (after Taylor,1948)

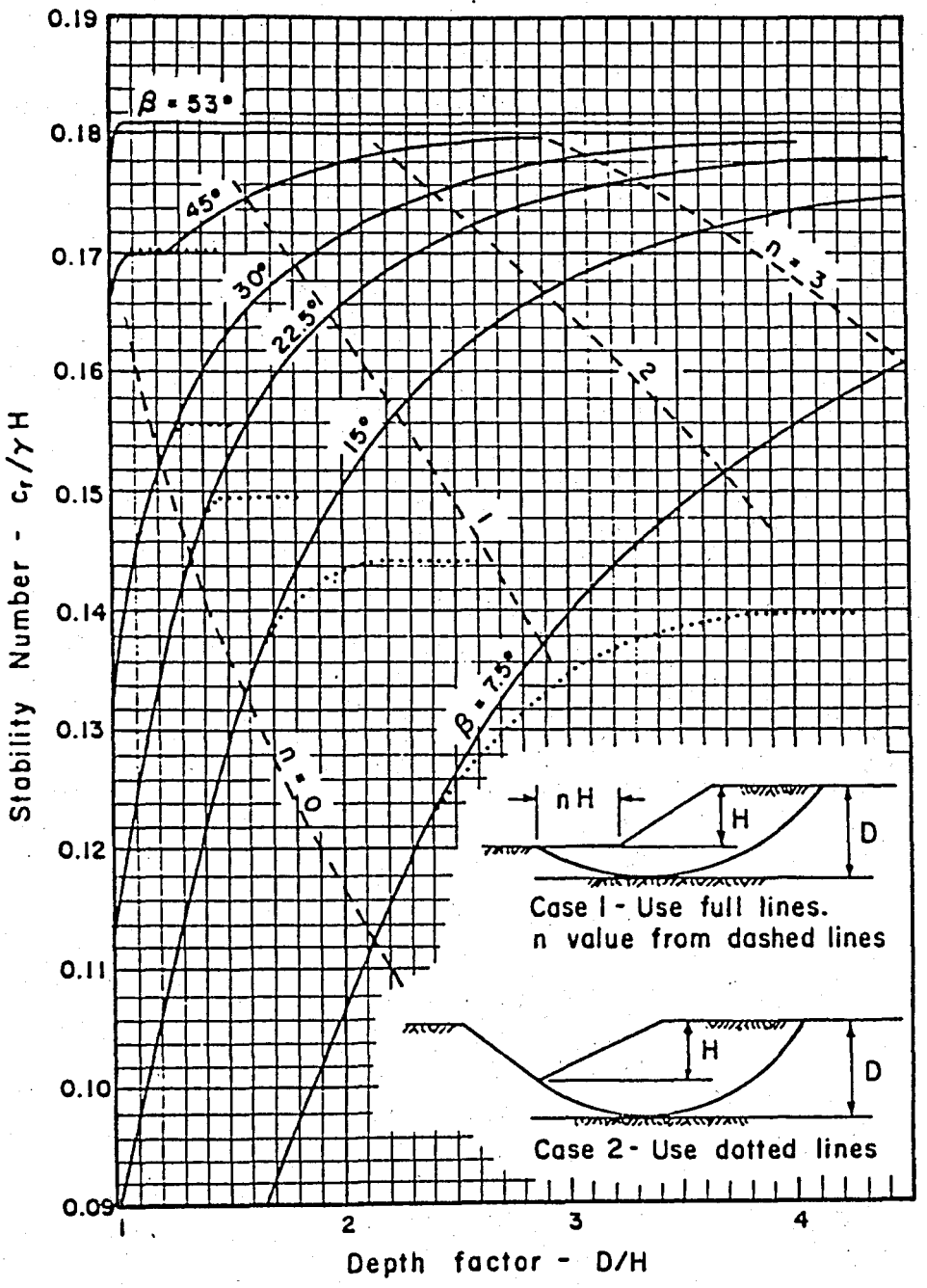

FIG.3.2 Stability Numbers for Homogeneous Simple Slopes for (ϕ = 0) (after Taylor, 1948)

which prevent the circle from passing below the toe, are represented by dotted lines.

If there is strong material at the elevation of the toe of the slope, the case is represented in Fig.3.2 by a D/H value of unity, and it is also covered in Fig.3.1 by case 3. For D/H equal to unity and ϕ greater than zero the solution has been carried out only for 15^0 slopes; therefore the short dashed lines for the larger friction angles are of short length in Fig.3.1.

The factor of safety for a ϕ=0 soil may be obtained directly from Fig.3.2, but a trial and error procedure is required for a c-ϕ soil. All points in the charts represent a factor of safety unity. In trial error procedure, a factor of safety with respect to friction, F_ϕ , is initially assumed and is compared with the resulting factor of safety with respect to cohesion, F_c. The assumed F_ϕ is adjusted until $F_\phi = F_c = F_s$.

3.2.2 Janbu's Charts

Janbu (1968) has developed the stability charts for slopes in in soils ϕ=0 which are given in Fig.3.3. Charts giving correction factors for surcharge loading at the top of the slope, submergence, and tension cracks are given in Figs.3.4 and 3.5.

Steps for use of charts:

1. Using the charts at the bottom of Fig.3.3, determine the position of the center of the critical circle, which is located at X_o, Y_o. For slopes flatter than 53^0, the critical circle passes tangent to the top of firm soil or

rock. For slopes steeper than 53°, the critical circle passes through the toe.

2. Using this estimated critical circle as a quide, estimate the average value of strength, c. This can be done by calculating the weighted average of the strengths along the failure arc, using the number of degrees intersected by each soil layer as the weighting factor. An example is shown in Fig.3.6.

3. The depth factor, d, can be calculated using the formula

$$d = \frac{D}{H} \qquad \ldots (3.3)$$

in which D=dept from the toe of the slope to the lowest point on the slip circle, (L; length)

H=slope height (L)

4. Calculate P_d using the formula below

$$P_d = \frac{\gamma H + q - \gamma_\omega H_\omega}{\mu_q \mu_\omega \mu_t} \qquad \ldots (3.4)$$

in which γ= average unit weight of soil (F/L^3 ; force/length^3)

H= slope height (L)

q= surcharge (F/L^2)

γ_ω=unit weight of water(F/L^3)

H_ω=depth of water outside slope (L)

μ_q=surcharge correction factor (Fig.3.4, top)

μ_ω=submergence correction factor (Fig.3.4, bottom)

μ_t=tension crack correction factor (Fig.3.5)

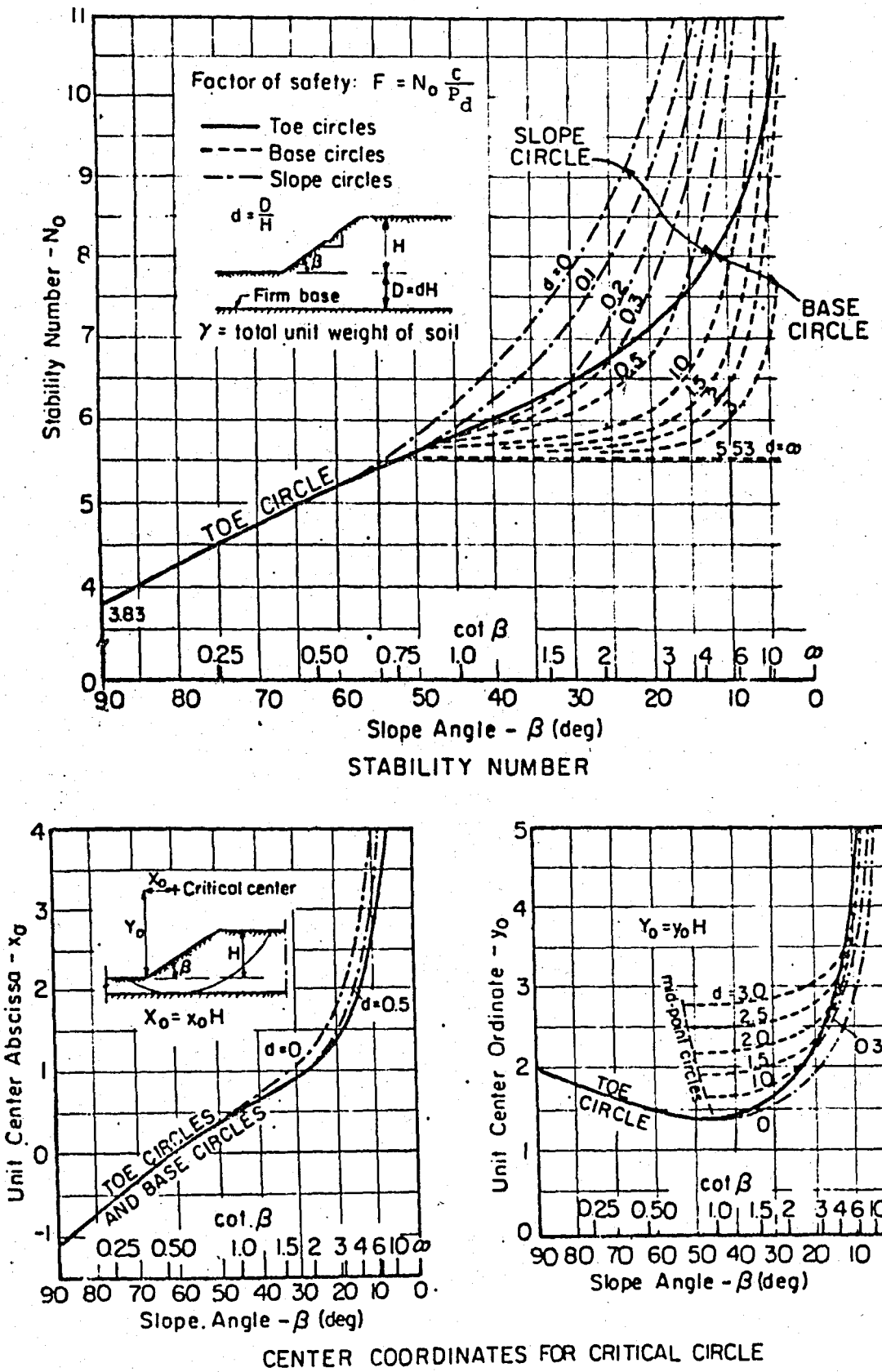

FIG.3.3 Slope Stability Charts for $\phi = 0$ Soils (after Janbu, 1968)

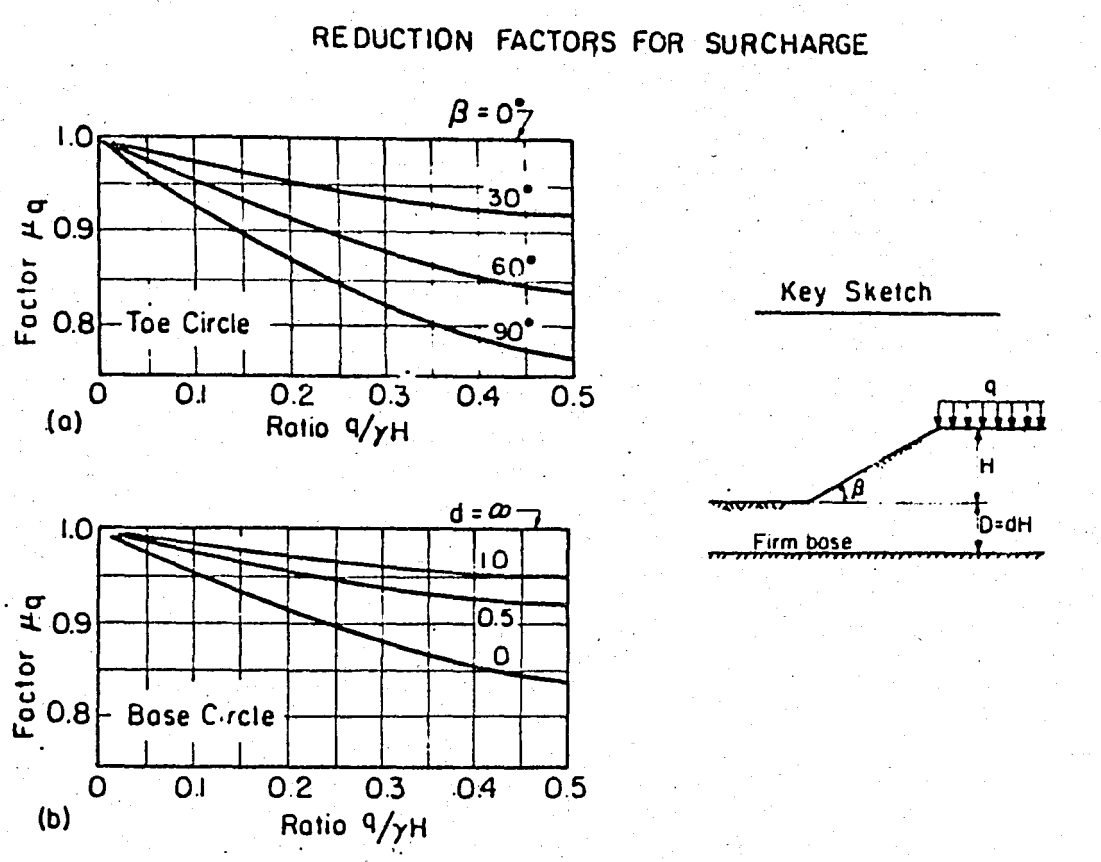

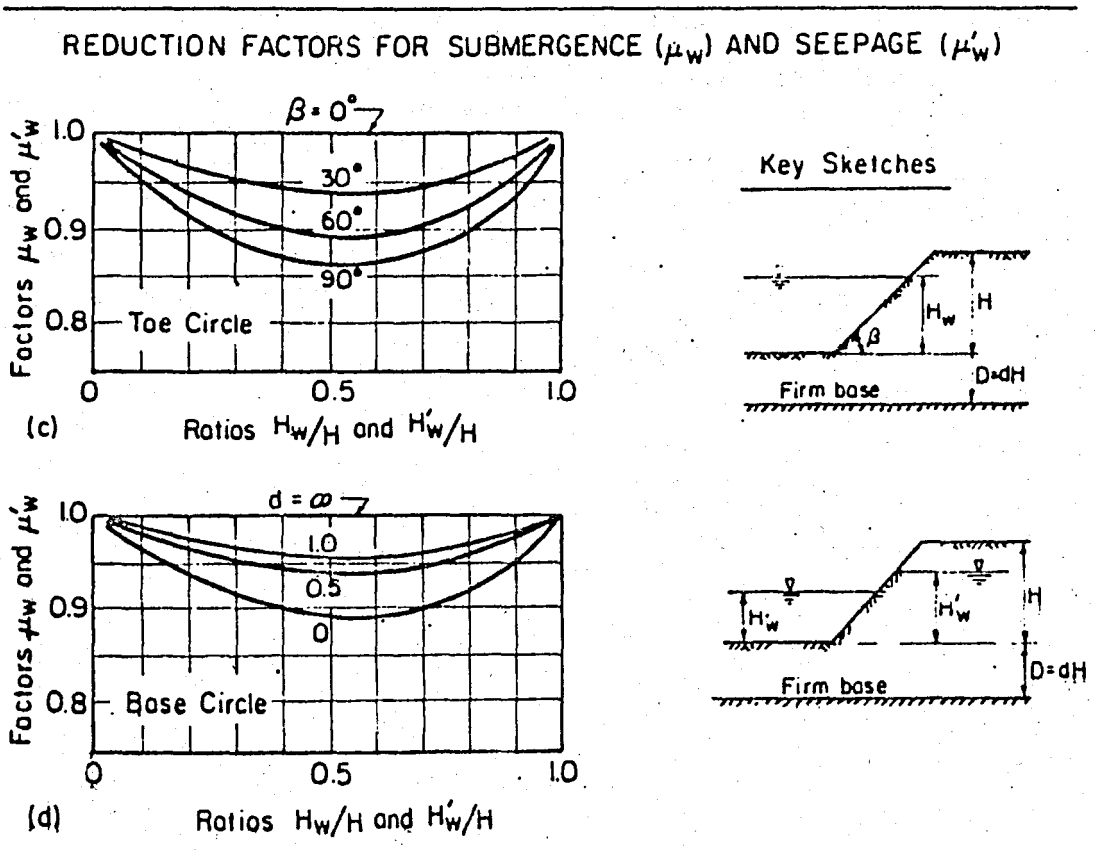

FIG.3.4 Reduction Factors for Slope Stability Charts for $\phi=0$ and $\phi>0$ Soils (after Janbu, 1968)

REDUCTION FACTOR FOR TENSION CRACK

No Hydrostatic Pressure in Crack

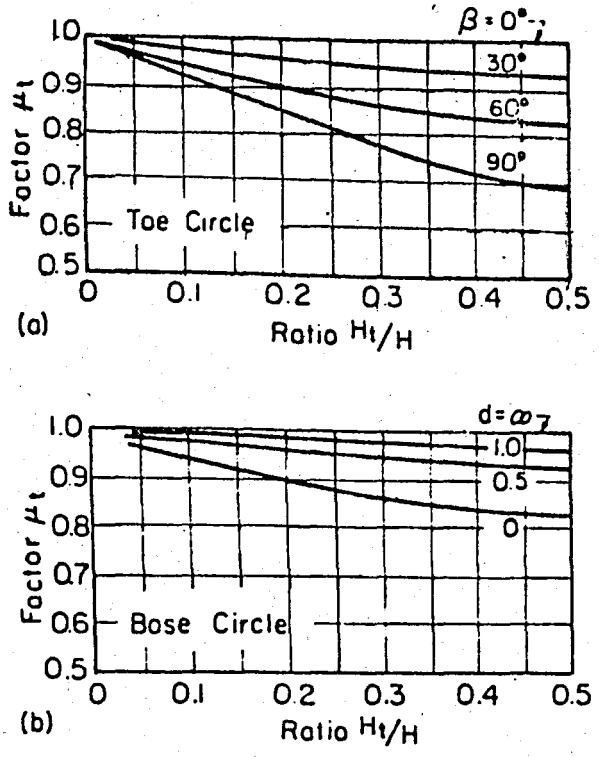

Key Sketch

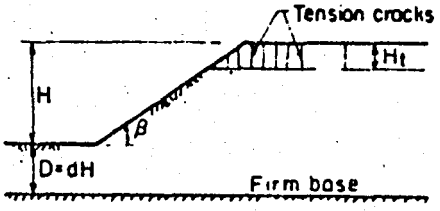

REDUCTION FACTOR FOR TENSION CRACK

Full Hydrostatic Pressure in Crack

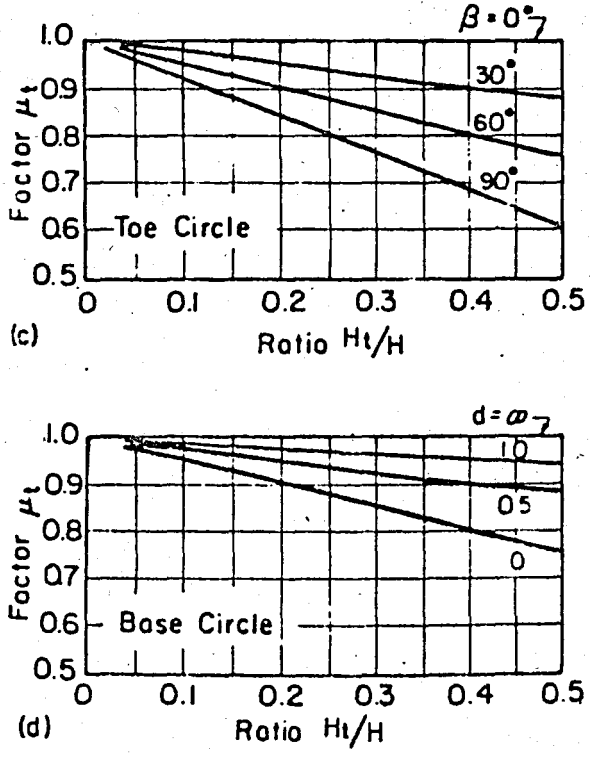

Key Sketch

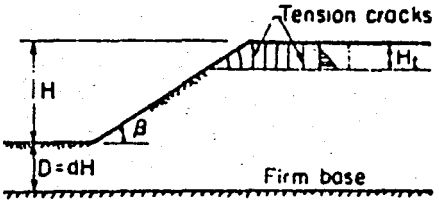

FIG.3.5 Reduction Factors for Slope Stability Charts for $\phi = 0$ and $\phi > 0$ Soils (after Janbu,1968)

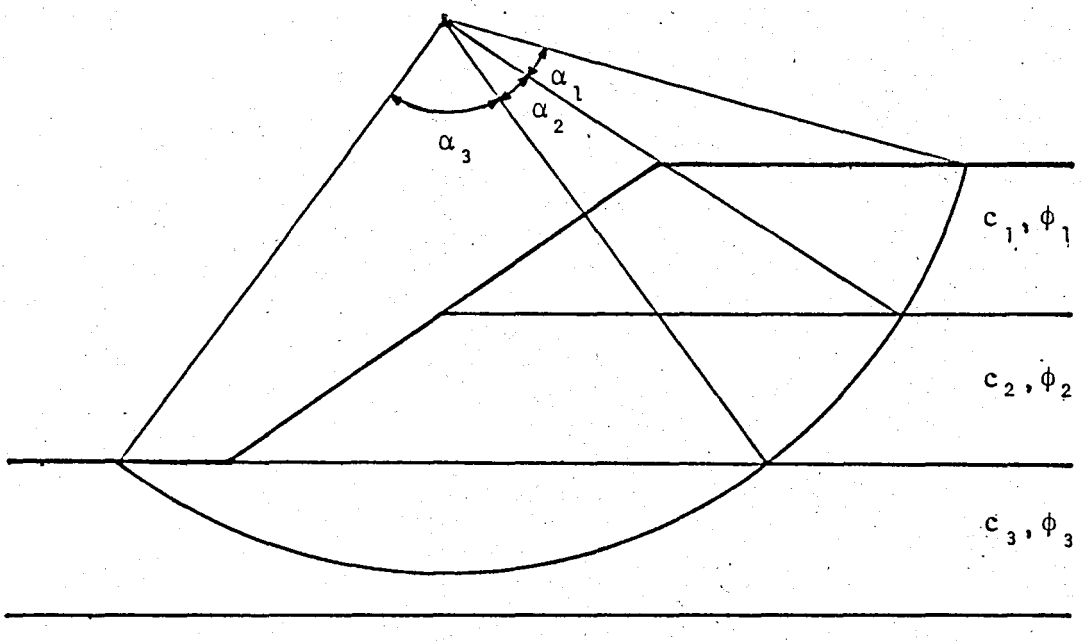

$$c_{ave} = \frac{c_1\alpha_1 + c_2\alpha_2 + c_3\alpha_3}{\alpha_1 + \alpha_2 + \alpha_3}$$

$$\tan\phi_{ave} = \frac{\alpha_1(\tan\phi_1) + \alpha_2(\tan\phi_2) + \alpha_3(\tan\phi_3)}{\alpha_1 + \alpha_2 + \alpha_3}$$

FIG.3.6 Figure Showing the Calculation of c_{ave} and ϕ_{ave}

If there is no surcharge, $\mu_q=1$; if there is no submergence, $\mu_\omega=1$; and if there are no tension cracks, $\mu_t=1$.

5. Using the chart at the top of Fig.3.3, determine the value of the stability number, N_o, which depends on the slope angle, β, and the value of d.

6. The factor of safety, F, can be obtained as follows

$$F = \frac{N_o c}{P_d} \qquad \ldots (3.5)$$

in which N_o=stability number

c =average shear strength (F/L^2)

7. If a slope contains more than one soil layer, it may be necessary to calculate the factor of safety for circles at more than one depth. The following criteria can be used to determine which possibilities should be examined:
   - If a soil layer is weaker than the layer above, the critical circle will be tangent to the base of the lower layer.
   - If a soil layer is stronger than the layer above, the critical circle may be tangent to the base of either the upper or the lower layer, and both possibilities should be examined.

3.3 CHARTS FOR SLOPES IN SOILS WITH STRENGTH LINEARLY INCREASING WITH DEPTH, AND ϕ=0

In this section the calculation of the stability number,N, for a variable shear strength case, by means of Hunter and Schuster (1968)

is shown. In general the shear strength of the soil for normally consolidated clays is not constant throughout of the layer and it is necessary to take into the account whether the shear strength of the soil is constant throughout of the layer or is increasing with depth in the stability analysis. The chart for slopes in soils with strength linearly increasing with depth,and ϕ=0, is shown in Fig.3.7.

Steps for use of chart:

1. Select the linear variation of strength with depth which best fits the measured strength data. Extrapolate this linear variation upward to determine H_o, the height at which the strength profile intersects zero, as shown in Fig.3.7.

2. Calculate $M=H_o/H$, where H=slope height.

3. Determine the dimensionless stability number, N, from the chart in Fig.3.7.

4. Determine the value of strength, c_b, at the elevation of the bottom of the slope

5. Calculate the factor of safety, F, using the formula

$$F = N \frac{c_b}{\gamma(H + H_o)} \qquad \ldots (3.6)$$

in which γ= total unit weight of soil for slopes above water,

γ= buoyant unit weight for submerged slopes, and

γ= weighted average unit weight for partly submerged slopes

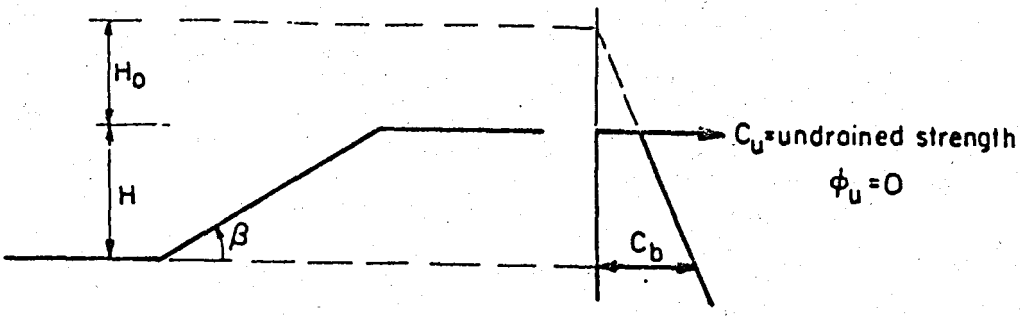

Steps:

① Extrapolate strength profile upward to determine value of H_0, where strength profile intersects zero

② Calculate $M = H_0/H$

③ Determine stability number N from chart below

④ Determine C_b = strength at bottom of slope

⑤ Calculate $F = N \frac{C_b}{\gamma(H+H_0)}$

Use $\gamma = \gamma_{buoyant}$ for submerged slope

Use $\gamma = \gamma_m$ for no water outside slope

Use average γ for partly submerged slope

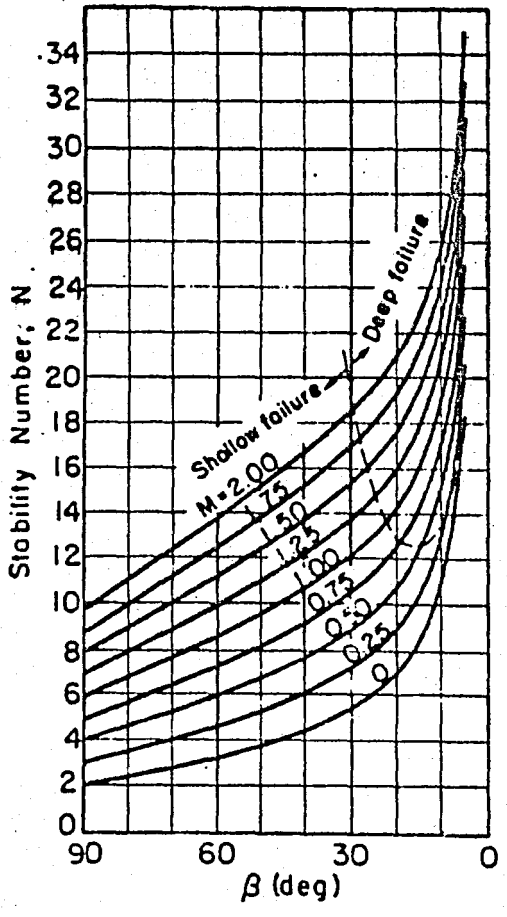

FIG.3.7 Slope Stability Charts for ϕ = 0, and Strength Increasing with Depth (after Hunter and Schuster, 1968)

3.4 CHARTS FOR SLOPES IN UNIFORM SOILS WITH $\phi>0$

For this type of soils Taylor's Charts which is given in section 3.2.1 and Janbu's Charts are also applicable only to the extremely simple conditions for which they were derived. However, many slopes that approximate the simple section and that are composed of more or less heterogeneous soils may be subjected to an approximate analysis by entering the charts with average values.

3.4.1 Taylor's Charts

The chart in Fig.3.1 developed by Taylor (1948) and discussed on section 3.2.1 is also applicable for uniform soils with $\phi>0$. For steeper slopes the failure arc goes through the toe of the slope as shown by key sketch A in Fig.3.1. In zone B the low point of the critical circle is not at the toe of the slope, and three cases that will be considered are shown in key sketch B in Fig.3.1. For small slope angles and for c-ϕ soils the critical circle may pass below the toe of the slope. For all ranges in which this case holds, stability numbers are given in the chart by long dashed curves. Stability numbers for the critical circles passing through the toe are given by solid lines in the chart.

3.4.2 Janbu's Charts

The stability chart for slopes in soils with $\phi>0$ is shown in Fig.3.8. Correction factors for surcharge loading at the top of the slope, submergence, seepage, and tension cracks are given in Figs.3.4 and 3.5.

Steps for use of charts:

1. Using judgment, estimate the location of the critical circle. For most conditions of simple slopes in uniform soils with $\phi>0$, the critical circle passes through the toe of the slope, and the stability numbers given in Fig.3.8 have been developed by analyzing toe circles.

   However, where the conditions are not uniform and there is a weak layer beneath the toe of the slope, a circle passing beneath the toe may be more critical than a toe circle. The chart shown in Fig.3.8 may be used to calculate the factor of safety for such cases provided the values of c and ϕ used represent the correct average values for the circle considered.

   If there is a weak layer above the toe of the slope, a circle passing above the toe of the slope may be more critical. Similarly, if there is water outside the toe of the slope, a circle passing above the water may be more critical. When these types of circles are analyzed, the value of H should be taken equal to the height from the base of the weak layer, or the water level, to the top of the slope.

2. Using this circle as a quide, estimate the average values of c and tan ϕ . This can be done by calculating the weighted average values of c and tan ϕ along the failure arc, using the number of degrees intersected along the arc by each soil layer as the weighting factor which is illustrated before.

3. Calculate P_d using the formula below.

$$P_d = \frac{\gamma H + q - \gamma_\omega H_\omega}{\mu_q \mu_\omega \mu_t} \quad \ldots (3.7)$$

in which γ=average unit weight of soil (F/L^3, force/length^3)

H=slope height (L)

q=surcharge (F/L^2)

γ_ω=unit weight of water (F/L^3)

H_ω=depth of water outside slope (L)

μ_q= surcharge correction factor (Fig.3.4, top)

μ_ω= submergence correction factor (Fig.3.4, bottom)

μ_t= tension crack correction factor (Fig.3.5)

If there is no surcharge, μ_q=1; if there is no submergence, μ_ω=1; and if there are no tension cracks, μ_t=1.

4. Calculate P_e using the formula

$$P_e = \frac{\gamma H + q - \gamma_\omega H'_\omega}{\mu_q \mu'_\omega} \quad \ldots (3.8)$$

in which H'_ω= height of water within slope (L)

μ'_ω= seepage correction factor (Fig.3.4, bottom)

and the other factors are as defined previosly.

If the surcharge is applied so quickly that there is not sufficient time for the soils to consolidate under the surcharge, take q=0 and μ_q=1 in the formula for P_e. If there is no surcharge, μ_q=1, and if there is no seepage, μ'_ω = 1.

5. Calculate the dimensionless parameter $\lambda_{c\phi}$ using the formula

$$\lambda_{c\phi} = \frac{P_e \tan\phi}{c} \qquad \ldots (3.9)$$

in which $\tan\phi$= average value of $\tan\phi$

c= average value of c (F/L^2)

For $c=0$, $\lambda_{c\phi}$ is infinite. In this case, skip step 6.

6. Using the chart at the left in Fig.3.8 , determine the value of the stability number, N_{cf}, which depends on the slope angle, β, and the value of $\lambda_{c\phi}$.

7. Calculate the factor of safety, F, using the formula

$$F = N_{cf} \frac{c}{P_d} \qquad (\text{for } c>0) \qquad \ldots (3.10)$$

For $c=0$, $\lambda_{c\phi}$ is infinite, and the factor of safety is calculated using the formula.

$$F = \frac{P_e}{P_d} b\tan\phi \qquad (\text{for } c=0) \qquad \ldots (3.11)$$

in which b=slope ratio=$\cot\beta$ and the other factors are as defined previously.

8. Determine the actual location of the critical circle, using the chart on the right side of Fig.3.8. The center of the circle is located at X_o, Y_o, and the circle passes through the toe of the slope. One exception is the case where a weak layer beneath the toe makes a circle passing beneath the toe more critical, as explained in connection with step 1. In this case the critical circle passes tangent to the base of the weak layer. A second exception is for

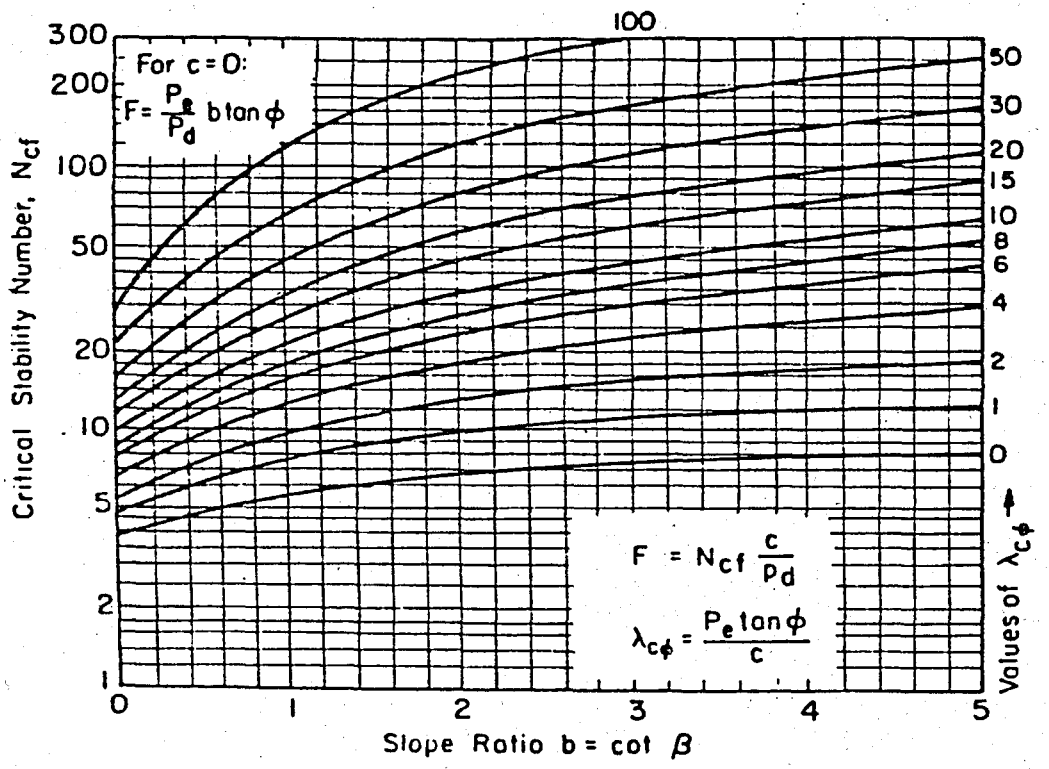

(In formula for P_e take q = 0, μ_q = 1 for unconsolidated condition)

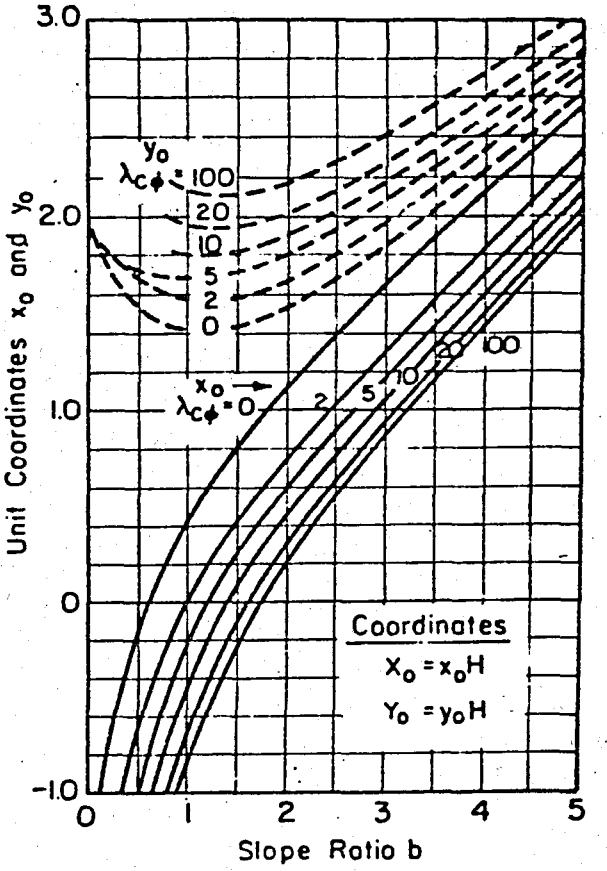

CENTER COORDINATES FOR CRITICAL CIRCLE

FIG.3.8 Slope Stability Charts for $\phi > 0$ Soils (after Janbu,1968)

$\lambda_{c\phi} = \infty$, in which case shallow sliding is the critical failure mechanism.

If the critical circle is much different from the one assumed in step 1 for the purpose of determining the average strength, steps 2 through 8 should be repeated.

9. If a slope contains more than one soil layer, it may be necessary to calculate the factor of safety for circles at more than one depth. The following criteria can be used to determine which possibilities should be examined.
   - If a soil layer is weaker than the layer above, the critical circle will extend into the lower layer, and either a toe circle or a deep circle within this layer will be critical.
   - If a soil layer is stronger than the layer above, the critical circle may or may not extend into the lower layer, depending on the relative strengths of the two layers. Both possibilities should be examined.

3.4.3 Log Spiral Slope Stability Charts

The Log Spiral Analysis procedure provides a convenient means of calculating values of the stability number(N_{cf}) for homogeneous slopes, because for all values of ϕ the procedure fully satisfies all conditions of equilibrium independently of any assumptions regarding the normal stress distribution along the shear surface. The stability numbers given by Wright (1969) for the critical log spiral shear surfaces passing through the toe of the slope are shown by the chart in Fig.3.9.

For relatively flat slopes having low values of the dimensionless parameter, $\lambda_{c\phi} = \frac{\gamma H \tan \phi}{c}$ which is defined by Janbu in the previous section a more critical spiral may be found which intersects the surface somewhat beyond the toe of the slope. The stability numbers for these most critical surfaces are tabulated in Table 3.1 together with the values calculated for the critical toe spirals as given by Wright (1969). From this table it may be noted that even for slopes as flat as 5:1 and for values of $\lambda_{c\phi}$ as low as 1 the difference in the stability numbers for these two surfaces is less than 1-1/2 %. For higher values of $\lambda_{c\phi}$ and steeper slopes the most critical spiral passes through the toe and the difference in stability numbers becomes zero.

If $\lambda_{c\phi}$ is zero it can be theoretically shown that the critical shear surface for slopes flatter than 53^0(≈0.75:1) will extend infinitely deep and have a stability number of 5.53 as indicated by the dashed line in Fig.3.9. However, the critical shear surface usually will be prevented from extending infinitely deep by the presence of some harder layer, and thus the appropriate stability number will lie somewhere between the values for an infinitely deep surface and one passing through the toe.

Although it was assumed that all critical toe spirals represented by the chart in Fig.3.9. could extend as deeply as necessary, in many instances they will be prevented from doing so by the presence of a firmer soil layer at relatively shallow depth. If the spirals cannot extend below the toe elevation, as representative of a slope on a rigid base, the stability numbers may be considerably higher. This is analyzed by Wright and illustrated in Fig.3.10. It is shown by Wright that for relatively flat slopes having low values of $\lambda_{c\phi}$ the critical surfaces intersect the slope above the toe. However, for steeper slope inclinations and higher values of $\lambda_{c\phi}$, the critical spirals pass through the

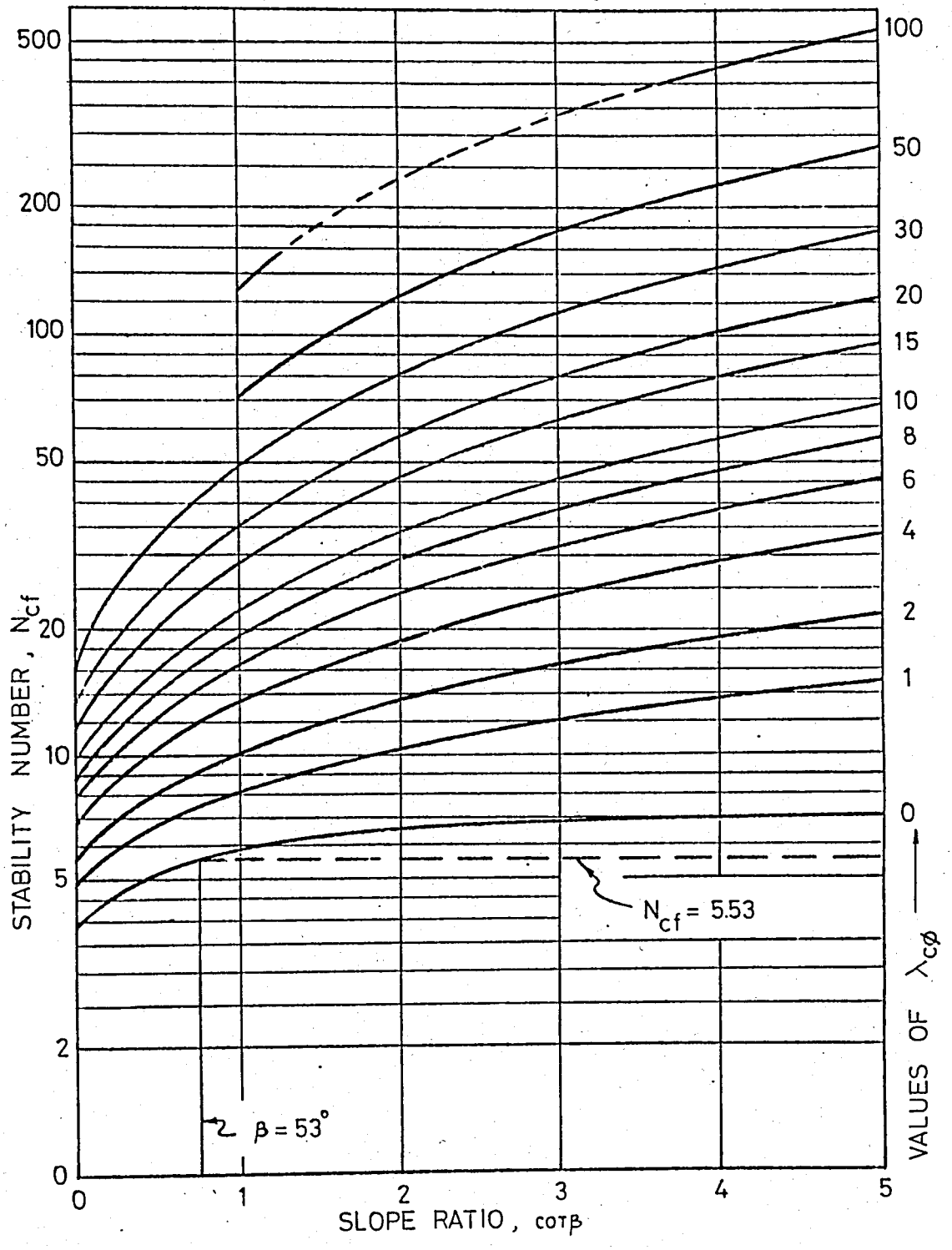

FIG.3.9 Log Spiral Stability Chart for Toe Circles. Total Stress Analysis (after Wright, 1969)

TABLE 3.1 Stability Numbers(N_{cf}) for Most Critical and Toe Log Spirals

Slope : / $\lambda_{c\phi}$	Vertical		1:1		2:1		3:1		4:1		5:1	
	Toe	Crit.	Toe	Crit.	Toe	Crit.	Toe	Crit.	Toe	Crit.	Toe	Crit.
1	4.74	4.74	8.1	8.1	10.3	10.2	12.0	11.9	13.6	13.4	15.0	14.8
2	5.50	5.50	10.0	10.0	13.4	13.4	16.3	16.3	19.1	18.9	21.7	21.5
4	6.77	6.77	13.3	13.3	18.9	19.0	24.1	24.1	29.1	29.1	33.9	33.9
6	7.83	7.83	16.3	16.3	24.2	24.2	31.5	31.5	38.6	38.6	45.6	45.5
8	8.76	8.76	19.2	19.2	29.1	29.2	38.6	38.7	47.9	47.9	56.9	56.9
10	9.61	9.61	22.0	22.0	34.0	34.1	45.6	45.6	56.9	56.9	68.0	68.0
15	11.45	11.45	28.6	28.6	45.8	45.8	62.6	62.6	79.1	79.1	95.4	95.4
20	13.03	13.03	34.9	34.9	57.2	57.2	79.2	79.2	101	101	122.3	122
30	15.72	15.72	47.0	47.0	79.5	79.6	111.8	111.9	144	144	175.3	175
50	-	-	70.2	70.2	123.0	123.2	176	176	228	228	280	280
100	-	-	125.6	125.6	-	-	-	-	-	435	537	-

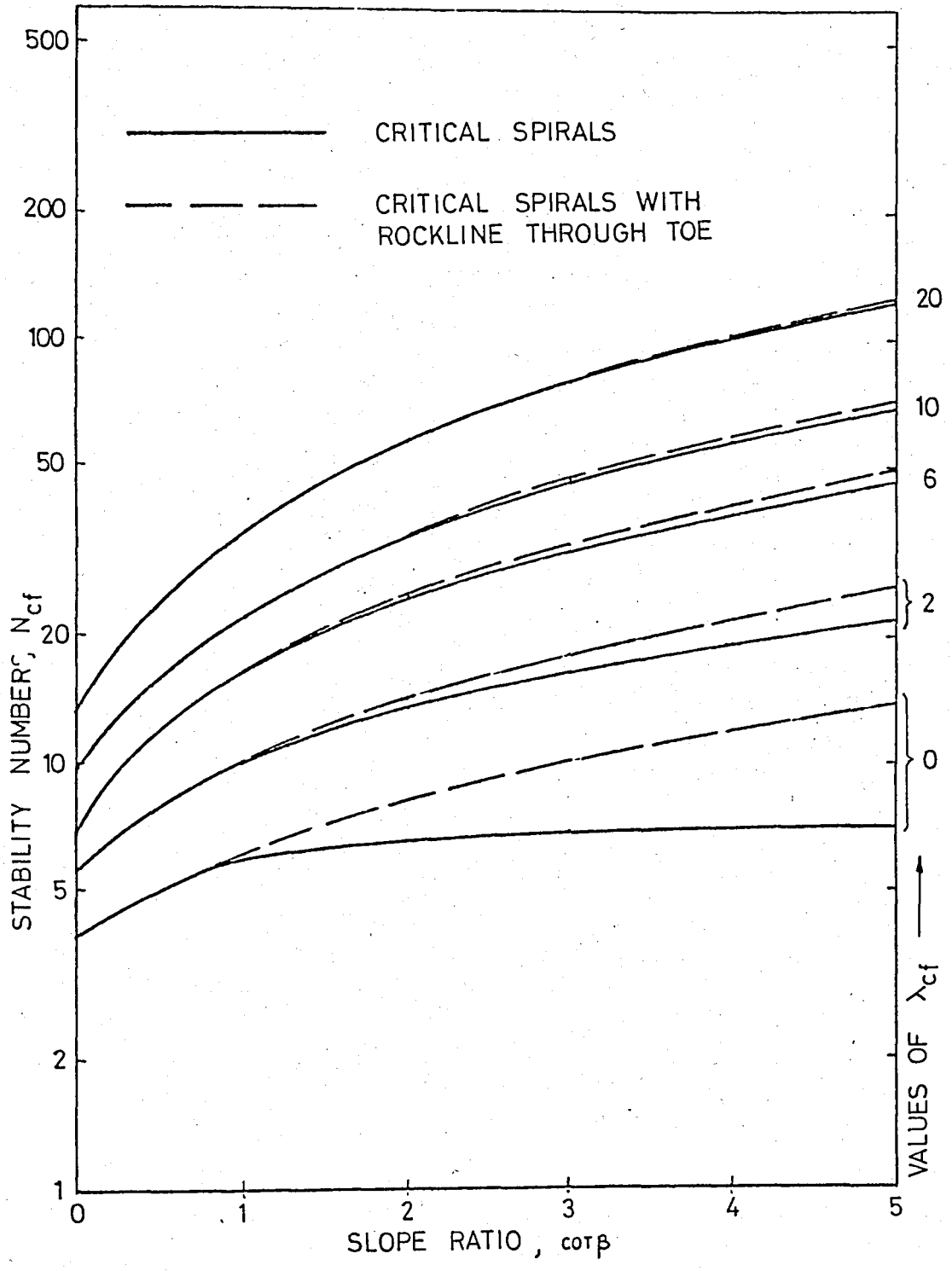

FIG.3.10 Comparison of Log Spiral Stability Numbers for Toe and Base Spirals (after Wright, 1969)

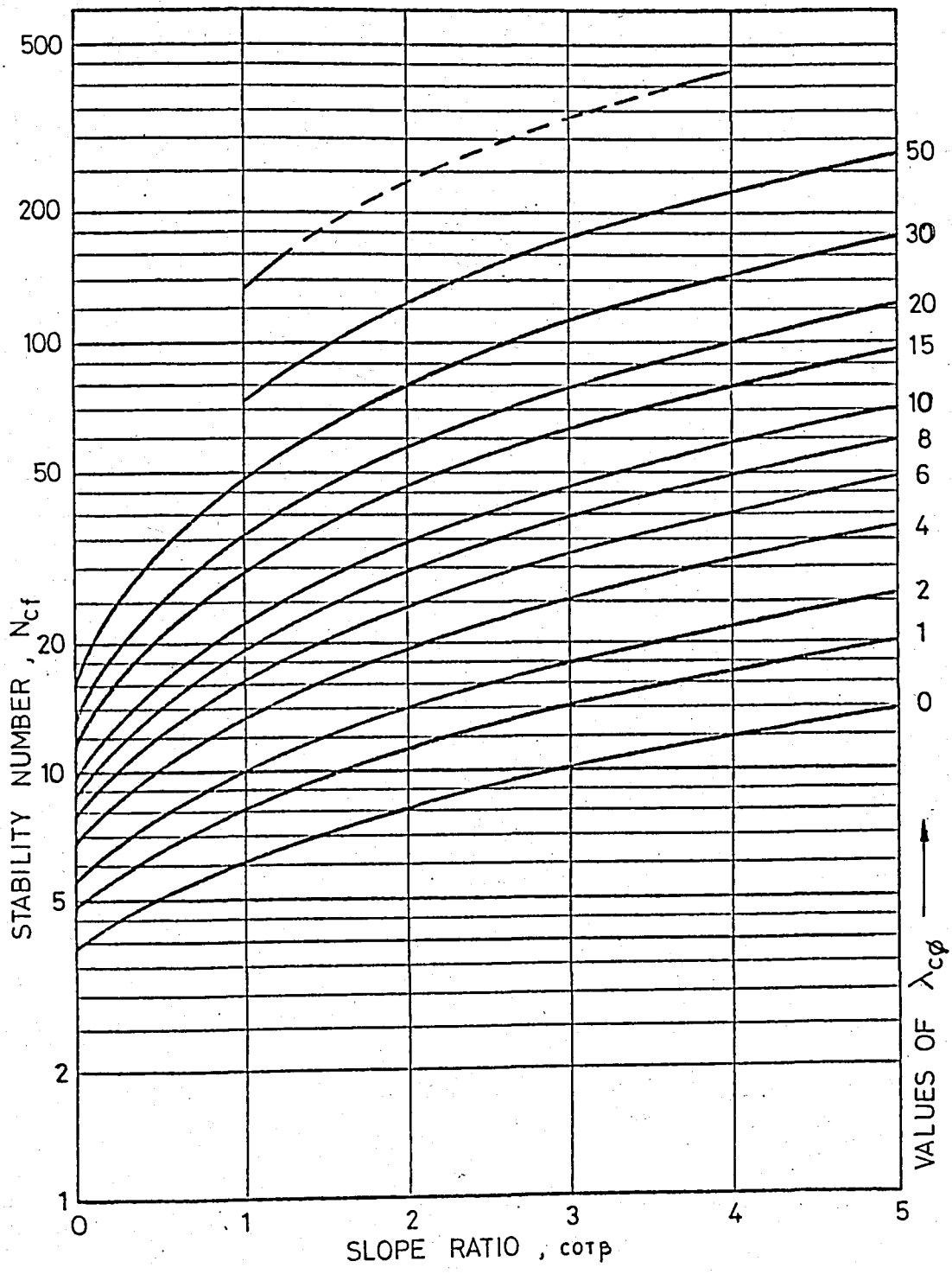

FIG.3.11 Log Spiral Stability Chart for Slopes on a Rigid Base-Total Stress Analysis (after Wright, 1969).

toe of the slope, and thus, stability numbers for slopes on a rigid base, which are given by the chart in Fig.3.11, correspond exactly to the stability numbers given in Fig.3.9 for critical toe circles.

Steps for use of the charts:

1. The slope ratio, cot β, is calculated

2. The dimensionless parameter $\lambda_{c\phi}$ is obtained from the following equation.

$$\lambda_{c\phi} = \frac{\gamma H \tan\phi}{c} \qquad \ldots (3.12)$$

where

γ= unit weight of the fill

H=slope height

ϕ=internal friction angle

c=cohesion intercept

3. Using the chart in Fig.3.9, the value of the stability number is determined for the critical log spiral shear surfaces passing through the toe of the slope.

4. The factor of safety is calculated, using the formula

$$F = N_{cf} \frac{c}{\gamma H} \qquad \ldots (3.13)$$

3.5 SLOPE STABILITY CHARTS FOR INFINITE SLOPES

Two types of conditions can be analyzed accurately using the charts shown in Fig.3.12, which are based on infinite slope analyses and presented by Duncan and Buchignani (1975). These conditions are:

1. Slopes in cohesionless materials, where the critical

failure mechanism is shallow sliding or surface ravelling.

2. Slopes in residual soils, where a relatively thin layer of soil overlies firmer soil or rock, and the critical failure mechanism is sliding along a plane parallel to the slope, at the top of the firm layer.

Steps for use of the charts for effective stress analyses:

1. Determine the pore pressure ratio r_u, which is defined by the formula

$$r_u = \frac{u}{\gamma H} \qquad \ldots (3.14)$$

in which u= pore-pressure (F/L^2 , force/length^2)

γ= total unit weight of soil (F/L^3)

H= depth corresponding to pore pressure, u (L)

For an existing slope, the pore pressure can be determined from field measurements, using piezometers installed at the depth of sliding.

For seepage parallel to the slope, which is a frequently encountered condition, the value of r_u can be calculeted using the following formula:

$$r_u = \frac{X}{T} \frac{\gamma_\omega}{\gamma} \cos^2\beta \qquad \ldots (3.15)$$

in which X = distance from the depth of sliding to the surface of seepage, measured normal to the surface of the slope(L)

T = distance from the depth of sliding to the surface of the slope, measured normal to the surface of the slope (L)

γ_ω= unit weight of water (F/L^3)

γ = total unit weight of soil (F/L^3)

β = slope angle

For seepage emerging from the slope, which is more critical than seepage parallel to the slope, the value of r_u can be calculated using the following formula

$$r_u = \frac{\gamma_\omega}{\gamma} \frac{1}{1 + \tan\beta \tan\theta} \quad \ldots (3.16)$$

in which θ= angle of seepage measured from the horizontal direction, and the other factors are as defined previously.

2. Determine the values of the dimensionless parameters A and B from the charts at the bottom of Fig.3.12.

3. Calculate the factor of safety, F, using the formula

$$F = A \frac{\tan\phi'}{\tan\beta} + B \frac{c'}{\gamma H} \quad \ldots (3.17)$$

in which ϕ'=angle of internal friction in terms of effective stress

c'=cohesion intercept in terms of effective (F/L^2)

β =slope angle

H =depth of sliding mass measured vertically (L)

and the other factors are as defined previously.

Steps for use of charts for total stress analyses:

1. Determine the value of B from the chart in the lower right corner of Fig.3.12.

2. Calculate the factor of safety, F, using the formula

$$F = \frac{\tan\phi}{\tan\beta} + B \frac{c}{\gamma H} \quad \ldots (3.18)$$

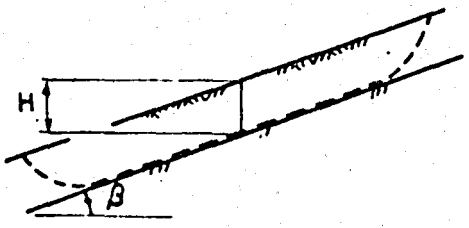

γ = total unit weight of soil

γ_w = unit weight of water

c' = cohesion intercept, ϕ = friction angle } Effective Stress

r_u = pore pressure ratio = $\frac{u}{\gamma H}$

u = pore pressure at depth H

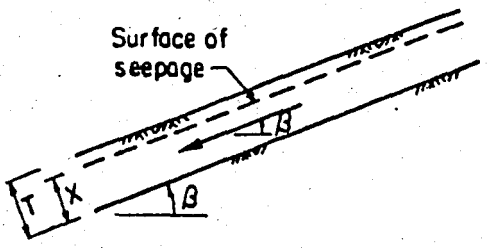

Seepage parallel to slope

$r_u = \frac{X}{T}\frac{\gamma_w}{\gamma}\cos^2\beta$

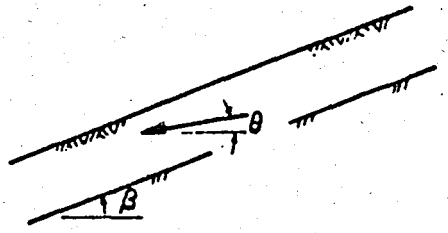

Seepage emerging from slope

$r_u = \frac{\gamma_w}{\gamma}\frac{1}{1+\tan\beta\tan\theta}$

Steps:

① Determine r_u from measured pore pressures or formulas at right

② Determine A and B from charts below

③ Calculate $F = A\frac{\tan\phi'}{\tan\beta} + B\frac{c'}{\gamma H}$

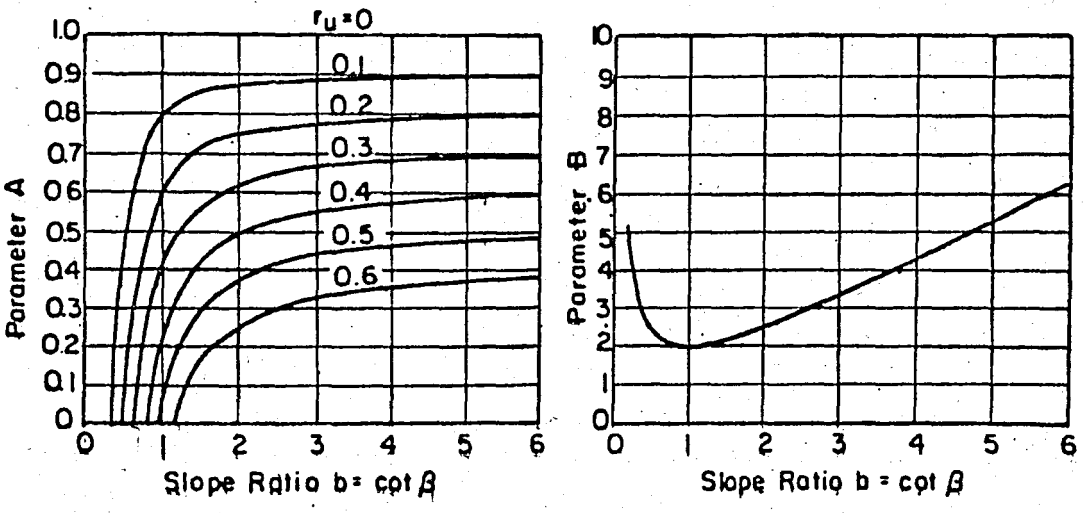

FIG.3.12 Stability Charts for Infinite Slopes

(after Duncan and Buchignani, 1975)

in which ϕ= angle of internal friction in terms of total stress

c= cohesion intercept in terms of total stress (F/L^2)

and the other factorsare as defined previously.

3.6 STABILITY CHARTS FOR ANALYSES WITH PORE PRESSURES

In this section Bishop's and Morgenstern's Procedure (1960), Janbu's Approximate Procedure(1967) and Wright's Chart (1969) are discussed.

3.6.1 Bishop and Morgenstern's Procedure

Bishop and Morgenstern (1960) have shown that the presentation of stability charts for analyses with pore pressures is considerably simplified by the observed linear relationship between the factor of safety and the value of the pore pressure coefficient, r_u. This linearity apparently exists in all procedures of slope analysis including the Modified Bishop solution. As illustrated in Fig.3.13, by Wright (1969), which shows the relationships between stability numbers and the value of r_u for the Ordinary Method of Slices, Lowe and Karafiath, Spencer, and Modified Bishop procedures, the only exception to linearity occurs for high values of r_u and steep slopes analyzed by the Ordinary Method of Slices procedure. The deviation from a straight line is the result of setting negative normal stresses equal to zero, and it may be noted that such a modification tends to partially offset the underestimate in stability which occurs by using the Ordinary Method of Slices.

The stability charts presented by Bishop and Morgenstern require the determination of the two dimensionless parameters, m and n are termed the stability coefficients, from which the factor of

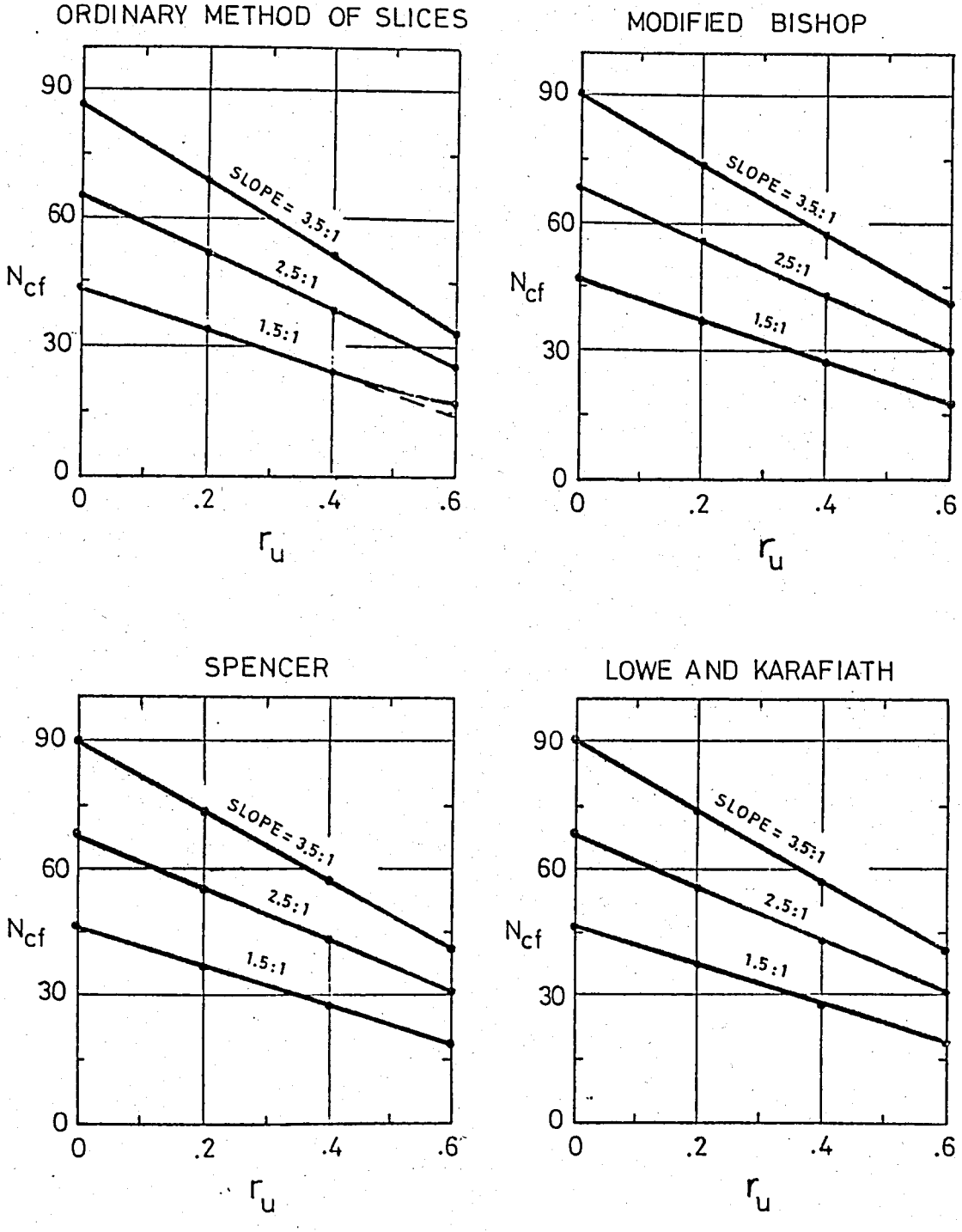

FIG.3.13 Relationships Between the Stability Numbers (N_{cf}) and r_u for Several Procedures of Analysis $-\lambda_{c\phi} = 20$ (after Wright, 1969)

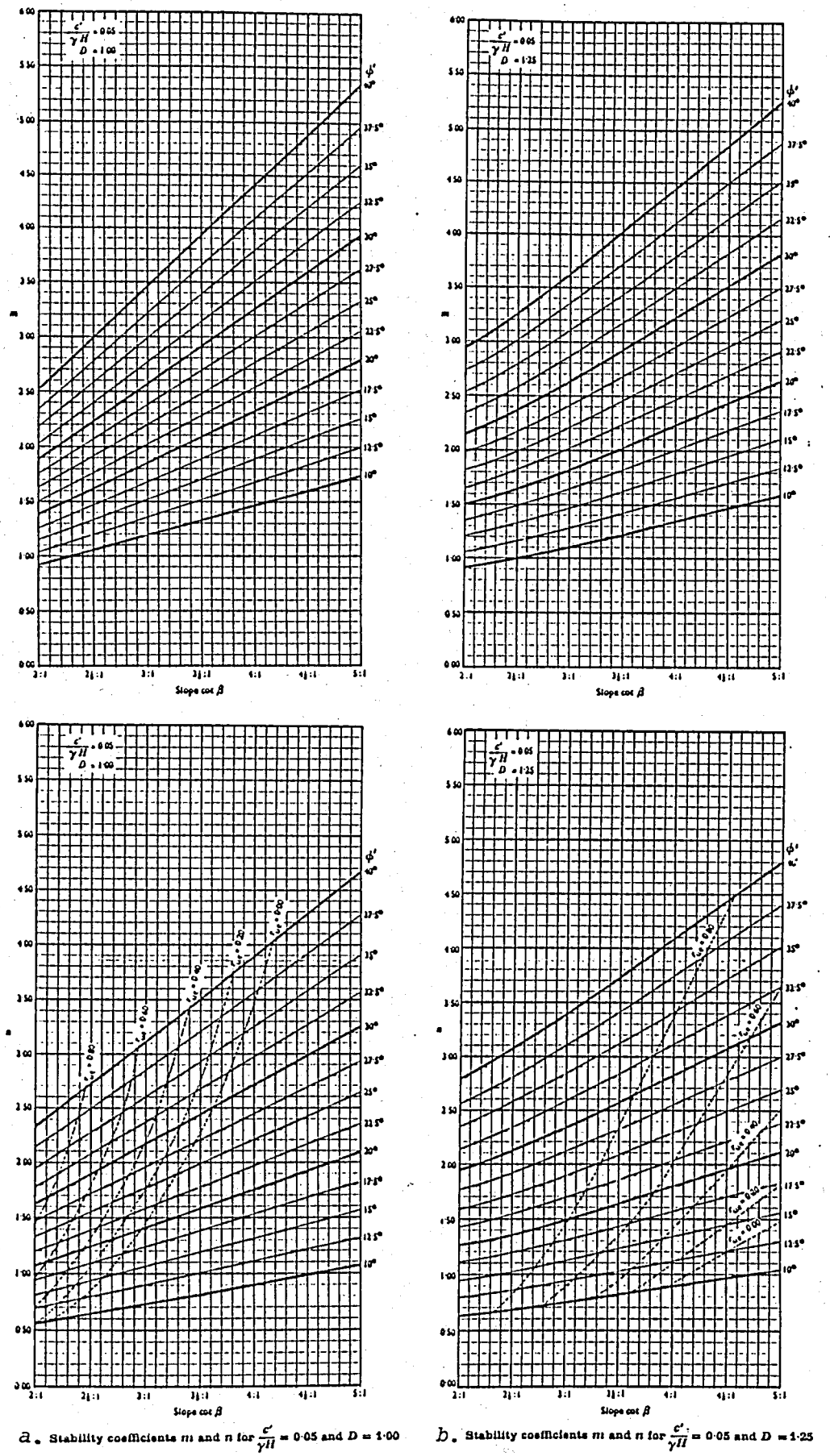

a. Stability coefficients m and n for $\frac{c'}{\gamma H} = 0.05$ and $D = 1.00$

b. Stability coefficients m and n for $\frac{c'}{\gamma H} = 0.05$ and $D = 1.25$

FIG.3.14 Stability Charts for Analysis with Pore Pressure (after Bishop and Morgenstern, 1960)

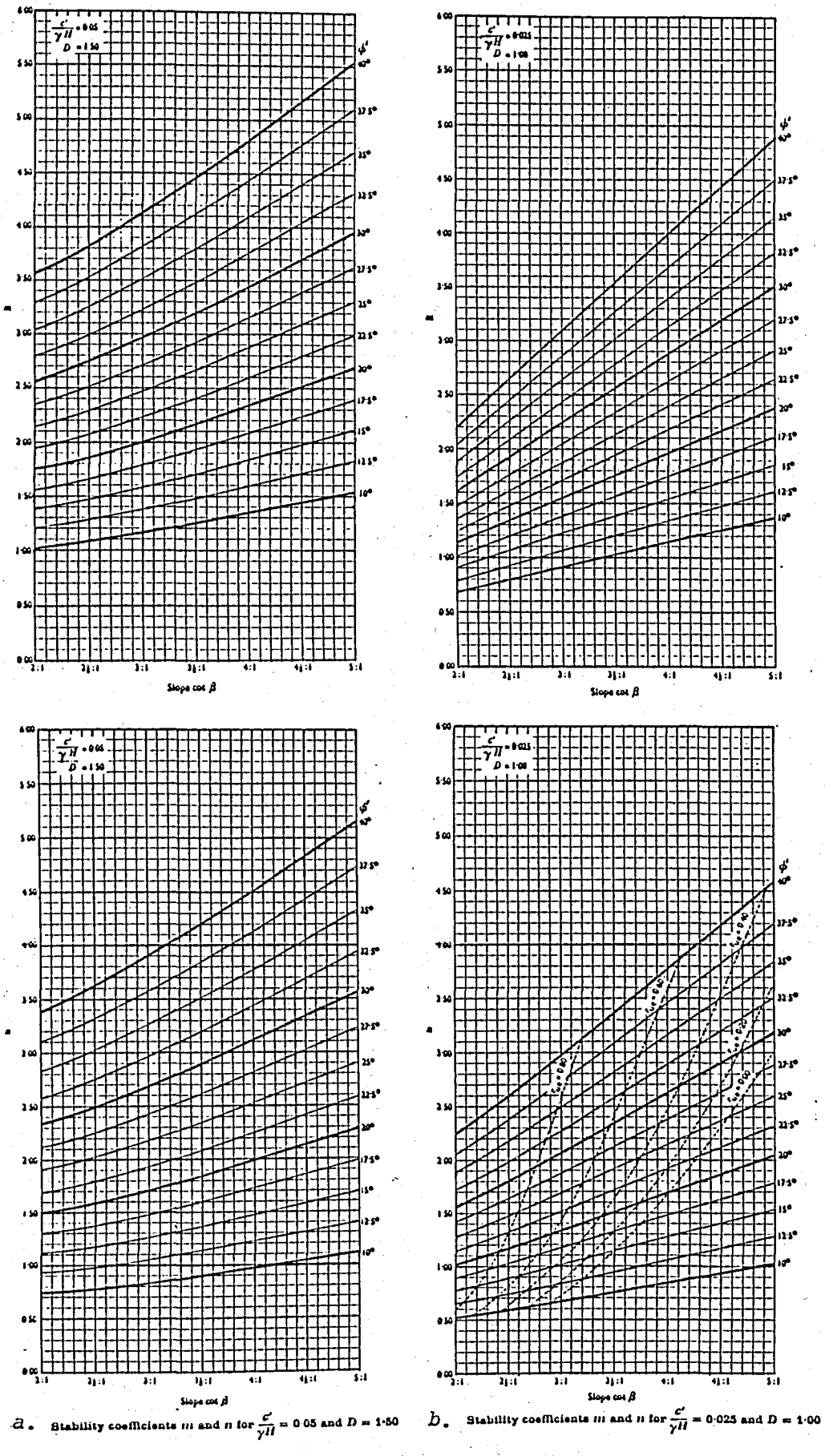

a. Stability coefficients m and n for $\frac{c'}{\gamma H} = 0.05$ and $D = 1.50$

b. Stability coefficients m and n for $\frac{c'}{\gamma H} = 0.025$ and $D = 1.00$

FIG.3.15 Stability Charts for Analysis with Pore Pressure (after Bishop and Morgenstern, 1960)

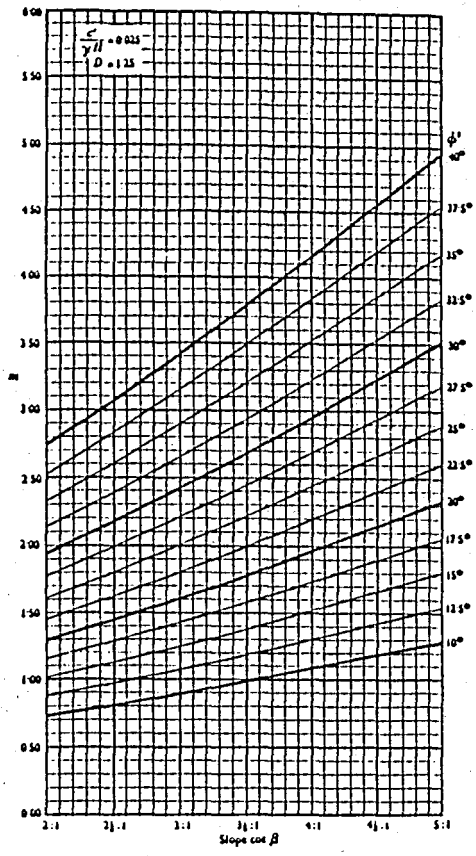

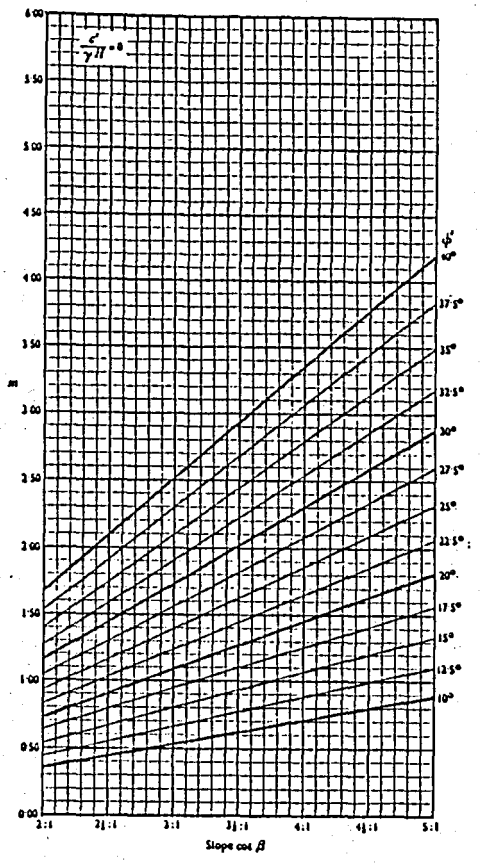

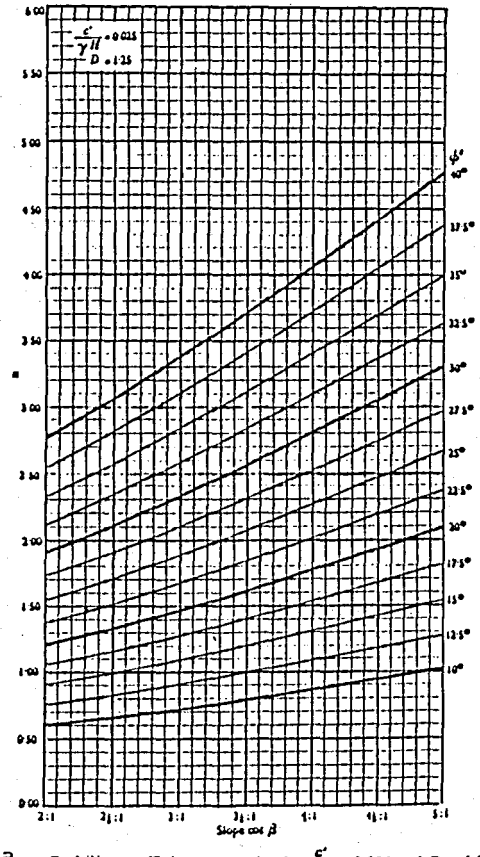

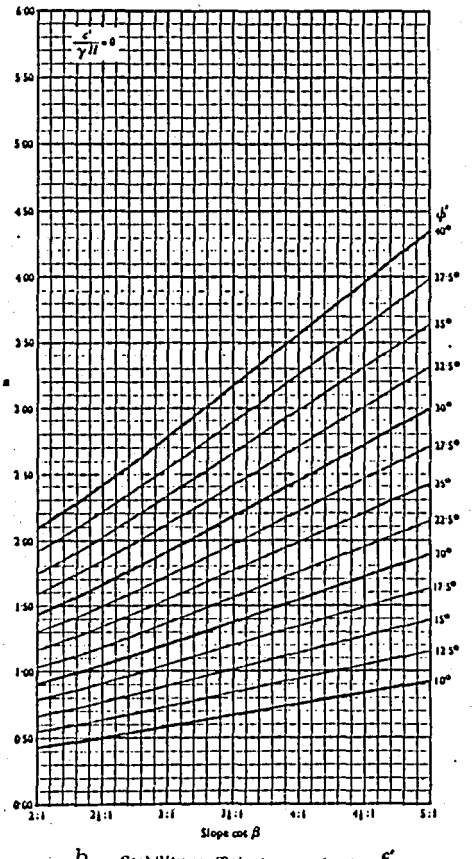

a. Stability coefficients m and n for $\frac{c'}{\gamma H} = 0.025$ and $D = 1.25$

b. Stability coefficients m and n for $\frac{c'}{\gamma H} = 0$

FIG.3.16 Stability Charts for Analysis with Pore Pressure (after Bishop and Morgenstern, 1960)

safety is calculated using the relationship,

$$F = m - nr_u \qquad \ldots (3.19)$$

The values of the stability coefficients have been plotted against β, the cotangent of the slope angle, for ϕ' varying between 10^0 and 40^0 in Fig.3.14 to 3.16 with values of $c'/\gamma H$ and D specified for each figure. The bold lines show values of m and n at intervals of 10^0, whereas the lighter lines indicate the intermediate values that have been obtained by interpolation. The broken lines are those of equal r_u (detoned by r_{ue})

If one wishes to determine the mininum factor of safety for sections not located directly on a hard stratum with specified values of $c'/\gamma H$, β, ϕ', and r_u, one enters the appropriate graph for the given $c'/\gamma H$ value and for D=1.00, initially (either Figs.3.14a or 3.15b). The values of β and ϕ' then define a point on the curves of n with which is associated a value of r_{ue} given by the broken lines. If that value is less than the design value, the next depth factor, D=1.25 , will give a more critical value of factor of safety. If one is operating with $c'/\gamma H$=0.05 a set of r_{ue} curves is available to determine in a similar manner whether the level given by D=1.50 is even more critical.

3.6.2 Janbu's Approximate Procedure

The stability charts shown in Figs 3.8, 3.9 and 3.11 were obtained for total stress analyses. (r_u=0); however, Janbu (1967) has suggested an approximate procedure by which these charts may be used for analyses with pore pressures. By Janbu's procedure a modified parameter, $\lambda'_{c\phi}$, is calculated from the relationship

$$\lambda'_{c\phi} = \lambda_{c\phi}(1-r_u) \qquad \ldots (3.20)$$

The value of $\lambda'_{c\phi}$ is then used to obtain the stability number from a chart for zero pore pressure, such as that shown in Fig.3.8. In determining the stability number from this chart, the value of $\lambda'_{c\phi}$ is used as if it were equivalent to $\lambda_{c\phi}$. Although Janbu (1967) has shown that for many slopes this procedure is acceptably accurate, a significiant overestimate in the factor of safety may result from the use of this approach for some cases.

To investigate the magnitude of the overestimate in the factor of safety by Janbu's approach, stability numbers were calculated by Wright (1969) for various values of $\lambda'_{c\phi}$ corresponding to zero pore pressure and to a pore pressure coefficient (r_u) equal to 0.6 The results are shown in Fig.3.17 for Lowe and Karafiath's analysis procedure. It may be noted from this figure that the curves representing the stability numbers corresponding to a value of r_u equal to 0.6 in many cases lie considerably below the curves for no pore pressures. For example, if an analysis was made, by Janbu's approach for values of $\lambda'_{c\phi}$ equal to 20 and r_u equal to 0.6, the stability number would be represented by the solid line in the upper part of Fig.3.17, corresponding to zero pore pressure stability numbers. However, for all but very flat slopes, the correct stability number, indicated by the dashed line in this figure, would be considerably lower.

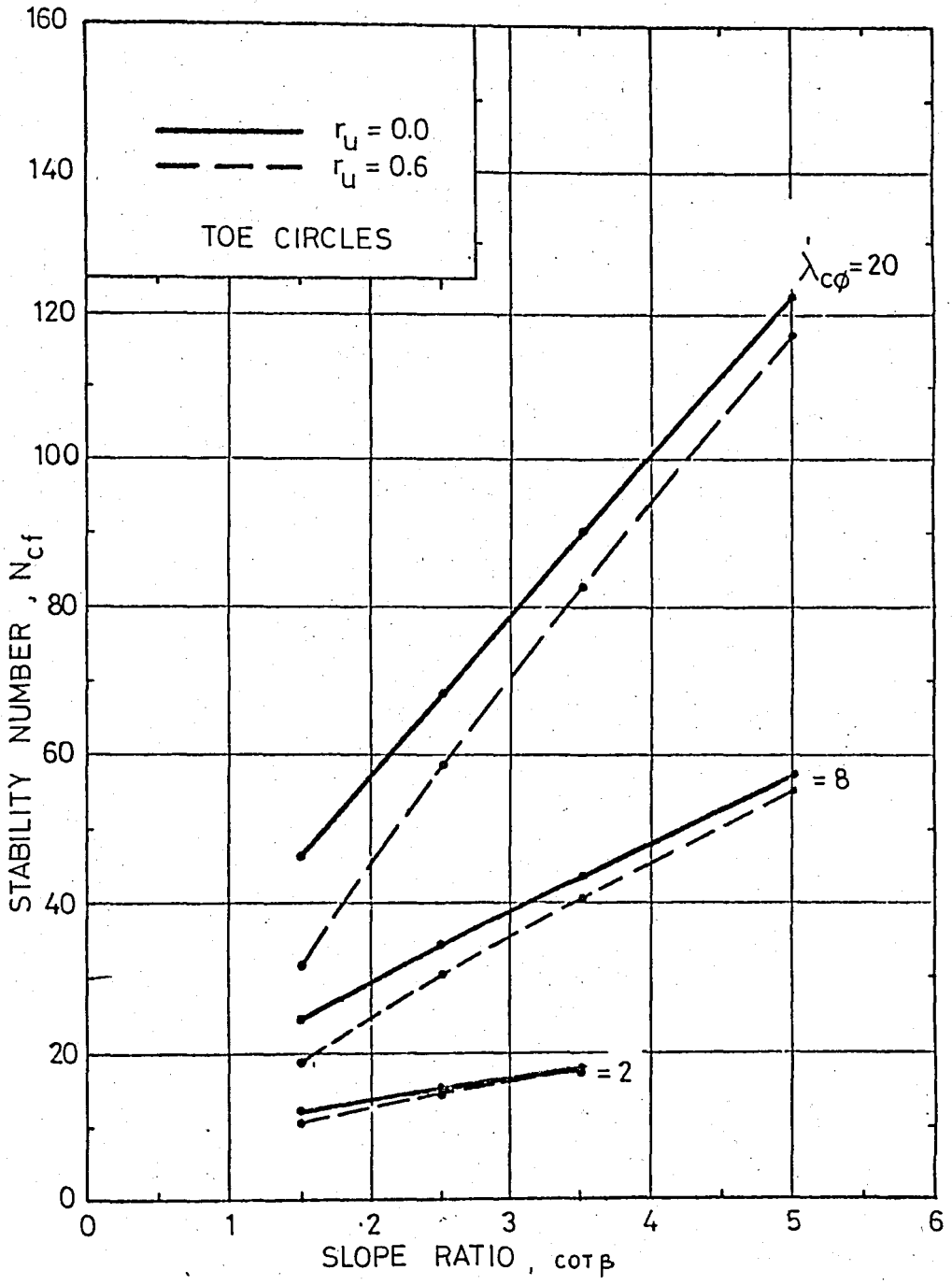

FIG.3.17 Stability Numbers for r_u = 0.0 and 0.6 by Lowe and Karafiath's Procedure (after Wright,1969).

3.6.3 Wright's Chart

An additional simplification to the stability charts presented by Bishop and Morgenstern may be achieved by making use of the linear relationship between the factor of safety, and r_u using Lowe and Karafiath's (1960) procedure. Such a simplified chart developed by Wright (1969) is illustrated in Fig.3.18.

Steps for use of the chart:

1. First, for a given slope ratio and $\lambda_{c\phi}$ value the stability numbers corresponding to values of r_u equal to zero and 1.0 are determined from the left and right sections of the chart respectively as shown by the dashed lines in Fig.3.18

2. Next, a straight line is drawn on the center portion of the chart connecting the values of the stability numbers corresponding to r_u equal to 0 and 1.0.

3. The value of N_{cf} corresponding to the desired r_u value may then be found as indicated by the arrows on the center portion of the chart.

The calculation of the factor of safety from such a chart may be illustrated by the following example for a slope of 2.5:1, a value of $\lambda_{c\phi}$ equal to 20, and a value of r_u equal to 0.4. For this example the stability number is equal to 43.

The preparation of stability charts such as shown in Fig.3.18 provides a convenient means of graphically determining the stability number for analyses with pore pressures.

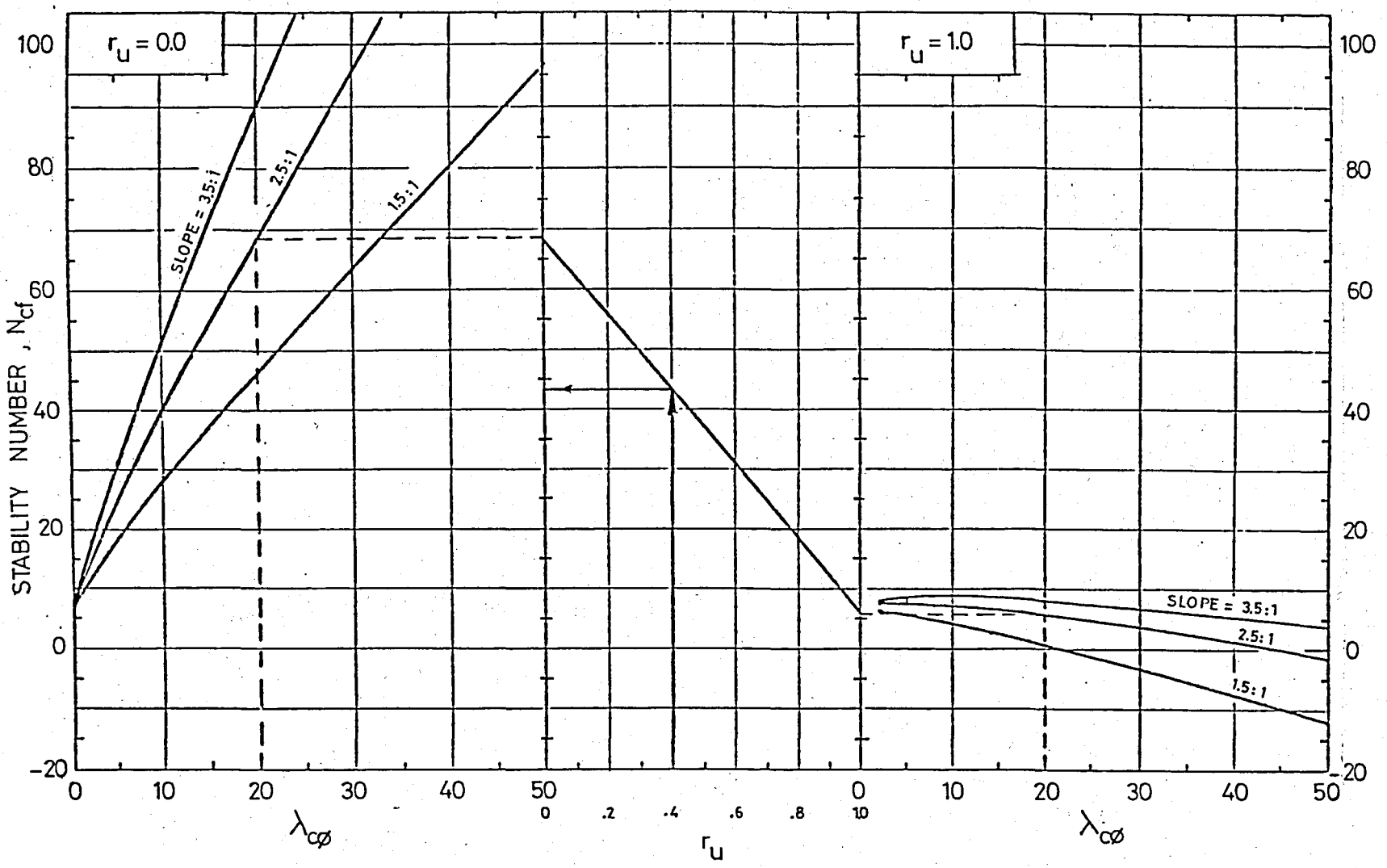

FIG.3.18 Stability Chart for Effective Stress Analyses-Lowe and Karafiath's Procedure (after Wright, 1969)

3.7 SUMMARY

Using slope stability charts, the factor of safety for a slope can be calculated within on accuracy of 15% in most cases. Thus, when the available data on site conditions and soil strengths are not extensive, calculations using slope stability charts provide sufficient accuracy for design. Slope stability charts are also very useful for preliminary design calculations, to compare alternatives which can be examined more thoroughly subsequently using detailed analysis procedures. Chart solutions also provide a rapid means of checking the results of detailed analyses.

A further use for slope stability charts is to back-calculate strength values for failed slopes to aid in planning remedial measures. This can be done by assuming a factor of safety of unity for the conditions at failure and solving for the unknown shear strength. Since soil strength usually involves both cohesion and friction, there is no unique value of cohesion (c) and angle of internal friction (ϕ)which will give a factor of safety equal to unity; therefore, several pairs of values should be calculated and judgment used to select the most reasonable values. If the material in the slide zone is clay and the slide occurred under undrained conditions, a unique solution for shear strength can be obtained by assuming ϕ=0 and back calculating a value of cohesion.

CHAPTER 4

MECHANICS OF STABILITY ANALYSIS OF FILLS ON SOFT CLAY FOUNDATIONS

4.1 INTRODUCTION

Many different methods of slope stability analysis have been developed based on the mechanics of limiting equilibrium. In most of these methods, the soil mass is divided into a number of vertical slices. To be in complete equilibrium, the forces acting on each slice must satisfy three conditions of equilibrium, namely:

(1) moment equilibrium

(2) horizontal force equilibrium

(3) vertical force equilibrium

In this type of analysis the factor of safety with regard to the slope stability is estimated by examining the conditions of equilibrium when incipient failure is postulated along a predefined failure plane, and then comparing the strength necessary to maintain equilibrium with the available strength of the soil. All limit equilibrium problems are statically indeterminate and, since the stress-strain relationship along the assumed failure surface is not known, it is necessary to make enough assumptions so that a solution using only the equations of equilibrium is possible. The number and type of assumptions that are made leads to the major difference in the various limit equilibrium methods

of analysis.

In this chapter the procedures of slices which are Ordinary Method of slices, Bishop's Procedure, Bishop's Modified procedure, Spencer's procedure, Morgenstern and Price's procedure, Wedge procedure, Janbu's Generalized Procedure of Slices, Lowe and Karafiath's procedure are discussed.

4.2 NUMERICAL FORMULATION OF SLICE EQUILIBRIUM

A number of numerical procedures of stability analysis, which are very similar to the graphical techniques, have been developed. Because of their increased simplicity and adaptability to computer solution, these numerical procedures have gained a wider acceptance than the graphical techniques. For the purpose of examining these various numerical solutions it is convenient to consider the three equations of equilibrium for an individual slice such as that shown in Fig.4.1. These equations may be expressed as:

a) Vertical Force Equilibrium :

$$-W + (X_{n+1} - X_n) + S\sin\alpha + N\cos\alpha = 0 \qquad \ldots (4.1)$$

b) Horizontal Force Equilibrium :

$$(E_{n+1} - E_n) + S\cos\alpha - N\sin\alpha = 0 \qquad \ldots (4.2)$$

and c) Moment Equilibrium about Point M :

$$X_n \Delta x + (X_{n+1} - X_n) \frac{\Delta x}{2} + E_n \Delta y_t - (E_{n+1} - E_n)(h_t + \Delta y_t - \frac{\Delta y}{2}) + (N\Delta g) = 0 \qquad \ldots (4.3)$$

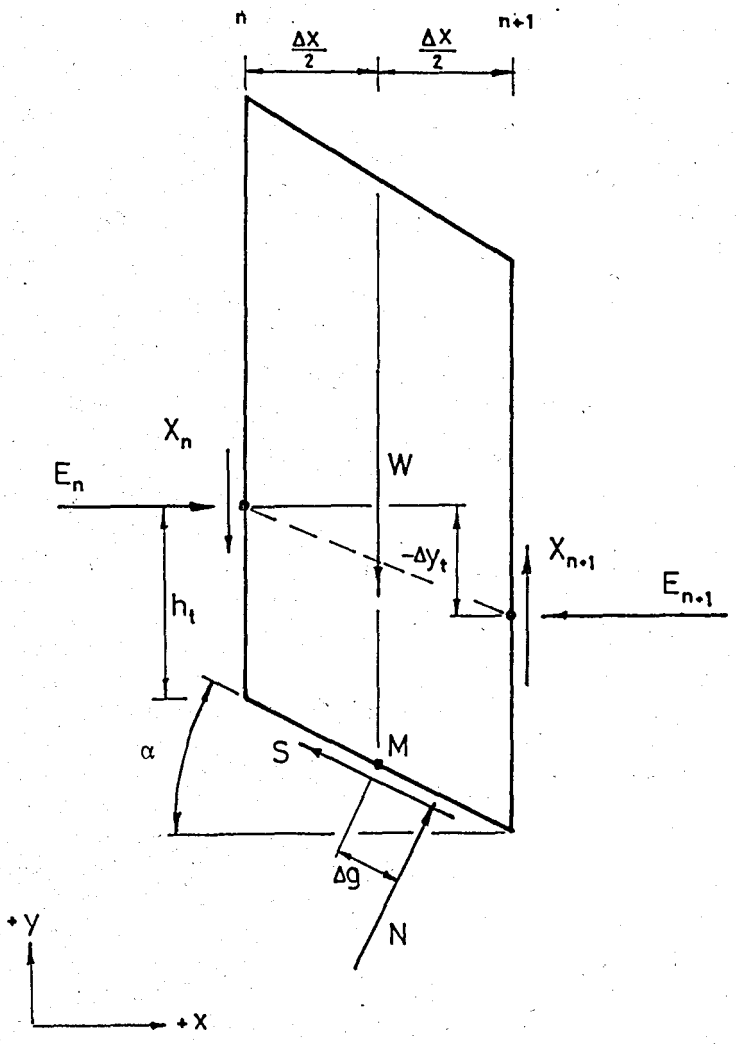

FIG.4.1 Forces and Locations Involved in the Equilibrium of an Individual Slice

For simplicity in deriving Eq.4.3 the weight force has been assumed to act at the center of the slice with the normal force being offset a distance, Δg, along the base. In addition to these three equations of equilibrium it is sometimes convenient to employ an alternate pair of force equilibrium equations for a second set of orthogonal axes. By resolving forces in the directions normal and parallel to the base of each slice the following equations of force equilibrium can be written:

a) Equilibrium Normal to Base of Slice :

$$N = W\cos\alpha - (X_{n-1} - X_n)\cos\alpha + (E_{n-1} - E_n)\sin\alpha \quad \ldots (4.4)$$

b) Equilibrium Parallel to Base of Slice :

$$S = -(E_{n-1} - E_n)\cos\alpha - (X_{n-1} - X_n)\sin\alpha + W\sin\alpha \quad \ldots (4.5)$$

Satisfaction of any two of these force equilibrium equations as well as the moment equilibrium equation for every slice is a necessary and sufficient condition for complete equilibrium. In the absence of any external loads on the slope the boundary conditions which the solution to these three sets of equations must satisfy may be expressed as:

$$\Sigma(X_{n-1} - X_n) = 0 \quad \ldots (4.6)$$

$$\Sigma(E_{n-1} - E_n) = 0 \quad \ldots (4.7)$$

$$\Sigma M_n = 0 \quad \ldots (4.8)$$

An alternate way of stating these same requirements is that the side forces and moments on the extreme ends of the shear surface are zero. In other words,

$$X_o = X_n \quad \ldots (4.9)$$

$$E_o = E_n \quad \ldots (4.10)$$

$$M_o = M_n \quad \ldots (4.11)$$

For this reason the unknown forces acting on the sides of the slices are not n+1 corresponding to the total number of sides but rather are n-1 corresponding to the number of boundaries between slices.

All procedures of slices assume that S and N are related by the Mohr-Coulomb strength criterion and a constant factor of safety expressed as,

$$S = \frac{1}{F}\left[c'\Delta l + (N - u\Delta l)\tan\phi'\right] \quad \ldots (4.12)$$

By employing this expression for the shear force (S) on the base of each slice, this force is reduced from an independent unkonwn to a dependent quantity defined in terms of the unkonwns F and N.

It is interesting to note the similarity between Eq.4.4 and the expression for the normal forces which is employed in the Ordinary Method of Slices. Bishop(1955) has shown that these two expressions involving the normal forces are identical if the resultant of all side forces acts parallel to the base of each slice. Thus, the Ordinary Method of Slices assumption of no interslice forces is equivalent to assuming that their resultant is parallel to the base; however, the magnitude of this resultant cannot be calculated without additionally satisfying moment equilibrium.

4.3 SOLUTIONS OF SLICE EQUILIBRIUM EQUATIONS

In order to achieve statical determinancy the 5n-2 unknowns which are shown in Table 4.1 must be reduced to 3n by making 2n-2 assumptions. The most commonly employed assumption is that the location of the normal forces on the base of each slice is known. This force is usually assumed to be located at the center of the base or the point at which the weight force intersects the base. However, even with this assumption n-2 assumptions still must be made before statical determinancy is achieved. The nature of these additional assumptions varies from procedure to procedure and for this reason it is appropriate to consider the specific techniques for solution on an individual basis.

4.4 METHOD OF SLICES

With this method the trial failure arc is divided into a reasonable number of slices, as shown in Fig.4.2. The overturning moment is determined by summing the moment of the weight of each slice about the trial center O. Note that slices to the left of O have a negative moment.

The overturning moment is

$$OM = \Sigma W_n a_n = r\Sigma W_n \sin\alpha_n \qquad \ldots (4.13)$$

The side forces on each slice are not included in the moment equations, since, when all slices are considered, the net moment of the side forces will be zero. The moment required for equilibrium is due to the tangential force $T = S_n'/F$ on the base of each slice. The force S_n'' is the sum of the cohesive and frictional strength at the base of each slice. For stability

TABLE 4.1 Equations and Unknowns Associated with Complete Slice Equilibrium

Equations	
n	Moment Equilibrium Equations for Each Slice
n	Vertical Force Equilibrium Equations for Each Slice
n	Horizontal Force Equilibrium Equations for Each Slice
3n	Total Equations
Unknowns	
1	Factor of Safety
n	Normal Forces on the Base of Each Slice(N)
n	Locations of the Normal Forces on the Base of Each Slice
n-1	Interslice Normal forces (E) and n-1 Resultant Interslice forces (Z)
	or
n-1	Interslice Shear Forces (X) and n-1 Inclinations of Resultant Interslice forces (β)
n-1	Locations of Interslice Forces (y_t) - (Line of Thrust)
5n-2	Total Unknowns

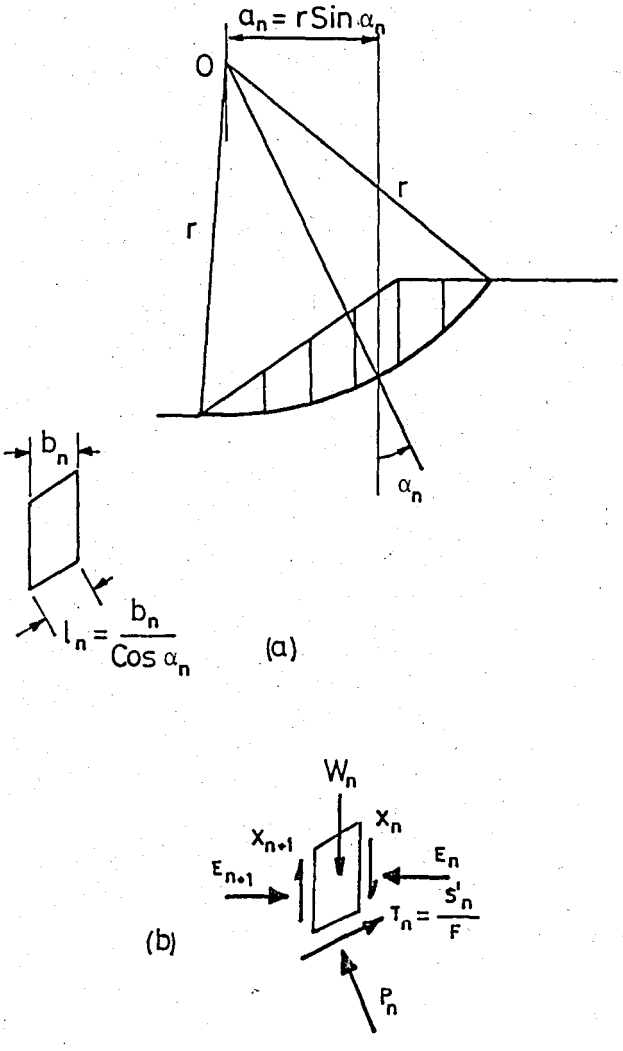

FIG.4.2 Method of Slices

$$r\Sigma W_n \sin\alpha_n = r\Sigma T_n = r\Sigma \frac{S'_n}{F} = \frac{r\Sigma(c_n l_n + P_n \tan\phi_n)}{F} \quad \ldots (4.14)$$

and the safety factor F is

$$F = \frac{RM}{OM} = \frac{\Sigma(c_n l_n + P_n \tan\phi_n)}{\Sigma W_n \sin\alpha_n} \quad \ldots (4.15)$$

The safety factor is defined as the ratio of resisting moment to overturning moment. When the analysis is based on total stress parameters c and ϕ, the equation for F is Eq.4.15.

If effective stresses c' and ϕ' are used, the normal force is reduced by the water force $U=u_n l_n$ where u_n is the average pore pressure on the bottom of the slice. The factor of safety based on effective stress parameters is Eq.4.16.

$$F = \frac{RM}{OM} = \frac{\Sigma\left[c'_n l_n + (P_n - u_n l_n)\tan\phi'_n\right]}{\Sigma W_n \sin\alpha_n} \quad \ldots (4.16)$$

Although the side forces cancel out of the overall moment equation, they do influence the magnitude of the normal reaction P_n on the base of the slice and thus the frictional shear strength at the base of the slice.

The side forces are actually indeterminate but can be approximated in various ways. Johnson (1975) has presented a summary of methods that consider side forces. Two commonly used methods of analysis, the Ordinary Method of Slices and Bishop's Simplified Method, are described in the following sections.

4.5 THE ORDINARY METHOD OF SLICES

The Ordinary Method of Slices can be used to calculate the factor of safety for a circular slip surface in soils whose strengths are governed by any of the following equations:

$s = c(\phi = 0)$

$s = \sigma \tan\phi$

or $s = c + \sigma \tan\phi$

in which s = shear strength

σ = normal stress on the failure plane

c = cohesion intercept

ϕ = friction angle

To be able to determine the strengths of soils with $\phi > 0$, the normal stress on the failure plane must be known. Therefore, to analyze the stability of slopes in such soils, it is necessary to determine the normal stress on the shear surface analyzed.

For analysis by the Ordinary Method of Slices, the mass above a trial circular slip surface is divided into a number of vertical slices. The most commonly employed assumptions in the procedures of slices are associated with the interslice forces. The basic assumption in the method can be made with regard to these forces is that they are zero. Therefore does not influence the normal stress on the base of the slice.

Each slice was considered to be in equilibrium under three forces, the weight W_n, the normal reaction $P_n = W_n \cos\alpha_n$, and the tangential force $T_n = W_n \sin\alpha_n$. The factor of safety by the Ordinary Method of Slices may be expressed as

$$F = \frac{\Sigma(W\cos\alpha - ul)\tan\phi + \Sigma cl}{\Sigma W\sin\alpha} \qquad \ldots (4.17)$$

in which F=factor of safety, c=cohesion ,ϕ=friction angle, W=slice weight, α= inclination of base of slice, u= pore pressure on base of slice, and l= lenght of base of slice

The factor of safety defined by this equation can be shown to be exactly the same as the ratio between the shear strength of the soil and the shear stress required for equilibrium of the slope. The factor of safety of a slope is calculated using the following procedure:

1. Select a trial slip surface.

2. Divide the mass bounded by the circular arc into a number of vertical slices. The slices should be chosen so that the base of any slice lies wholly within a single soil layer. If there is water outside the slope, it should be represented by one or more slices, just as if it was a soil with weight but no strength.

3. Calculate the weight of each vertical slice. When a slice crosses more than one layer having different unit weights, the weights within each layer are summed to determine the total weight of the slice. This may be done conveniently using the tabular computation form in Fig.4.3.

4. For each slice, determine the length of the base(l), the angle of inclination of the base (α), the cohesion of the soil at the base(c), the friction angle of the soil at the base (ϕ), and the pore pressure at the base(u). (If the analysis is being done with total stresses, use u=o) Enter these values, along with the weight of each slice,

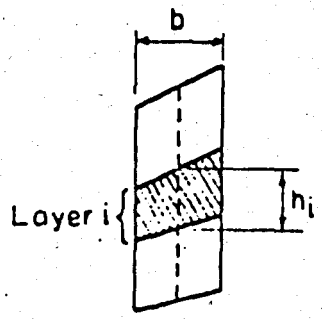

γ_i = unit weight of layer i

h_i = height of layer at center of slice

W_i = partial weight = $b\, h_i\, \gamma_i$

ΣW_i = total weight of slice

Slice No.	b	h_i	γ_i	W_i	ΣW_i

FIG.4.3 Tabular Form for Computing Weights of Slices

Slice No.	W	ℓ	α	C	ϕ	u	$u\ell$	$W\cos\alpha$	$W\cos\alpha - u\ell$	$(W\cos\alpha - u\ell)\tan\phi$	$C\ell$	$W\sin\alpha$
									Σ			

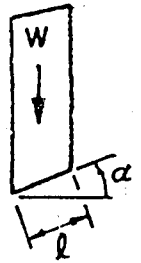

C = cohesion intercept
ϕ = friction angle
u = pore pressure
} of base of slice

$$F = \frac{\Sigma (W\cos\alpha - u\ell)\tan\phi + \Sigma c\ell}{\Sigma W\sin\alpha}$$

$$F = \frac{\qquad\qquad}{\qquad\qquad} =$$

FIG. 4.4 Tabular Form for Calculating Factor of Safety by Ordinary Method of Slices

in the tabular computation form shown in Fig.4.4

5. Calculate the factor of safety following the procedure indicated on the computation form.

6. Repeat steps(1) through(5) for a number of circles tangent to the same elevation as the first, until the most critical circle (the one with the lowest value of F) tangent to this elevation has been located.

7. Repeat for other tangent elevations until the overall critical circle has been located.

4.6 BISHOP'S PROCEDURE

In 1955 Bishop presented a procedure for slope analysis which satisfies the 3n conditions of static equilibrium. Although Bishop restricted his formulation to a circular shear surface, Nonveiller (1965) has shown that Bishop's approach may also be applied to a surface of any shape. In this procedure more generally the "slices" method is used, with a simplifying assumption about the effect of the forces between the slices.

The significance of this assumption may be examined by considering the equilibrium of the mass of soil (of unit thickness) bounded by the circular arc ABCD, of radius R and centre at O (Fig.4.5(a)). In the case where no external forces act on the surface of the slope, equilibrium must exist between the weight of the soil above ABCD and the resultant of the total forces acting ABCD.

Let E_n, E_{n+1} denote the resultants of the total horizontal

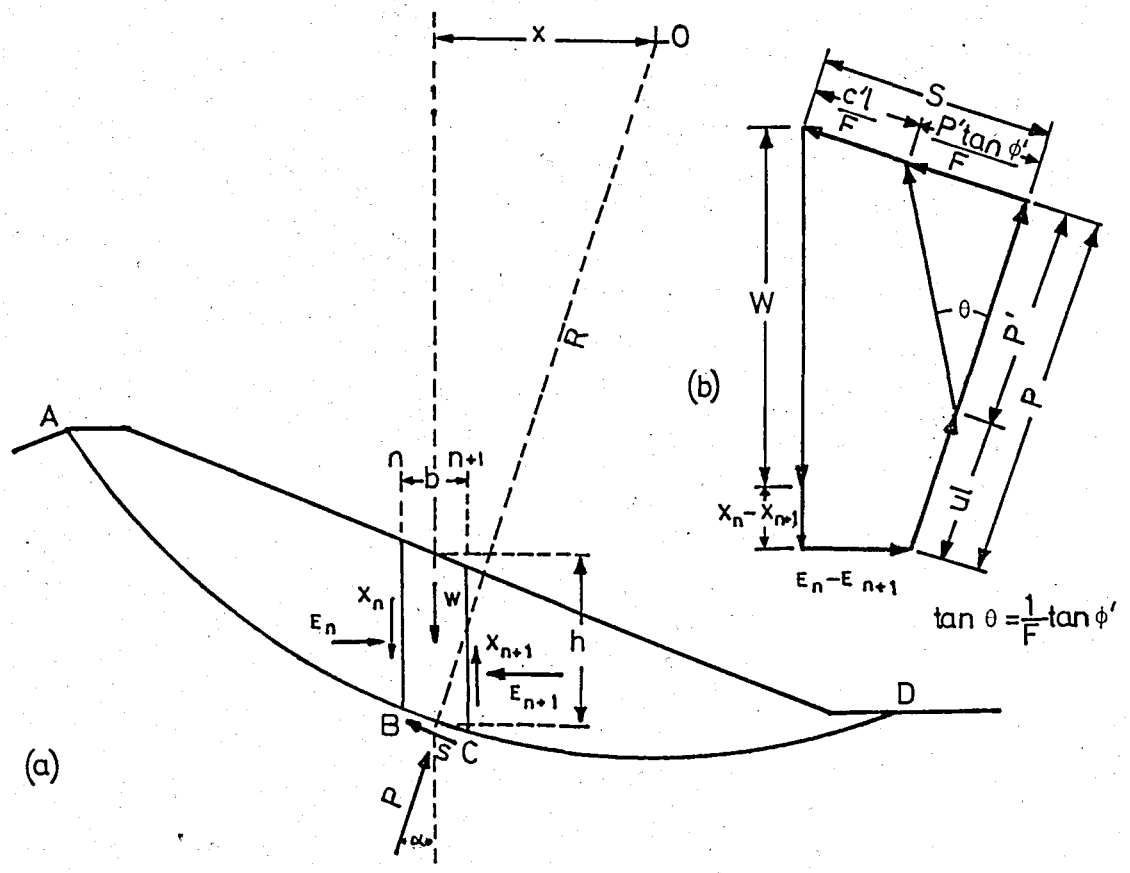

FIG.4.5 Forces in the Slices Method

forces on the sections n and n+1 respectively.

X_n, X_{n+1} = the vertical shear forces,

W = the total weight of the slice of soil,

P = the total normal force acting on its base,

S = the shear force acting on its base,

h = the height of the element,

b = the breadth of the element,

l = the length BC,

α = the angle between BC and the horizontal

x = the horizontal distance of the slice from the centre of rotation

The factor of safety (F) is defined as the ratio of the available shear strength of the soil to that required to maintain equilibrium. The shear strength mobilized is, therefore, equal to s, where:

$$s = \frac{1}{F}\left\{c' + (\sigma_n - u)\tan\phi'\right\} \qquad \ldots (4.18)$$

where

c' = cohesion in terms of effective stress,

ϕ' = angle of shearing resistance in terms of effective stress,

σ_n = total normal stress,

u = pore pressure

The total normal stress is σ_n, where

$$\sigma_n = \frac{P}{l} \qquad \ldots (4.19)$$

Hence, from Equation (4.18), the magnitude of the shear strength mobilized to satisfy the conditions of limiting equilibrium is s where:

$$s = \frac{1}{F}\left\{c' + \left(\frac{P}{l} - u\right)\tan\phi'\right\} \qquad \ldots (4.20)$$

Bishop assumed that the normal and weight forces act through a point on the center of the base of each slice. The shear force S acting on the base of the slice is equal to sl, and thus,equating the moment about O of the weight of soil within ABCD with the moment of the external forces acting on the sliding surface, we obtain:

$$\Sigma\, Wx = \Sigma\, SR = \Sigma\, slR \qquad \ldots (4.21)$$

It follows, therefore, from equation 4.20 that:

$$F = \frac{R}{\Sigma Wx}\,\Sigma\left[c'l + (P - ul)\,\tan\phi'\right] \qquad \ldots (4.22)$$

From the equilibrium of the soil in the slice above BC, we obtain P, by resolving in a direction normal to the slip surface:

$$P = (W + X_n - X_{n+1})\,\cos\alpha - (E_n - E_{n+1})\,\sin\alpha \qquad \ldots (4.23)$$

The expression for F thus becomes:

$$F = \frac{R}{Wx}\,\Sigma\left[c'l + \tan\phi'\,(W\cos\alpha - ul) + \tan\phi'\left\{(X_n - X_{n+1})\,\cos\alpha - (E_n - E_{n+1})\,\sin\alpha\right\}\right] \qquad \ldots (4.24)$$

Since there are no external forces on the face of the slope, it follows that:

$$\Sigma\ (X_n - X_{n+1}) = 0 \qquad \ldots\ (4.25\ a)$$

$$\Sigma\ (E_n - E_{n+1}) = 0 \qquad \ldots\ (4.25\ b)$$

However, except in the case where ϕ' is constant along the slip surface and α is also constant (i.e, a plane slip surface), the terms in equation (4.24) containing X_n and E_n do not disapper. A simplified form of analysis, suggested by Krey (1926) and Terzaghi (1929) and also presented by May (1936) as a graphical method, implies that the sum of these terms

$$\Sigma\ \tan\phi' \left\{ (X_n - X_{n+1})\ \cos\alpha - (E_n - E_{n+1})\ \sin\alpha \right\}$$

may be neglected without serious loss in accuracy.

Putting $x = R\sin\alpha$, the simplified form may be written:

$$F = \frac{1}{\Sigma\ W\ \sin\alpha}\ \Sigma \left[c'l + \tan\phi' (W\ \cos\alpha - ul) \right] \qquad \ldots\ (4.26)$$

In earth dam design the construction pore pressures are often expressed as a function of the total weight of the column of soil above the point considered, i.e.

$$u = r_u \left(\frac{W}{b} \right) \qquad \ldots\ (4.27)$$

where r_u is a soil parameter based either on field data or laboratory tests.

In this case, putting $l = b\sec\alpha$, the expression for factor of safety can be further simplified to:

$$F = \frac{1}{\Sigma\ W\ \sin\alpha} \Sigma\left[c'l + \tan\phi'\ W\ (\cos\alpha - r_u \sec\alpha)\right] \quad \ldots\ (4.28)$$

This expression permits the rapid and direct computation of the value of F which is necessary if sufficient trial circles are to be used to locate the most critical surface. The values of F are, in general, found to be conservative, and may lead to uneconomical design. This is especially marked where conditions permit deep slip circles round which the variation in α is large.

To derive a method of analysis which largely avoids this error it is convenient to return to equation (4.22). If we denote the effective normal force (P-ul) by P' (as shown in Fig.4.5(b)), and resolve the forces on the slice vertically, then we obtain, on re-arranging:

$$P' = \frac{W + X_n - X_{n+1} - l(u\cos\alpha + \frac{c'}{F}\sin\alpha)}{\cos\alpha + \frac{\tan\phi'\ \sin\alpha}{F}} \quad \ldots\ (4.29)$$

Substituting in equation (4.22) and putting $l = b.\sec\alpha$ and $x = R.\sin\alpha$, an expression for the factor of safety is obtained:

$$F = \frac{1}{\Sigma W \sin\alpha} \Sigma\left[\left\{c'b + \tan\phi'(W(1-r_u) + (X_n - X_{n+1}))\right\} \frac{\sec\alpha}{1 + \frac{\tan\phi'\tan\alpha}{F}}\right] \quad \ldots\ (4.30)$$

The values of the interslice shear forces (X_{n+1}) in this equation must also satisfy the boundary condition:

$$\Sigma\ (X_n - X_{n+1}) = 0 \quad \ldots\ (4.25a)$$

A solution to Eq.(4.30), however, is not necessarily a solution satisfiying all conditions of equilibrium. In order to assure satisfaction of complete equilibrium it is necessary, in addition, to satisfy force equilibrium in a direction other than vertical. For this purpose Bishop chose to consider equilibrium in a direction parallel to the base of each slice which may be expressed in Eq.4.31 as,

$$(E_n - E_{n+1}) = S \sec\alpha - (W + X_n - X_{n+1}) \tan\alpha \quad \ldots (4.31)$$

Summing this equation for all slices and introducing the boundary condition that the sum of the E forces for all slices must be zero yields,

$$\Sigma S\sec\alpha - (W + X_n - X_{n+1}) \tan\alpha = 0 \quad \ldots (4.32)$$

If the values of the X forces satisfy Eq.4.32, then the implied E forces will satisfy their boundary condition and the system will be in horizontal as well as vertical equilibrium. If Eq.4.32 is not satisfied a new set of values of X must be assumed until one is found which satisfies both Eqs. 4.30 and 4.32.

Even though these two equations may be satisfied, their particular solution may not be resonable. So far the n moment equilibrium equations for individual slices have not been considered; however, since the overall moment equilibrium equation which has been employed makes one of these equations redundant, only n-1 independent equations remain to be satisfied. From these equations the n-1 unknown coordinates for the line of thrust (y_t), which define the locations of the side forces, may be calculated. Even though it is not

necessary to solve these remaining equations to find a solution for the factor of safety which satisfies all conditions of equilibrium, the reasonableness of the solution may be judged from the position of the line of thrust. If an unreasonable line of thrust is calculated from these equations, it is necessary to find another of the infinite number of possible solutions to Eqs.4.30 and 4.32 by assuming new sets of values for X.

4.7 BISHOP'S MODIFIED PROCEDURE

The simplest solution satisfying Eq.4.31 is obtained by assuming that there are no interslice shear forces ($X=0$). For this assumption the boundary condition (Eq.4.25a) is satisfied and Eq.4.30 may be solved for the single unknown factor of safety. Alhough the normal forces (N) need not be evaluated to calculate the factor of safety, they may be determined from Eqs.4.1 and 4.12 . The assumption that there are no interslice shear forces was made by Bishop to simplify the solution and is commonly referred to as the Modified Bishop Procedure . The balance of equations and unknowns which are involved in the solution by this procedure are:

Equations

1	Overall moment equilibrium equation
n	Vertical force equilibrium equations for individual slices
n+1	Total equations

Unknowns

1	Factor of Safety
n	Normal forces on the base of each slice
n+1	Total unknowns

Seldom will the assumption that X=0 ever result in a solution satisfying complete equilibrium and having a reasonable line of thrust. Therefore, the solutions satisfying complete equilibrium will generally have non-zero values for X and give a somewhat different value for the factor of safety than the value calculated by Bishop's Modified Procedure.

4.8 SPENCER'S PROCEDURE

In application, the rigorous analysis proposed by Bishop was extremely lengthy and , as the intention was to examine a large number of problems extending over a wide range of soil properties in embankments of various slopes, it was necessary to derive an alternative method which would satisfy both force and moment equilibrium conditions and which would take the inter-slice forcesinto account.

Spencer (1967) has presented a procedure for satisfying complete slice equilibrium for a circular shear surface. Assuming that the normal forces were located at the center of the base of each slice, Spencer achieved statical determinancy with the additional assumption that all side forces (Z) are parallel. Although the solution presented by Spencer was only directly applicable to a circular shear surface , his procedure may be readily extended to slip surfaces of a general shape.

Figure 4.6(a) shows a section through an embankment of height H and slope β. The slope of the embankment is in the form cotβ:1. In the same figure, a circular slip surface and a typical slice of mean height h and width b are shown. An enlarged sketch of the slice with the forces acting upon it is given in Fig.4.6(b). The five forces can be described as follows:

(a) the weight (W);

(b) the total reaction (P) normal to the base of the slice; this force will have two components:

(i) the force (P') due to the effective or inter-granular stress,

(ii) the force (ubsecα) due to the pore pressure (u);

thus

$$P = P' + ub\sec\alpha \qquad \ldots (4.33)$$

(c) the mobilized shear force ($S_m = \frac{S}{F}$), where $S = c'b\sec\alpha + P'\tan\phi'$, i.e.

$$S_m = \frac{c'b}{F}\sec\alpha + P'\frac{\tan\phi'}{F} \qquad \ldots (4.34)$$

(d) the inter-slice forces (Z_n) and (Z_{n+1}); for equilibrium, the resultant (Q) of these two forces must pass through the point of intersection of the three other forces.

If the presence of the inter-slice forces is ignored, the three remaining forces are, of course, concurrent and in this case both conditions of equilibrium can be satisfied either by resolving or by taking moments. In either case the following expression is obtained for the factor of safety of the embankment:

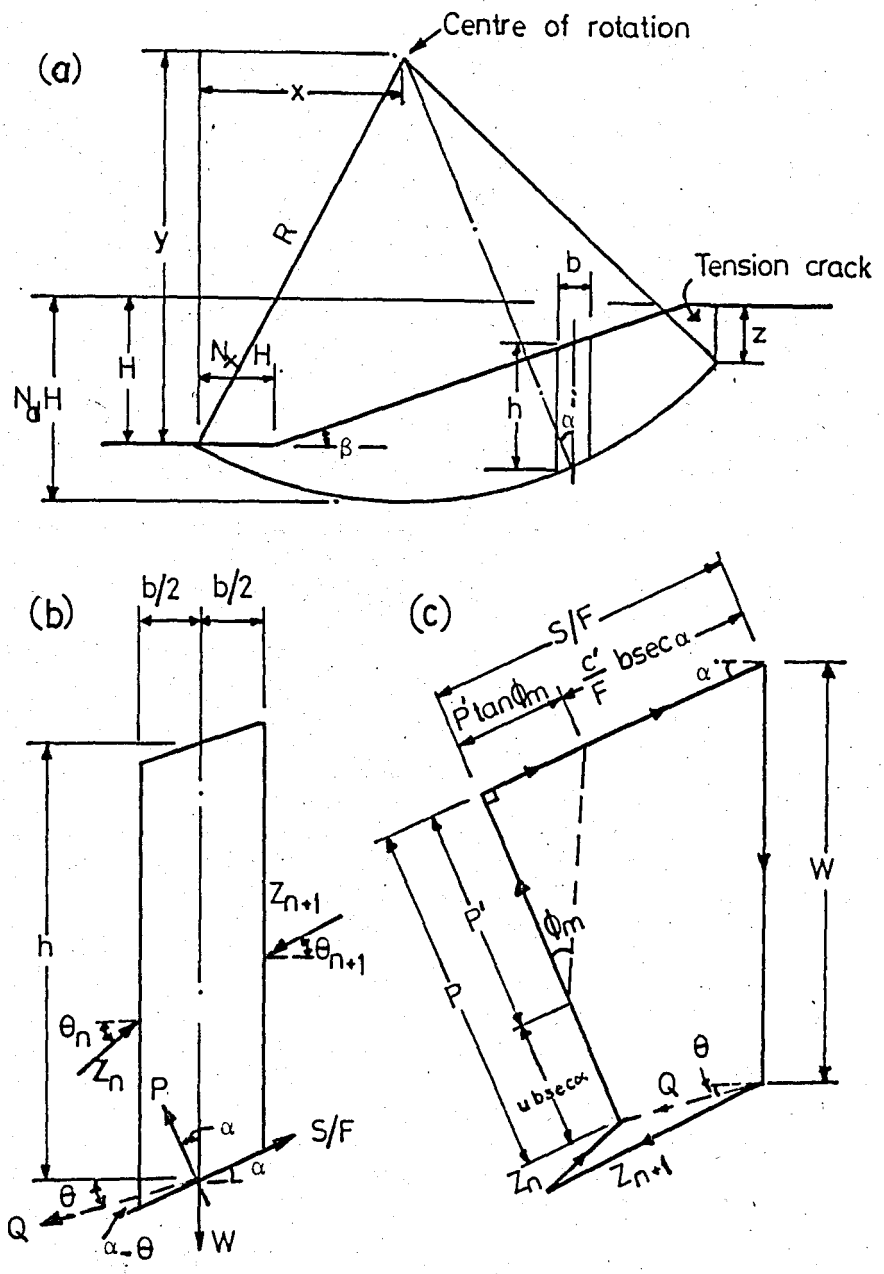

FIG.4.6 Dimensions of Slip Surface and Forces on a Slice

$$F = \frac{1}{\Sigma[W \sin\alpha]} \Sigma \left[c'b\sec\alpha + \tan\phi' \left(W\cos\alpha - ub\sec\alpha \right) \right] \quad \ldots (4.35)$$

The value for F given by this expression is appreciably less than that obtained when the effect of the inter-slice forces is taken into account.

Returning to the consideration of the inter-slice forces, these forces in a fully rigorous solution would be separated into two components like force P. One of these components would be derived from effective stress and the other from pore pressure. In this analysis, for the sake of simplicity, the total force is used.

By resolving normal and parallel to the base of the slice the five forces shown in Figs.4.6(b) and 4.6(c), the following expression is obtained for the resultant (Q) of the two inter-slice forces:

$$Q = \frac{\frac{c'b}{F}\sec\alpha + \frac{\tan\phi'}{F}(W\cos\alpha - ub\sec\alpha) - W\sin\alpha}{\cos(\alpha - \theta)\left[1 + \frac{\tan\phi'}{F}\tan(\alpha - \theta)\right]} \quad \ldots (4.36)$$

In this expression, u is the mean pore pressure on the base of the slice of weight W. If the soil is assumed to be uniform and of density γ, the weight of a slice of mean height h and width b can be written:

$$W = \gamma bh \quad \ldots (4.37)$$

Furthermore, assuming a homogeneous pore-pressure distribution as proposed by Bishop and Morgenstern (1960), the mean pore-pressure on the base of the slice can be written:

$$u = r_u \gamma h \quad \ldots (4.38$$

where r_u is a pore-pressure coefficient.

Making these assumptions, equation 4.39 can now be transposed and re-written in a dimensionless form as follows:

$$Q = \gamma Hb \frac{\frac{c'}{F\gamma H} + \frac{1}{2}\frac{h}{H}\frac{\tan\phi'}{F}(1-r_u+\cos 2\alpha) - \frac{1}{2}\frac{h}{H}\sin 2\alpha}{\cos\alpha\cos(\alpha-\theta)\left[1+\frac{\tan\phi'}{F}\tan(\alpha-\theta)\right]} \quad \ldots (4.39)$$

Now if the external forces on the embankment are in equilibrium, the vectorial sum of the interslice forces must be zero. In other words, the sum of the horizontal components of the inter-slice forces must be zero and the sum of their vertical components must also be zero.

$$\Sigma \; Q\cos\theta = 0 \qquad \ldots (4.40a)$$

$$\Sigma \; Q\sin\theta = 0 \qquad \ldots (4.40b)$$

Furthermore, if the sum of the moments of the external forces about the centre of rotation is zero, the sum of the moments of the inter-slice forces about the centre of rotation must also be zero:

$$\Sigma \left[QR\cos(\alpha - \theta)\right] = 0$$

And since the slip surface is assumed to be circular, the radius of curvature (R) is constant and:

$$\Sigma \left[Q\cos(\alpha - \theta)\right] = 0 \qquad \ldots (4.41)$$

In a given problem, there are thus three equations to be solved: two in respect of forces (4.40a, 4.40b) and one in respect of moments (4.41). Values of F and of θ must be found which satisfy all three equations and it must be noted that although , for a given slice, the value of θ will be the same in each equation, the inter-slice forces

will not necessarily be parallel throughout.

It has been shown by Morgenstern and Price(1965) that, within limits, the variation in θ can be assumed arbitrarily. They also found, however, that the range of values obtanied for F for different types of distribution in θ was quite small . The limiting factor which controls the variation in θ is that soil is able to withstand only a small intensity of tensile stress. Consequently, the point of application of an inter-slice force must not be far outside the middle third of the vertical boundary on which the force acts.

If it can be assumed that the inter-slice forces are parallel (i.e. that θ is constant throughout), equations (4.40a) and (4.40b) becomes identical:

$$\Sigma Q = 0 \qquad \ldots (4.40)$$

In this case, there are only two equations to solve (4.40) and (4.41), and the solution is therefore greatly simplified.

The result of assuming that the inter-slice forces are parallel was checked in a few trial cases in which the procedure was as follows.

1. A circular slip surface was chosen arbitrarily, the area inside it divided into vertical strips of equal width and the mean height (h) and base slope (α) of each slice determined graphically.

2. Several values of θ were chosen and , for each, the value of F was found which would satisfy both equations (4.40) and (4.41). The values of F obtained using the force

equilibrium equation (4.40) are designated F_f ,and those obtained using the moment equilibrium equation (4.41) as F_m . The value of the factor of safety obtained using the moment equation and taking θ as zero is designated F_{mo} .

3. A curve was then plotted showing the relationship between F_f and θ and, on the same graph, a second curve was plotted showing the relationship between F_m and θ . The type of graph resulting is shown in Fig.4.7. The intersection of the two curves gives the value of the factor of safety (F_i) which satisfies both equations (4.40) and (4.41) and the corresponding slope (θ_i) of the inter-slice forces.

4. The values of F_i and θ_i were then substituted in equation (4.39) to obtain the values of the resultants of the inter-slice forces. Hence, working from the first slice to the last, the values of the inter-slice forces themselves were obtained.

5. Then, working again from the first slice to the last, the points of action of the interslice forces were found by taking moments about the middle of the base of each slice in turn. The positions of the points of action were then marked on the section of the embankment.

Spencer's procedure of analysis satisfies all conditions of equilibrium and may be used to obtain an unique solution in a relatively straight-forward manner. However, there are two possible shortcomings of this procedure. First, the solution is not readily amenable to hand calculation and, second, the assumption of parallel interslice forces may

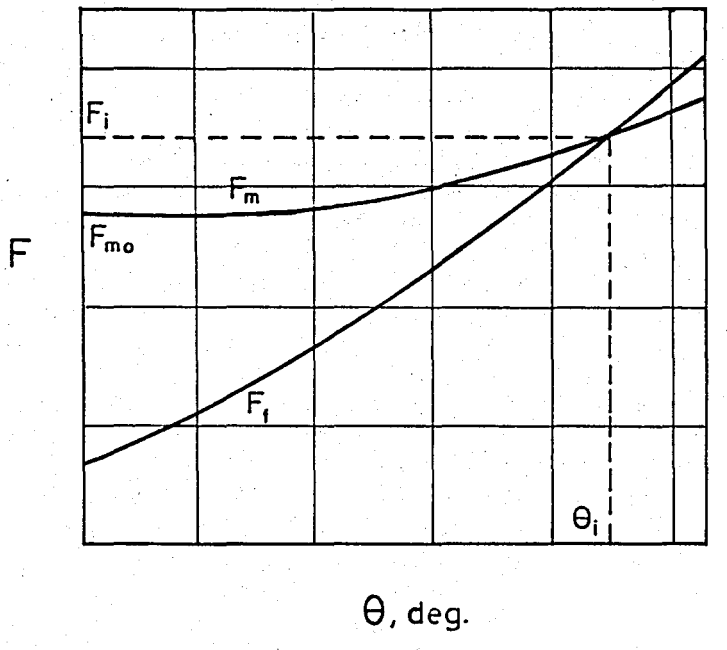

FIG.4.7 Variation of F_m and F_f with θ

not always lead to the most reasonable solution as judged from the calculated line of thrust. It is interesting to note that if the solution for the side force inclination is zero (horizontal side forces) then Spencer's and the Modified Bishop procedures are identical and the Modified Bishop solution will be one satisfying complete equilibrium.

4.9 JANBU'S GENERALIZED PROCEDURE OF SLICES

An expression for the factor of safety based on the requirements of force equilibrium for each slice may be obtained by using the following equations of vertical force equilibrum and force equilibrium parallel to the base of each slice as shown below.

$$S = \frac{1}{F}\left\{c' \Delta x + \left[W - (X_{n+1} - X_n) - u \Delta x \right] \tan\phi \right\} k_\alpha \quad \ldots (4.42)$$

in which,

$$k_\alpha = \frac{\sec\alpha}{1 + \frac{\tan\alpha \tan\phi}{F}}$$

and

$$\Sigma\left[W - (X_{n+1} - X_n)\right] \tan\alpha - \Sigma S \sec\alpha = 0 \quad \ldots (4.43)$$

As previously explained the horizontal force equilibrium boundary condition $\left[\Sigma (E_n - E_{n+1}) = 0\right]$ is satisfied by the formulation of Eq.4.43. These two equations of force equilibrium were combined by Janbu (1955) to obtain the following expression for the factor of safety:

$$F = \frac{\Sigma\left\{c'\Delta x + \left[W - (X_{n+1} - X_n) - u\Delta x\right] \tan\phi'\right\} \sec\alpha \; k_\alpha}{\Sigma\, W - (X_{n+1} - X_n) \tan\alpha} \quad \ldots (4.44)$$

This equation satisfies all conditions of force equilibrium providing that the values of the forces, X, satisfy the boundary condition:

$$\Sigma(X_{n+1} - X_n) = 0 \qquad \ldots (4.6)$$

Janbu (1957,1968) has shown that values of the vertical side forces for use in force equilibrium solutions may be obtained by systematic use of the requirements of moment equilibrium. These vertical forces may be expressed by the moment equation as:

$$X = -E \frac{dy_t}{dx} - h_t \frac{dE}{dx} \qquad \ldots (4.45)$$

Thus, if the values of y_t are assumed, the forces, X, are given by Eq.4.45 as a function of E alone. However, although satisfaction of either this differential moment equation on the moment equation for a finite slice (Eq.4.3) is desirable, this cannot be done in a straight forward manner if the n-1 values of y_t are assumed. The difficulty in using the above procedure may be readily seen from the equations and unknowns given in Table 4.1. If the n locations of the normal force on the base of each slice and the n-1 coordinates of the line of thrust are assumed, the number of unknowns is reduced to 3n-1. Thus, the system of 3n equations is overdetermined by one known.

Statical determinancy for fixed normal force locations may only be achieved by assuming a relationship for the line of thrust such as,

$$h_t = y_t - y = a(y_s - y) \qquad \ldots (4.46)$$

in which a is a single unknown describing the fraction of the height above the shear surface at which the line of thrust acts, and y_t, y and y_s are the y coordinates of the line of thrust, shear surface, and

slope surface respectively.

Janbu (1957,1968) has presented a more logical procedure for using the conditions of moment equilibrium to estimate values of the vertical side force, X. A solution by Janbu's Generalized Procedure of Slices (GPS) is begun by assuming the values of X in Eq.4.44.These values are commonly assumed zero for the first step of the analysis. Once the initial factor of safety (F_o) has been calculated, Eqs.4.42 and 4.31 are used to evaluate the magnitudes of the horizontal side forces (E) using an assumed line of thrust. From these calculated values of E a numerical or graphical approximation of $\frac{dE}{dx}$ is made for each interslice boundary and new values of X, which are not equal to zero, are calculated using Eq.4.45. This procedure is then repeated until the change in the calculated value of F is within the desired accuracy on consecutive iterations

Occasional convergence difficulties may arise in the application of Janbu's GPS procedure to some problems. Because the force equilibrium equation (Eq.4.44) and differential moment equilibrium equation (Eq.4.45) are treated independently at each step in the analysis it is not possible to prove that the solution will converge. However in the majority of practical cases convergence has been found to occur within a reasonable number of iterations. Janbu's Generalized Procedure of Slices has been included with the force equilibrium solutions because for any calculated values of X it always provides a convergent solution satisfying force equilibrium. It has the advantage over other force equilibrium procedures in that moment equilibrium is also satisfied at least approximately.

4.10 WEDGE METHOD

The Wedge Method can be used to calculate the factor of safety for a noncircular slip surface in soils whose strengths are governed by any of the following equations:

$$s = c(\phi = 0)$$

$$s = \sigma \tan\phi$$

$$s = c + \sigma \tan\phi$$

in which s=shear strength, σ=normal stress on the failure plane, c= cohesion intercept, and ϕ=friction angle. To be able to determine the strengths of soils with $\phi > 0$, the normal stress on the failure plane must be known. Therefore, to analyze the stability of slopes in such soils, it is necessary to determine the normal stress on the shear surface analyzed.

For analysis by the Wedge Method the mass above the trial slip surface is divided by vertical lines into a number of wedges or slices as shown in Fig.4.8. This method satisfies both horizontal and vertical force equilibrium. The basic assumption in the Wedge Method is that the side forces between slices are horizontal. This assumption is conservative, and the method gives factors of safety which are lower than the values calculated by more accurate methods. For most cases the error due to this assumption is no more than 15%. Greater accuracy can be achieved using methods which satisfy all conditions of equilibrium, such as Janbu's Generalized Procedure of Slices (Janbu, 1973), Spencer's Method (Wright, 1969) or Morgenstern and Price's Method (Morgenstern and Price, 1965)

The Wedge Method is most appropriate for conditions where the failure surface is not likely to be circular. For example, the

embankment shown in Fig.4.8 rests on a thin layer of weak clay, and it is likely that a considerable portion of the critical failure surface will lie within this layer. For this type of problem the wedge mechanism may be more critical than a circular surface.

The factor of safety calculated by the Wedge Method is defined as the ratio between the shear strength and the shear stress required for equilibrium. The factor of safety is the factor by which the strength parameters (c and $\tan\phi$) for each soil would have to be divided to bring the slope into a state of barely stable equilibrium. The factor of safety should always be at least as large as the margin of uncertainty regarding soil strengths.

The Wedge Method factor of safety is calculated by trial and error. A value for F is assumed, and then checked to determine if the assumed value satisfies equilibrium. The analysis can be performed either graphically or numerically. The first three steps are the same whether the graphical or the numerical method is used.

1. Select a trial slip surface.

2. Divide the mass above the slip surface into wedges. The wedges should be chosen so that the base of any wedge lies wholly within a single soil layer. Three to five wedges are usually sufficient. If there is water outside the slope, it should be represented by a wedge, just as if it was a soil with weight but no strength.

3. Calculate the weight of each wedge. If the top as well as the bottom of each wedge is a straight line, the weights can be calculated using the tabular computation form

described previously for the Ordinary Method of Slices. If the top boundary of a wedge is a broken line, as for wedge 2 in Fig.4.8, the weight of the wedge can be calculated by dividing it into two parts.

To solve for the factor of safety graphically, follow steps(4) through (9) below.

4.Assume a value for the factor of safety, and calculate trial values of mobilized cohesion and mobilized friction angles for each soil using the following formulas:

$$c_m = \frac{c}{F} \qquad \ldots (4.47)$$

and

$$\tan\phi_m = \frac{\tan\phi}{F} \qquad \ldots (4.48)$$

in which F= assumed value for the factor of safety, c= cohesion, c_m=mobilized cohesion, ϕ=friction angle, and ϕ_m= mobilized friction angle.

5.Construct the force polygon for wedge 1. An example is shown in Fig.4.8. First draw the weight vector vertically, to scale. Next, draw the mobilized cohesion vector, which is equal to the mobilized cohesion multiplied by the length of the base of a slice, and acts parallel to the base of the slice. The tail of this vector connects to the head of the weight vector. (In the example the cohesion is zero on the first slice.) Then, if the analysis is done in terms of effective stress, draw the pore pressure vector, which is equal to the pore pressure on the base of the slice multiplied by the length of the base, and acts perpendicular to the base. The tail of this vector connects to the head

of the cohesion vector. If the analysis is done in terms of total stresses, as the example in Fig.4.8, the pore pressure is taken as zero, and there is no pore pressure force in any of the force polygons. Next, lay off the direction of the resultant of the normal and frictional forces on the base of the slice. This resultant acts at an angle of ϕ_m from the normal direction, and the head of this vector connects to the tail of the weight vector. The remaining force, which closes the polygon, is the side force exerted on wedge 1 by wedge 2. This vector is assumed to act horizontally, as discussed previously. The position of the intersection of the resultant of the normal and frictional forces with the side force determines the lengths of these two vectors, which are unknown until the intersection point is determined.

6. Construct the force polygon for wedge 2. First draw the weight vector vertically, to scale. Then draw the side force exerted on wedge 2 by wedge 1. Note that this is equal but opposite to the force exerted on wedge 1 by wedge 2, and that the head of this vector connects to the tail of the weight vector. Next, draw the mobilized cohesion vector, which is equal to the mobilized cohesion multiplied by the length of the base of the slice, and acts parallel to the base of the slice, with its tail connected to the head of the weight vector. Then, if the analysis is done in terms of effective stresses, lay off the pore pressure force, from the head of the cohesion force, acting perpendicular to the base of the slice. Next, lay off the

direction of the resultant of the normal and frictional forces on the base of the slice. This resultant acts at an angle of ϕ_m from the normal direction, and the head of this vector connects to the tail of the vector which represents the side force exerted on wedge 2 by wedge 1. (In the example, ϕ=0 for the second slice, and there is therefore no frictional force. In this case the vector consists of only the normal force and acts normal to the base of the slice.) The remaining force, which closes the polygon, is the side force exerted on wedge 2 by wedge 3. This vector is assumed to act horizontally. The position of the intersection of the resultant of the normal and frictional forces with the side force determines the lengths of these two vectors, which are unknown until the intersection point is determined.

7. Construct the force polygons for the remaining wedges in sequence, using the same procedures as for wedges 1 and 2. If the assumed factor of safety is correct, the force polygon for the last wedge will close, with no unbalanced force. However, if the assumed factor of safety is not correct, an additional force will be required to close the polygon. If the force required to close the polygon would have to act in the direction which would make the slope more stable, the assumed factor of safety is too high. If the required force would have to act in the direction which would make the slope less stable, the assumed factor of safety is too low. This is true for the trial solution with F=1.50 in Fig.4.8.

8. Assume a new factor of safety and repeat steps (4) through (7). This has been done in Fig. 4.9. Try additional factors of safety until the unbalanced force on the last slice is negligibly small compared to the magnitudes of the other forces. Then the assumed value of F is the correct one for the assumed failure mechanism. Usually no more than two trials are needed to determine F. By plotting the assumed factor of safety against the magnitude of the unbalanced force for the first two trials, a third trial value of F can usually be estimated which will be very close to the correct value, as shown in Fig. 4.10. If the value of F determined by this procedure differs greatly from both of the first two trial values, a third trial may be necessary.

9. Select a new failure mechanism and repeat steps (1) through (8). Try several different failure mechanisms in order to find the one with the lowest factor of safety.

To solve for the Wedge Method factor of safety numerically, use the tabular computation form shown in Fig.4.11. Steps (1) through (3), as described previously, are the same for the numerical analysis as for the graphical analysis. Steps (4) through (9) proceed as described below.

4. For each wedge, determine the inclination of the base (α), the length of the base (l), the cohesion of the soil at the base(c), the friction angle of the soil at the base (ϕ), and the pore pressure at the base (u). (If the analysis is being done with total stresses, use u=0.) Enter these

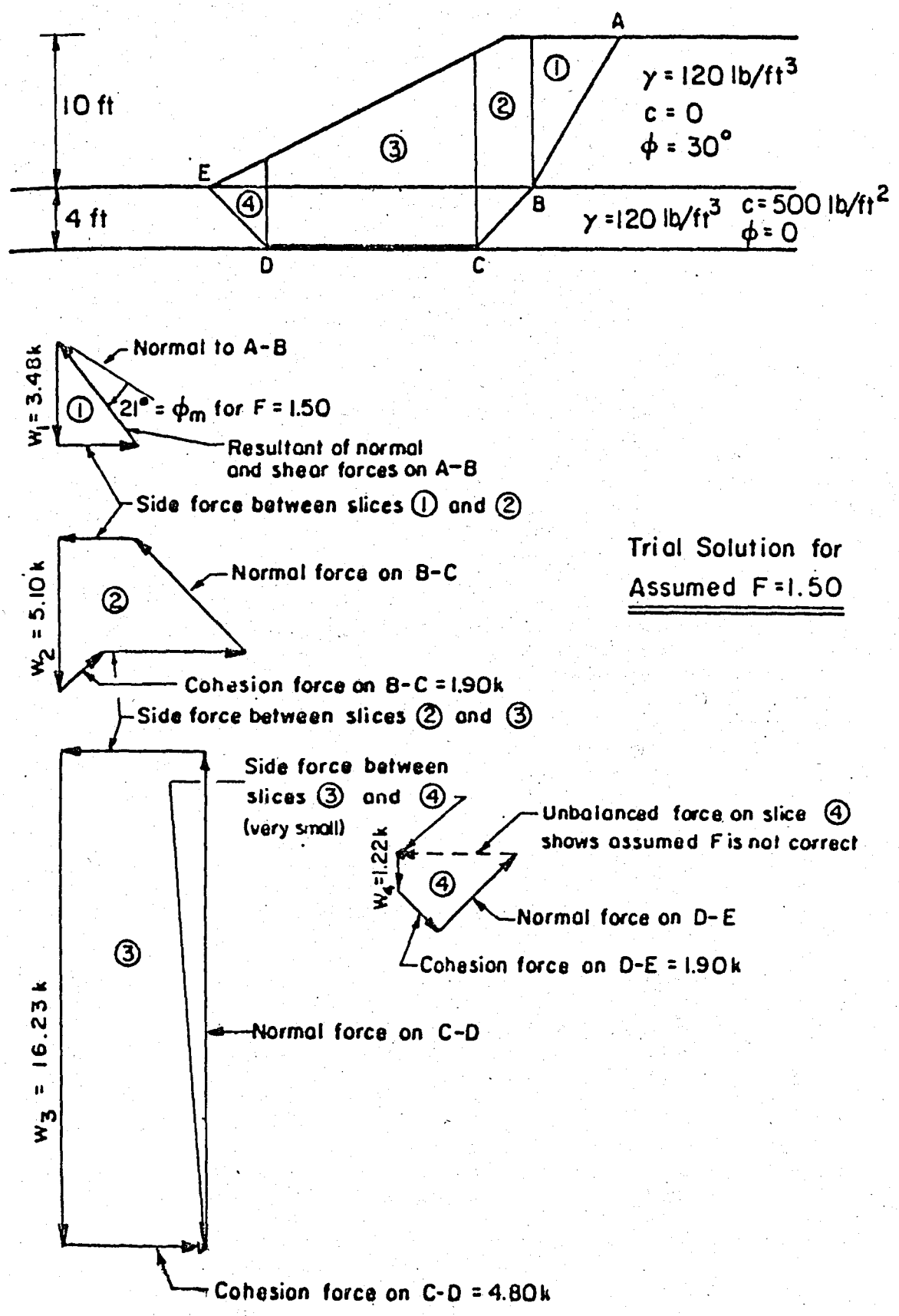

FIG.4.8 Example of Graphical Procedure for Wedge Method (after Duncan and Buchignani, 1975).

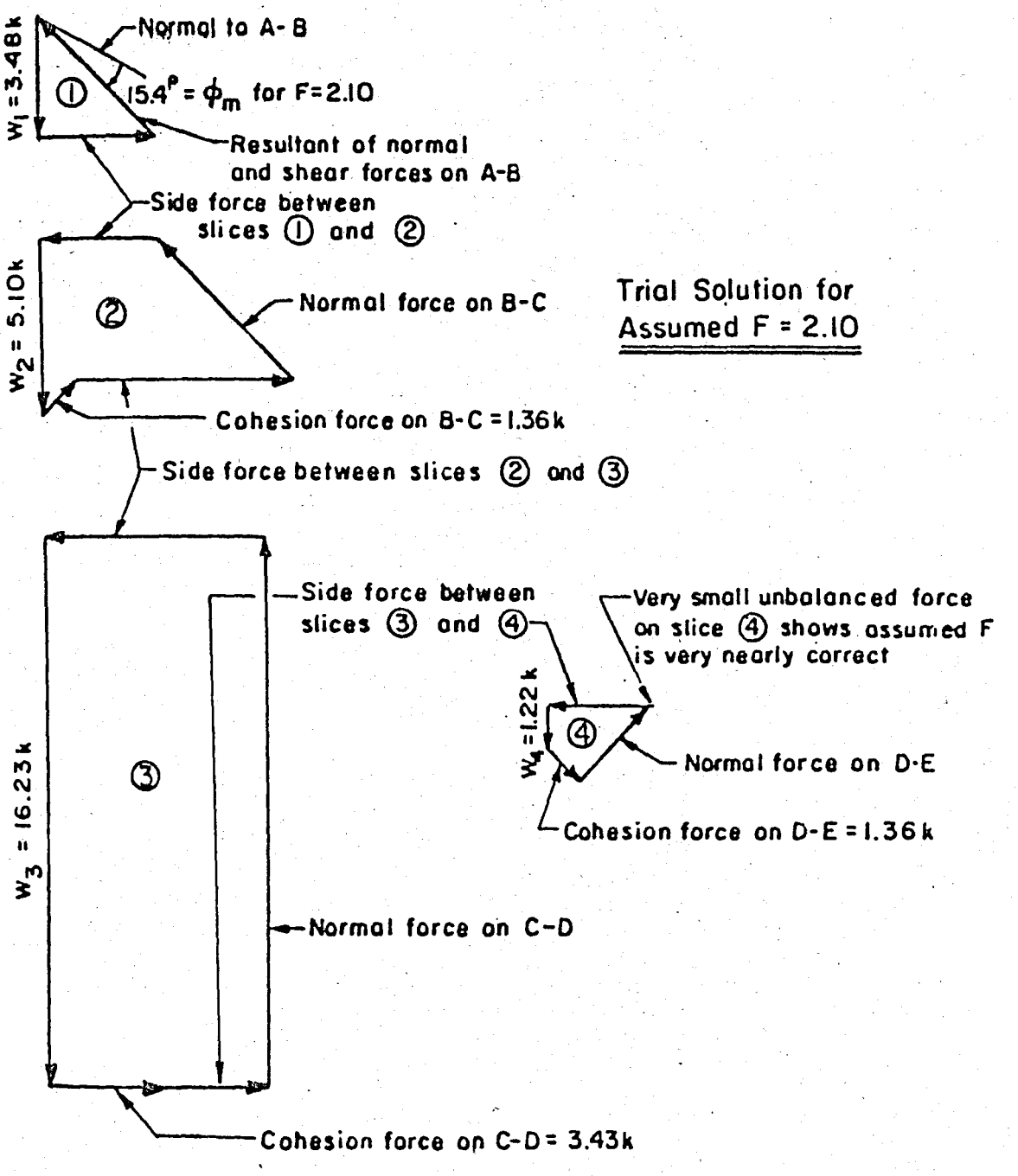

FIG.4.9 Example of Graphical Procedure for Wedge Method (after Duncan and Buchignani, 1975)

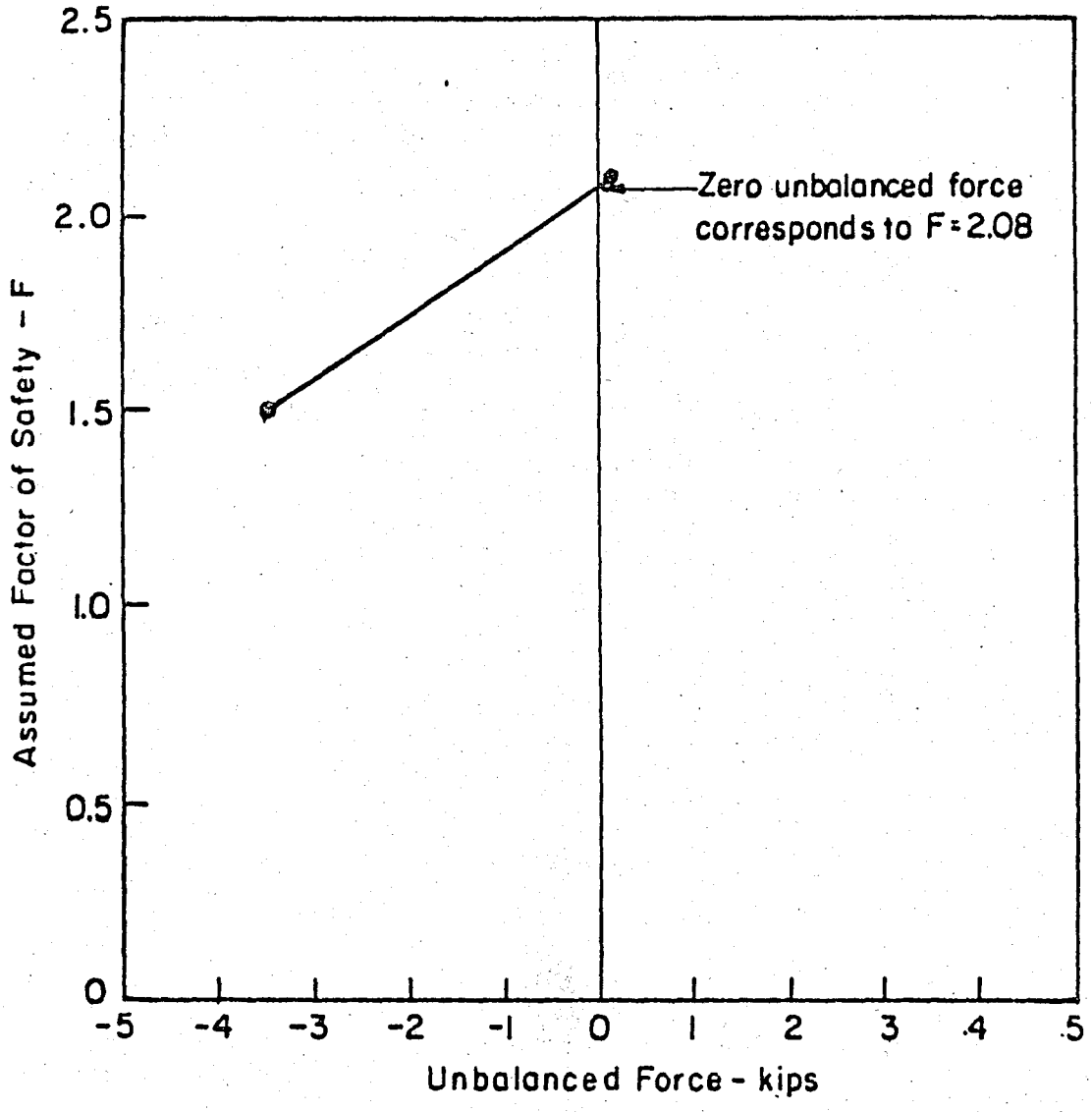

FIG.4.10 Determining Factor of Safety by Wedge Method

values, along with the weight of each slide, in the tabular computation form shown in Fig.4.11.

5.Calculate the quantities $cl/\cos\alpha$, $W\tan\phi$ and $ul\tan\phi/\cos\alpha$ for each wedge, and enter these in the table.

6.Assume a trial value for the factor of safety, and calculate the value of ΔE for each wedge as indicated in the table. ΔE is the difference between the side forces on the left and right sides of each slice, and is given by the equation.

$$\Delta E = \frac{FW\tan\alpha - \frac{cl}{\cos\alpha} - W\tan\phi + \frac{ul\tan\phi}{\cos\alpha}}{F + \tan\phi\tan\alpha} \quad \ldots (4.49)$$

7.Calculate the sum of the terms ΔE for all slices. If the assumed factor of safety is correct, this sum will be zero. If its value is less than zero, the assumed value of F is too low. If it is greater than zero the assumed value of F is too high.

8.Assume a new value of F and repeat steps (6) and (7). Try additional values of F until the sum of the ΔE's is negligibly small. Then the assumed value of F is the correct one for the assumed failure mechanism. Usually no more than two trials are needed to determine F. By plotting the assumed factor of safety against the value of $\Sigma\,\Delta E$ for the first two trials, a value of F can usually be estimated which will be very close to the correct value, as shown in Fig.4.10. If the value of F determined by

$$\Delta E = \frac{N_4 - N_1 - N_2 + N_3}{N_5}$$

Slice No.	W	α	ℓ	C	ϕ	u	N_1 $\frac{C\ell}{\cos\alpha}$	N_2 $W\tan\phi$	N_3 $\frac{u\ell\tan\phi}{\cos\alpha}$

Trial	F	Slice No.	N_4 $FW\tan\alpha$	N_5 $F+\tan\phi\tan\alpha$	ΔE	$\Sigma\Delta E$

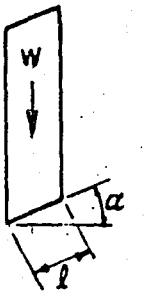

C = cohesion intercept

ϕ = friction angle

u = pore pressure at base of slice

FIG.4.11 Tabular Form for Calculating Factor of Safety by Wedge Method (after Duncan and Buchignani, 1975)

this procedure differs greatly from both of the first two values, a third trial may be necessary .

9. Select a new failure mechanism and repeat steps(1) through (8). Try several failure mechanisms in order to find the one with the lowest factor of safety.

4.11 MORGENSTERN AND PRICE'S PROCEDURE

Morgenstern and Price (1965,1967) have presented a somewhat different approach to the solution of complete slice equilibrium. While Bishop and Spencer considered the overall moment equilibrium equations for circular shear surfaces, Morgenstern and Price have considered only the moment equations of individual slices. The advantage of the latter approach rests in its simplification of the numerical formulations of equilibrium for a non-circular shear surface.

The assumption made by Morgenstern and Price is that the shear and normal forces between slices are related by an expression of the form,

$$X_j = \lambda f(x) E_j \qquad \ldots (4.50)$$

in which the assumed function f(x) represents the variational relationship between the X and E forces along the shear surface. Although the assumption for f(x) may be made arbitrarily, only an assumption resulting in reasonable values for the unknowns is considered acceptable. The parameter λ is an unknown scaling factor defining the relationship between X and E in terms of f(x). Although a continuous function, f(x), is assumed, only the values of this function at interslice boundaries are directly used in the solution. This procedure assumes that f(x)

varies linearly between each interslice boundary at which its values are specified. By assuming this variation for f(x), the locations of the normal forces on the base of each slice are thus fixed; however, their exact locations may only be determined once the necessary equilibrium solution is found for the differential moment equilibrium equation which may be expressed from Eq.4.3 as,

$$-X = E \frac{dy_t}{dx} + h_t \frac{dE}{dx} \qquad \ldots (4.45)$$

The complete solution to this moment equation for each slice and the remaining equations of force equilibrium involves the following unknowns:

Unknowns	
1	Factor of safety (F)
1	Side force scaling factor (λ)
n	Normal forces on the base of each slice (N)
n-1	Interslice normal forces (E)
n-1	Locations of the interslice forces (y_t), (Line of thrust)
3n	Total unknowns

4.12 LOWE AND KARAFIATH'S PROCEDURE

Lowe and Karafiath(1960) have suggested that the inclinations of the side forces may be reasonably assumed to be equal to the average inclinations of the shear surface and slope face. This assumption is equivalent to assuming that the side forces are parallel to an imaginary tangent line drawn at midheight through each interslice boundary. In general the line of thrust will be somewhat below this midheight line

TABLE 4.2 Equations and Unknowns Associated with Force Equilibrium for Each Slice

Equations	
n	Vertical Force Equilibrium Equations for Individual Slices
n	Horizontal Force Equilibrium Equations for Individual Slices
2n	Total Equations
Unknowns	
1	Factor of Safety (F)
n	Normal Forces on the Base of Each Slice (N)
n-1	Interslice Normal Forces (E)
n-1	Resultant Interslice Forces (Z)
	or
n-1	Interslice Shear Forces (X)
n-1	Inclinations of Resultant Interslice Forces (β)
3n-1	Total Unknowns

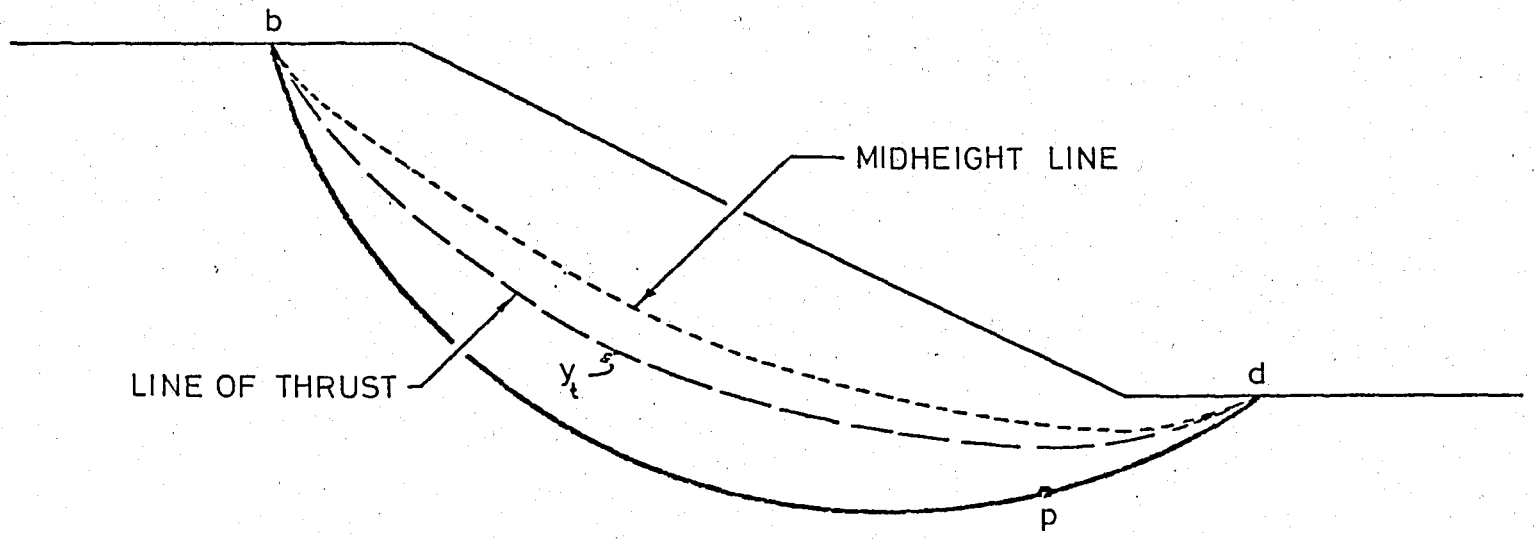

FIG.4.12 Line of Thrust and Midheight Line for a Typical Shear Surface

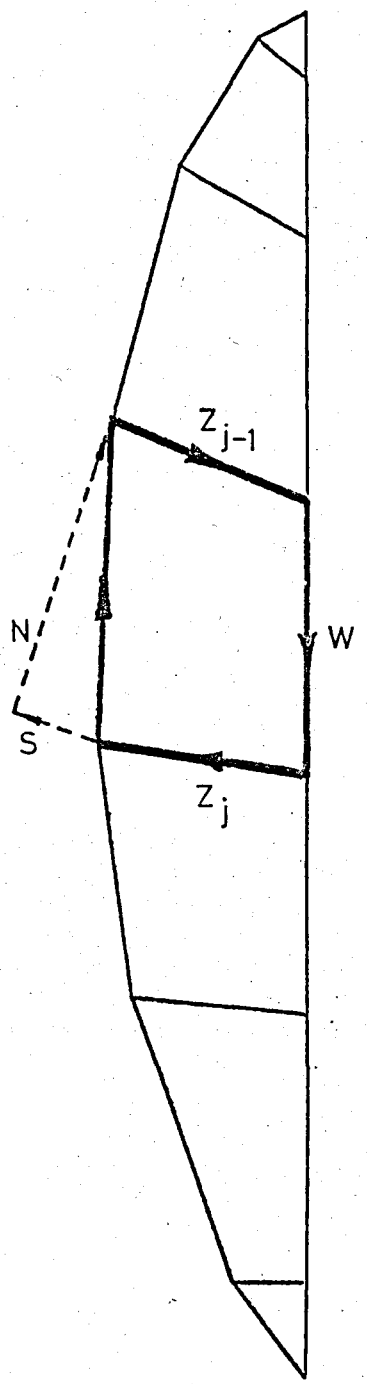

TABLE 4.13 Force Equilibrium Polygons

as illustrated in Fig.4.12 and therefore it may be noted that this midheight line is somewhat flatter than line of thrust above the center of the shear surface and somewhat steeper than the line of thrust along much of the lower portion of the shear surface. Thus , it may also be noted that the inclination of the side forces, which are assumed tangent to the midheight line, will have the same characteristics as those side forces satisfying moment equilibrium. Although the side force assumption suggested by Lowe and Karafiath cannot be directly verified from the moment equation, it appears that the assumption is that least qualitatively correct over a major portion of the slope.

Lowe and Karafiath have presented a relatively simple procedure for obtaining a force equilibrium solution. As previously explained, they assumed that the side forces act at the average inclination of the shear and slope surfaces; thus, eliminating the n-1 unknowns relating to side force inclinations which are shown in Table 4.2 and making the system of 2n equations statically determinant.

A solution by this procedure is commonly obtained graphically by first assuming a factor of safety and drawing the force polygons from slice to slice as illustrated in Fig.4.13. If the polygon for the last slice fails to close, then a new factor of safety is assumed and the procedure repeated until closure is obtained.

4.13 SUMMARY

The similarities and differences in the various procedures of stability analysis discussed in this chapter may be examined in terms of the conditions of equilibrium which they satisfy and the assumptions

they employ to achieve statical determinancy. Some of these procedures satisfy only one or two conditions of equilibrium, whereas others satisfy all three conditions, and they all involve some assumptions to make the problem statically determinant. In making the assumptions, a balance between the number of equilibrium equations satisfied and the number of unknown quantities must be maintained to achieve statical determinancy in the solution.

Several procedures may satisfy the same conditions of equilibrium, but due to the fact that they involve different assumptions, they may result in different values for the factor of safety. Others may satisfy the same conditions and employ the same assumptions, but differ only in the manner in which the solution is obtained; thus, although the techniques may be different, all such procedures should result in the same value for the factor of safety.

The number of equilibrium conditions satisfied does not provide a sufficient basis for selecting the best procedure for analysis . In this respect the studies conducted show that the condition of moment equilibrium is more important than the conditions of horizontal or vertical force equilibrium.

For example, in the Ordinary Method of Slices, overall moment equilibrium is only satisfied. Bishop's Modified method (Bishop, 1955) satisfies the conditions of overall moment and vertical force equilibrium. The basic assumption of this method is that the side forces are horizontal.

Morgenstern and Price's method (Morgenstern and Price 1965) satisfies all conditions of equilibrium. Although it is more complex than nearly any other method. Morgenstern and Prices 's method has been used quite extensively. The method has been

regarded by many engineers as the most accurate method of slope stability analysis from the point of view of mechanics. The basic assumption made in this method is that the inclinations of the forces between the slices θ , varies in accordance with the equation $\theta_i=\lambda f(x)$, in which the function $f(x)$ is an assumed function which describes the pattern of variation of the side force inclinations.

Spencer's method, described by Spencer(1967) and Wright (1969) also satisfies all conditions of equilibrium. The basic assumption is that the side forces are parallel, or θ=constant. This corresponds exactly to Morgenstern and Price's method with $f(x)$ = constant. Spencer's method is equally as accurate from the point of view of mechanics.

In the Wedge method. The inclinations which are assumed for the side forces vary from paralel to the slope to horizontal. This method satisfies both horizontal and vertical force equilibrium.

Janbu's Generalized Procedure of Slices has the advantage over other force equilibrium procedures in that moment equilibrium is also satisfied at least approximately.

The procedures may involve different assumptions to satisfy a given set of equilibrium conditions, the relative accuracy of the various procedures is best evaluated from the results of numerical analyses.

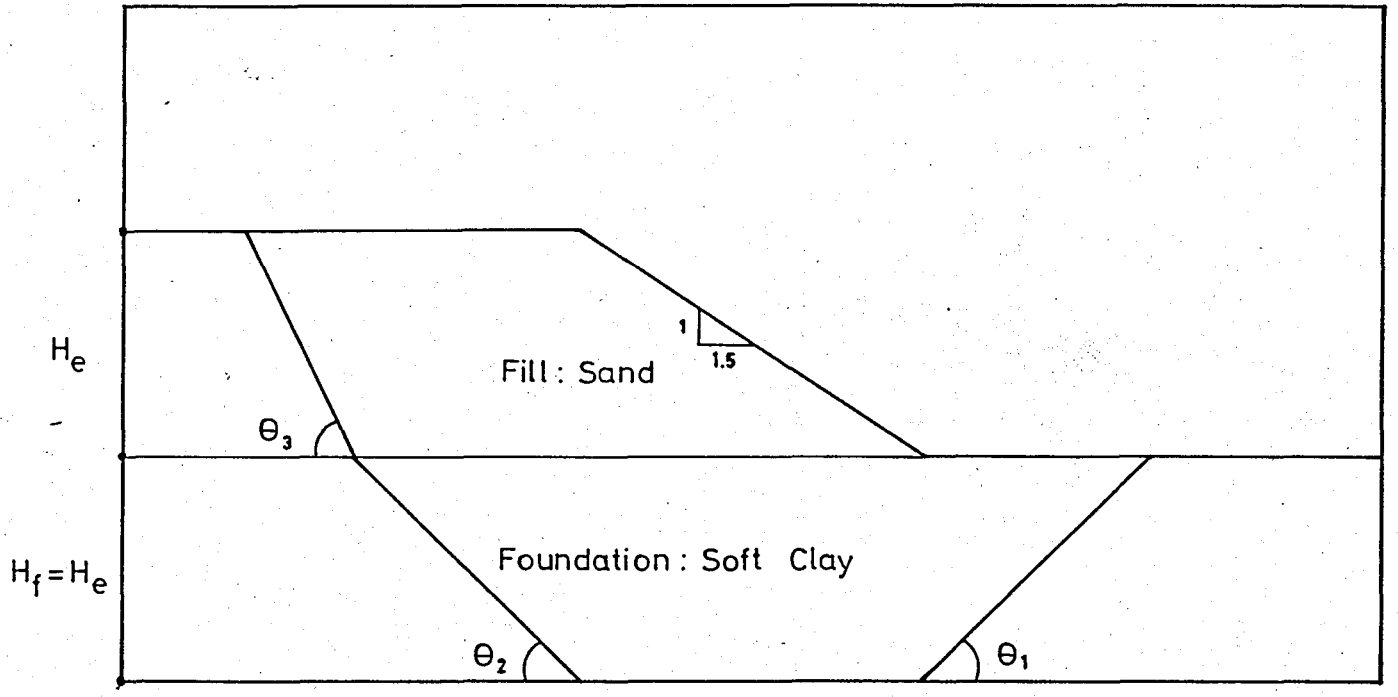

FIG.5.1 Geometry of the Embankment and Foundation and the Failure Surface Used in the Analyses

in the other methods.

In the non-circular failure surface analysis slip surface is defined with respect to the terms of θ_1, θ_2 and θ_3 where

$$\theta_1 = 45 - \frac{\phi_{foundation}}{2}, \quad \theta_2 = 45 + \frac{\phi_{foundation}}{2}, \text{ and } \quad \theta_3 = 45 + \frac{\phi_{fill}}{2}$$

The parametric study is performed using the computer programs for each method. More than 200 runs are achieved, whence more than 2000 possible factor of safety values are checked to solve the problems.

5.2 THE COMPUTER PROGRAMS

The computer programs SLOPE 22R, SLOPE 8R, and SLOPE 9 were written by Stephen G.Wright at the University of California Berkeley.

SLOPE 22R consists of a main program and four subroutines (CENER, OMS, BISHOP, and READER). This computer program calculates the factors of safety for specified circles using both the Ordinary Method of Slices and Bishop's Modified Method.

SLOPE 8R consists of a main program and seven subroutines (EFLAG, MESAGE, CGXY, BISRIG, EFORCE, THRUST, and READER). It calculates the factor of safety for specified non-circular slip surfaces by the procedure developed by Spencer (1967) and extended by Wright to non-circular surfaces. By assuming parallel side forces this procedure satisfies all equilibrium conditions for each slice. The two unknown parameters, F(the factor of safety) and THETA(the side force inclination) are varied simultaneously by iteration until a convergent solution is found with net force and moment inbalance less than specified values.

SLOPE 9 consists of a main program and eight subroutines, NOTE, EFLAG, IN,INITL, OUT, GENER, SETUP and JANBU2. The program calculates the factor of safety by Janbu's Generalized Procedure of Slices (GPS procedure) for an arbitrarily assumed line of thrust. The solution by the GPS procedure is by iteration and occasionally a convergent solution cannot be obtained. If the solution for the factor of safety diverges, the program will normally abort the particular problem being solved and continue with the next problem; however, provisions are available in the program to override the abort allowing the iterations to continue, add in some cases a convergent solution may then be found even though divergency has been once encountered. A provision for a tension crack of specified depth is available when circular slip surface coordinates are generate by the program, and the specification of the tension crack is described in the data input description.

The computer program WEDGE 1 is developed in this study. It calculates the factor of safety using Corps of Engineers' Wedge Analysis. This computer program has iteractive characteristic and reads the input data iteractively. It prints the factor of safety when the given accuracy is greater than the sum of the difference between the side forces. WEDGE 1 also takes into the account the effect of linear variation of foundation shear strength. This computer program is developed on CDC Cyber 170/815 system.

5.3 EFFECT OF UNIT WEIGHT AND FRICTION ANGLE OF COHESIONLESS FILL

5.3.1 For Variable Fill Density

In order to find the factor of safety of the typical case of the soil profile and failure surface shown in Fig.5.2, the height of the embankment, H_e, the friction angle and the unit weight of the fill material are varied respectively while all other factors are held constant. The parameters used in these analyses are shown in Fig.5.2. The slope of the fill material is taken as 1/1.5 and is kept constant during the investigation. Analyses are performed using three different slope heights-4 m, 8 m, 12 m. For unit weight of the sand layer again three different values as γ = 1.9, 2.0, 2.1 t/m^3 , for friction angle of the sand layer three different values as ϕ=35^0, 40^0, 45^0 are chosen respectively. The foundation material is taken as normally consolidated clay which has undrained shear strength of 4 t/m^2 , and unit weight of 2.0 t/m^3. The thickness of the foundation layer is constant and equals to the height of the fill, H_e.

The factors of safety corresponding to the given soil profile and failure surface for each method are given in Table 5.1.

The values determined are plotted as a function of the slope height, H_e, and the fill material shear strength as shown in Figs. A.1 through A.5 in Appendix A.

To make the comparison of various analysis procedures a specific case (γ=2.1 t/m^3, ϕ=45^0) is studied. For this condition of the soil profile and failure surface shown in Fig.5.2 the corresponding

factors of safety are given in Table 5.1. The result of this study is shown in Fig.5.3.

The effect of the unit weight (γ) and the friction of angle (ϕ) of cohesionless fill material is studied using the typical embankment shown in Fig.5.2. The fill was assumed to consist of a homogeneous sand. It can be seen from the Figs. A.1. through A.5 in Appendix A that a large change in the value of ϕ results in a relatively small change in the factor of safety for each method. If the results of the study are considered, when the unit weight and the friction angle of the fill increases, the factor of safety decreases as shown in Figs A.1 through A.5. At the same time, it is found that the factor of safety decreases while the height of the fill which equals to the foundation thickness increases.

For the example slope shown in Fig.5.2, the values of the factor of safety calculated by the Modified Bishop procedure are about 7-9 % higher than the values obtained by the Ordinary Method of Slices. Due to differences in the corresponding normal stress distributions along the shear surface, the differences between the values of the factor of safety calculated by the Modified Bishop and Ordinary Method of Slices procedures should be considerably larger for inhomogeneous slopes of the type shown in Fig. 5.2 than for slopes in homogeneous soil conditions. On the other hand, the difference between the values of the factor of safety calculated by the Modified Bishop and Spencer's procedure is small. The values of the factor of safety obtained by Janbu's GPS procedure are similar to the values of the factor of safety calculated by the other methods. The values of the factor of safety obtained by Wedge Method is about 30 % less than the Janbu's GPS procedure value.All results

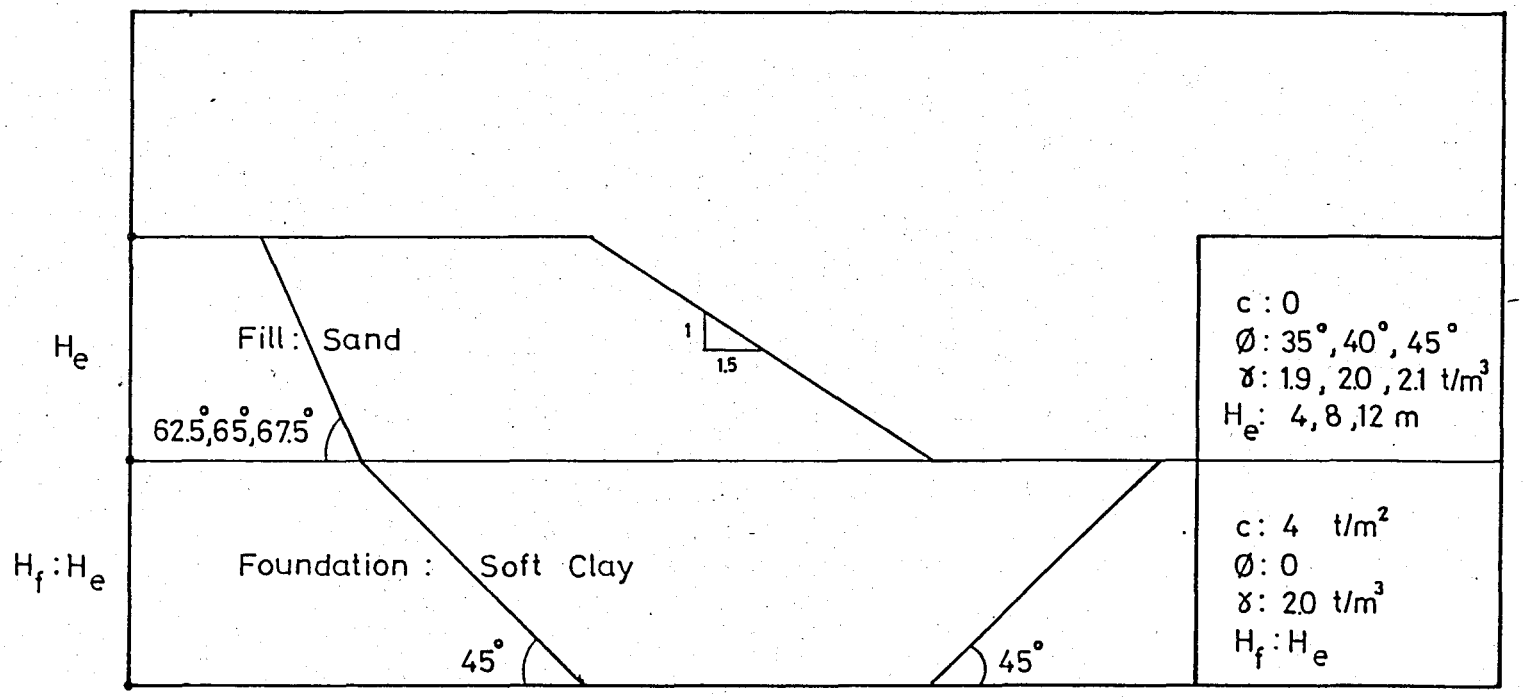

FIG.5.2 Dimensions and Properties of the Embankment and Foundation for Variable and Constant Fill Density

TABLE 5.1 Summary of Results

(for Variable Fill Density)

Fill Properties	Methods	Factor of Safety		
		Height of Fill, H_e, m		
		4.0	8.0	12.0
$\gamma = 1.9 t/m^3$, $\phi = 35^0$	OMS[1]	2.551	1.313	0.900
	BM[2]	2.736	1.434	0.984
	SM[3]	2.299	NC*	0.807
	GPS[4]	2.951	1.577	1.123
	WM[5]	2.288	1.238	0.867
$\gamma = 2.0 t/m^3$, $\phi = 40^0$	OMS	2.442	1.265	0.873
	BM	2.639	1.385	0.950
	SM	2.866	1.487	1.014
	GPS	2.860	1.561	1.090
	WM	2.236	1.210	0.845
$\gamma = 2.1 t/m^3$, $\phi = 45^0$	OMS	2.347	1.226	0.853
	BM	2.552	1.340	0.919
	SM	2.176	1.120	0.758
	GPS	2.798	1.526	1.064
	WM	2.194	1.183	0.821

1. Ordinary Method of Slices
2. Bishop's Modified Method
3. Spencer's Method
4. Janbu's Generalized Procedure of Slices
5. Wedge Method

*Solution did not converge

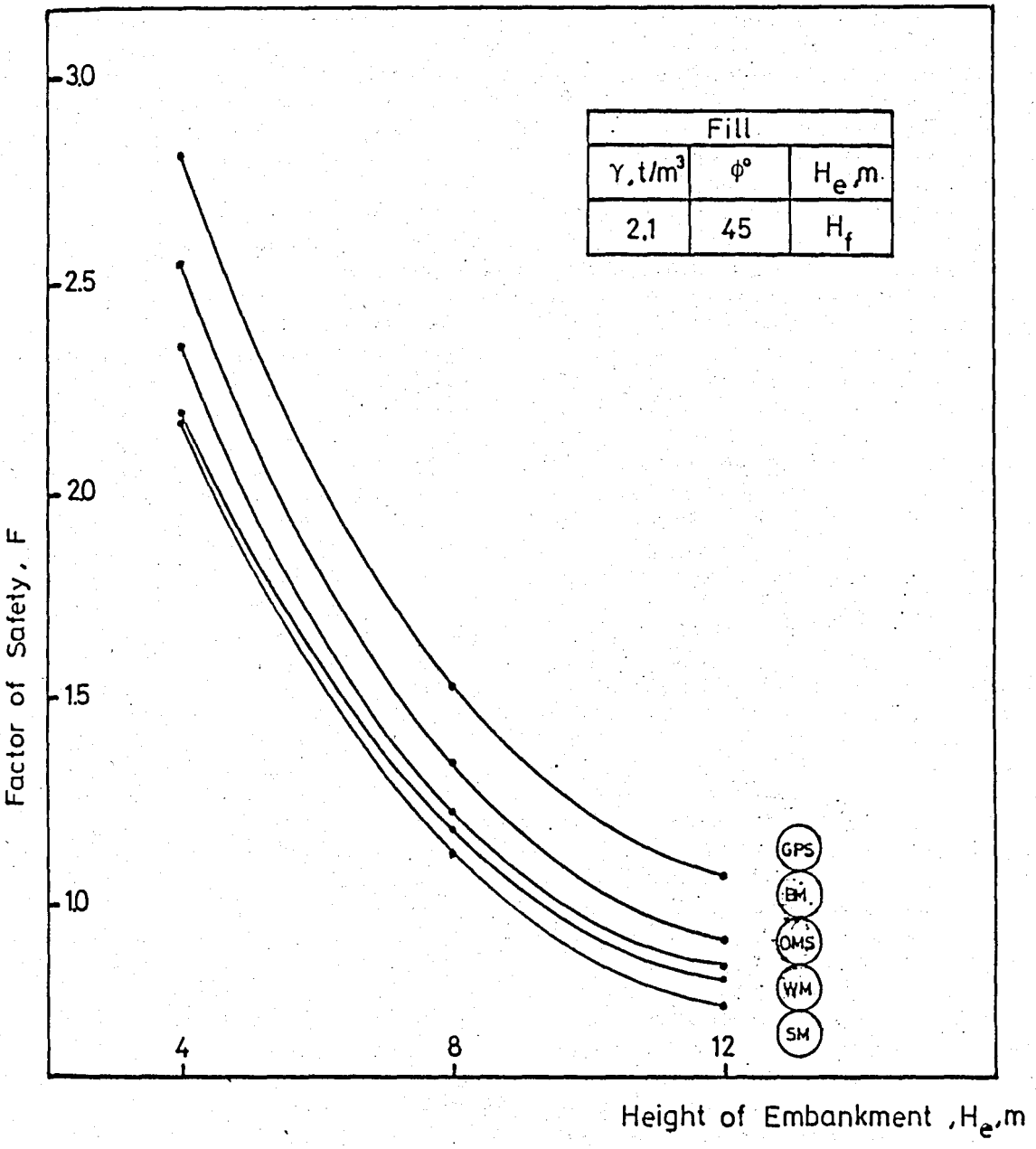

FIG.5.3 Variation of Factor of Safety with Embankment Height for Different Procedures (Variable Fill Density)

mentioned above are given in Fig.5.3.

5.3.2 For Constant Fill Density

In this analysis, the same soil cross-section and properties with the previous study which is shown in Fig. 5.2 are used. The only exception is that the fill material has a constant unit weight which is taken as γ=2.0 t/m^3 while the friction angle of the fill material is varied.

The safety factors corresponding to the given soil profile and failure surface for each method are given in Table 5.2. The values determined are plotted as a function of the fill height, H_e and the fill material shear strength as shown in Figs A.6 through A.10 in Appendix A.

The differences in the values of the factor of safety calculated by various procedures of analysis for a specific case (γ=2.0 t/m^3 and ϕ=45^0) may be conveniently represented by a family of curves. Such a family of curves is shown in Fig. 5.4.

The effect of the unit weight (γ) and the friction of angle (ϕ) of cohesionless fill material is again studied for constant fill density. The factor of safety increases while the internal friction angle of the fill increases as presented in Figs A.6 through A.10 in Appendix A. At the same time, it can be seen that the factor of safety decreases rapidly with increase in the height of the fill.

In this study, for the Ordinary Method of Slices and Bishop's Modified procedure similar results are obtained as mentioned previous subsection. The values of the factor of safety calculated by Spencer's procedure are slightly less than the value calculated by Janbu 's GPS procedure. The lowest values of the factor of safety in the analysis are obtained by the Wedge method.

TABLE 5.2 Summary of Results

(for Constant Fill Density)

Fill Properties	Methods	Factor of Safety		
		Height of Fill H_e, m		
		4.0	8.0	12.0
$\gamma = 2.0 t/m^3$, $\phi = 35^0$	OMS	2.427	1.251	0.858
	BM	2.608	1.367	0.938
	SM	2.831	1.469	1.003
	GPS	2.810	1.504	1.072
	WM	2.186	1.183	0.828
$\gamma = 2.0 t/m^3$, $\phi = 40^0$	OMS	2.442	1.265	0.873
	BM	2.639	1.385	0.950
	SM	2.866	1.487	1.014
	GPS	2.860	1.561	1.090
	WM	2.236	1.210	0.845
$\gamma = 2.0 t/m^3$, $\phi = 45^0$	OMS	2.459	1.282	0.890
	BM	2.670	1.403	0.962
	SM	2.898	1.505	1.023
	GPS	2.933	1.598	1.117
	WM	2.291	1.236	0.859

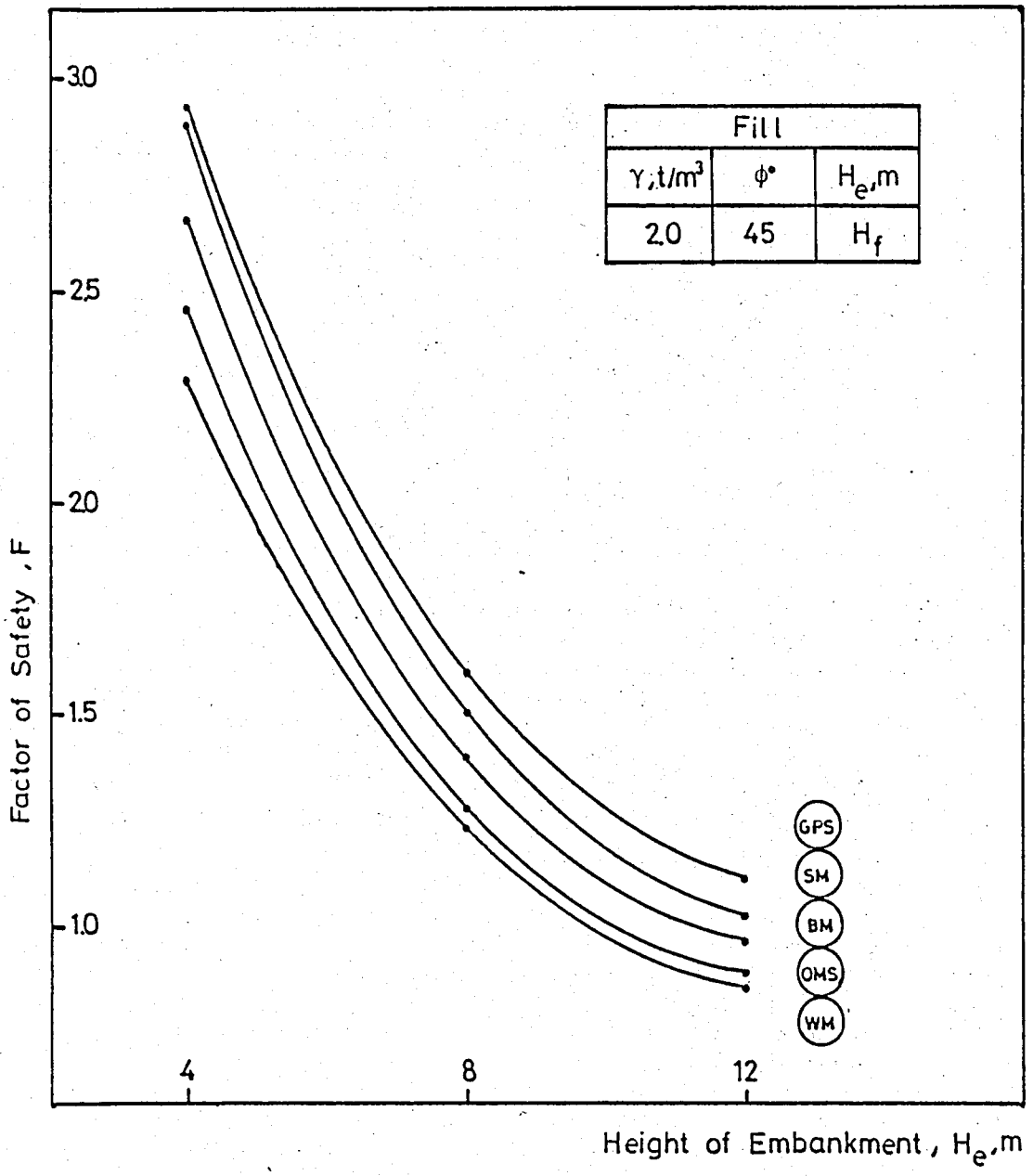

FIG.5.4 Variation of Factor of Safety with Embankment Height for Different Procedures (Constant Fill Density)

This case study is performed to study the effect of the foundation depth on the factor of safety. The foundation thickness H_f and the height of the fill, H_e, are varied while all other factors are held constant. Analyses are performed using three different foundation depth-4,6,8 m. For the height of the fill material three values as $H_e = H_f/2$, $H_f/3$, $H_f/4$ are chosen. The unit weight of both the fill material and foundation clay layer are taken as 2.0 t/m^3. The friction angle of fill material as $\phi=40^0$ and the cohesion intercept of the foundation clay layer as $c=3$ t/m^2 are taken. The geometry of the fill and the foundation, the properties of the fill and foundation material are shown in Fig.5.5. The safety factors corresponding to the given soil profile and failure surface for each method are given in Table 5.3 The values obtained during the investigation are plotted as a function of thickness of the foundation, H_f, and the height of fill, H_e, as given in Figs.A.11 through A.13 in Appendix A.

To present the variation of the factors of safety calculated by various procedures a specific case ($H_e=H_f/2$ and $\phi=40^0$) is studied. A family of curves is shown in Fig 5.6.

The effect of the thickness of the foundation is studied using three different depth values as mentioned above. As the thickness of the foundation increases, the factor of safety decreases. On the other hand, the factor of safety rapidly increases with decreasing height of the embankment. However, for Spencer's Method and Janbu's Generalized Procedure of Slices the reasonable solitions are not obtained because of the non-convergence.

It can be seen from Fig.5.6 that the values of the factor of safety calculated by the Modified Bishop procedure are about 3-5%

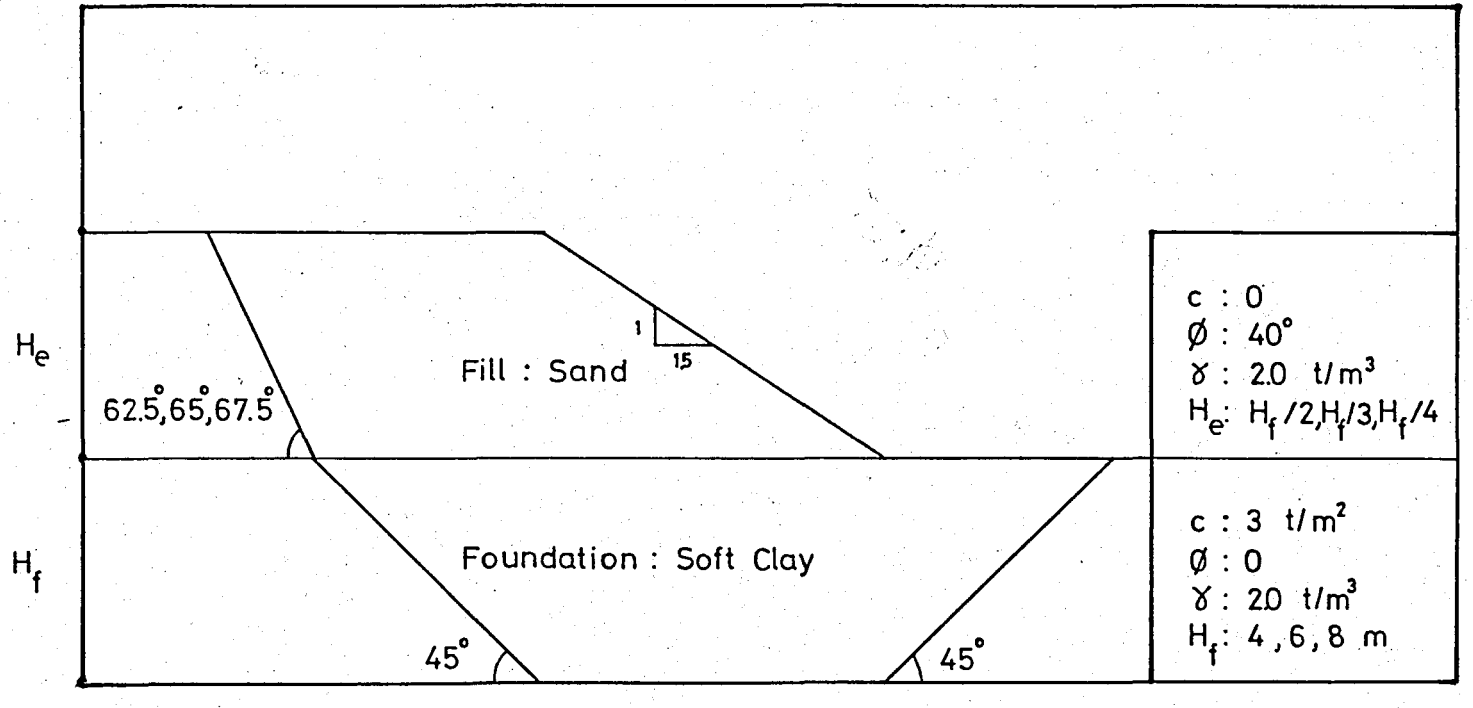

FIG.5.5 Geometry and Soil Properties of the Embankment and Foundation for the Effect of Foundation Depth

TABLE 5.3 Summary of Results

(for the Effect of Foundation Depth)

Height of Fill	Methods	Factor of Safety		
		Foundation Depth H_f, m		
		4.0	6.0	8.0
$H_e = H_f/2$	OMS	3.913	2.623	1.975
	BM	4.055	2.735	2.067
	SM	3.963	2.666	1.999
	GPS	NC	3.411	NC
	WM	3.121	2.137	1.634
$H_e = H_f/3$	OMS	6.141	4.069	3.074
	BM	6.254	4.162	3.151
	SM	NC	NC	NC
	GPS	NC	NC	1.775
	WM	4.558	3.085	2.352
$H_e = H_f/4$	OMS	8.415	5.586	4.181
	BM	8.505	5.663	4.248
	SM	NC	NC	NC
	GPS	NC	NC	NC
	WM	6.003	4.054	3.068

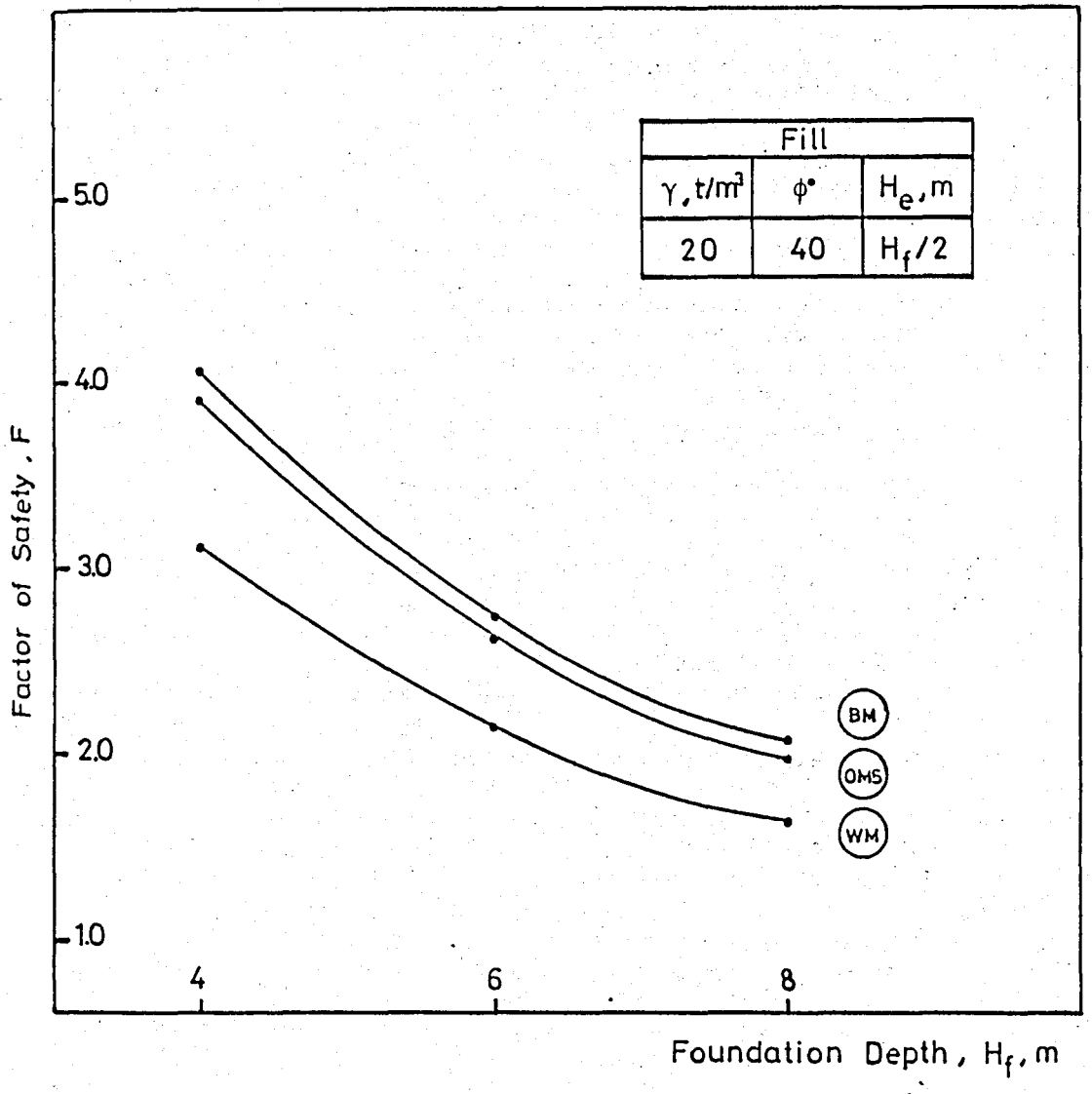

FIG.5.6 Variation of Factor of Safety with Foundation Depth for Different Procedures

higher than the values obtained by the Ordinary Method of Slices. The values of the factor of safety obtained by the Wedge procedure are greatly less than the Modified Bishop value. For Spencer's procedure and Janbu's GPS procedure a reasonably convergent solution could not be obtained.

5.5 EFFECT OF VARIABLE SHEAR STRENGTH OF FOUNDATION

In order to find the factor of safety of the typical case of the soil profile and failure surface shown in Fig.5.7, the friction angle of fill, ϕ, and the cohesion intercept of the foundation, c, are varied while all other factors are held constant. The parameters used in these analyses are shown in Fig 5.7. Analyses are performed using three different internal friction angle of the fill material- 35^0 , 40^0 , 45^0. For shear strength of the clay layer again four values as c=1,2,4,6 t/m^2 are chosen. The unit weight of both the fill material and foundation clay layer are taken as 2.0 t/m^3. The slope height, H_e, is taken as 4 m and the foundation clay layer depth , H_f is constant and equals to the slope height, H_e.

The safety factors corresponding to the given soil profile and failure surface for each method are given in Table 5.4. The values obtained during the investigation are plotted as a function of the shear strength of the foundation, c, and the friction angle of fill, ϕ, as shown in Figs A.14 through A.18 in Appendix A.

On the other hand, for $\phi=35^0$ a family of curves showing the variation of the factor of safety for each method is given in Fig.5.8.

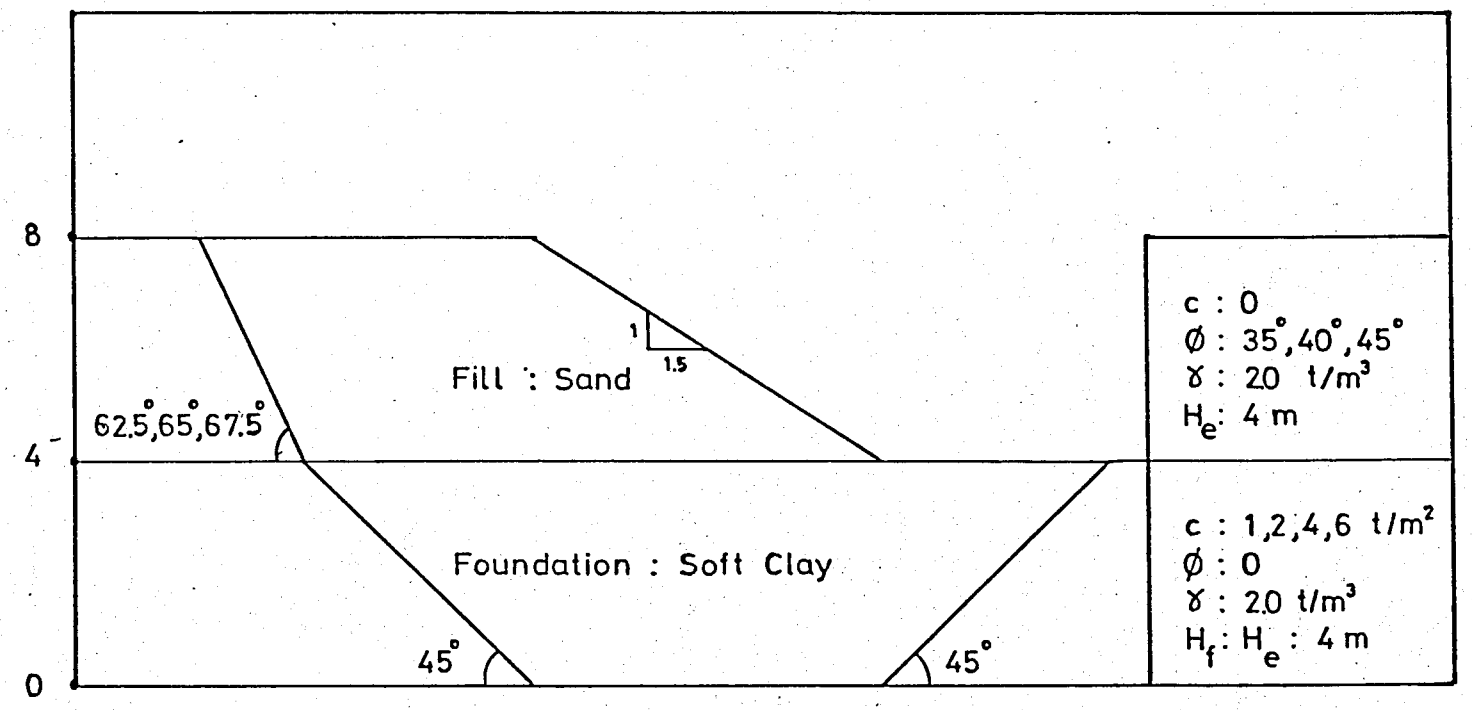

FIG.5.7 Dimensions and Properties of the Embankment and Foundation for Variable Shear Strength of Foundation

TABLE 5.4 Summary of Results

(for Variable Shear Strength of Foundation)

Shear Strength of Foundation	Methods	Factor of Safety		
		Friction Angle of Fill, ϕ^0		
		35^0	40^0	45^0
c = 1 t/m^2	OMS	0.662	0.677	0.694
	BM	0.718	0.727	0.735
	SM	0.749	0.752	NC
	GPS	0.836	0.854	0.875
	WM	0.643	0.653	0.661
c = 2 t/m^2	OMS	1.251	1.265	1.282
	BM	1.367	1.385	1.403
	SM	1.469	1.487	1.496
	GPS	1.504	1.561	1.598
	WM	1.183	1.210	1.236
c = 4 t/m^2	OMS	2.427	2.442	2.459
	BM	2.608	2.639	2.670
	SM	2.831	2.866	2.898
	GPS	2.810	2.860	2.933
	WM	2.186	2.236	2.291
c = 6 t/m^2	OMS	3.604	3.619	3.636
	BM	3.819	3.858	3.900
	SM	4.163	4.218	4.277
	GPS	4.096	4.170	4.256
	WM	3.150	3.125	3.294

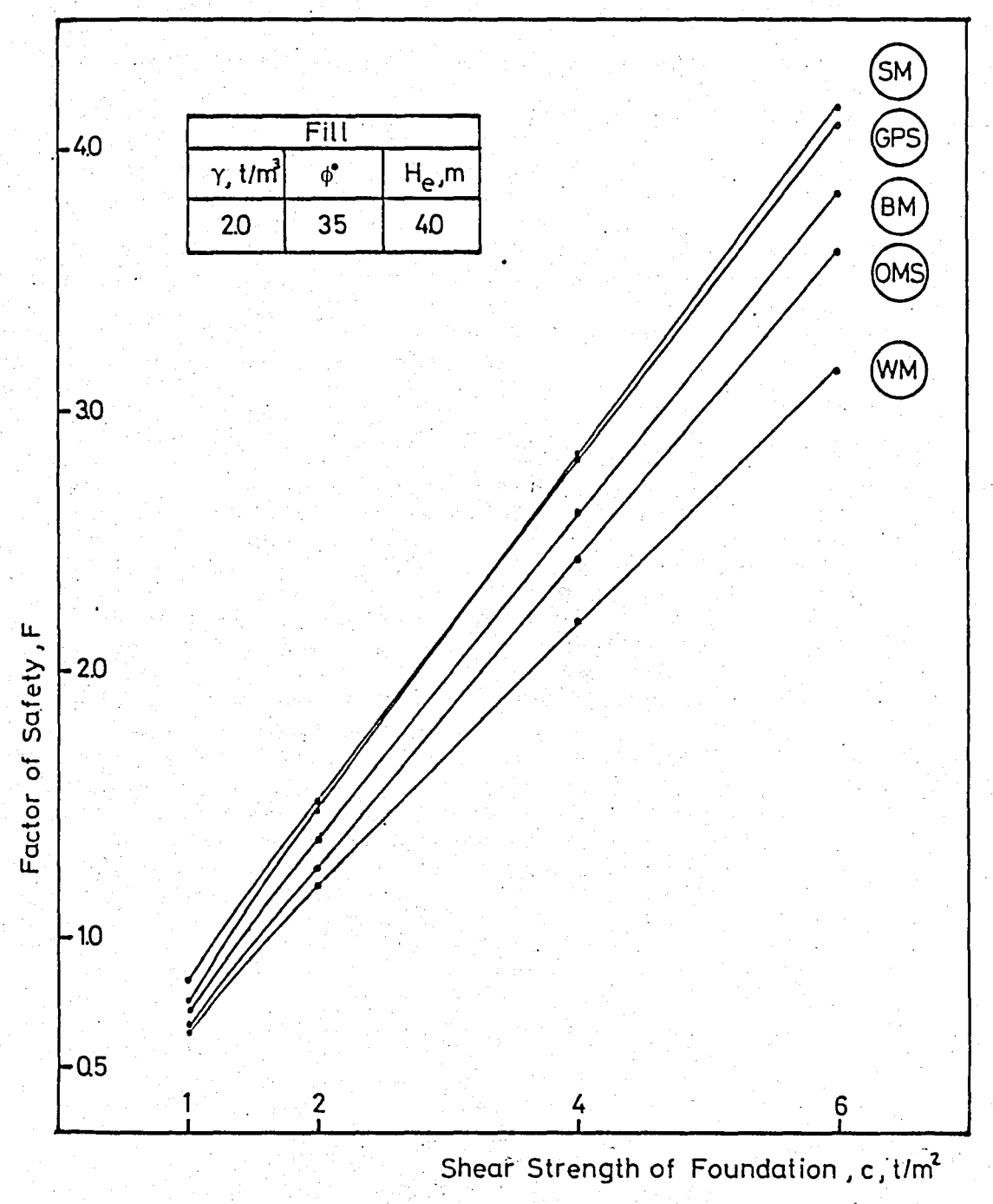

FIG.5.8 Variation of Factor of Safety with Variable Shear Strength of Foundation for Different Procedures

The effect of variable shear strength of foundation is studied using four different shear strength values as mentioned above. As the variable shear strength of foundation increases, the factor of safety rapidly increases. At the same time, the factor of safety also increases with increasing friction angle of the fill. However, it can be seen that a large change in the value of ϕ results in a relatively small change in the factor of safety. As shown in Figs A.14 through A.18 the factor of safety increases in direct proportion to the shear strength of foundation between the values of 2 and 6.

The results in Fig.5.8, show that the values of the factor of safety calculated by the Ordinary Method of Slices are almost 6-9% less than the values calculated by Bishop's Modified method. The difference between the values of the factor of safety obtained by Spencer's procedure and Janbu's GPS procedure is small. Wedge method appears to give very similar results.

5.5.1 The Use of Dimensionless Parameter

In these analyses, it is observed the variation of the factor of safety with respect to a dimensionless parameter in order to obtain directly the value of the factor of safety when foundation shear strength is known. The dimensionless parameter, d, is given as follows :

$$d = \frac{c}{\gamma_e H_e} \qquad \ldots (5.1)$$

where

c = foundation shear strength

γ_e = unit weight of the fill material

H_e = height of the fill material

For each value of which is shown in Table 5.4 the dimensionless parameter is calculated by the equation mentioned above and is given in Table 5.5. The friction angle of fill, ϕ, and the cohesion intercept of the foundation, c, are varied while all other factors are held constant. These parameters are shown in Fig.5.7. Analyses are performed using three different internal friction angle of the fill material-35^0, 40^0, 45^0. For shear strength of the clay layer again four values as c=1,2,4,6 t/m^2 are chosen. The unit weight of both the fill material and foundation clay layer are taken as 2.0 t/m^3. The slope height, H_e, is taken as 4 m and the foundation clay layer thickness, H_f is held constant being equal to the slope height, H_e.

The graphs which are given in Figs A.19 through A.23 in Appendix A show the variation of the factor of safety, as a function of the dimensionless parameter, d, and the internal friction angle of the fill material.

The comparison of the various procedures is shown in Fig. 5.9. These curves are given for the case which $\phi=35^0$.

The results of the analyses are shown in Figs A.19 through A.23 . It is found that as the dimensionless parameter increases, the factor of safety increases. It is also seen that while the friction angle of the fill increases, the factor of safety increases. Between the dimensionless parameter values of 0.25 and 0.75 the factor of safety increases in direct proportion to the dimensionless parameter. Moreover, it decreases with the increasing values of the slope height and the unit weight of the fill material.

It can be seen from Fig. 5.9 that the variation of the factor of safety for each method is the similar with the previous study.

TABLE 5.5 Summary of Results

(for Dimensionless Parameter)

Dimensionless parameter	Methods	Factor of Safety		
		Friction Angle of Fill, ϕ^0		
		35^0	40^0	45^0
$c = 1 t/m^2$, d = 0.125	OMS	0.662	0.677	0.694
	BM	0.718	0.727	0.735
	SM	0.749	0.752	NC
	GPS	0.836	0.854	0.875
	WM	0.643	0.653	0.661
$c = 2 t/m^2$, d = 0.250	OMS	1.251	1.265	1.282
	BM	1.367	1.385	1.403
	SM	1.469	1.487	1.496
	GPS	1.504	1.561	1.598
	WM	1.183	1.210	1.236
$c = 4 t/m^2$, d = 0.500	OMS	2.427	2.442	2.459
	BM	2.608	2.639	2.670
	SM	2.831	2.866	2.898
	GPS	2.810	2.860	2.933
	WM	2.186	2.236	2.291
$c = 6 t/m^2$, d = 0.750	OMS	3.604	3.619	3.636
	BM	3.819	3.858	3.900
	SM	4.163	4.218	4.277
	GPS	4.096	4.170	4.256
	WM	3.150	3.215	3.294

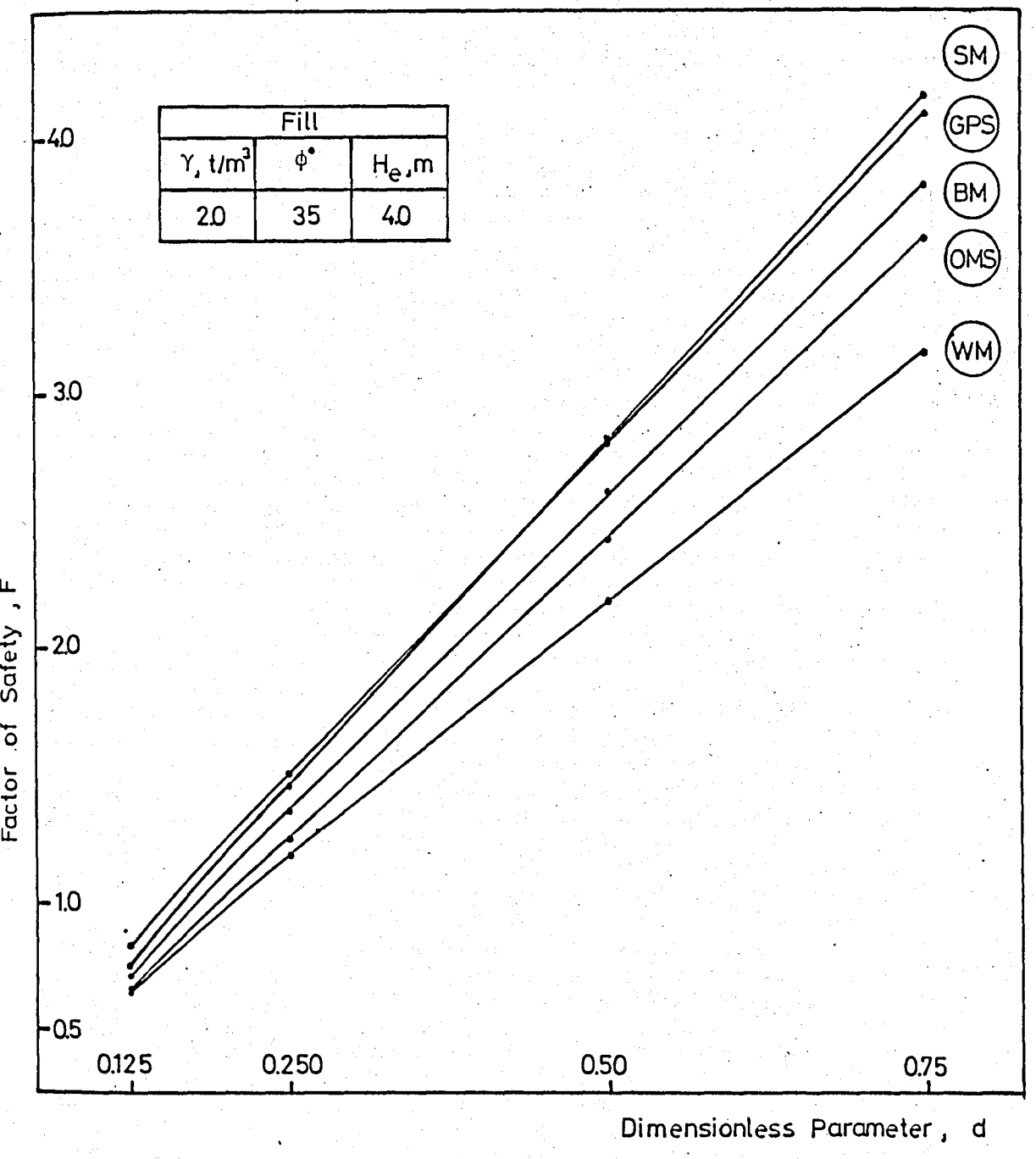

FIG.5.9 Variation of Factor of Safety with Dimensionless Parameter for Different Procedures (Variable Shear Strength of Foundation)

5.6 EFFECT OF LINEAR VARIATION OF FOUNDATION SHEAR STRENGTH

In this case for investigation of the effect of the linear variation of foundation shear strength on the factor of safety using different methods this parametric study is performed. The rate of the shear strength of the clay layer is shown as the following expression.

$$v = \frac{dc}{dz} \qquad \ldots(5.2)$$

where

c= cohesion intercept of the foundation material

z= depth of foundation from which the failure surface passes.

In order to obtain the factor of safety, cross-section of the typical embankment analyzed is shown in Fig.5.10

5.6.1 Cohesion Intercept at the Foundation Surface, c=0

The soil profile and failure surface considered in this study are shown in Fig. 5.10. The values of the internal friction angle, ϕ, of the fill material and the rate of the cohesion intercept with respect to the depth of the foundation, v, are varied. Analyses are performed again using three different internal friction angle of the fill material 35^0, 40^0,45^0. For the rate of the increase in shear strength of the clay layer four values v=1,5, 3, 4.5,6 $t/m^2/m$ are chosen by considering that the cohesion intercept value of the foundation at the foundation surface is taken as c=0 t/m^2 for each v value.

The unit weight of both the fill material and foundation clay layer are taken as 2.0 t/m^3. The slope height, H_e, is taken as 4 m and the foundation clay layer thickness, H_f is constant and equal to the slope height, H_e.

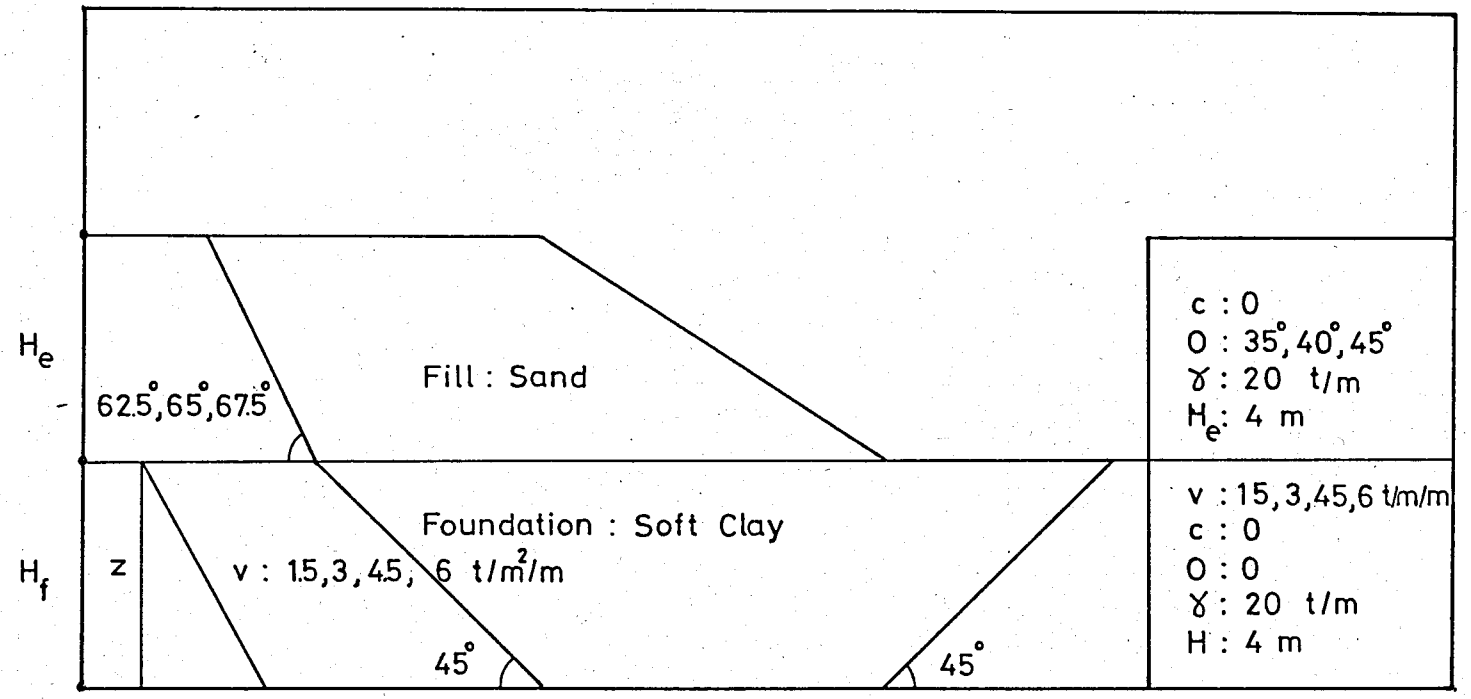

FIG.5.10 Dimensions and Properties of the Embankment and Foundation for Linear Variation of Foundation Shear Strength

TABLE 5.6 Summary of Results (c=0)

(for Linear Variation of Foundation Shear Strength)

v, $t/m^2/m$	Methods	Factor of Safety		
		Friction Angle of Fill, ϕ		
		35^0	40^0	45^0
1.5	OMS	2.385	2.399	2.416
	BM	2.563	2.594	2.625
	SM	2.974	3.014	3.055
	GPS	2.951	3.005	3.088
	WM	2.096	2.146	2.200
3.0	OMS	4.696	4.710	4.727
	BM	4.931	4.975	5.024
	SM	5.791	5.858	5.935
	GPS	5.677	5.746	NC
	WM	3.925	4.000	4.090
4.5	OMS	7.006	7.020	7.038
	BM	7.268	7.320	7.379
	SM	8.599	8.685	8.791
	GPS	8.327	8.468	NC
	WM	5.710	5.803	5.920
6.0	OMS	9.317	9.331	9.349
	BM	9.594	9.652	9.716
	SM	11.420	11.516	11.641
	GPS	11.039	NC	NC
	WM	7.480	7.587	7.720

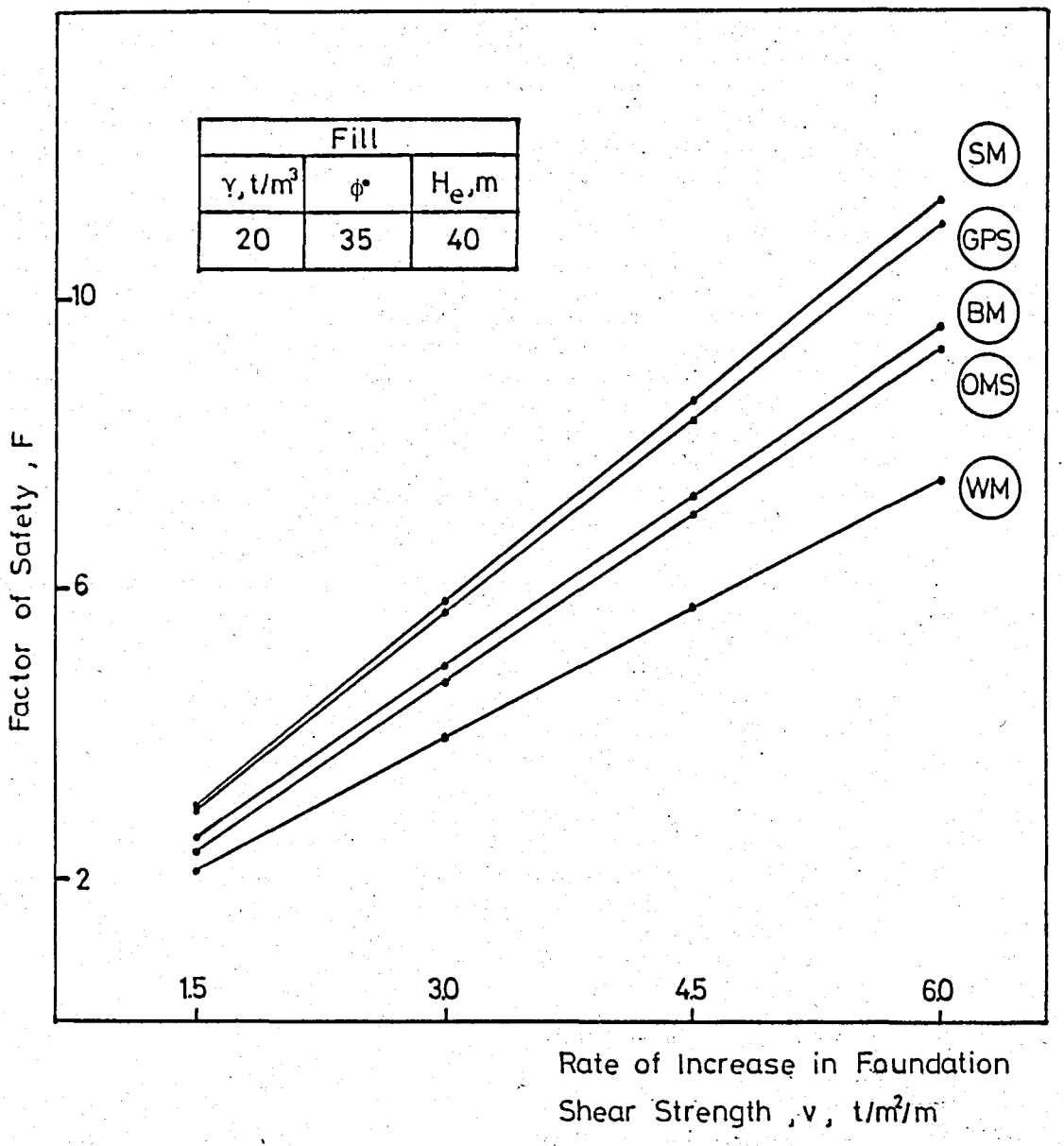

FIG.5.11 Variation of Factor of Safety with Rate of Increase in Foundaiton Shear Strength for Different Procedures (c=0)

The safety factors corresponding to the given soil profile and failure surface for each method are given in Table 5.6. The values obtained are plotted as a function of the internal friction angle of the fill, ϕ, and the rate of increase in the cohesion intercept with respect to the depth of the foundation ,v, as shown in Figs. A.24 through A.28 in Appendix A.

The values of the factors of safety calculated for a specific case using various procedures of analysis are also shown in Fig.5.11.

When both the rate of the cohesion intercept with respect to the depth of the foundation and the friction angle of the fill increase, the factor of safety increases. As shown in Figs. A. 24 through A.28, the factor of safety increases in direct proportion to the rate of the cohesion intercept with respect to the depth of the foundation.

The results in Fig.5.11 show that the maximum difference between the Ordinary Method of Slices and Bishop's procedure does not exceed 7 % for the case studied. The values of the factor of safety calculated by Spencer's procedure are virtually identical to the values calculated by Janbu's GPS procedure. The similar results are also obtained by Wedge method.

5.6.2 Finite Value of Cohesion Intercept at the Foundation Surface

This case study is also performed on a typical embankment with the same cross-section shown in Fig.5.10. The values of the internal friction angle ,ϕ, of the fill material and the rate of the cohesion intercept with respect to the depth of the foundation ,v, are varied. Case study is performed for three different internal friction angle of

the fill material 35^0, 40^0, 45^0. For the rate of the shear strength of the foundation four values v = 1.5,3,4.5,6, $t/m^2/m$ are chosen. The cohesion intercept value of the foundation clay layer at the foundation surface is assumed as c=2 t/m^2 for each v value.

The unit weight of both the fill material and foundation clay layer are taken as 2.0 t/m^3. The slope height, H_e, is taken as 4 m and the foundation clay layer depth, H_f is constant and equals to the slope height, H_e.

For the given slip circle of the embankment shown in Fig. 5.10 the values of factor of safety calculated by various methods are summarized in Table 5.7. The values obtained are plotted as a function of the internal friction angle of the fill, ϕ, and the rate of the cohesion intercept with respect to the depth of the foundation, v, as shown in Figs. A.29 through A.39 in Appendix A.

For the case which ϕ=35 the comparison of the various procedures is given in Fig.5.12.

The results of these analyses, which are shown in Figs. A.29 through A.33, show that the greater the friction angle of the fill, the greater the factor of safety. It is also seen that the rate of the cohesion intercept with respect to the foundation depth is directly proportional to the factor of safety. The results of this analysis are the similar with the results of the analysis for c=0.

It can be seen from Fig.5.12 that the values of the factor of safety calculated by the Modified Bishop procedure are almost 3-6% greater than the values obtained by the Ordinary Method of Slices.The values of the factor of safety calculated by Spencer procedure and Janbu's GPS procedure are identical to the values obtained by the other

TABLE 5.7 Summary of Results ($c=2\ t/m^2$)
(for Linear Variation of Foundation Shear Strength)

v, $t/m^2/m$	Methods	Factor of Safety		
		Friction Angle of Fill, ϕ		
		35^0	40^0	45^0
1.5	OMS	3.561	3.576	3.593
	BM	3.775	3.814	3.855
	SM	4.304	4.359	4.424
	GPS	4.223	4.320	4.404
	WM	3.062	3.127	3.205
3.0	OMS	5.872	5.886	5.904
	BM	6.123	6.172	6.226
	SM	7.125	7.193	7.288
	GPS	6.932	7.046	NC
	WM	4.861	4.950	5.054
4.5	OMS	8.183	8.197	8.215
	BM	8.453	8.509	8.571
	SM	9.928	10.016	10.134
	GPS	9.625	NC	NC
	WM	6.642	6.740	6.860
6.0	OMS	10.494	10.508	10.525
	BM	10.777	10.836	10.903
	SM	12.730	12.849	12.983
	GPS	12.315	NC	NC
	WM	8.410	8.510	8.650

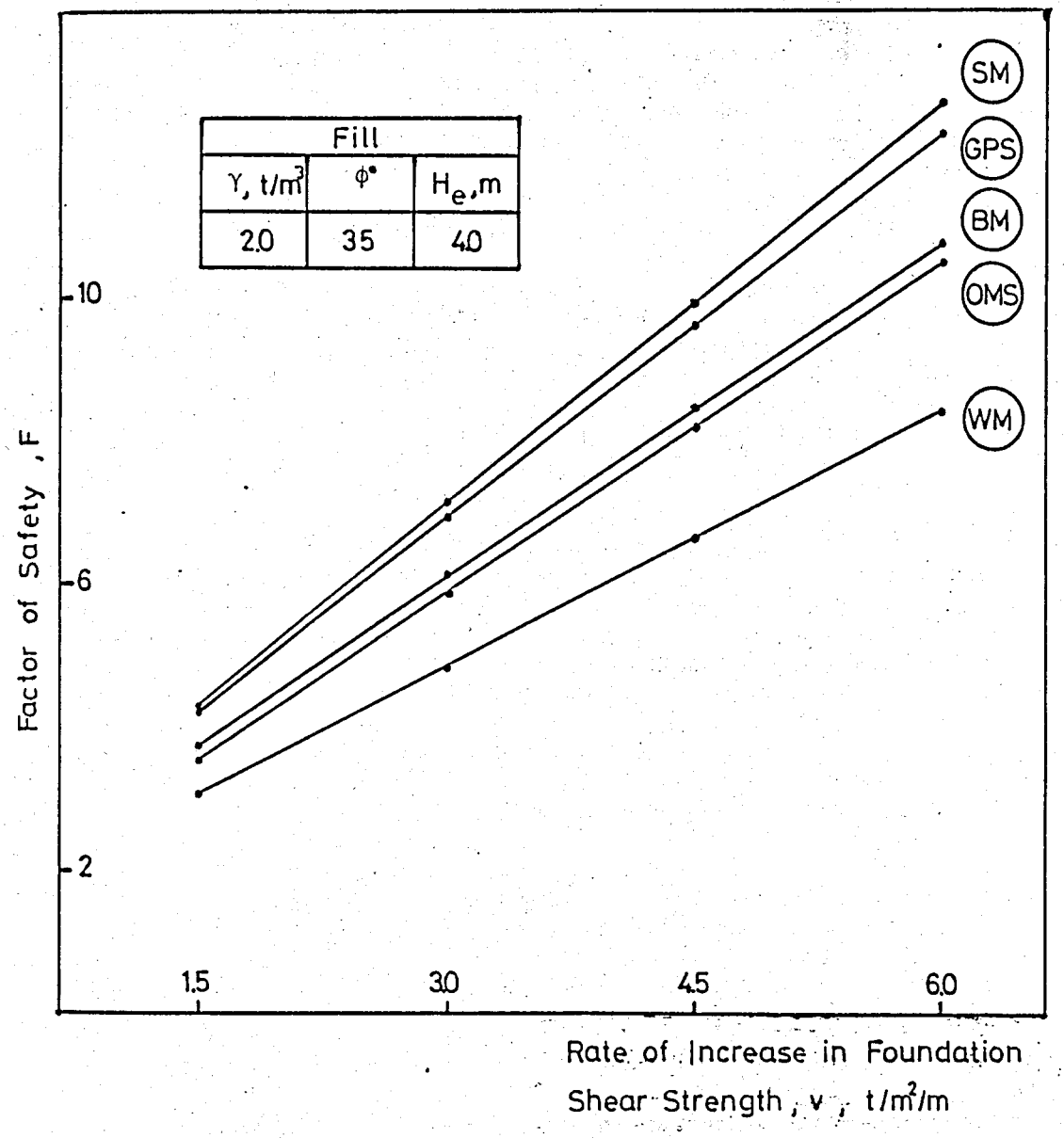

FIG.5.12 Variation of Factor of Safety with Rate of Increase in Foundation Shear Strength for Different Procedures ($c=2\ t/m^2$)

methods. The values calculated by Wedge method are greatly less than the Spencer's procedure.

5.6.3 The Use of Dimensionless Parameter

The purpose of this study is to obtain the variation of the factor of safety with respect to a dimensionless parameter, a

$$a = \frac{vh}{\gamma_e H_e} \qquad \ldots (5.3)$$

where

v = rate of the foundation shear strength

h = depth within the foundation from which the failure surface passes.

γ_e=unit weight of the fill

H_e=height of the fill

In order to obtain directly the value of the factor of safety when the rate of the foundation shear strength is known, for each value of which is shown in Table 5.6 the dimensionless parameter, a, is calculated by the equation mentioned above and is given in Table 5.8. The parameters which are used in this analysis are the same as the study which is given in section 5.5.1.The soil profile is also shown in Fig.5.10.The results are plotted as a function of the internal friction angle of the fill, ϕ, and the dimensionless parameter, a , as presented in Figs A.34 through A.38 in Appendix A.

For the variation of the factors of safety calculated by various procedures a specific case (ϕ=35^0) is investigated. A family of curves is shown in Fig 5.13.

TABLE 5.8 Summary of Results
(for Dimensionless Parameter)

Dimensionless Parameter	Methods	Factor of Safety		
		Friction angle of Fill, ϕ		
		35^0	40^0	45^0
a = 0.75	OMS	2.385	2.399	2.416
	BM	2.563	2.594	2.625
	SM	2.974	3.014	3.055
	GPS	2.951	3.005	3.088
	WM	2.096	2.146	2.200
a = 1.5	OMS	4.696	4.710	4.727
	BM	4.931	4.975	5.024
	SM	5.791	5.858	5.935
	GPS	5.677	5.746	NC
	WM	3.925	4.000	4.090
a = 2.25	OMS	7.006	7.020	7.038
	BM	7.268	7.320	7.379
	SM	8.599	8.685	8.791
	GPS	8.327	8.468	NC
	WM	5.710	5.803	5.920
a = 3	OMS	9.317	9.331	9.349
	BM	9.594	9.652	9.716
	SM	11.420	11.516	11.641
	GPS	11.039	NC	NC
	WM	7.480	7.587	7.720

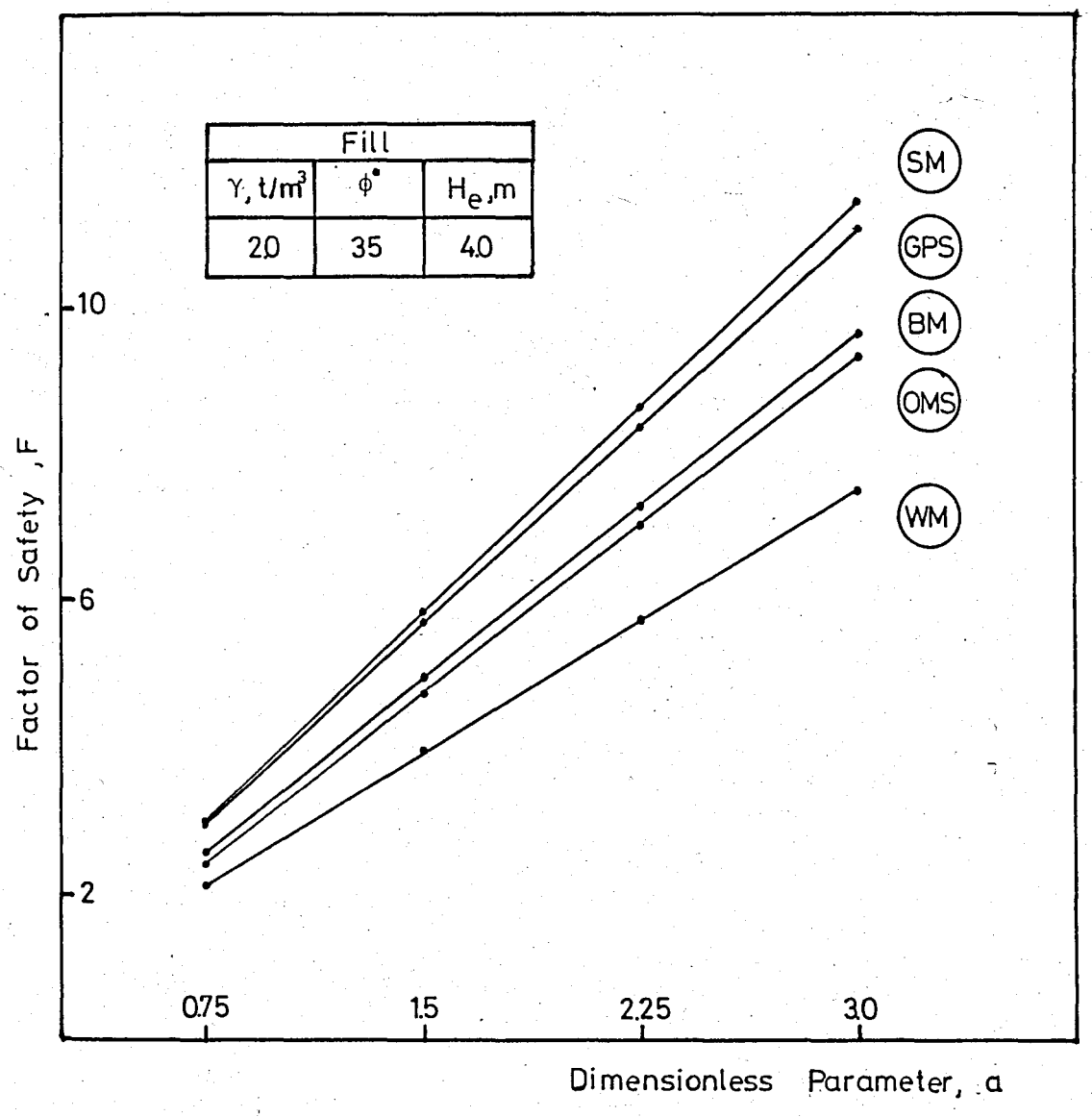

FIG.5.13 Variation of Factor of Safety with Dimensionless Parameter for Different Procedures (Linear Variation of Foundation Shear Strength)

From the results it can be seen that the factor of safety increases in direct proportion to the dimensionless parameter, a, while the friction angle of the fill increases. The increase of the unit weight and the height of the fill material have decreasing effect on the factor of safety.

The differences in the values of the factor of safety calculated by various procedures for a specific case which are shown in Fig. 5.13, follow a pattern very similar to that shown previously.

5.7 SUMMARY

The stability of fill slopes built on soft subsoils depends on (a) strength of the fill, as characterized by the parameters c and ϕ, (b) the unit weight of the fill, (c) the height of the fill, (d) the slope angle, (e) the strength of the foundation, as characterized by the parameters c and ϕ. The critical failure mechanism is usually sliding on a deep surface tangent to the top of a firm layer within the foundation. A large part of the failure surface lies within the foundation, especially in cases where the soft subsoils extend to great depths, and the stability of the embankment depends to a large extent on the strength of the foundation soils.

The purpose of this chapter is to show, by means of various examples, the effect of embankment and foundation shear strength on factor of safety calculated by various procedures for a typical case of the soil profile and failure surface. In these studies the embankment is a sand fill on a normall consolidated clay foundation. Additionally, a comparison of various procedures and the effects of these methods on factor of safety are also made in each subsequent section.

When the results of the Chapter 5 are examined it can be seen that while the friction angle of the fill increases for variable fill density, the factor of safety decreases, but for constant fill density the factor of safety increases. On the other hand,for both the variable and constant fill density as the height of the fill increases, the factor of safety decreases.

As the thickness of the foundation increases, the factor of safety decreases. On the other hand, the factor of safety rapidly increases with decreasing height of the embankment.

If one considers the effect of the variable shear strength of foundation it is found that the factor of safety increases with increasing foundation strength and also increases while the friction angle of the fill increases.

The findings of the studies for given slope profile for variable foundation shear strength result lower factor of safety when compared to the linear variation of foundation shear strength. As shown in this chapter, the factor of safety increases in direct proportion to the rate of the cohesion intercept with respect to the depth of foundation.

The comparison of various procedures for a specific case indicates that relatively large differences in the values of the factor of safety may exist even for analyses by procedures satisfying complete equilibrium. The most important factor influencing the values of the factor of safety appears to be the result of different in the normal stress distributions along the shear surface.

In these analyses,the computer programs which are SLOPE 22R, SLOPE 8R, SLOPE 9, WEDGE 1 are used and the results obtained from the analyses are given at each subsequent section.

CHAPTER 6

EFFECT OF FOUNDATION SHEAR STRENGTH ON MINIMUM FACTOR OF SAFETY

6.1 INTRODUCTION

In the previous chapter, using various procedures the effect of embankment and foundation shear strength on the calculated factors of safety for typical embankments on soft foundations have been performed and the results have been discussed in detail.

The studies presented in this chapter were performed so as to determine the effect of foundation shear strength on the minimum factors of safety for a given embankment. The case studies in this chapter are given in two sections. In the first section, case analyzed for the effect of constant shear strength of foundation on minimum factor of safety, are presented. In the second section, other case study is given, in which, the effect of linear variation of foundation shear strength on minimum factor of safety is investigated. For this purpose, the computer program WEDGE 2 is also developed in this study.

6.2 FOR CONSTANT SHEAR STRENGTH OF FOUNDATION

The effect of the constant shear strength (c) of foundation is studied using the embankment shown in Fig. 6.1. The height of the fill is given as 4 meters and the depth of the bedrock is located at 8.0 meters below ground surface. It is assumed that an average shear strength of the foundation material is given as c_{ave}=3 t/m^2. The parameters used in this analysis are shown in Fig.6.1. Analyses are performed using three different internal friction angle of the fill material 35^0, 40^0, 45^0. For unit weight of the sand layer again three different values as γ_f=1.9, 2.0, 2.1 t/m^3 are chosen respectively. The foundation material has unit weight of 2.0 t/m^3.

The results of the study are tabulated in Tables B.1-B.3 which are given in Appendix B for Ordinary Method of Slices and Bishop's Modified Method.

For Spencer's Method, Janbu's Generalized Procedure of Slices and Wedge Method,to investigate the minimum factor of safety, the cross-sections typical of the embankments analyzed are shown in Fig. 6.2. In each of these cases, the properties of the fill and the foundation material are the same shown in Fig.6.1. The results of these analyses are tabulated in Table B.4 for these methods.

The results for all methods are summarized in Table 6.1. The values obtained during the investigation are plotted as a function of the friction angle of the fill material, ϕ, as shown in Fig. 6.3. It can be seen that a large change in the value of ϕ results in a relatively small change in the factor of safety for each method. Reducing ϕ from 45 to 35 results in an increase of only about 5 %

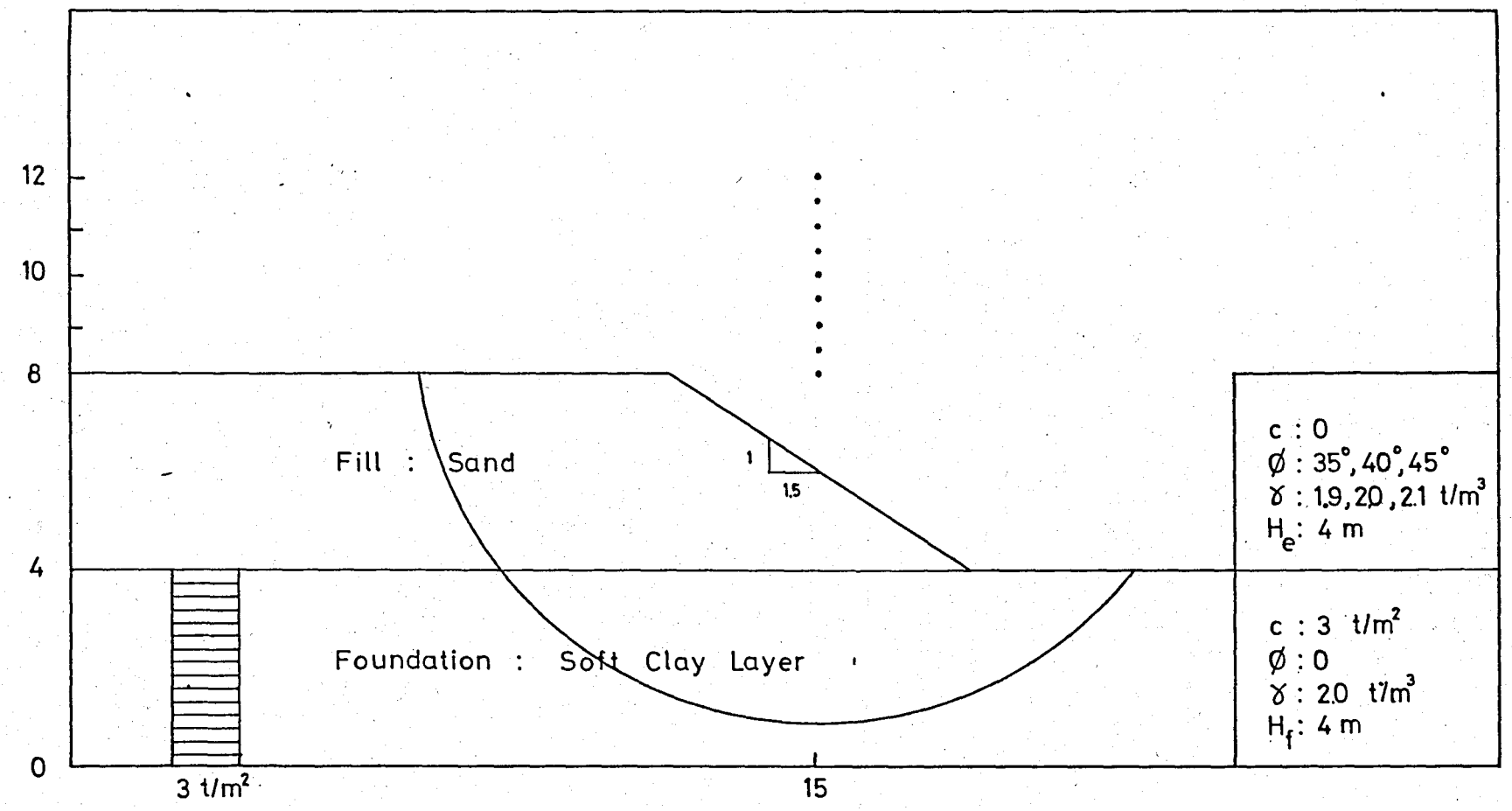

FIG.6.1 Geometry and Soil Properties of the Embankment and Foundation, and the Circular Failure Surface Used in the Analyses (For Constant Shear Strength of Foundation)

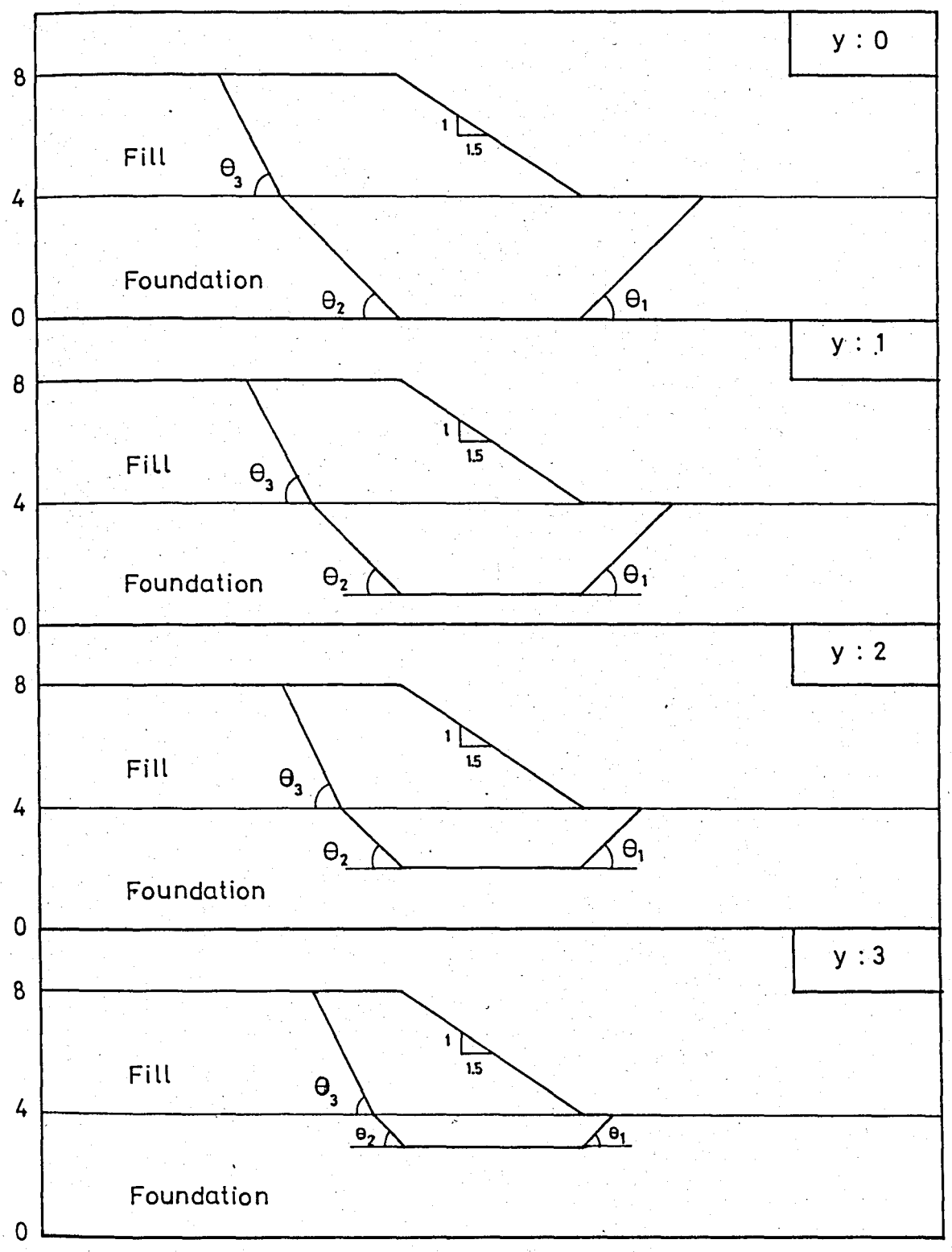

FIG.6.2 Dimensions and Profiles of the Embenkment and Foundation, and the Failure Surfaces Used in the Analyses

TABLE 6.1 Summary of Results
(for Constant Shear Strength of Foundation)

Fill Properties	Factor of Safety				
	OMS	BM	SM	GPS	WM
$\gamma = 1.9 t/m^3$ $\phi = 35^0$	1.882	2.084	1.695	2.271	1.764
$\gamma = 2.0 t/m^3$ $\phi = 40^0$	1.833	2.015	1.976	2.150	1.726
$\gamma = 2.1 t/m^3$ $\phi = 45^0$	1.780	1.952	1.379	2.162	1.690

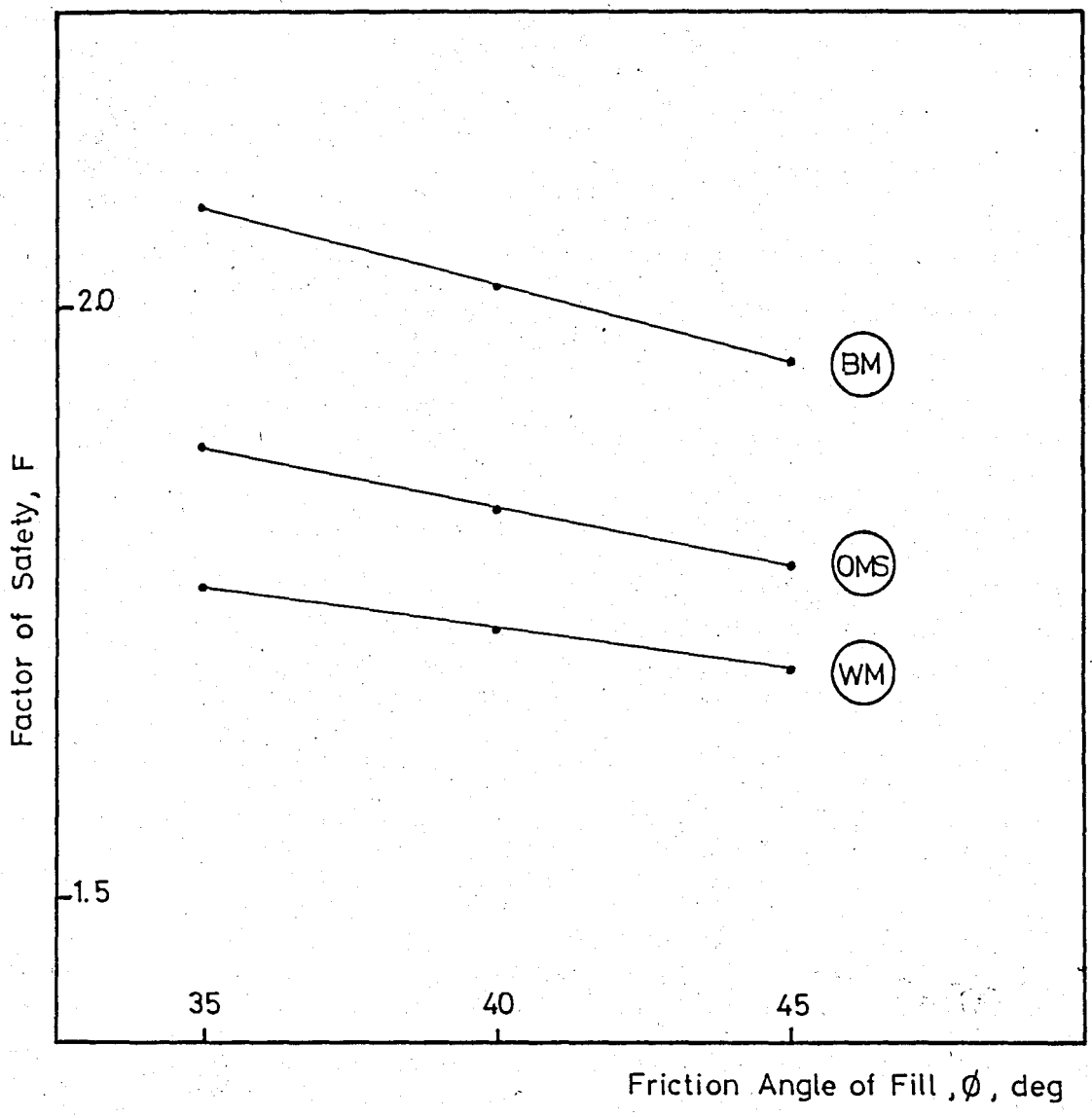

FIG.6.3 Variation of Factor of Safety with Friction Angle of Cohesionless Fill Material for Different Procedures (Constant Shear Strength of Foundation)

on the factor of safety. The factor of safety decreases in direct proportion to the friction angle and unit weight of the fill.

Variation of the factor of safety with the friction angle of the fill is almost the similar exhibiting straight lines throughout the analysis except for the results of the Spencer's Method and Janbu's Generalized Procedure of Slices. It is observed that the deep circles give smaller factor of safety than the toe circles for the Modified Bishop's Method and Ordinary Method of Slices. It can be seen from Tables B.1 through B.3 the circles studied by the Modified Bishop's Method go deeper than circles obtained by Ordinary Method of Slices. On the other hand, for Wedge Method the deeper failure surfaces give the smaller factor of safety as shown in Table B.4

6.3 FOR LINEAR VARIATION OF FOUNDATION SHEAR STRENGTH

In the analysis described in the previous sections, it was assumed that the foundation material has constant shear strength. In this study the foundation shear strength varies linearly with depth but the case result in average shear strength of $c_{ave} = 3$ t/m^2 for the slope which is shown in Fig.6.4. The parameters used in the analysis are also given in Fig.6.4. Analyses are performed using three different internal friction angle of the fill material 35^0, 40^0, 45^0. For unit weight of the sand layer again three different values as γ=1.9,2.0,2.1 t/m^3 are chosen respectively. The foundation material has unit weight of 2.0 t/m^3 and the rate of the cohesion intercept of the foundation is 1.5 t/m^2/m.

The results of the study are tabulated in Tables B.5-B.7 which are given in Appendix B for Ordinary Method of Slices and

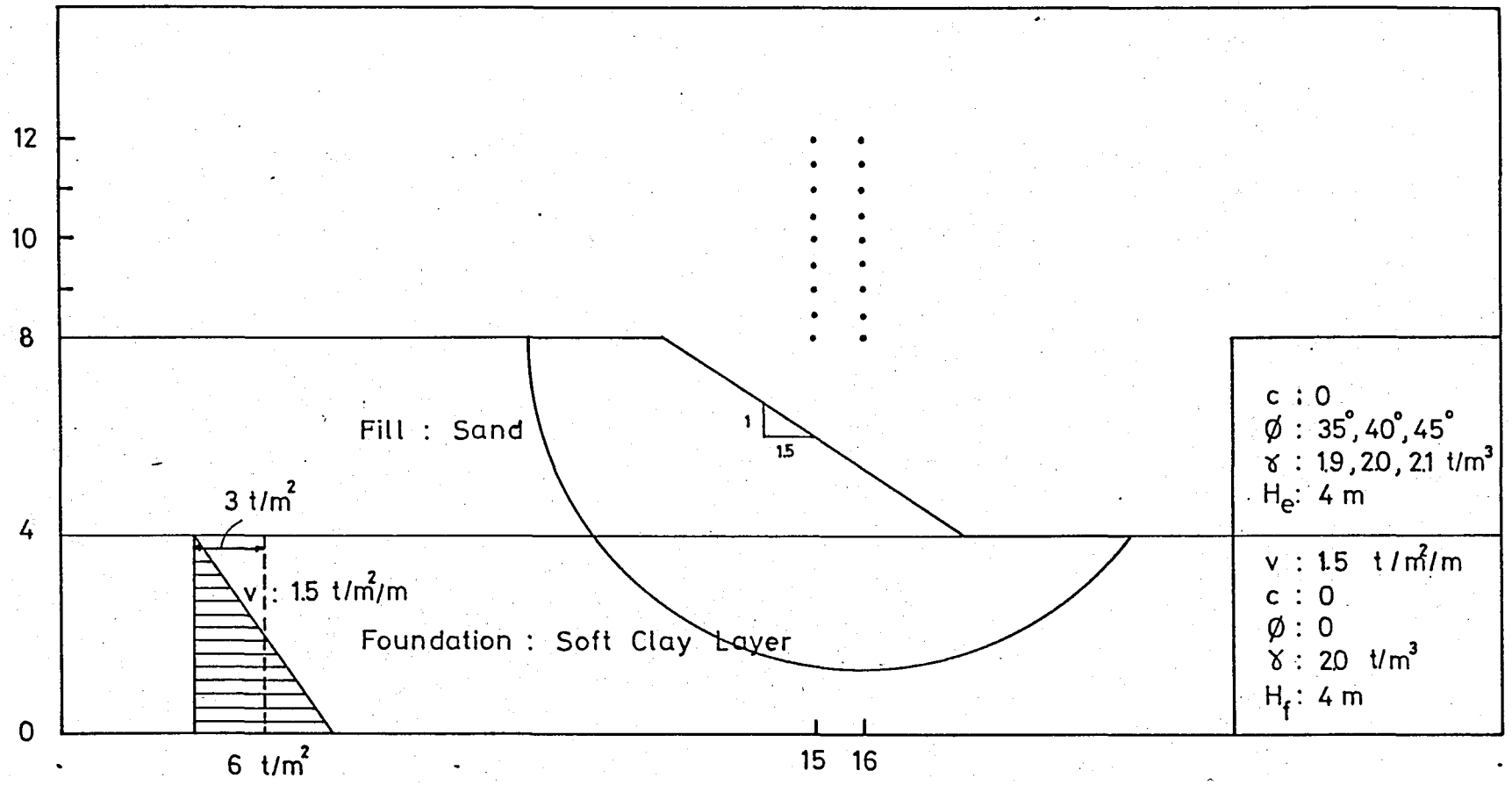

FIG.6.4 Geometry and Soil Properties of the Embankment and Foundation, and the Circular Failure Surface Used in the Analyses (For Linear Variation of Foundation Shear Strength)

Bishop's Modified Method.

For Spencer's Method, Janbu's Generalized Procedure of Slices and Wedge Method to investigate the minimum factor of safety the cross-sections typical of the embankments analyzed are shown in Fig.6.2. In each of these cases, the properties of the fill and the foundation material are the same as shown in Fig.6.4. The results of the analyses are tabulated in Table B.8 for these methods.

The results for all methods are summarized in Table 6.2 The values obtained during the investigation are plotted as a function of the friction angle of the fill material, ϕ as shown in Fig. 6.5. It is found that the factor of safety increases in direct proportion to the friction angle and unit weight of the fill.

If the results of the analysis are considered, variation of the factor of safety with the friction angle of the fill is almost the similar exhibiting straight lines throughout the analysis except for Spencer's Method.

When the linear variation of foundation shear strength is investigated,it is observed that the critical circles for the Modified Bishop's Method and Ordinary Method of Slices and the failure surfaces for Spencer's Method, Janbu's GPS Procedure, and Wedge Method pass from the higher layers when compared to the constant shear strength of foundation but result lower factor of safety values as presented in Table B.8.

TABLE 6.2 Summary of Results
(for Linear Variation of Foundation Shear Strength)

Fill Properties	Factor of Safety				
	OMS	BM	SM	GPS	WM
$\gamma = 1.9 t/m^3$ $\phi = 35^0$	0.791	0.907	1.120	1.148	1.018
$\gamma = 2.0 t/m^3$ $\phi = 40^0$	0.895	1.005	1.223	1.151	1.033
$\gamma = 2.1 t/m^3$ $\phi = 45^0$	0.975	1.093	1.200	1.155	1.047

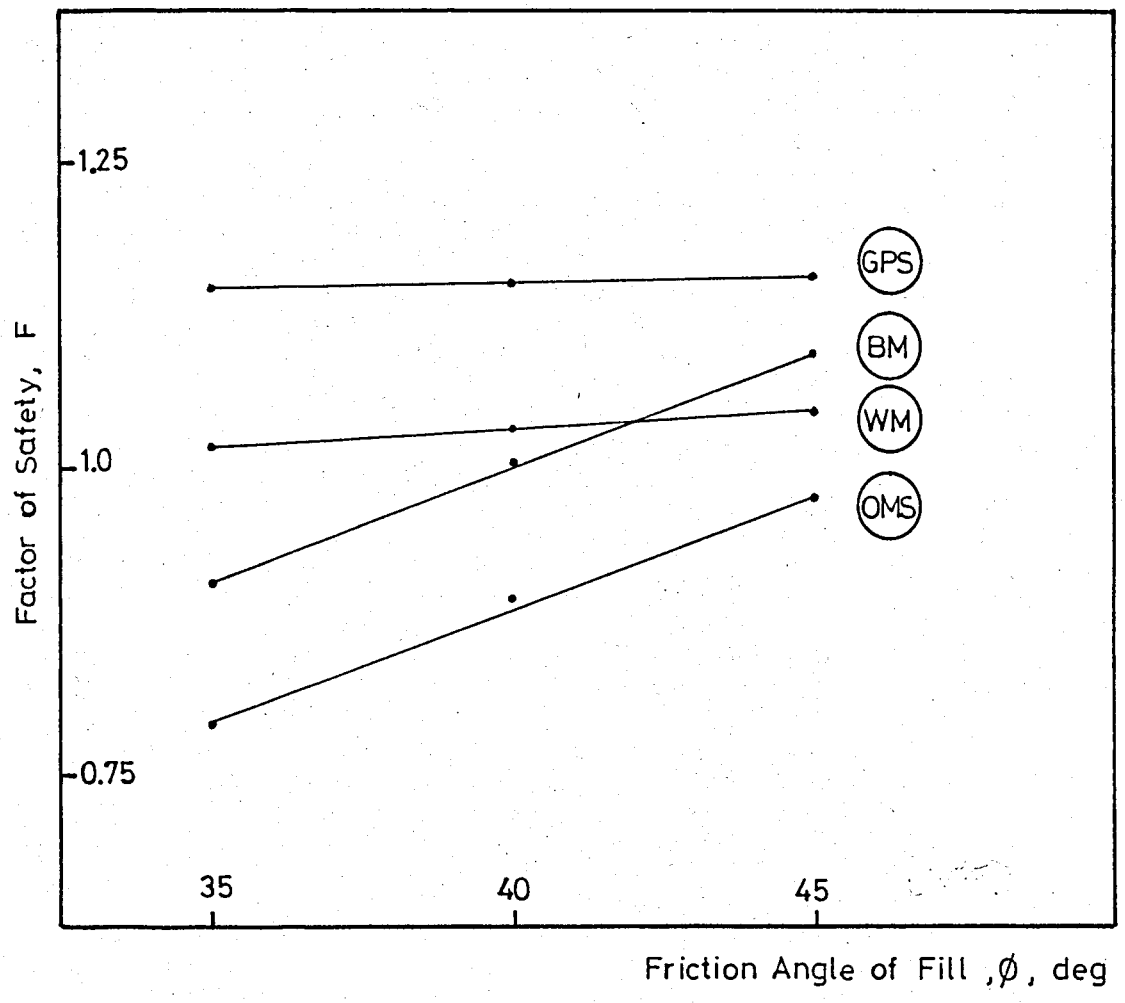

FIG.6.5 Variation of Factor of Safety with Friction Angle of Cohesionless Fill Material for Different Procedures (Linear Variation of Foundation Shear Strength)

6.4 SUMMARY

In this chapter, a parametric study has been conducted in order to establish the effect of foundation shear strength on minimum factor of safety. For this reason, two groups of analyses are discussed.

As the results for constant shear strength foundation indicate, a large change in the value of ϕ results in a relatively small change in the factor of safety for each method. Reducing ϕ from 45 to 35 results in an increase of only about 5 % on the factor of safety. The factor of safety decreases in direct proportion to the friction angle and unit weight of the fill. Variation of the factor of safety with the friction angle of the fill is almost the similar exhibiting straight lines throughout the analysis except for the results of the Spencer's Method and Janbu's GPS procedure.

On the other hand, for linear variation of foundation shear strength it is found that the factor of safety increases in direct proportion to the friction angle and unit weight of the fill. If the results of the analysis are considered, variation of the factor of safety with the friction angle of the fill is almost the similar for each method except for Spencer's method.

When the constant shear strength case is replaced by the varying shear strength case it can be seen that the critical circles and the failure surfaces go less deeper and the associated factor of safety decreases.

In these analyses, the computer programs which are SLOPE 22R, SLOPE 8R, SLOPE 9, and WEDGE 2 are also used and the results obtained from the analyses are given at each subsequent section.

CHAPTER 7

STABILITY OF SLOPES DURING EARTHQUAKES

7.1 INTRODUCTION

Earthquakes may cause the failure of earth embankments which under ordinary conditions would be amply safe.

The general practise of assessing slope stability of embankments in earthquake zones is based on an equivalent static approach. The method involves the computation of the factor of safety against sliding, when a horizontal force equal to the product of seismic coefficient and the weight of the potential failure wedge acts in additon to the already existing static forces. Any of the conventional static methods of analysis is used to ensure a minimum value of factor of safety.

Thus, any pseudo-static analysis involves the following steps:

1. Steps involved with respect to the chosen procedure of analysis.

2. Evaluation of the seismic coefficient values.

Additionally, at the end of this chapter, a illustrative example using the computer program WEDGE 3 is also presented for the Wedge Method-Earthquake case.

7.2 ACTION OF EARTHQUAKES ON SLOPES

Sudden ground displacements during earthquakes induce large inertia forces in embankments. Thus, for example, in a rigid embankment such as that shown in Fig.7.1, a ground acceleration to the right would induce inertia forces acting to the left on all elements of the embankment. These forces would tend to increase the stability of the right slope of the embankment but would decrease the stability of the left slope. However, the reduction in stability would only exist during the short period of time for which the inertia force is induced. As soon as the ground acceleration is reversed, which might occur after approximately, 0.25 sec during an earthquake, the direction of the inertia forces is also reversed with a corresponding increase in stability of the right slope. Thus, any one slope of an embankment will be subjected to inertia forces that alternate in direction many times during an earthquake and it is necessary to assess the effects of these pulsating stresses, superimposed on the initial dead load stresses, on the embankment configuration.

7.3 PROCEDURES OF ANALYSIS

The various steps involved in the computation of minimum factor of safety vary with the adopted procedure of analysis.Different conventional procedures are available for evaluating the slope stability. In this Chapter the effect of earthquakes using pseudo-static analysis for Wedge method is studied. Formulation of the problem is used on a practical problem. For this purpose,a typical slope profile is taken from Alaybey Shipyard Construction for the analysis.

During construction from the subsoil conditions,it is clear that the critical failure surface would be non-circular. Therefore,

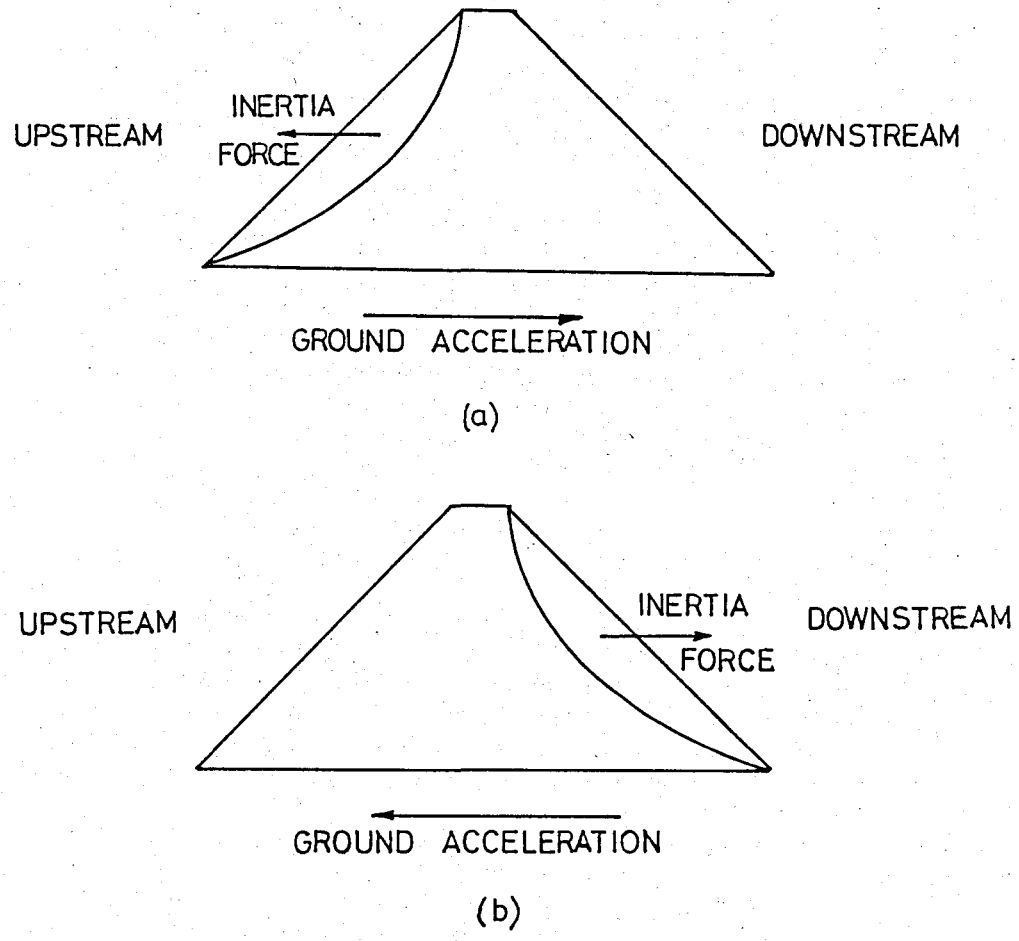

FIG.7.1 Inertia Force on Rigid Embankments

Wedge method of analysis is performed for the determination of proper factor of safety against the stability of the fill.

7.4 SELECTION OF SEISMIC COEFFICIENT IN PSEUDOSTATIC ANALYSIS

One of the major problems facing the engineer using this type of approach is that of selecting the value of the seismic coefficent to be used for design purposes.

The adopted practices in the world may be classified into three groups.

1. Empirical Approach
2. Rigid Body Response Consideration
3. Elastic Response Considerations

7.4.1 Empirical Approach

Most engineers in the United States, who adopt a pseudostatic method of seismic stability analysis, adopt some empirical value for the design seismic coefficient; typically this lies in the range of 0.05 to 0.15. These values are taken to be constant along the height of the dam.

It is interesting to note that, whereas the design seismic coefficient is typically on the order of 0.1 in the United States , somewhat higher values are used in Japan. They range between 0.12 to 0.25.

7.4.2 Rigid Body Response Consideration

If an embankment is assumed to behave as a rigid body, the accelerations will be uniform throughout the section and equal at all

times to the ground accelerations. This assumption simplifies the problem to a great extent. Thus, it is sometimes arqued that the design seismic coefficient should be equal to the maximum ground acceleration.

7.4.3 Elastic Response Considerations

The deficiencies in the use of empirical rules or the assumption of rigid body response have led a number of investigators to propose the use of elastic response solutions for the determination of design seismic coefficients. In effect, the embankment is considered to consist of a series of infinitely thin horizontal slices, the slices being connected by linearly elastic shear springs and viscous damping devices, and the response at different levels resulting from a uniformly distributed base motion is determined.

7.5 NUMERICAL TECHNIQUE FOR WEDGE METHOD

Most current practice in the analysis of embankment stability against earthquake forces involves the computation of the mimimum factor of safety against sliding, when a static, horizontal force of some magnitude is included in the analysis. The analysis is treated as a static problem and the horizontal force is expressed as the product of a seismic coefficient, k, and the weight, W, of the potentiel sliding mass. If the factor of safety approaches unity, the section is generally considered unsafe, although there is no generally recognized limit for the minimum acceptable factor of safety. In effect, the dynamic effects are replaced by a static force, and the approach might therefore be termed a pseudo-static method of analysis.

This horizontal force can be at the middle of the slice or at the base of the slice. Even though the horizontal force is considered at the middle of the slice in this section, for both case the numerical formulation of the factor of safety is the same in the Wedge method of analysis.

If it is considered the dimensions of slip surface and forces on a slice as shown in Fig.7.2, from the equilibrium in a direction normal to the base of the slice, the following equation is obtained.

$$\sigma.1 = W\cos\alpha + \Delta E \sin\alpha - Wk \sin\alpha \qquad \ldots (7.1)$$

The magnitude of the shear strength mobilized to satisfy the equilibrium conditions is s where

$$s = \frac{1}{F}\left\{c' + (\sigma - u)\tan\phi'\right\} \qquad \ldots (4.18)$$

The shear force S acting on the base of the slice may be expressed as

$$S = s.1 \qquad \ldots (7.2)$$

Substituting Eq.4.18 into Eq.7.2, one may obtain the following equation :

$$S = \frac{1}{F}(c'1 + \sigma l\tan\phi' - ul\tan\phi') \qquad \ldots (7.3)$$

If the group of terms in Eq 7.1 are substituted into Eq.7.3, this equation can be expressed in terms of the forces which act on an individual slice.

$$S = \frac{1}{F}(c'.1+W\cos\alpha.\tan\phi'+\Delta E\sin\alpha.\tan\phi'-Wk\sin\alpha.\tan\phi'-ul\tan\phi') \qquad \ldots (7.4)$$

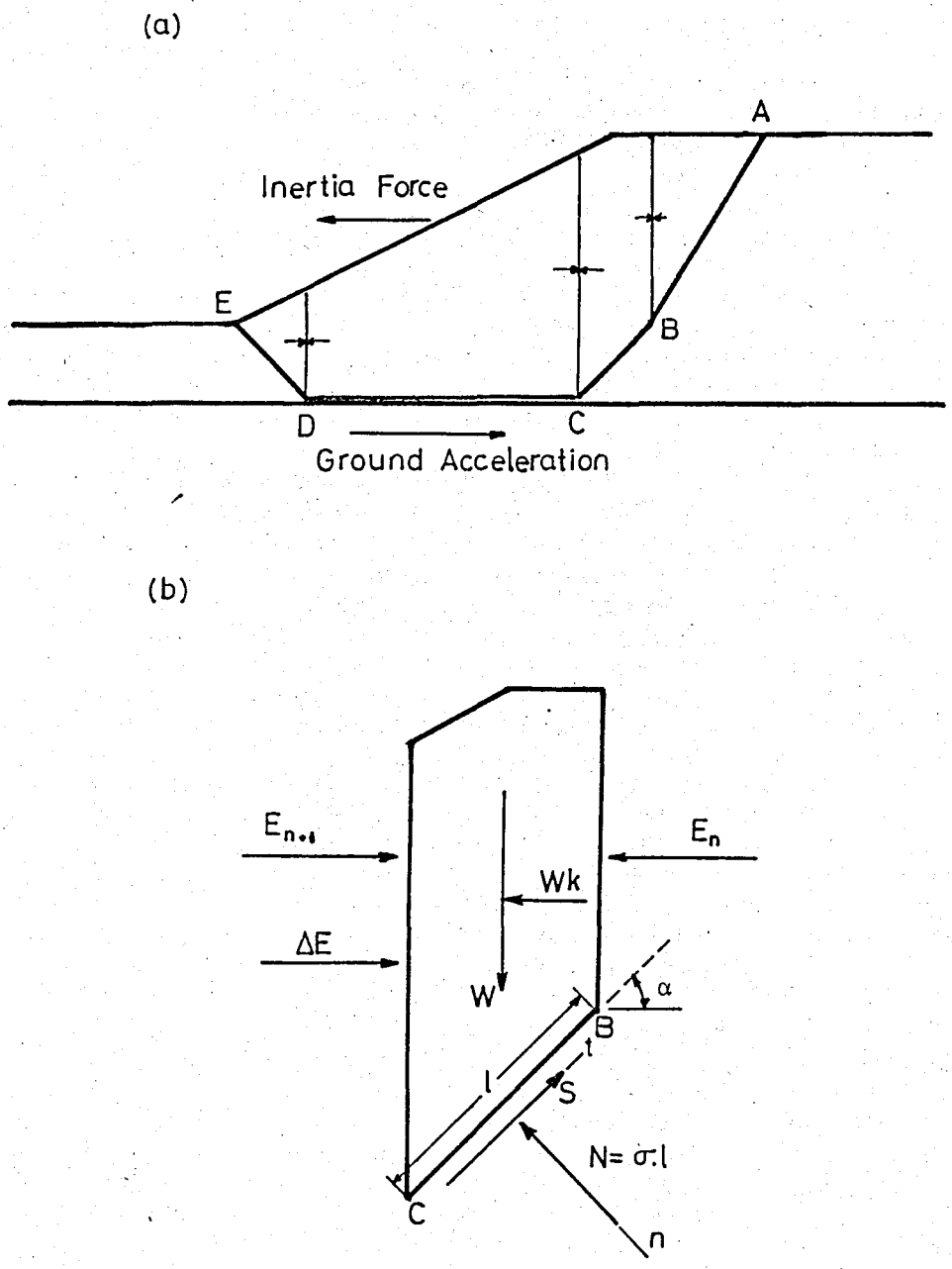

FIG.7.2 Forces and Locations Involved in the Equilibrium of an Individual Slice for Wedge Method-Earthquake Case

The value of ΔE obtained from Eq 7.5 can be written as

$$\Delta E = \frac{WF\tan\alpha - \frac{cl}{\cos\alpha} - W\tan\phi + \frac{ul\tan\phi}{\cos\alpha} + Wk\tan\alpha\tan\phi}{F + \tan\alpha\tan\phi} \quad \ldots (7.5)$$

If the quantities in Eq 7.6 are written with respect to the terms which are given in Fig. 4.11, the following equation may be obtained.

$$\Delta E = \frac{N_4 - N_1 - N_2 + N_3 - N_6}{N_5} \quad \ldots (7.6)$$

In this equation, the earthquake force is also introduced into the analysis as used in the solution of the example problem in the following section.

7.6 THE EXAMPLE PROBLEM

A typical slope taken from Alaybey Shipyard Construction is investigated in this section. As shown in Fig. 7.3, the slope profile has four different layers. The parameters used in the analysis are also given in Fig.7.3. The results which are obtained by using Wedge method seem to be reasonable. They compare well with the results performed by the designer. If the earthquake force is not considered (k=0), the factor of safety is found as 3.002. When the earthquake force is introduced into the analysis (k=0.1), the factor of safety has the value of 1.672.

7.7 SUMMARY

There can be no doubt that major and catastropic slope failures have occurred during medium and large earthquakes, and the development of reliable methods for preventing such failures is a major cause for concern to the soil engineer working in seismically active

LAYER	γ', kN/m^3	c', kN/m^2	ϕ'°
1	10	0	32.5
2	7	10	0
3	7	15	20
4	10	0	30

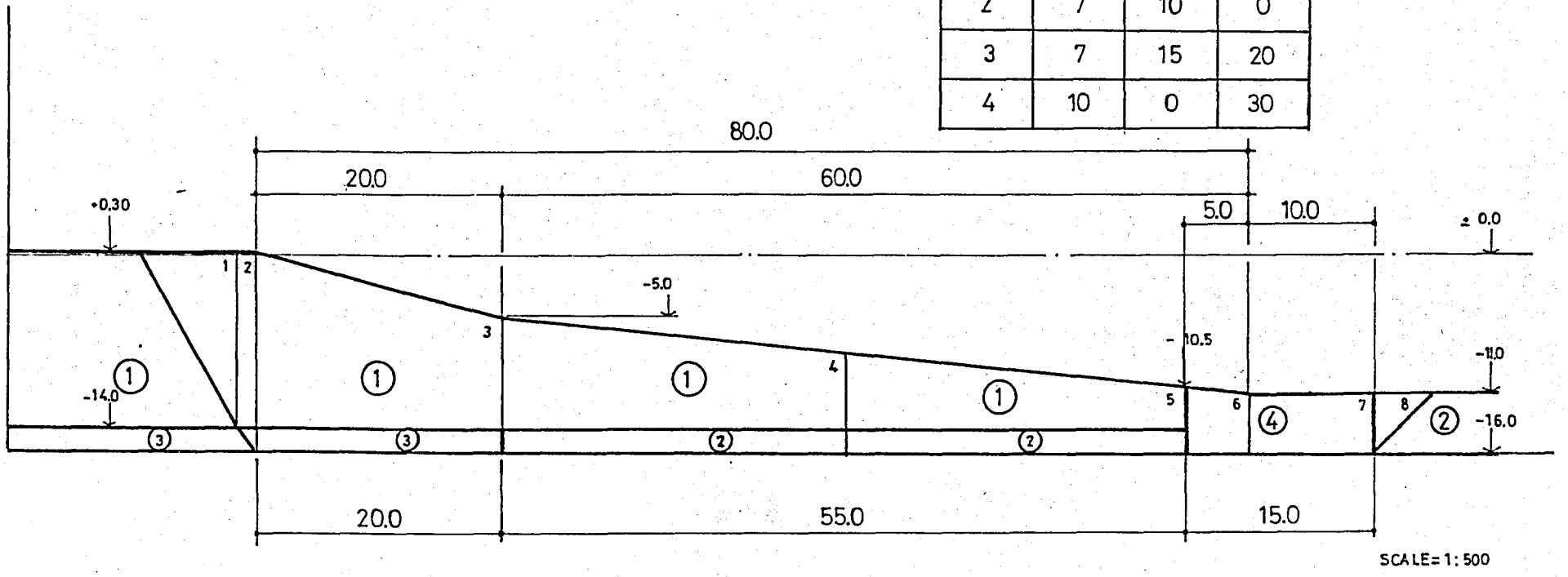

FIG.7.3 Dimensions and Properties of Embankment and Foundation, and Failure surface used in the Example

areas. Qualitative assessments of slope stability during earthquakes can often be made on the basis of experience and judgment. Pseudostatic methods of analysis provide a means for comparing the merits of different embankment sections and for assuring increased conservatism in design sections on an empirical basis. However, there is little to quide the design engineer in selecting an appropriate value for the seismic coefficient and furthermore, this method of analysis in inadequate to explain the mechanics of a considerable number of embankment failures . Thus,the method leaves much to be desired.

In recent years considerable progress has been made in the development of new concepts in earthquake resistant design of embankments. These developments provide a framework for evaluating previous failures and thereby offer the possibility for a a more meaningful categorization of experience and an improved quide to engineering judgment in the evaluation of slope stability during earthquakes.

CHAPTER 8
SUMMARY AND CONCLUSIONS

The slope stability methods which are plane failure surfaces, Circular arc method of analysis, ϕ=0 analysis, Friction circle method, and Logarithmic Spiral method are provided in Chapter 2.

The solutions of the slope stability problems have been obtained for simple slopes and uniform soil conditions and are available in the form of charts. A considerable amount of labor is required to obtain such charts but, once obtained, solutions by their use are simple. Many slopes that approximate the simple section and that are composed of more or less heterogeneous soils may be subjected to an approximate analysis by entering the charts with average values. Such estimates in some cases give no more than rough results, but in other instances the dependability of results is essentially as good as can be obtained by long and detailed analyses. These slope stability charts are given in Chapter 3.

The slope stability methods in which the mass of soil enclosed by the slip surface is divided into vertical slices are discussed in Chapter 4. Whitman and Bailey (1967) and Wright (1969) have shown that if the soil mass is divided into n slices, there will be 5n-2 unknowns to be evaluated, but only 3n equations can be obtained from the three conditions of equilibrium. Thus, the problem is indeterminate.

In order to find a solution, 2n-2 assumptions are needed. Because assumptions are inevitably involved, the solution is not unique. Some of these procedures satify only one or two conditons of equilibrium, whereas others satisfy all three conditions, and they all involve some assumptions to make the problem statically determinant. The number of equilibrium conditions satisfied does not provide a sufficient basis for selecting the best procedure for analysis. In this respect the studies conducted show that the condition of moment equilibrium is more important than the conditions of horizontal or vertical force equilibrium. For this reason,the Ordinary Method of Slices and Bishop's Modified Method and Spencer's Method are used in the investigations in Chapter 5. On the other hand,additionally,Janbu's Generalized Procedure of Slices and Wedge method are also used in these calculations for comparison purposes.

Previous studies have shown that methods of slope stability analysis which satisfy all three conditions of equilibrium will give accurate values of factor of safety from the point of view of mechanics. Although Bishop's Modified method has been found to be quite accurate and efficient for many problems, Whitman and Bailey (1967) have shown that numerical difficulties may occur because the normal force on the base of a slice may become very large or negative when the failure surface is steeply inclined. Convergence difficulties are often encountered for these types of problems in Chapter 5 when Spencer's method or Janbu's Generalized Procedure of slices are used. Under these conditions, the solutions by the Ordinary Method of Slices appears to be more reliable than solutions of the other methods. Consequently, in Chapter 5,using different procedures,the effect of embankment and foundation shear strength on the factor of safety calculated for a

given soil profile is discussed. In addition to these, a comparison of various procedures and the effects of these methods on factor of safety are also made in each subsequent section. The computer programs SLOPE 22R, SLOPE 8R, and SLOPE 9 developed for comparing the effect of these methods on factor of safety are employed. Additionally, the computer program WEDGE 1 is also developed in this study.

As presented in Chapter 6, the effect of foundation shear strength on minimum factor of safety using the various procedures as mentioned above has also been investigated. The computer program WEDGE 2 is developed for this purpose.

The effect of earthquakes on slope stability is discussed in Chapter 7. Formulation of the problem for Wedge Method is shown in this chapter. According to numerical technique of Wedge Method, the illustrative example which is taken from Alaybey Shipyard Construction is analyzed using the computer program WEDGE 3.

REFERENCES

1. Bell J.M.(1969), *"Noncircular Sliding Surfaces"*, Journal of the Soil Mechanics and Foundations Division, ASCE, Vol.95, No.SM3, May 1969, pp.829-844.

2. Bishop A.W.(1955), *"The Use of the Slip Circle in the Stability Analysis of Slopes"*, Geotechnique, Vol.5, No.1, March 1955,pp. 7-17.

3. Bishop A.W. and Morgenstern N.R.(1960), *"Stability Coefficients of Earth Slopes"*, Geotechnique, Vol.10, No.4 December 1960, pp.129-150.

4. Bowles J.E.(1979), *"Physical and Geotechnical Properties of Soils"*, McGraw-Hill, New York, 1979.

5. Chirapuntu S. and Duncan J.M.(1976), *"The role of Fill Strength in the Stability of Embankments on Soft Clay Foundations"*, Department of Civil Engineering Institute of Transportation and Traffic Engineering, University of California, Berkeley, June 1976.

6. Duncan J.M. and Buchignani A.L.(1975), *"An Engineering Manual For Slope Stability Studies"*; Department of Civil Engineering Institute of Transportation and Traffic Engineering, University of California, Berkeley, March 1975.

7. Dunn, I.S., Anderson L.R., Kiefer F.W.(1980), *"Fundamentals of Geotechnical Analysis"*, John Wiley and Sons Inc., New York,1980.

8. Frohlich O.K.(1955), *"General Theory of Stability of Slopes"*, Geotechnique, Vol.5, No.1, March 1955, pp.37-47.

9. Janbu N.(1957), *"Earth Pressures and Bearing Capacity Calculations by Generalized Procedure of Slices"*, Proceedings of the Fourth International Conference on Soil Mechanics and Foundation Engineering,Vol.2, London 1957, pp.207-212.

10. Janbu N.(1968), *"Slope Stability Computations"*, Soils Mechanics and Foundation Engineering Report, The Technical University of Norway, Trandheim, 1968.

11. Jumikis A.R.(1962), *"Soil Mechanics"*, D. Van Nostrand Company Inc., New York, 1962.

12. Little A.L. and Price V.E.(1958), *"The Use of an Electronic Computer for Stability Analysis"*, Geotechnique, Vol.8, No.3, September,1958,pp. 113-120.

13. Lowe J.(1967), *"Stability Analysis of Embankments"*, Journal of the Soil Mechanics and Foundations Division, ASCE, Vol.93,No.SM4,July 1967, pp.1-33.

14. Mongenstern N.R. and Price V.E.(1965), *The Analysis of the Stability of General Slip Surfaces"*, Geotechnique, Vol.15, No.1, March 1965, pp.79-93.

15. Morgenstern N.R. and Price V.E.(1967), *"A Numerical Method for Solving the Equations of Stability of General Slip Surfaces"*,

The Computer Journal, Great Britain, Vol.9, No.4, February 1967, pp.388-393.

16. Peck R.B.(1967), *"Stability of Natural Slopes"*, Journal of the Soils Mechanics and Foundations Division, ASCE, Vol.93, No.SM4, July 1967, pp.403-417.

17. Sarma S.K.(1979), *"Stability Analysis of Embankments and Slopes"*, Journal of the Soil Mechanics and Foundations Division, ASCE, Vol.105, No.GT12, December 1979, pp.1511-1524.

18. Seed H.B.(1966), *"A Method for Earthquake Resistant Design of Earth Dams"*, Journal of the Soil Mechanics and Foundations Division, ASCE, Vol.92, No.SM1, January 1966, pp.13-41.

19. Seed H.B.(1967), *"Slope Stability During Earthquakes"*,Journal of the Soil Mechanics and Foundations Division, ASCE, Vol.93, No.SM4, July 1967, pp.299-323.

20. Sherard J.L.(1967), *"Earthquake Considerations in Earth Dam Design"*, Journal of the Soil Mechanics and Foundations Division, ASCE, Vol.93, No.SM4, July 1967, pp.377-401.

21. Smith G.N.(1974), *"Elements of Soil Mechanics for Civil and Mining Engineers"*, Crosby Lockwood Staples, London, 1974.

22. Spencer E.(1967), *"A method of Analysis of the Stability of Embankments Assuming Parallel Inter-Slice Forces"*, Geotechnique, Vol.17, No.1, March 1967, pp.11-26.

23. Spencer E.(1969), *"Circular and Logarithmic Spiral Slip Surfaces"*, Journal of the Soil Mechanics and Foundation Division, ASCE, Vol.95, No.SM1, January 1969, pp.227-234.

24. Spencer E.(1981), *"Slip Circles and Critical Shear Planes"*, Journal of the Soil Mechanics and Foundations Division, ASCE, Vol.107, No.GT7, July 1981, pp.929-942.

25. Taylor D.W. (1948), *"Fundamentals of Soil Mechanics"*, John Wiley and Sons Inc., New York 1948.

26. Terzaghi K. and Peck R.B.(1958), *"Soil Mechanics in Engineering Practice"*, John Wiley and Sons Inc., New York, 1958.

27. Terzaghi K.(1963), *"Theoretical Soil Mechanics"*, John Wiley and Sons Inc., New York, 1963.

28. Whitman R.V. and Bailey W.A. (1967), *"Use of Computers for Slope Stability Analysis"*, Journal of the Soil Mechanics and Foundations Division, ASCE, Vol.93, No.SM4, July 1967, pp.475-498.

29. Wright S.G.(1969), *"A Study of Slope Stability and the Undrained Shear Strength of Clay Shales"*, Ph.D. Thesis, Department of Civil Engineering, University of California, Berkeley, 1969.

APPENDICES

APPENDIX A

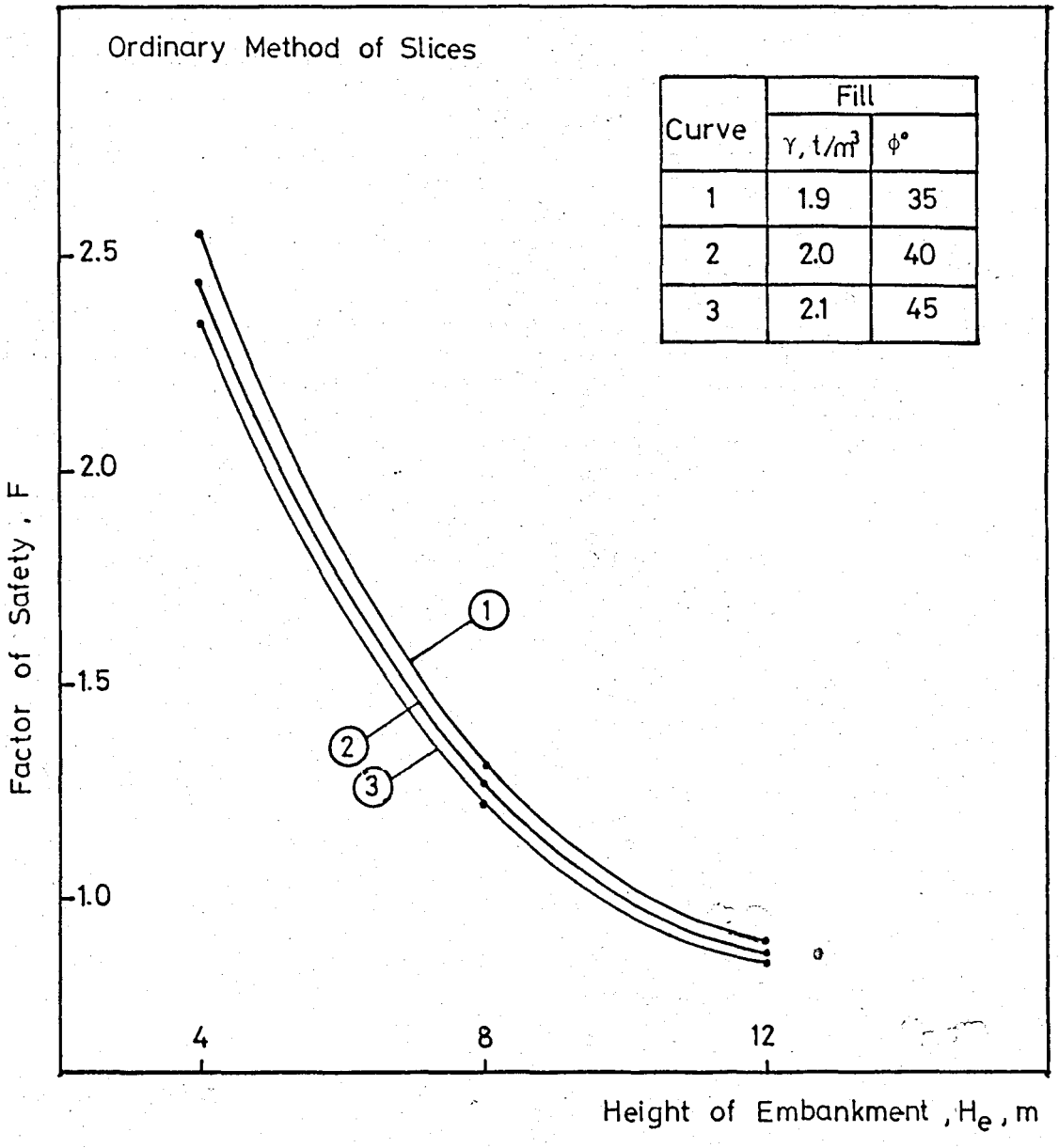

FIG.A.1 Effect of Embankment Height for Variable Unit Weight of Cohesionless Fill Material on Factor of Safety of the Typical Embankment Shown in Fig.5.2 by Ordinary Method of Slices

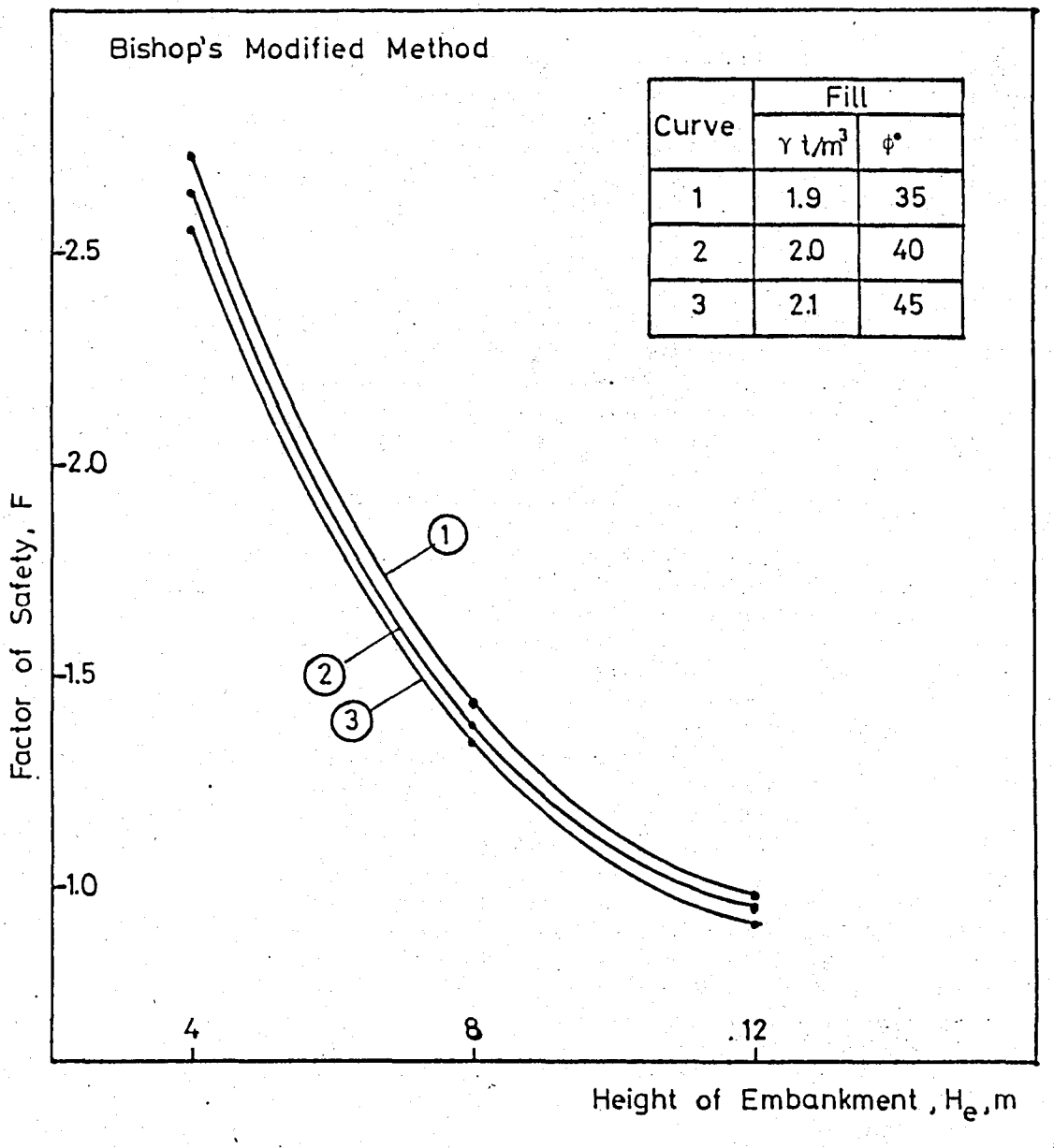

FIG.A.2 Effect of Embankment Height for Variable Unit Weight of Cohesionless Fill Material on Factor of Safety of the Typical Embankment, Shown in Fig.5.2 by Bishop's Modified Method

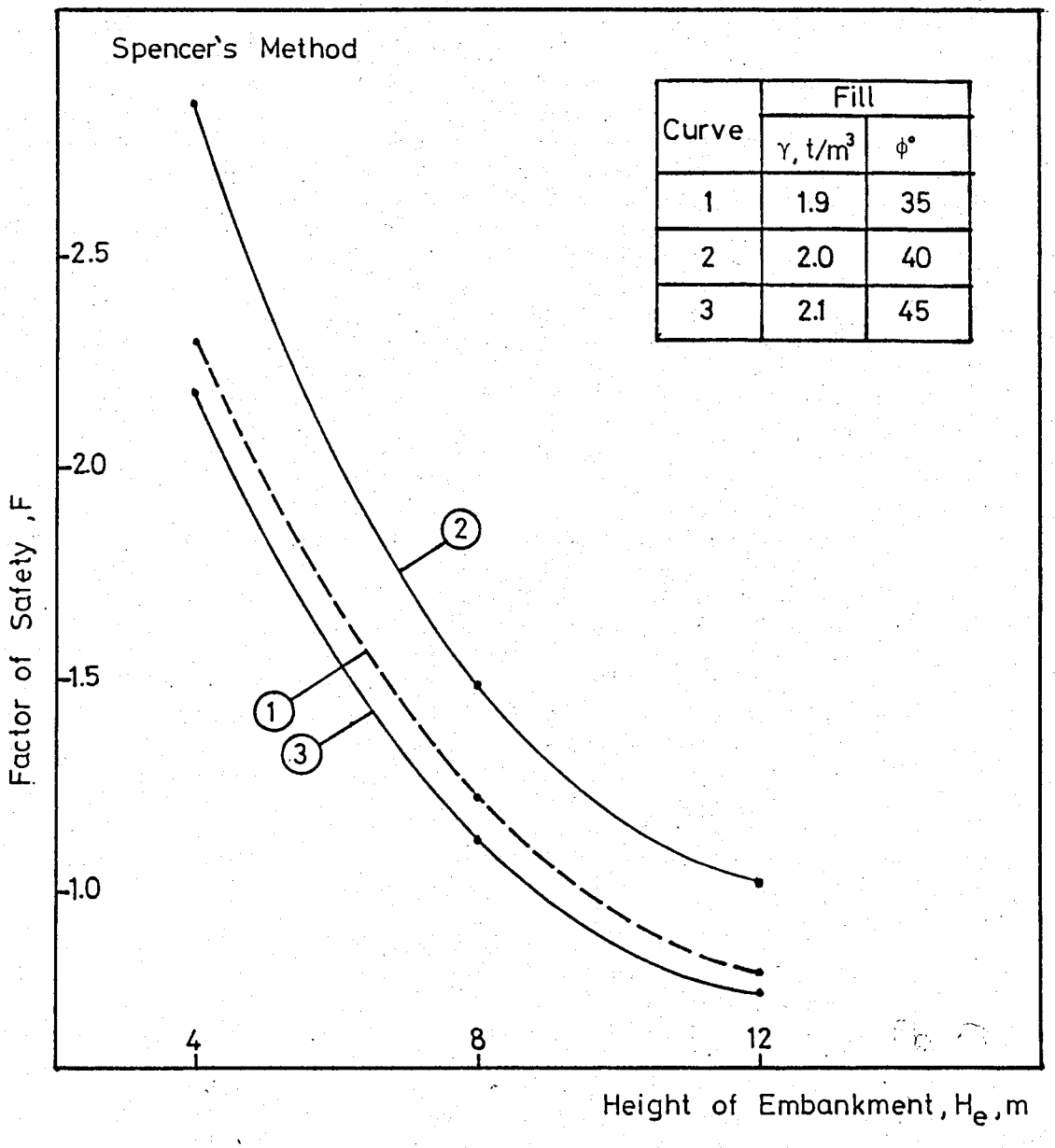

FIG.A.3 Effect of Embankment Height for Variable Unit Weight of Cohesionless Fill Material on Factor of Safety of the Typical Embankment Shown in Fig.5.2 by Spencer's Method

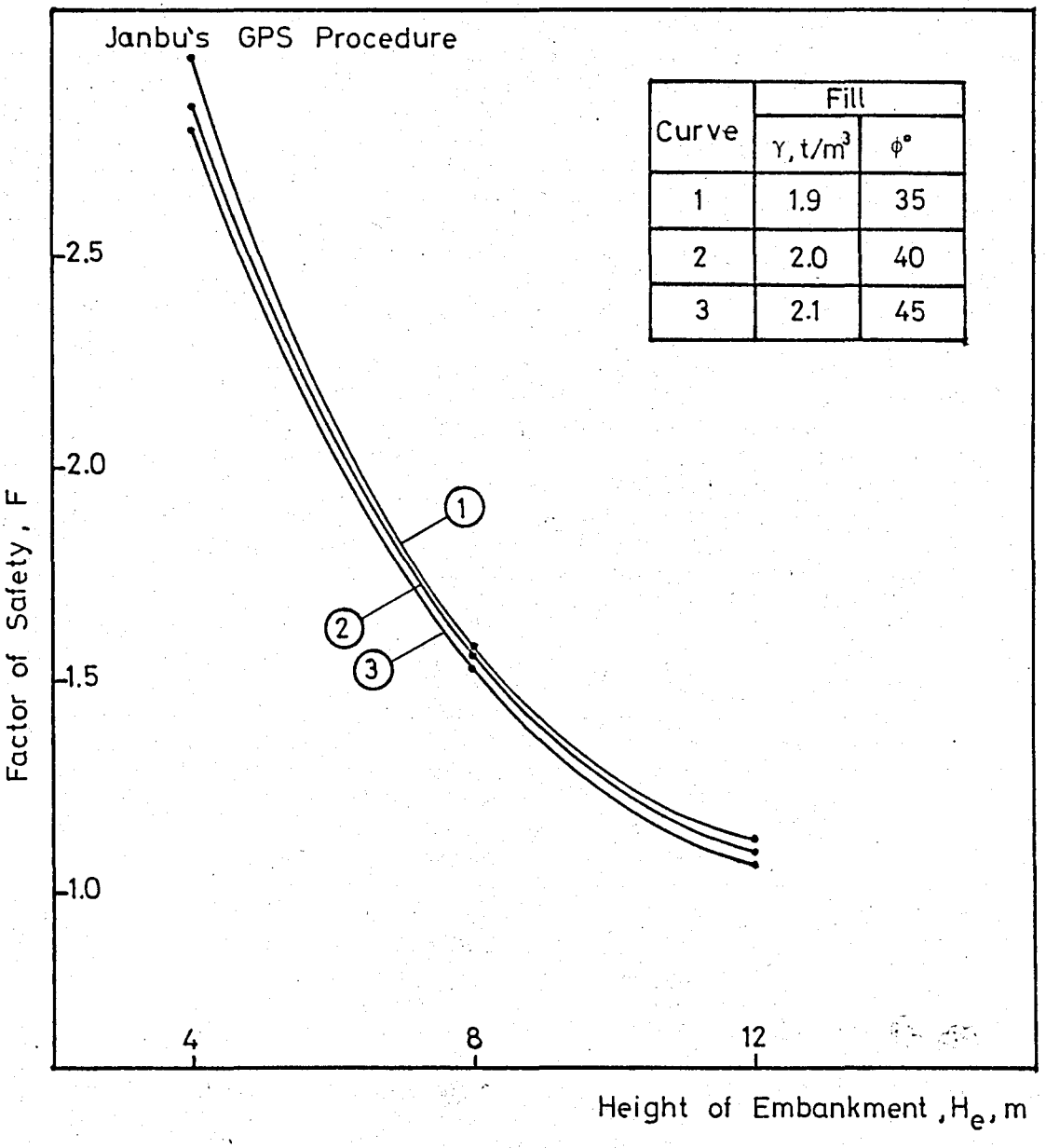

FIG.A.4 Effect of Embankment Height for Variable Unit Weight of Cohesionless Fill Material on Factor of Safety of the Typical Embankment Shown in Fig.5.2 by Janbu's Generalized Procedure of Slices

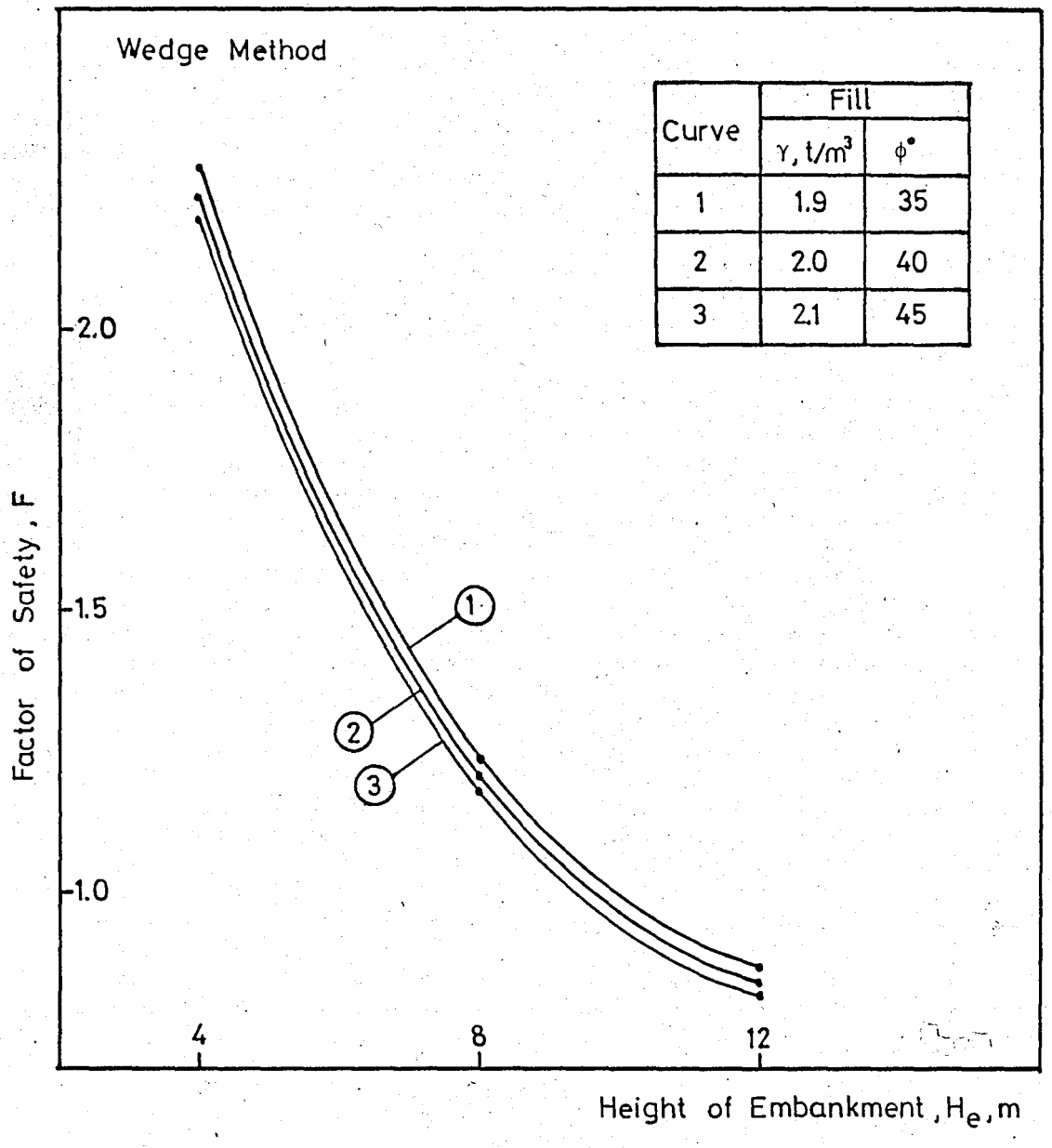

FIG.A.5 Effect of Embankment Height for Variable Unit Weight of Cohesionless Fill Material on Factor of Safety of the Typical Embankment Shown in Fig.5.2 by Wedge Method

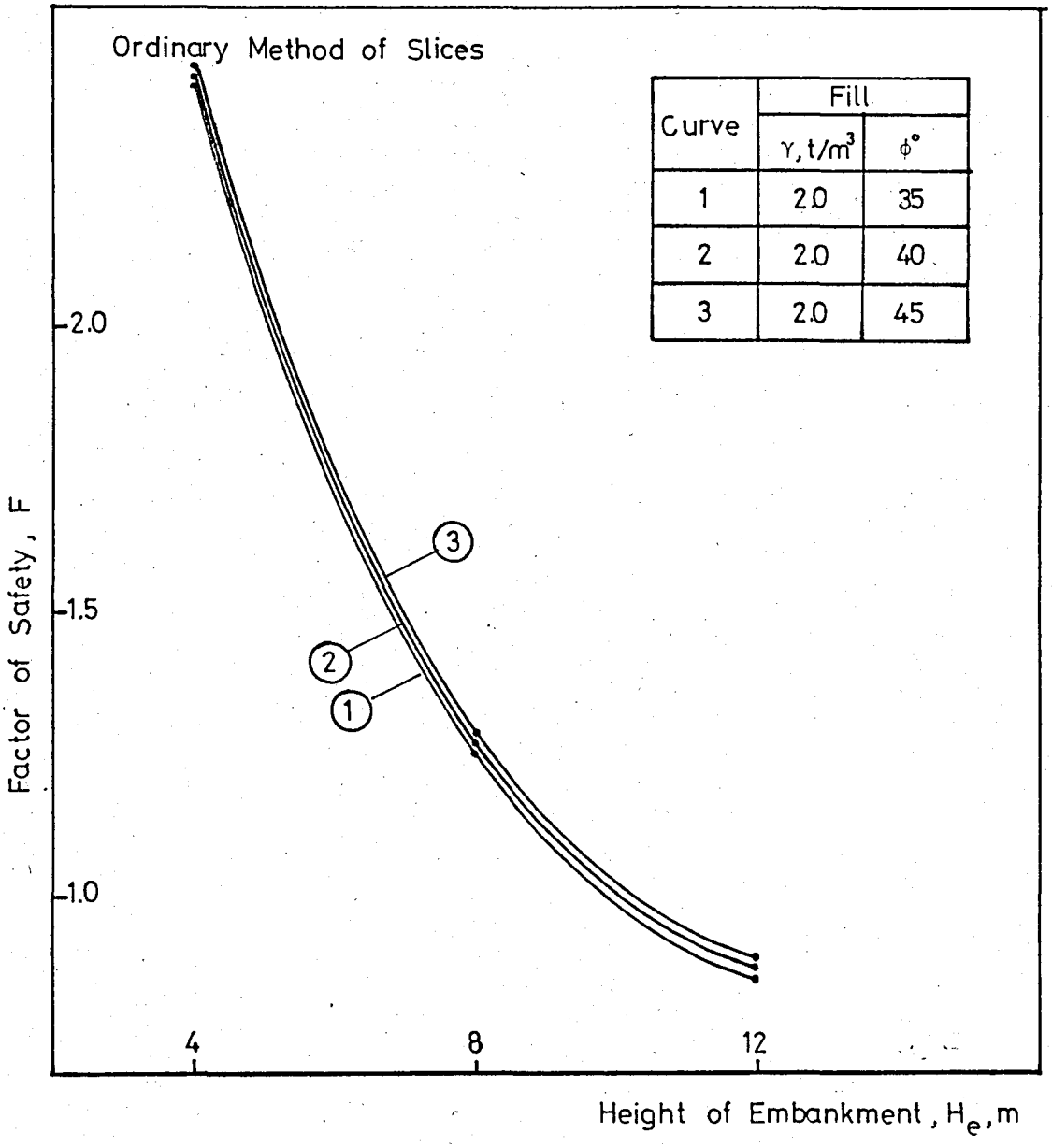

FIG.A.6 Effect of Embankment Height for constant Unit Weight of Cohesionless Fill Material on Factor of Safety of the Typical Embankment Shown in Fig.5.2 by Ordinary Method of Slices

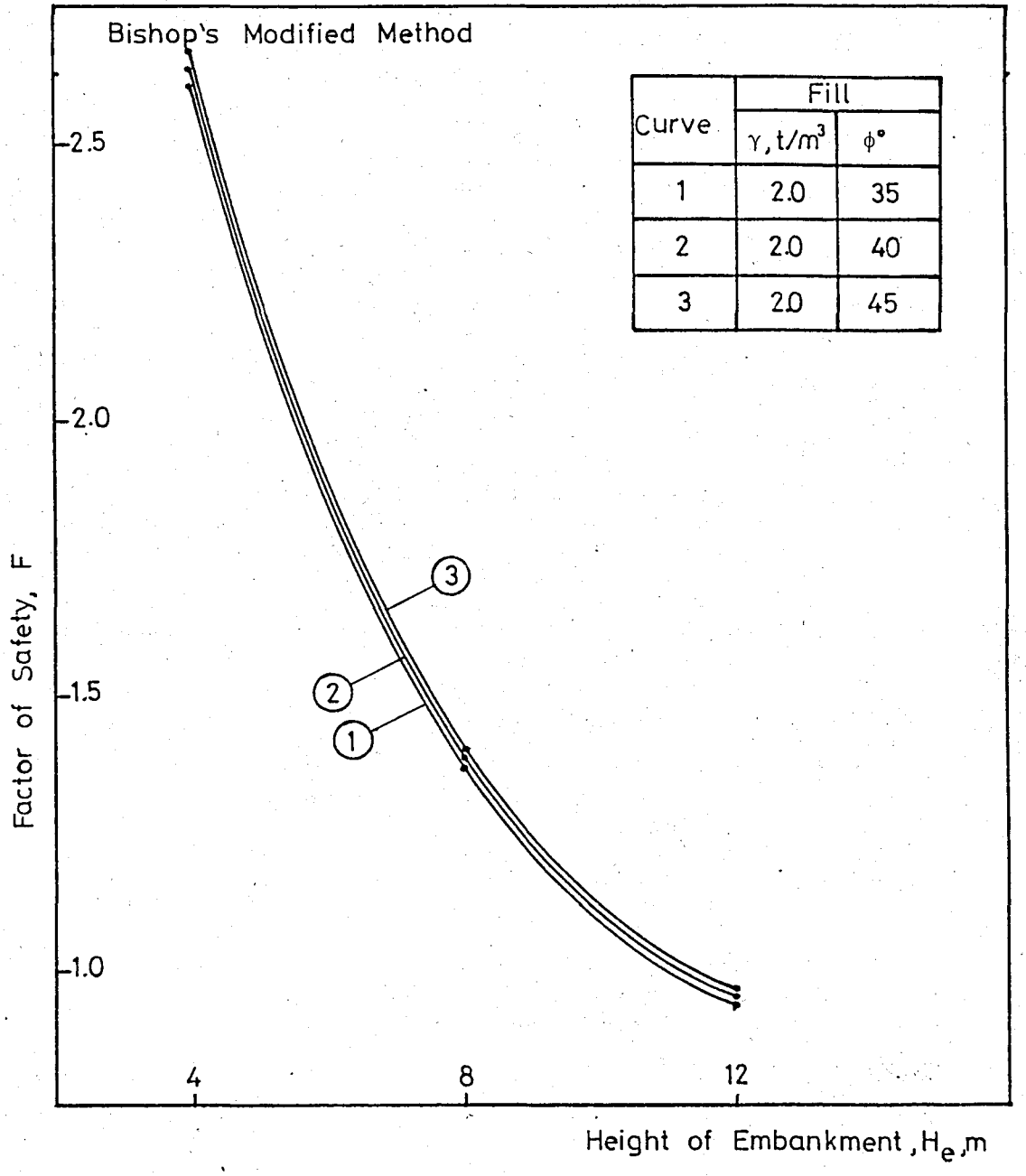

FIG.A.7 Effect of Embankment Height for constant Unit Weight of Cohesionless Fill Material on Factor of Safety of the Typical Embankment Shown in Fig.5.2 by Bishop's Modified Method

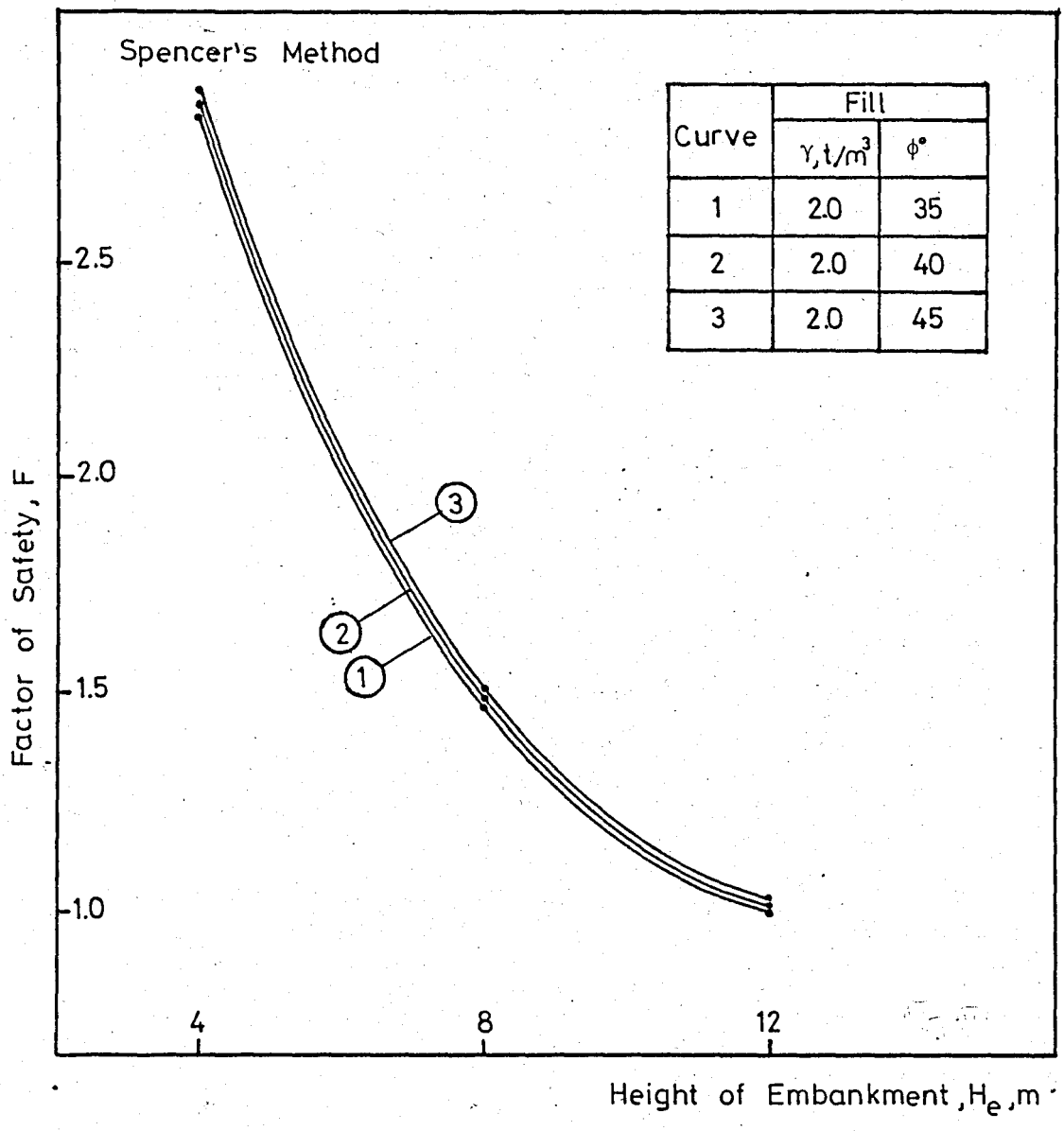

FIG.A.8 Effect of Embankment Height for constant Unit Weight of Cohesionless Fill Material on Factor of Safety of the Typical Embankment Shown in Fig.5.2 by Spencer's Method

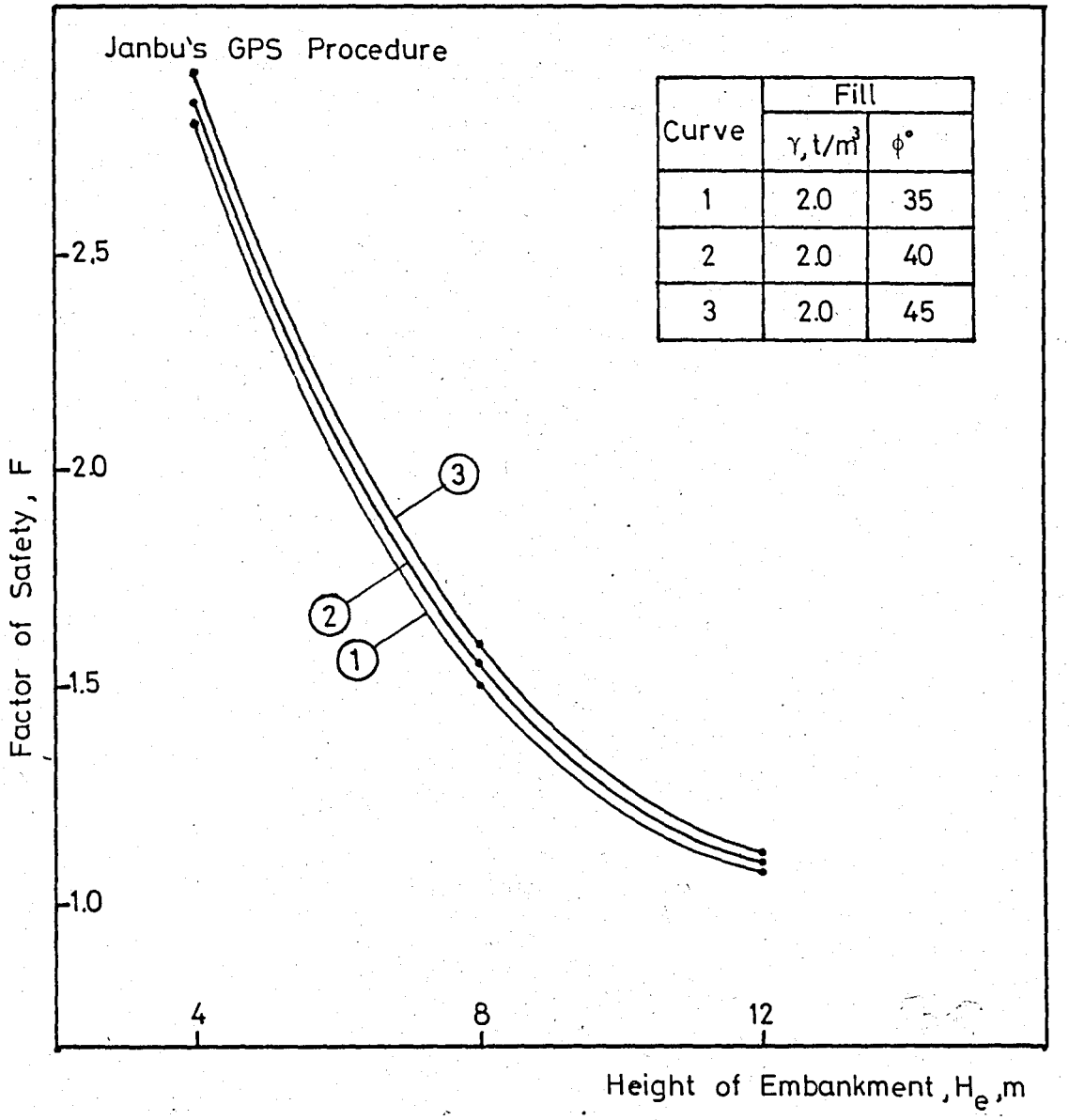

FIG.A.9 Effect of Embankment Height for constant Unit Weight of Cohesionless Fill Material on Factor of Safety of the Typical Embankment Shown in Fig.5.2 Janbu's Generalized Procedure of Slices

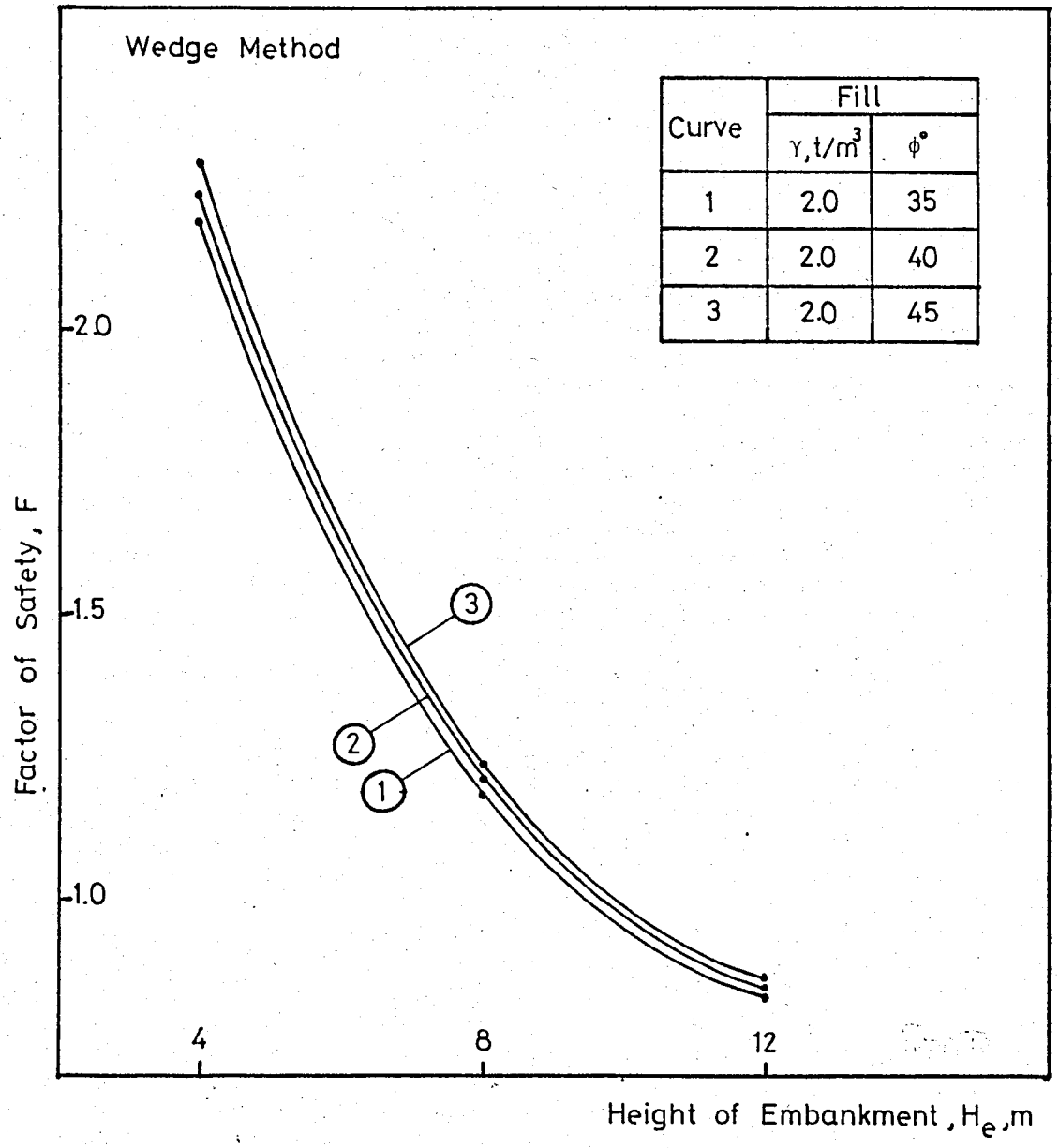

FIG.A.10 Effect of Embankment Height for constant Unit Weight of Cohesionless Fill Material on Factor of Safety of the Typical Embankment Shown in Fig.5.2 by Wedge Method

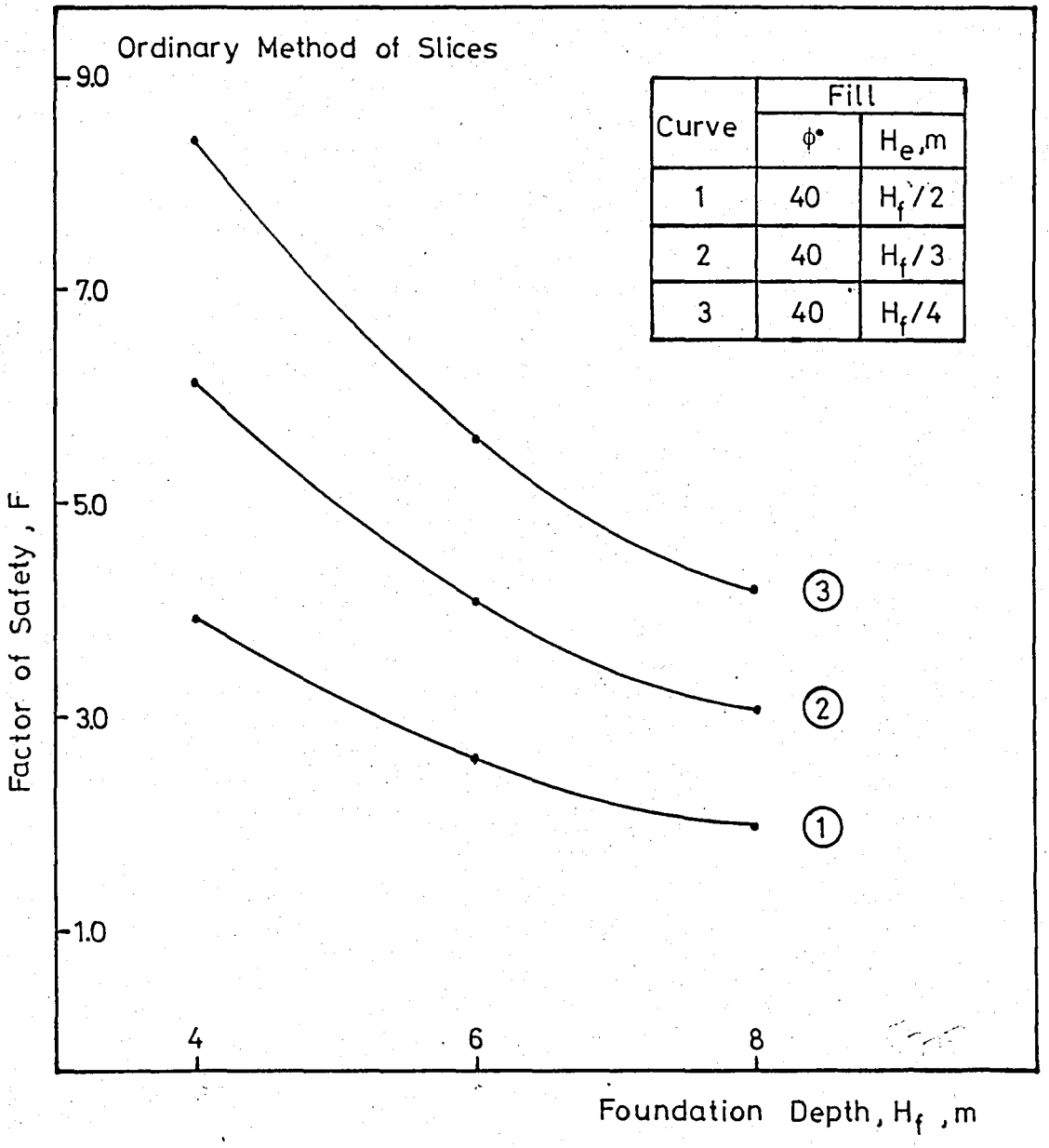

FIG.A.11 Effect of Foundation Depth for Variable Embankment Height on Factor of Safety of the Typical Embankment Shown in Fig.5.5 by Ordinary Method of Slices

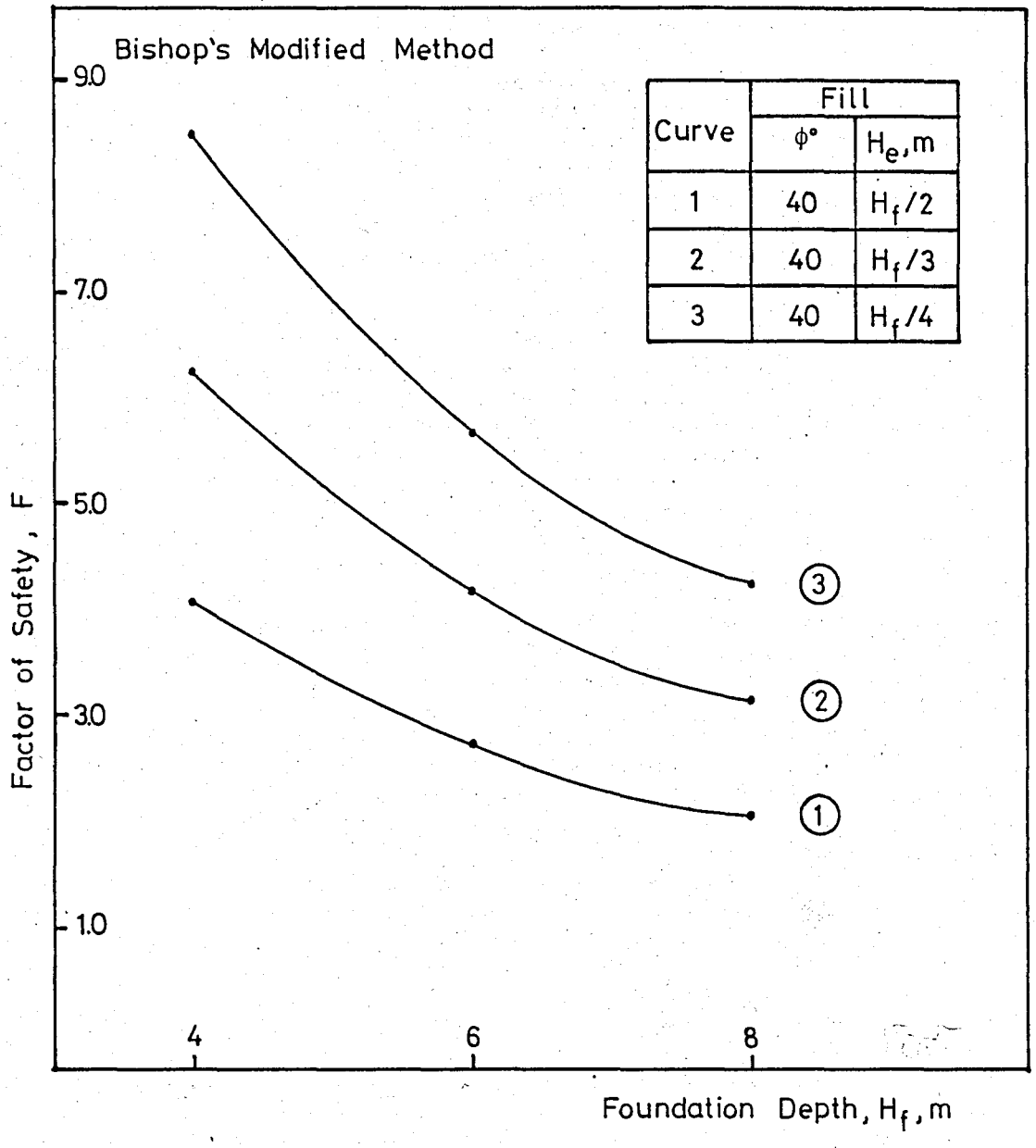

FIG.A.12 Effect of Foundation Depth for Variable Embankment Height on Factor of Safety of the Typical Embankment Shown in Fig.5.5 by Bishop's Modified Method

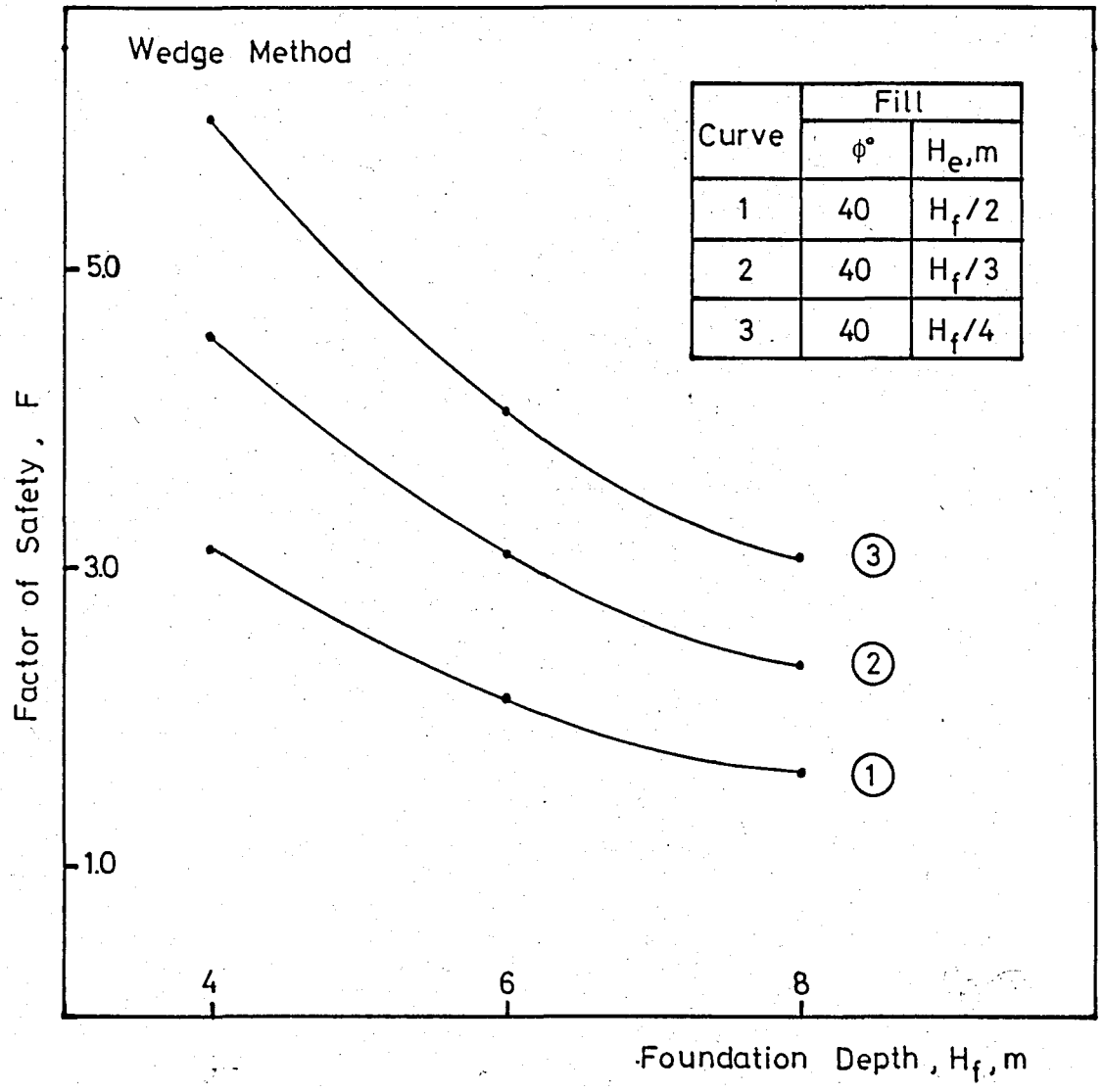

FIG.A.13 Effect of Foundation Depth for Variable Embankment Height on Factor of Safety of the Typical Embankment Shown in Fig.5.5 by Wedge Method

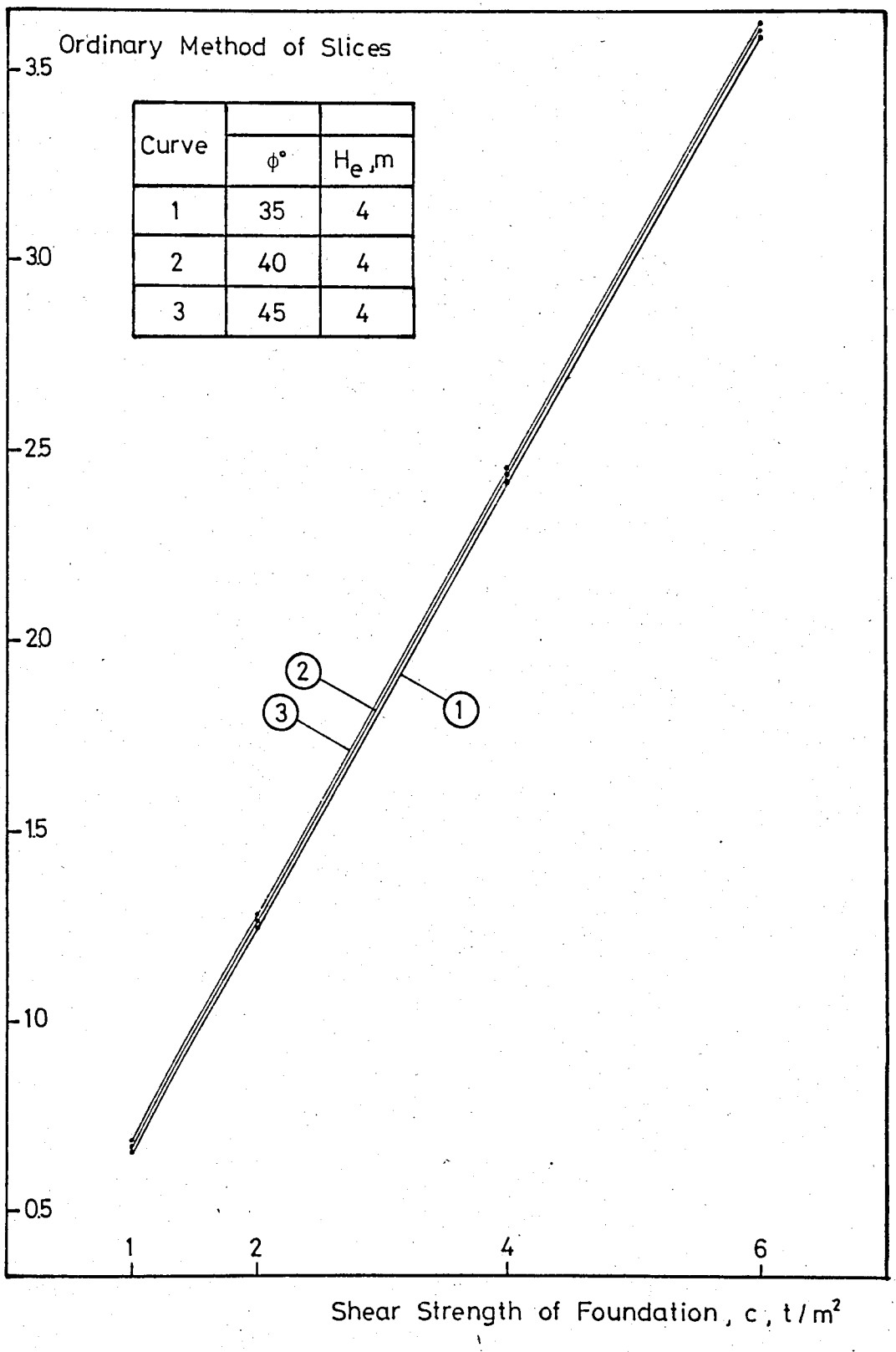

FIG.A.14 Effect of Variable Shear Strength of Foundation on Factor of Safety of the Typical Embankment Shown in Fig.5.7 by Ordinary Method of Slices

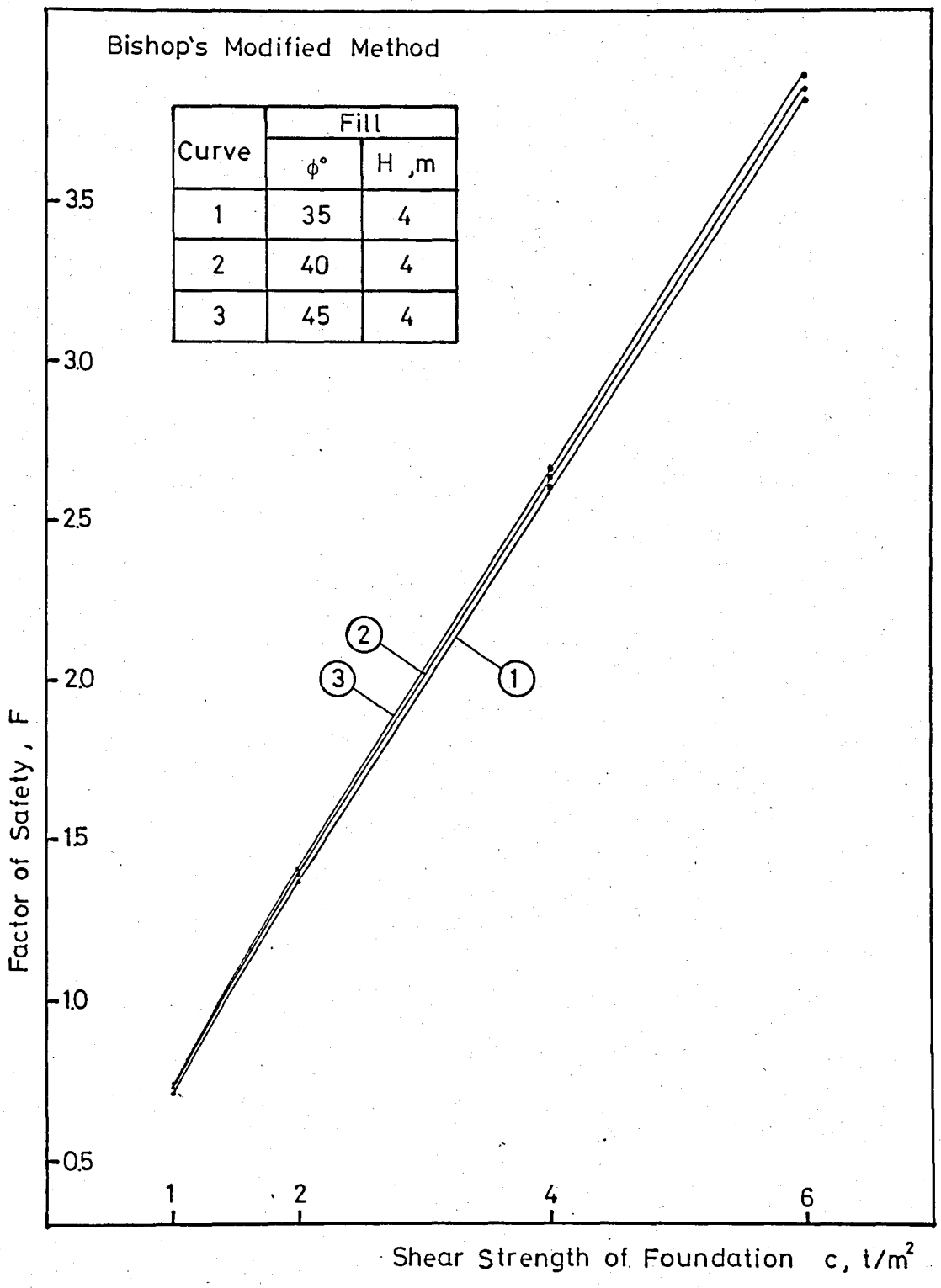

FIG.A.15 Effect of Variable Shear Strength of Foundation on Factor of Safety of the Typical Embankment Shown in Fig.5.7.by Bishop's Modified Method

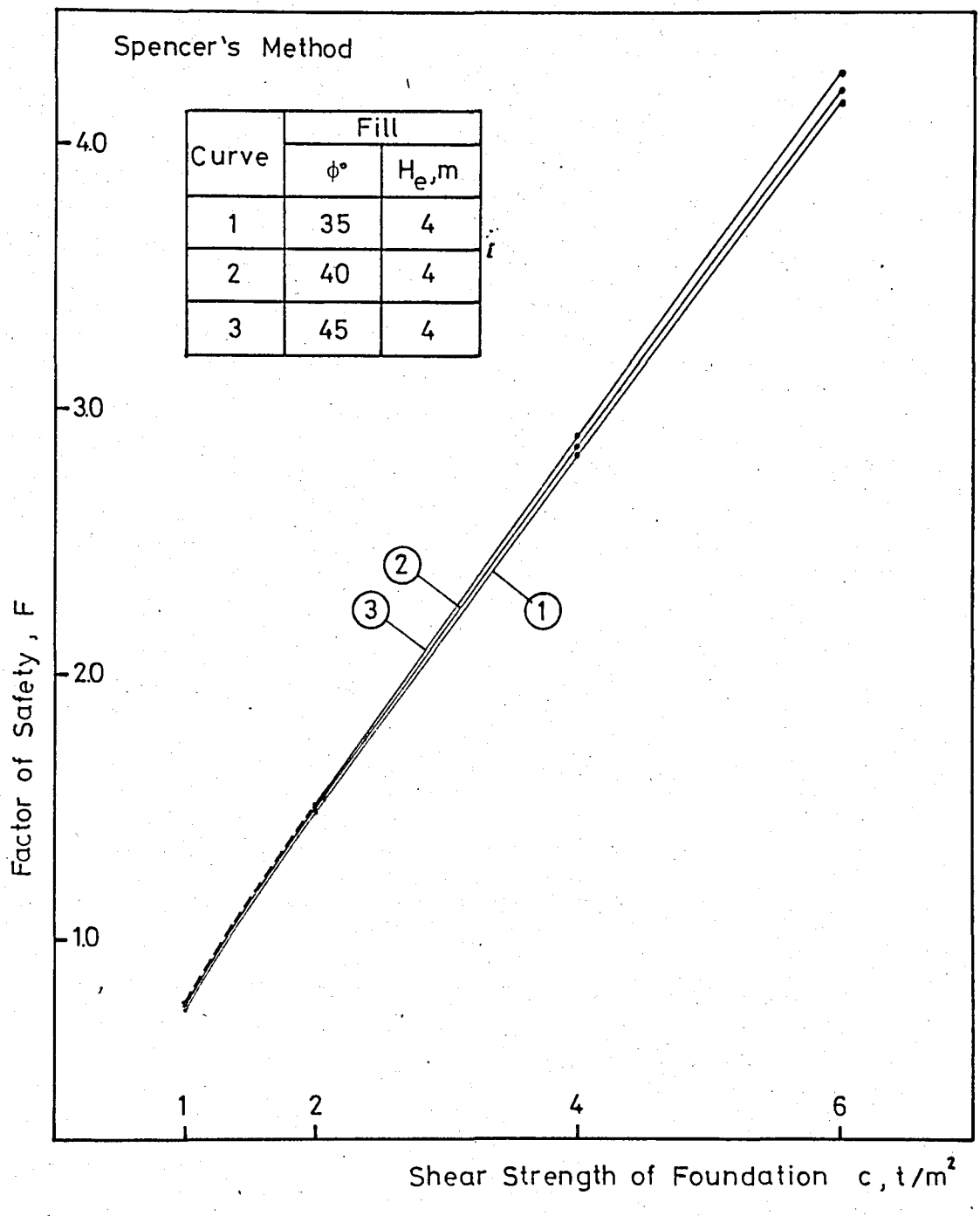

FIG.A.16 Effect of Variable Shear Strength of Foundation on Factor of Safety of the Typical Embankment Shown in Fig.5.7 by Spencer's Method

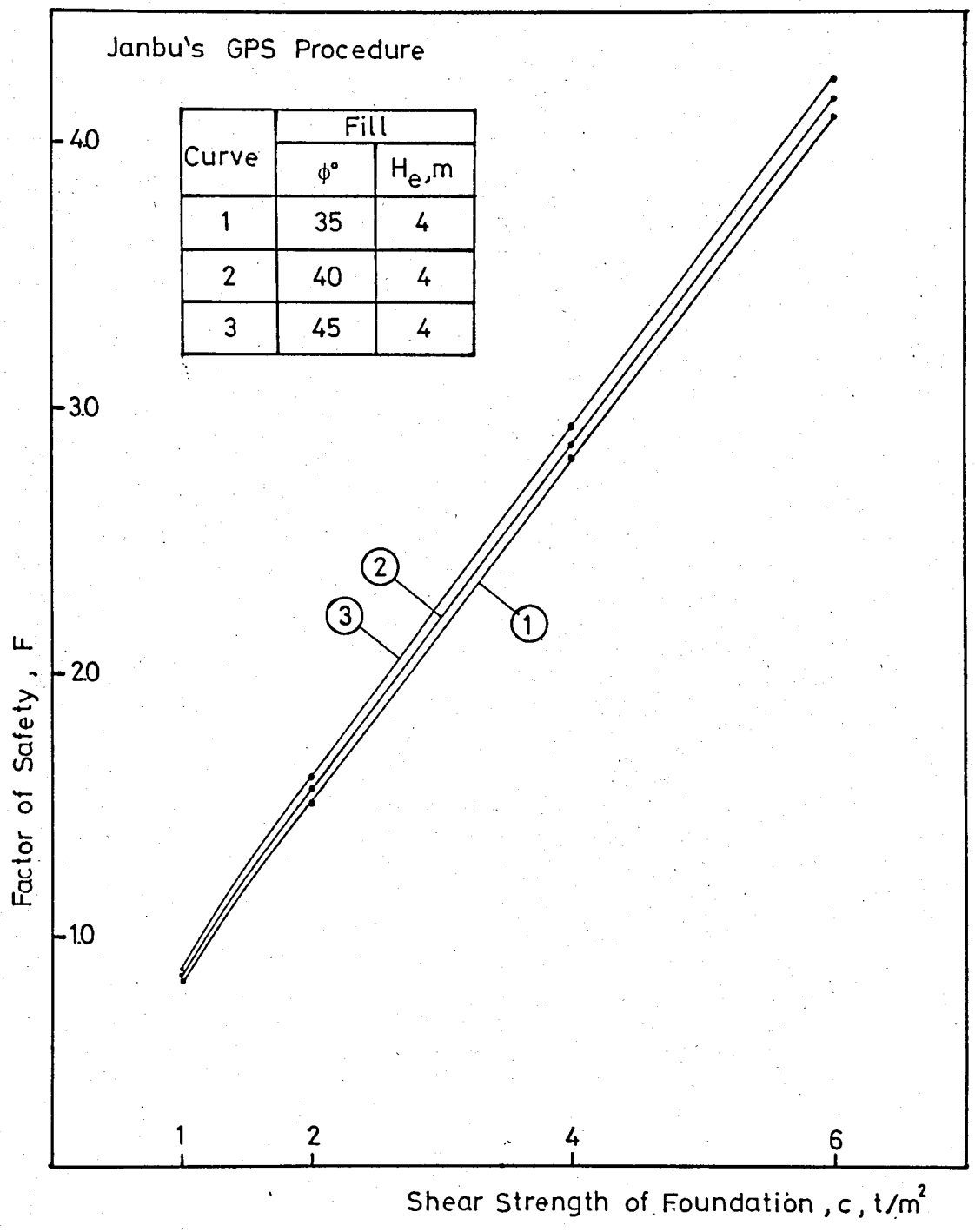

FIG.A.17 Effect of Variable Shear Strength of Foundation on Factor of Safety of the Typical Embankment Shown in Fig.5.7 by Janbu's Generalized Procedure of Slices

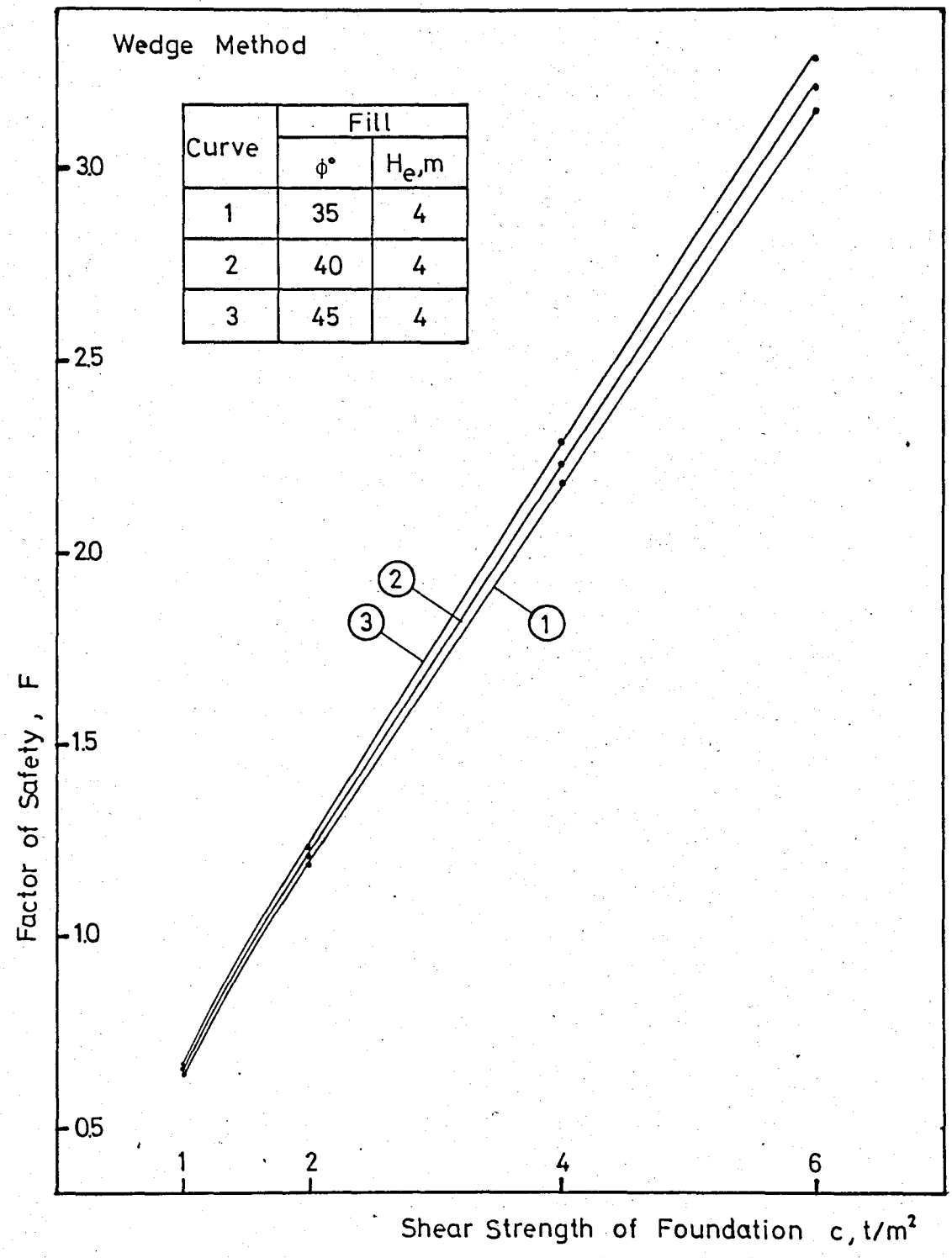

FIG.A.18 Effect of Variable Shear Strength of Foundation on Factor of Safety of the Typical Ebankment Shown in Fig.5.7 by Wedge Method

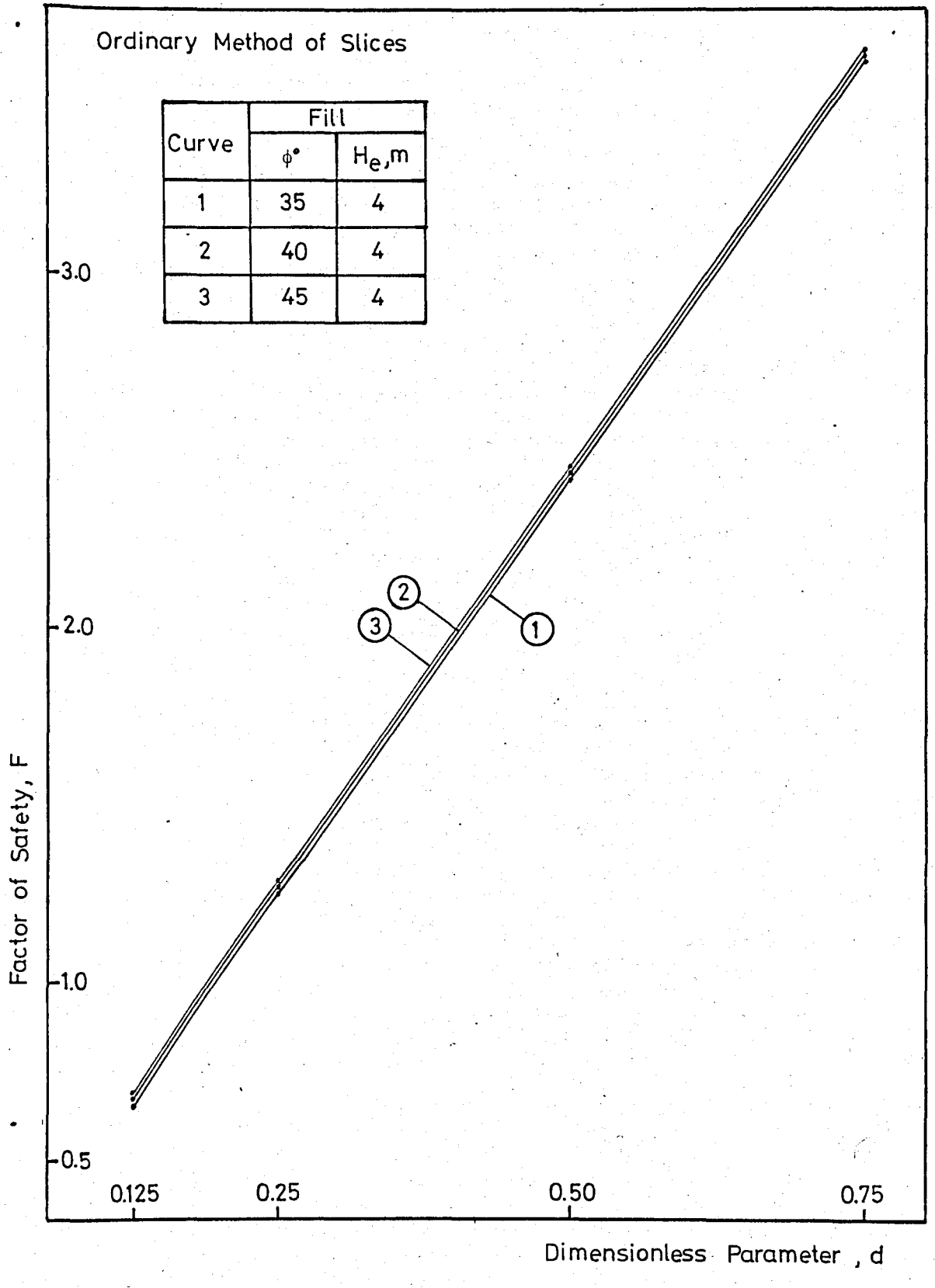

FIG.A.19 Effect of Dimensionless Parameter ,d, on Factor of Safety of the Typical Embankment Shown in Fig.5.7 by Ordinary Method of Slices

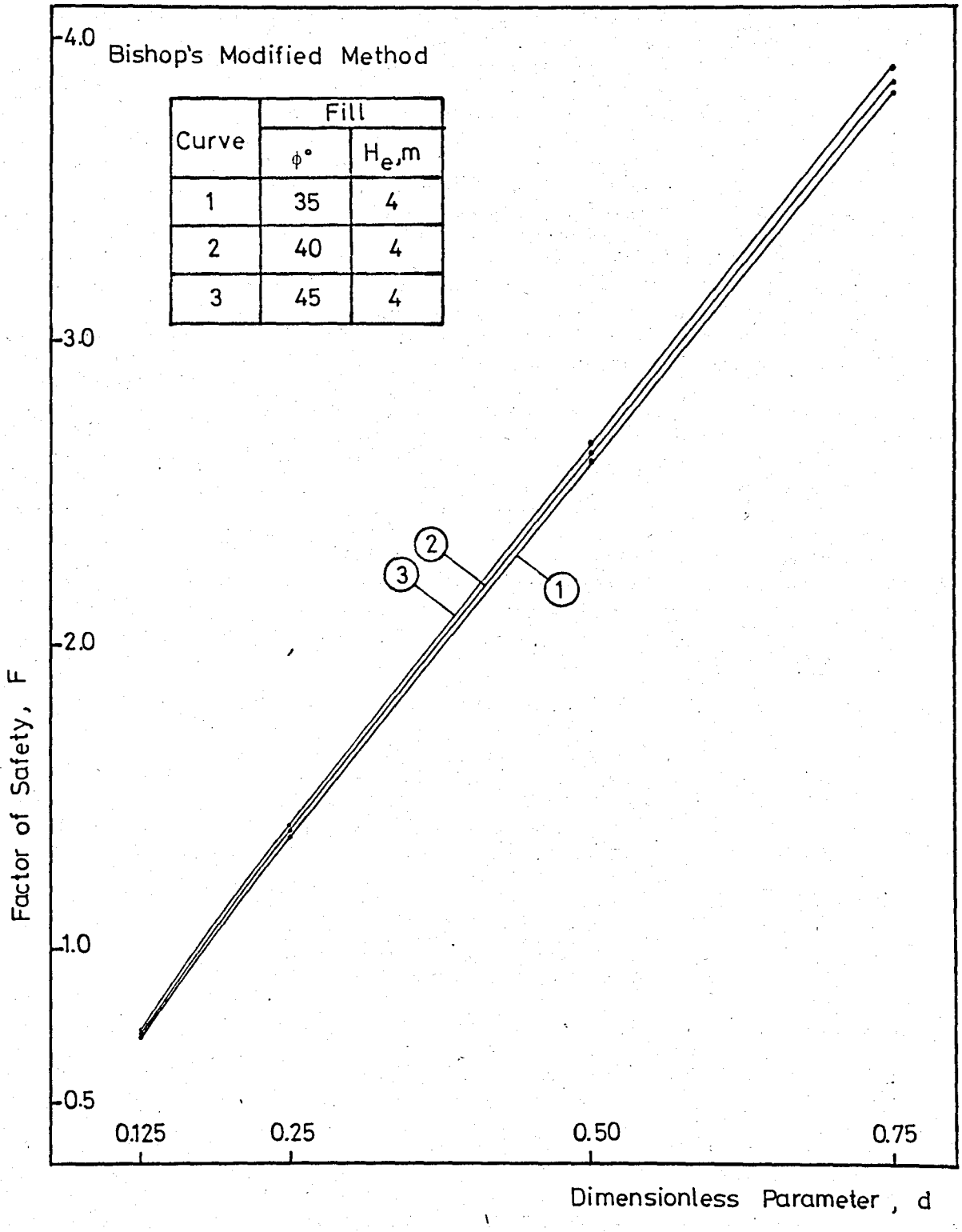

FIG.A.20 Effect of Dimensionle Parameter, d, on Factor of Safety of the Typical Embankment Shown in Fig.5.7 by Bishop's Modified Method

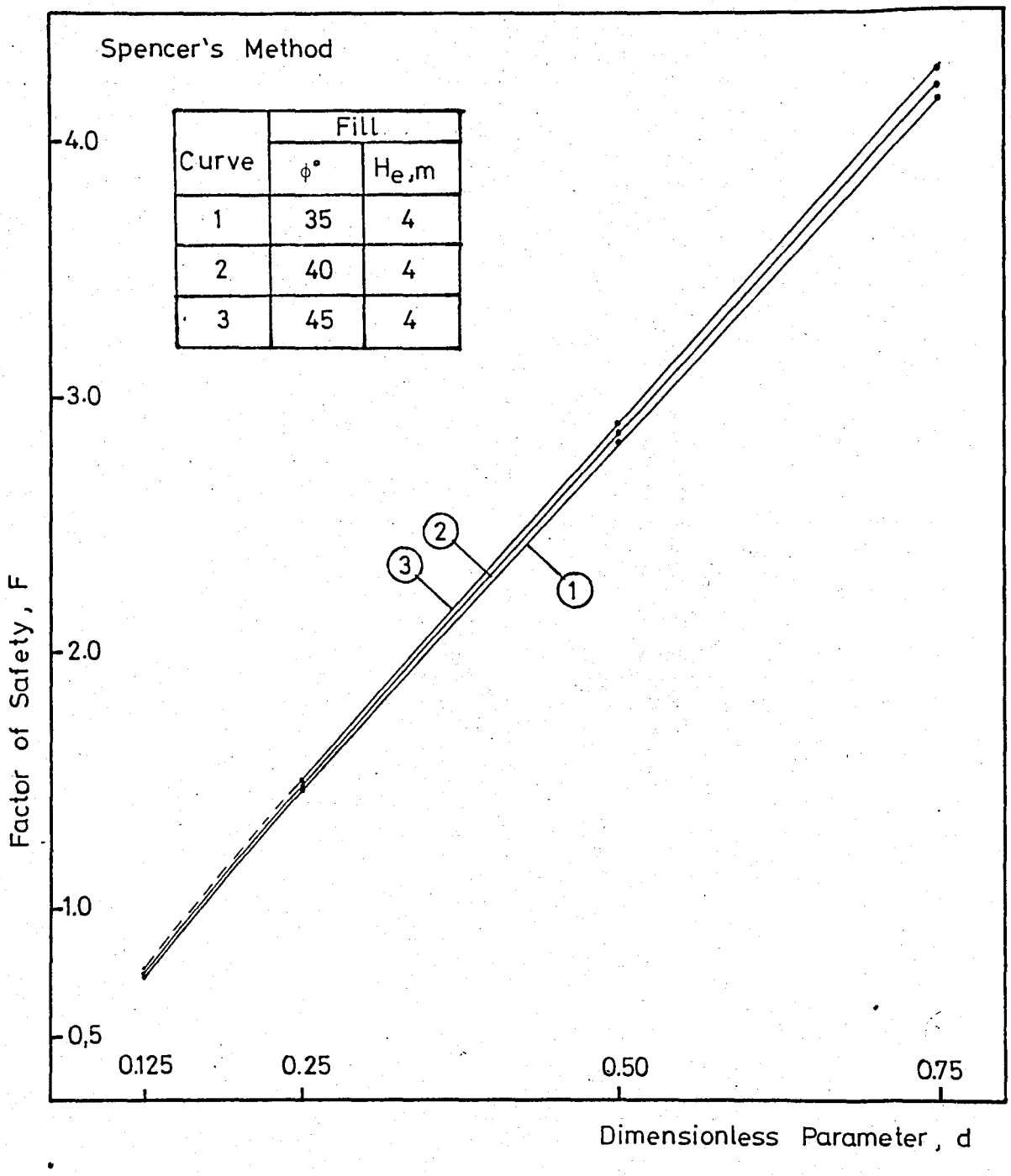

FIG.A.21 Effect of Dimensionless Parameter, d, on Factor of Safety of the Typical Embankment Shown in Fig.5.7 by Spencer's Method

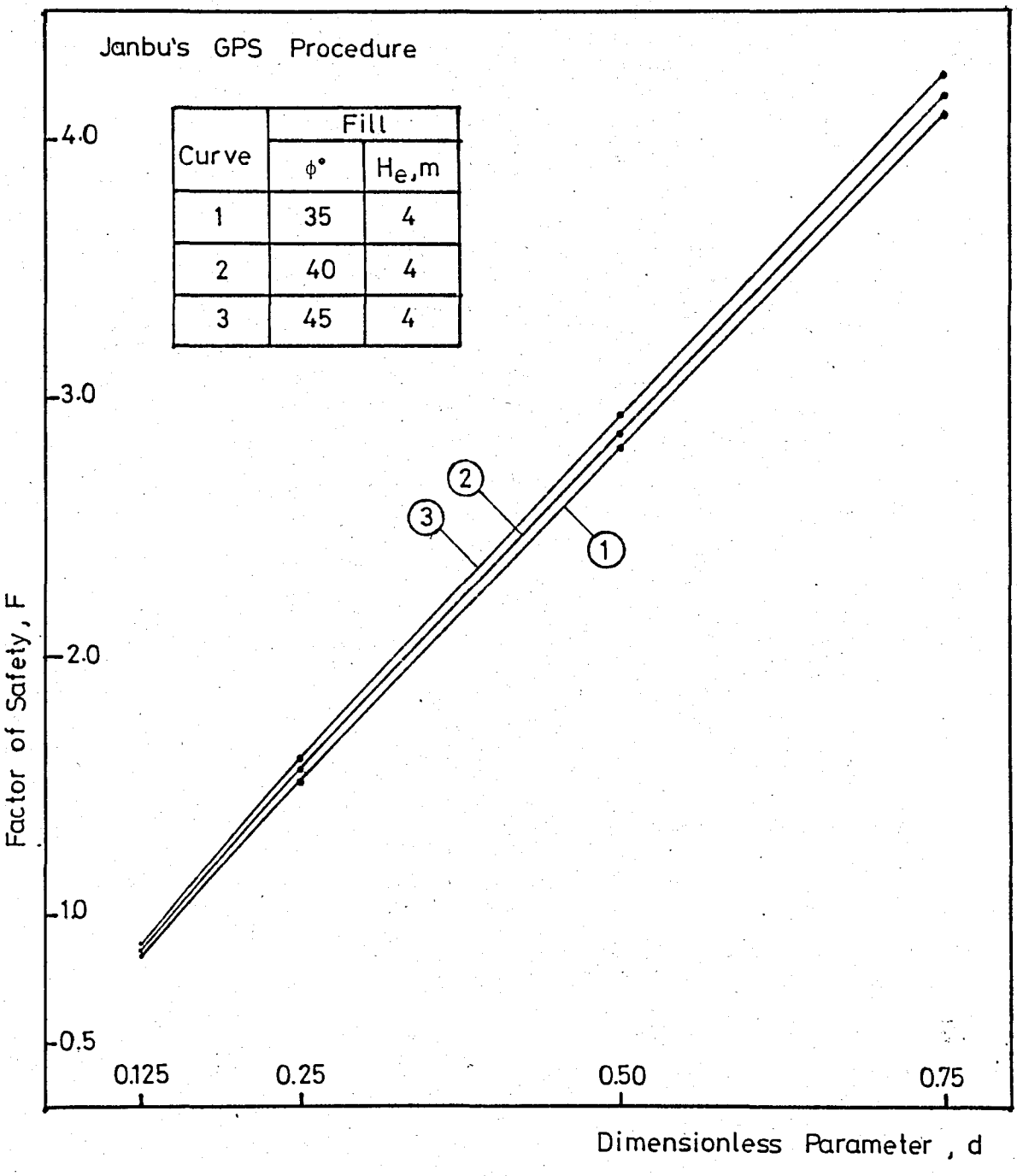

FIG.A.22 Effect of Dimensionless Parameter,d, on Factor of Safety of the Typical Embankment Shown in Fig.5.7 by Janbu's Generalized Procedure of Slices

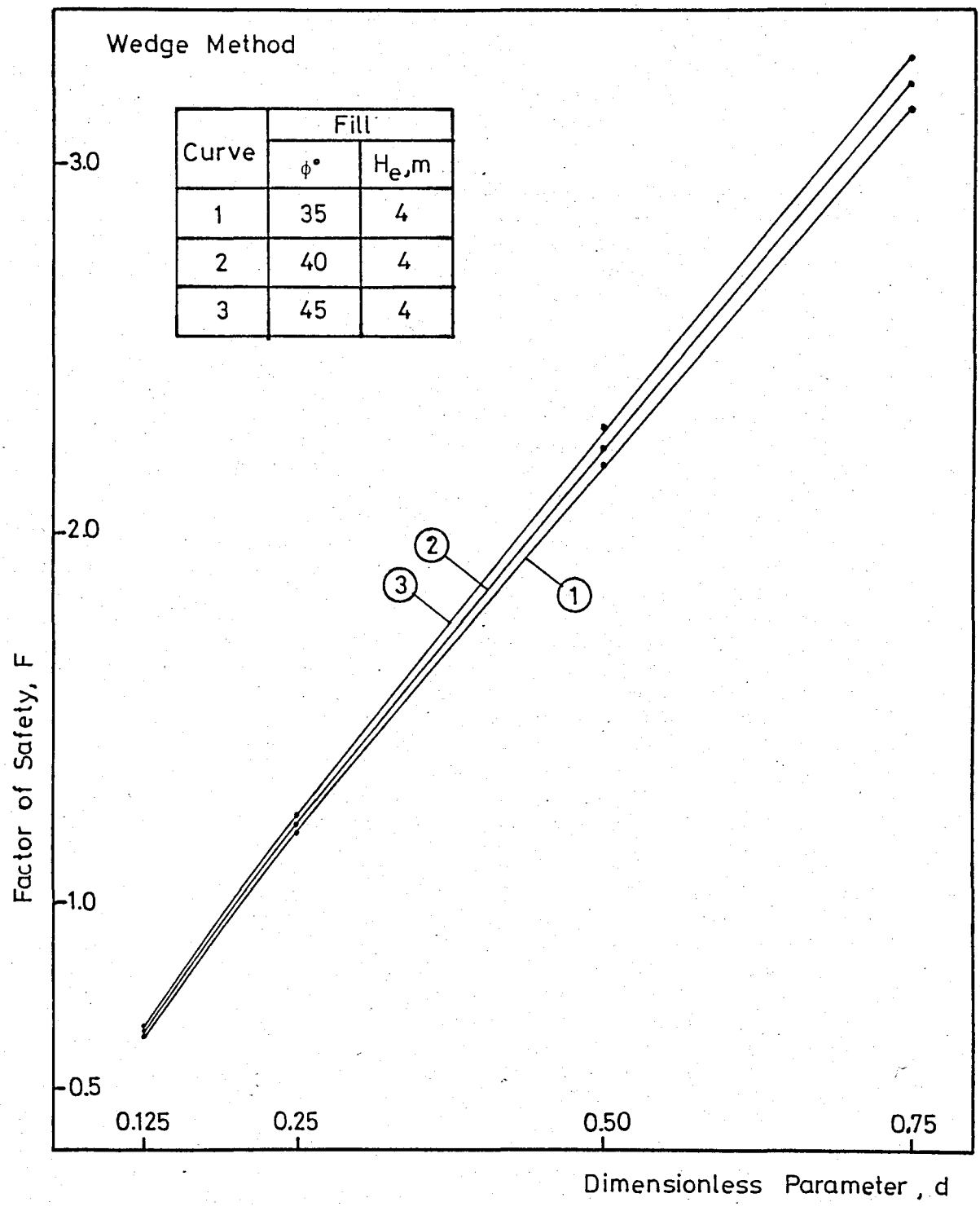

FIG.A.23 Effect of Dimensionless Parameter,d, on Factor of Safety of the Typical Embankment Shown in Fig.5.7 by Wedge Method

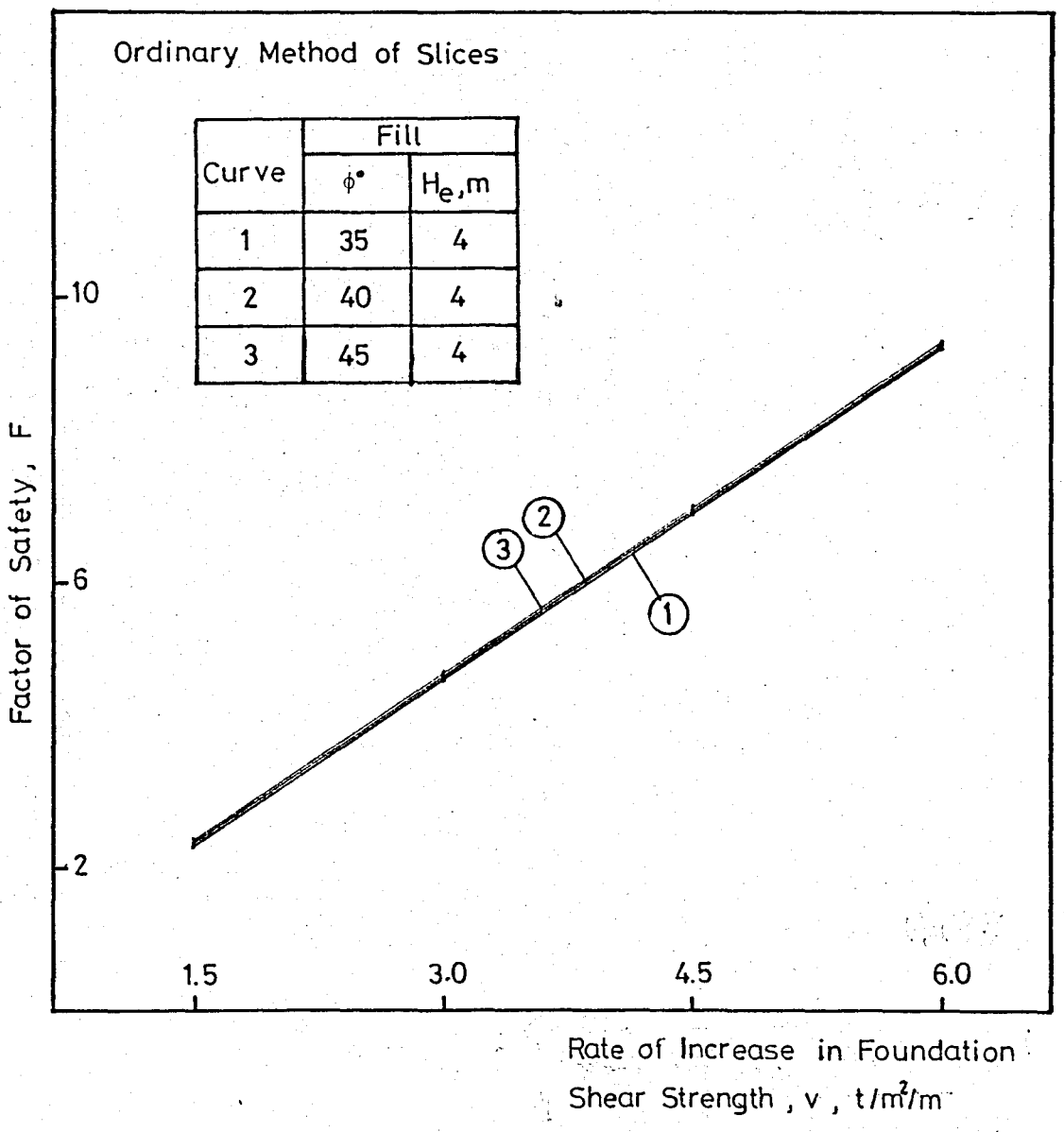

FIG.A.24 Effect of Rate of Increase in Foundation Shear Strength ,v, on Factor of Safety of the Typical Embankment Shown in Fig.5.10 by Ordinary Method Of Slices (for c=0)

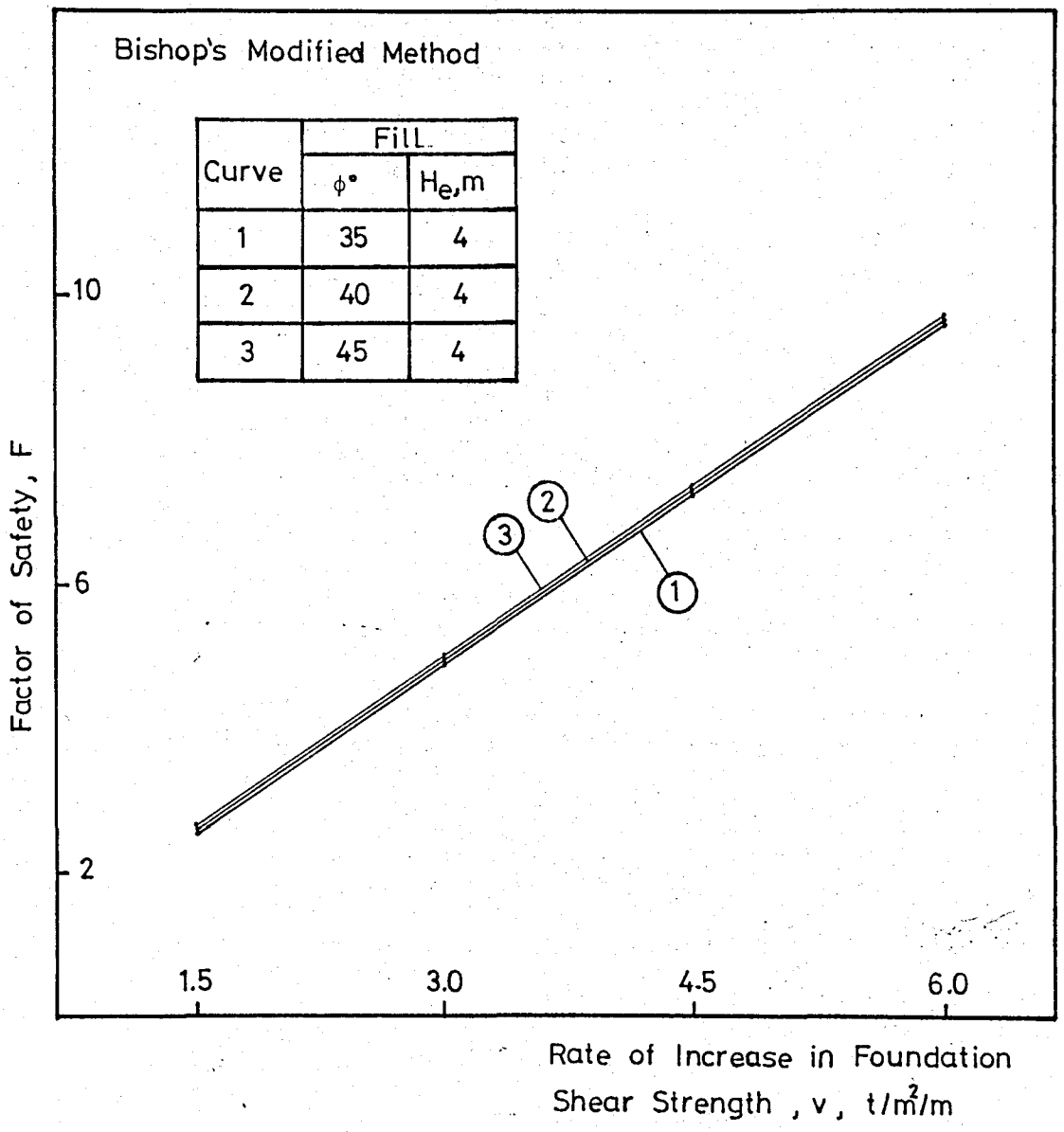

FIG.A.25 Effect of Rate of Increase in Foundation Shear Strength ,v, on Factor of Safety of the Typical Embankment Shown in Fig.5.10 by Bishop's Modified Methor (for c=0)

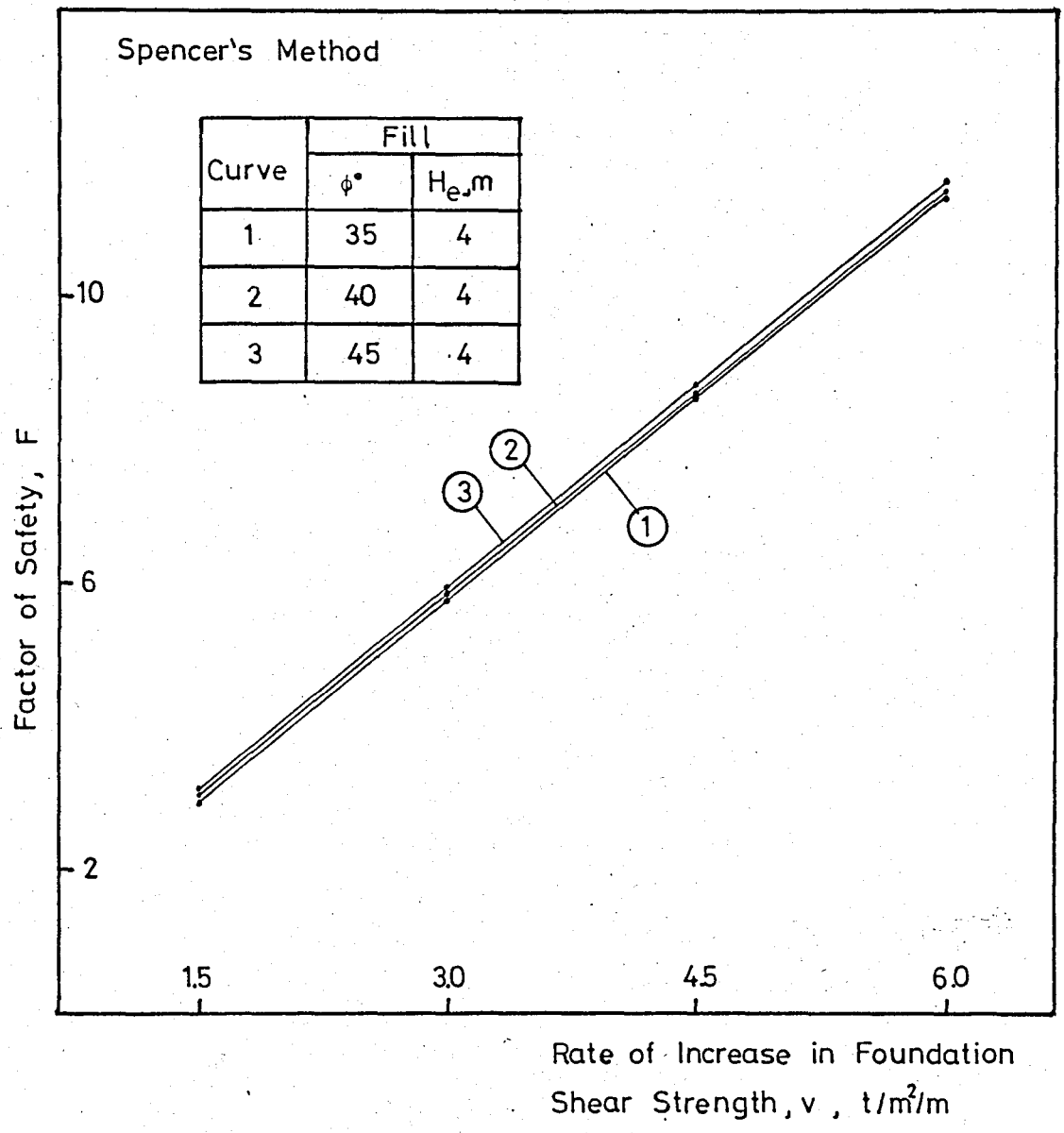

FIG.A.26 Effect of Rate of Increase in Foundation Shear Strength ,v, on Factor of Safety of the Typical Embankment Shown in Fig.5.10 by Spencer's Method (for c=0)

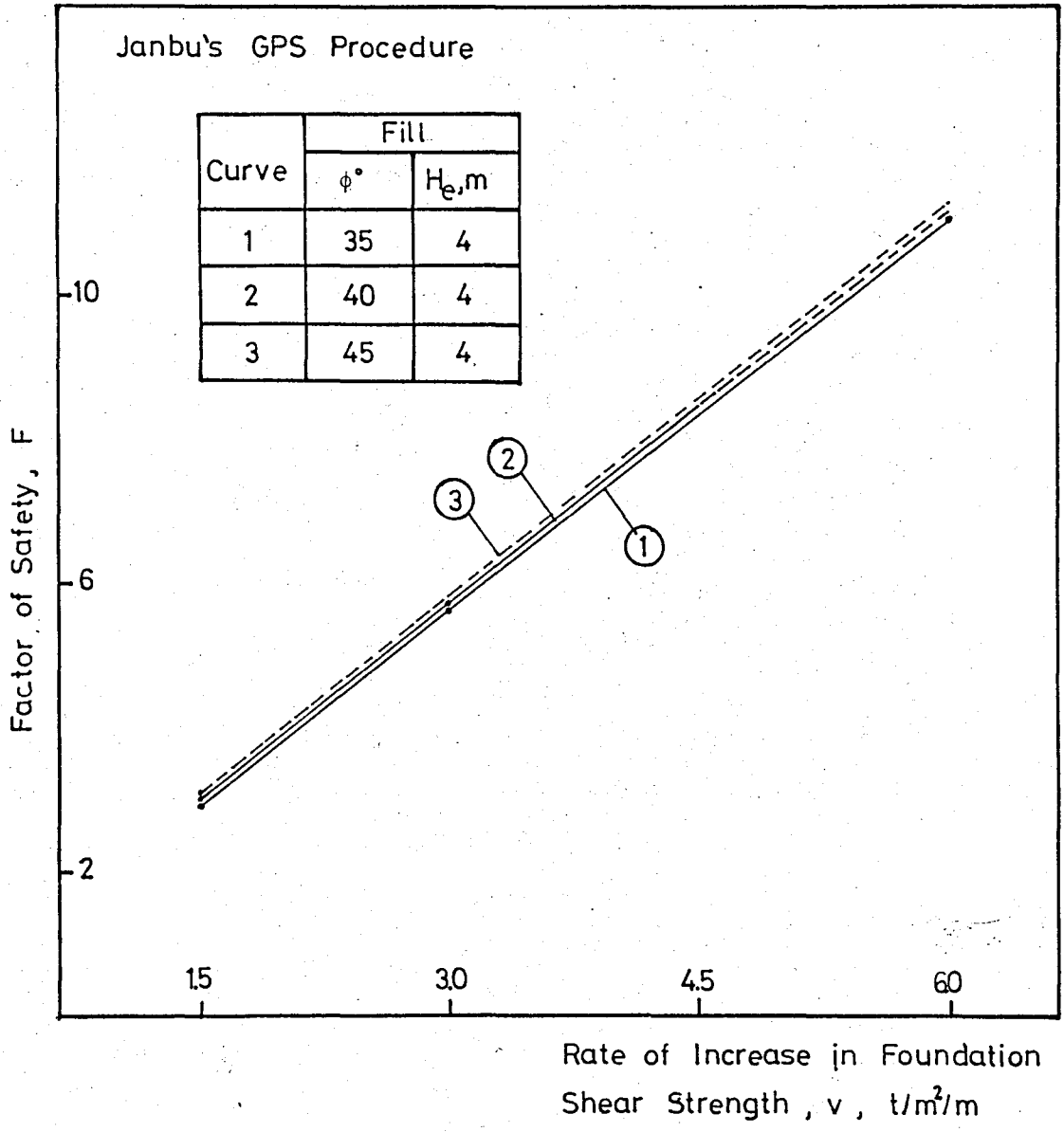

FIG.A.27 Effect of Rate of Increase in Foundation Shear Strength ,v, on Factor of Safety of the Typical Embankment Shown in Fig.5.10 by Janbu's Generalized Procedure of Slices (for c=0)

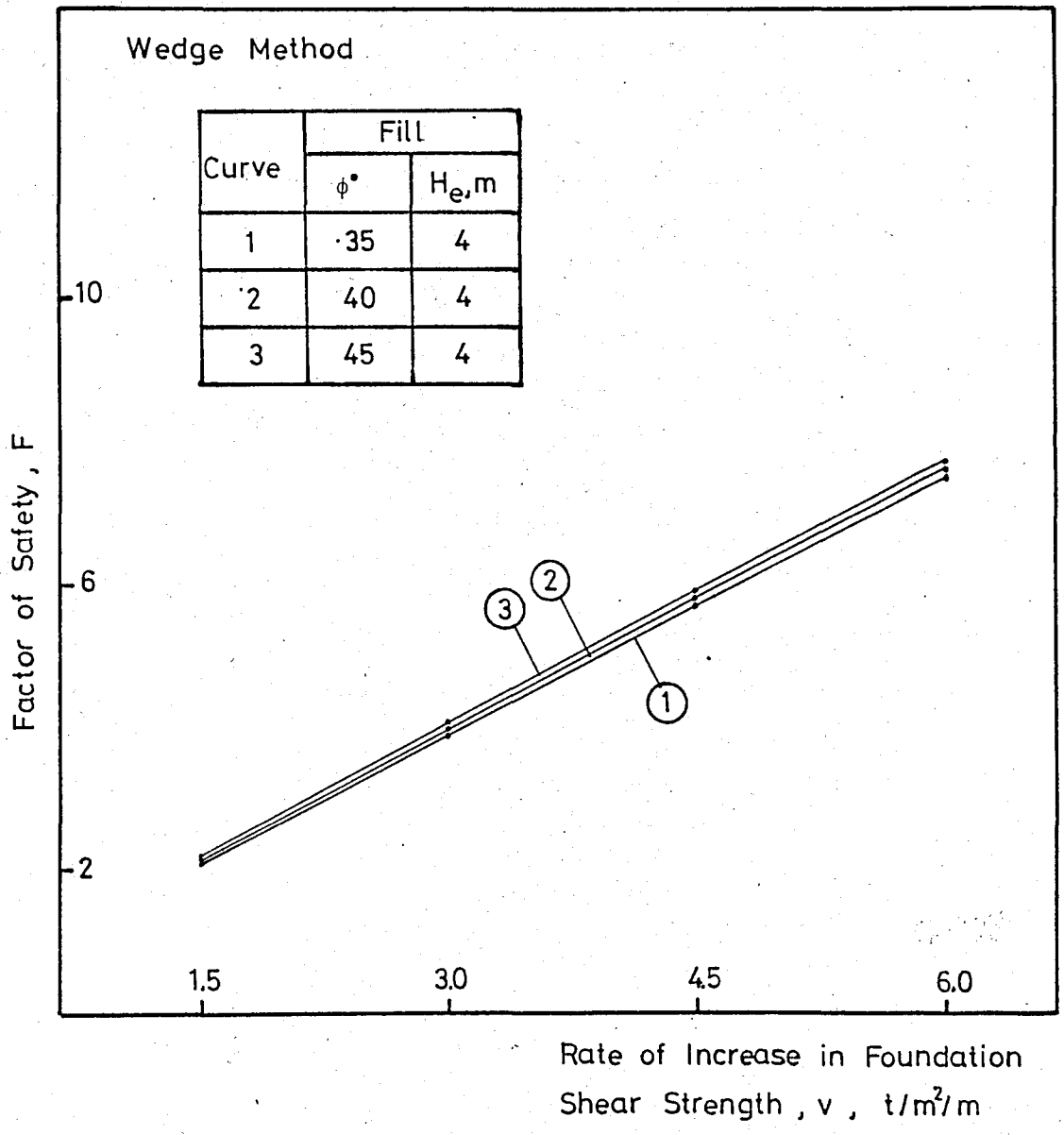

FIG.A.28 Effect of Rate of Increase in Foundation Shear Strengtn.,v, on Factor of Safety of the Typical Embankment Shown in Fig.5.10 by Wedge Method (for c=0)

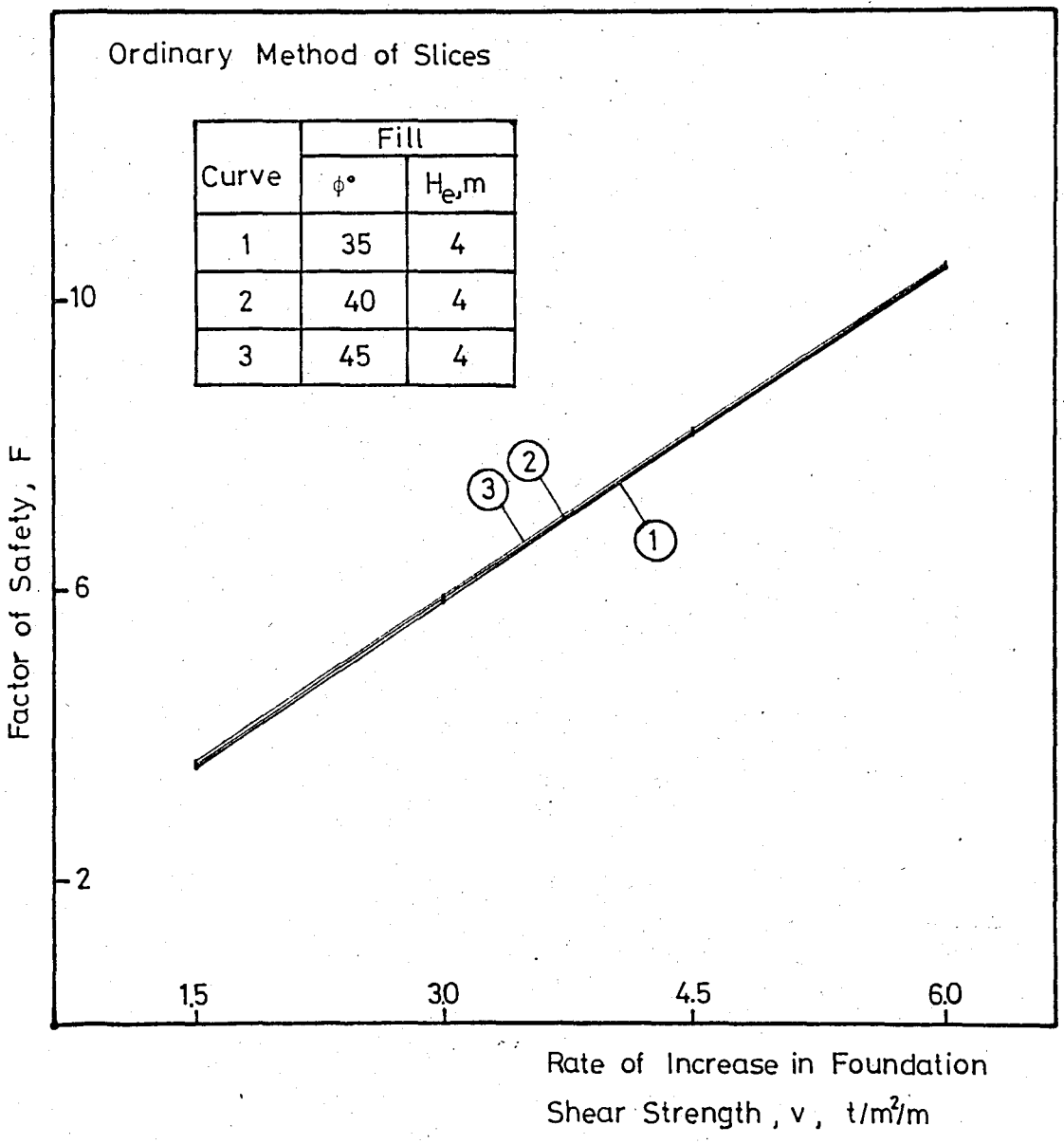

FIG.A.29 Effect of Rate of Increase in Foundation Shear Strength ,v, on Factor of Safety of the Typical Embankment Shown in Fig.5.10 by Ordinary Method Slices (for c=2 t/m²)

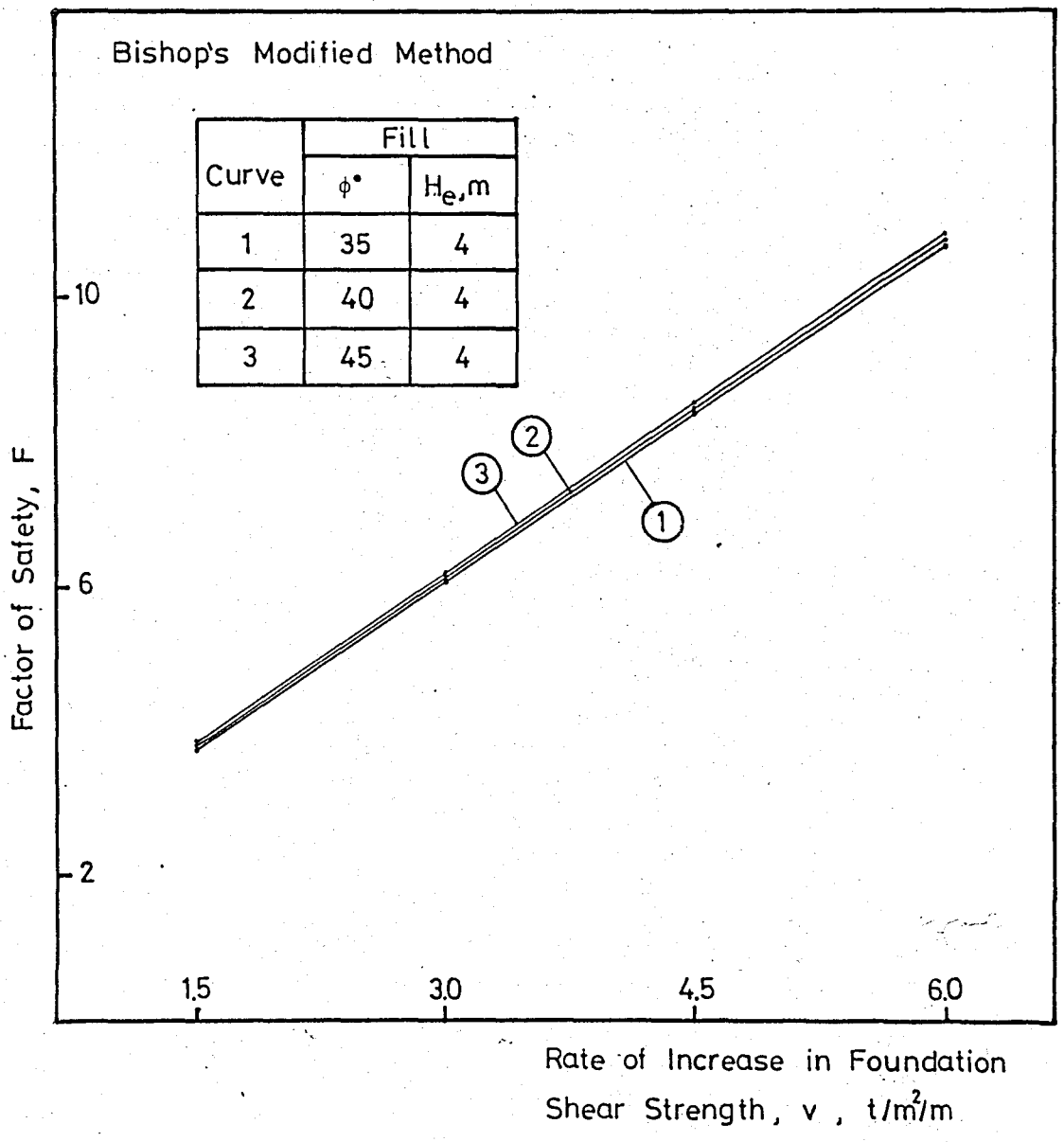

FIG.A.30 Effect of Rate of Increase in Foundation Shear Strength ,v, on Factor of Safety of the Typical Embankment Shown in Fig.5.10 by Bishop's Modified Method (for c=2 t/m²)

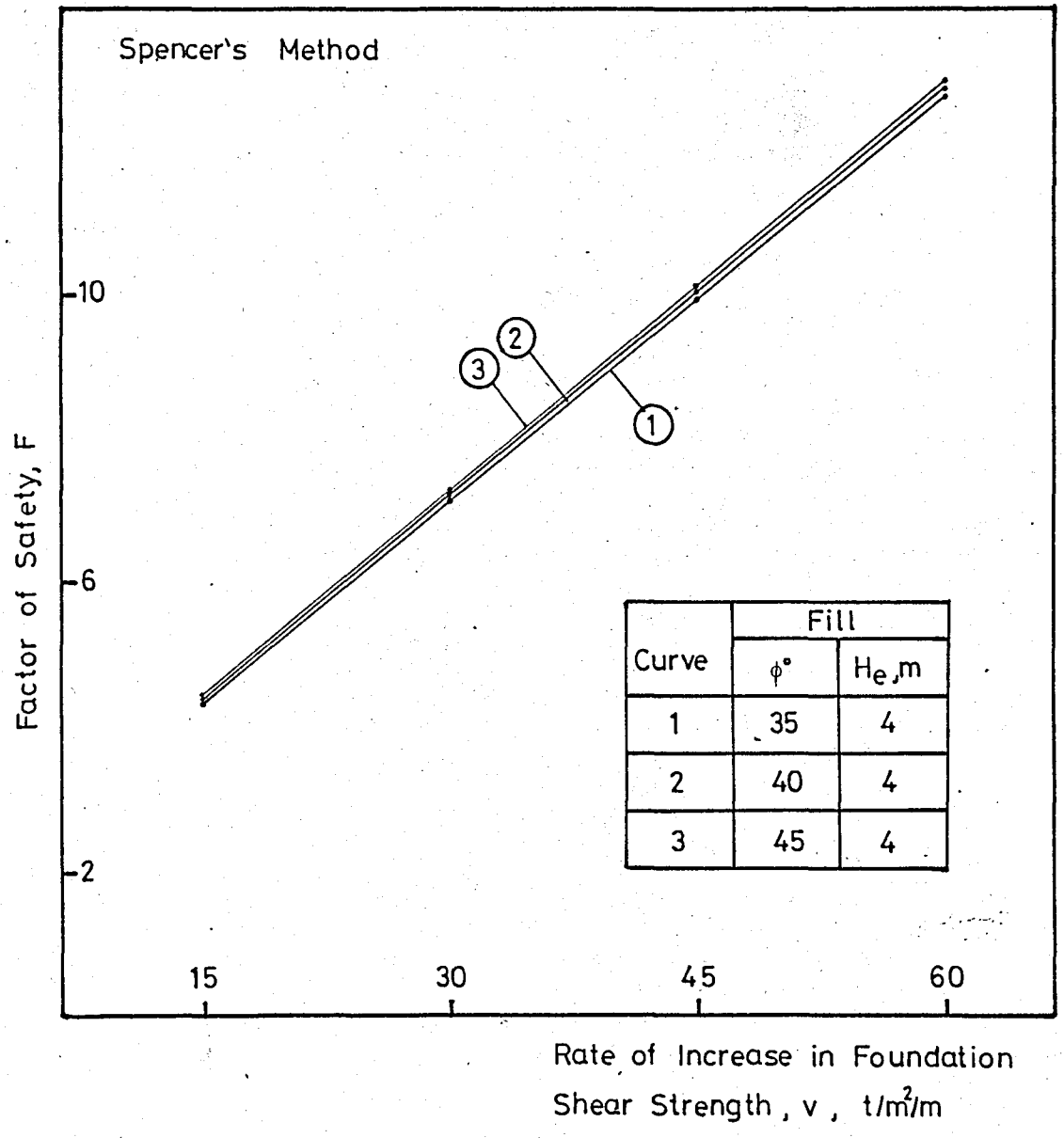

FIG.A.31 Effect of Rate of Increase in Foundation Shear Strength ,v, on Factor of Safety of the Typical Embankment Shown in Fig.5.10 by Spencer's Method (for c=2 t/m²)

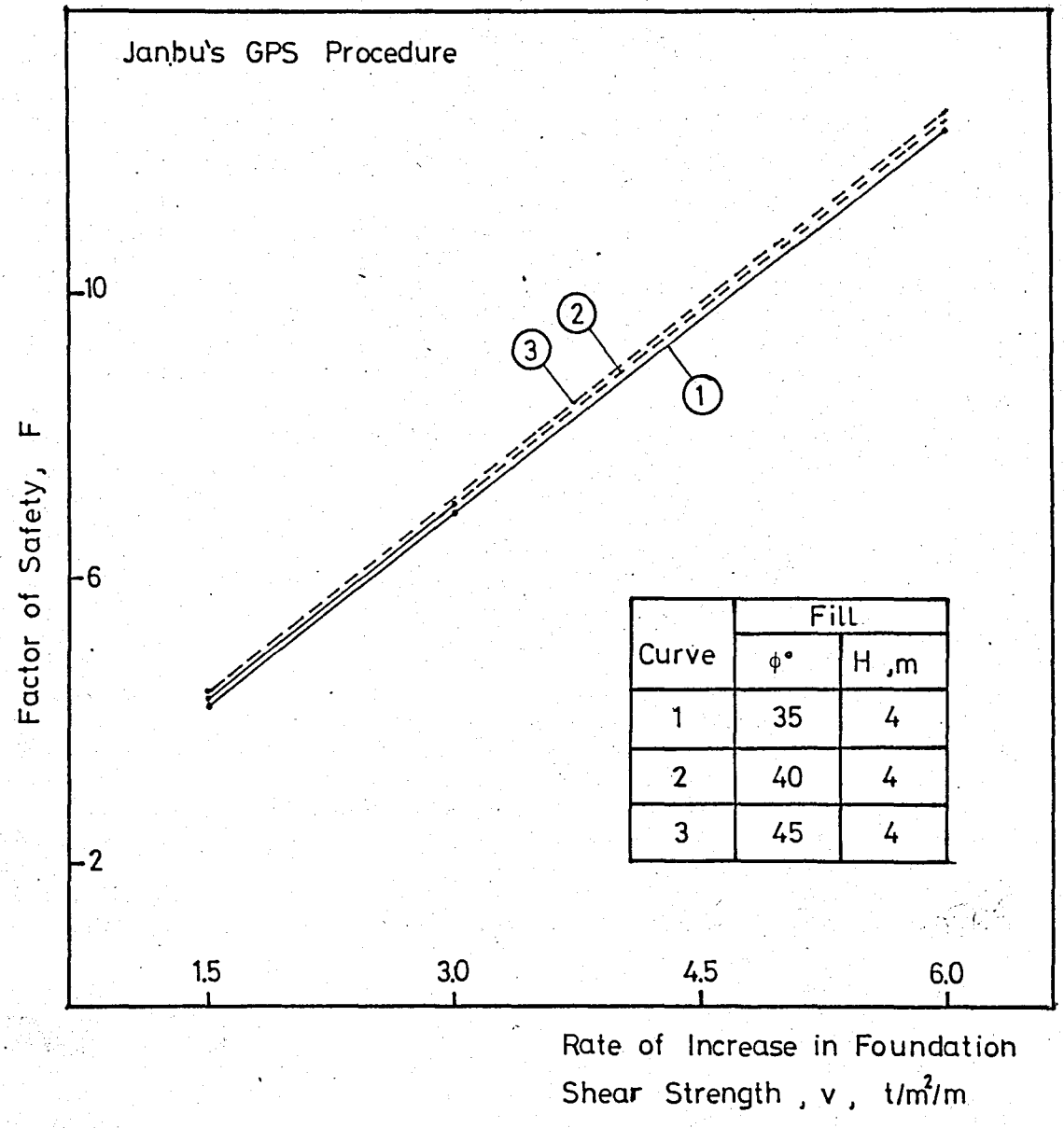

FIG.A.32 Effect of Rate of Increase in Foundation Shear Strength ,v, on Factor of Safety of the Typical Embankment Shown in Fig.5.10 by Janbu's Generalized Procedure of Slices (for c=2 t/m²)

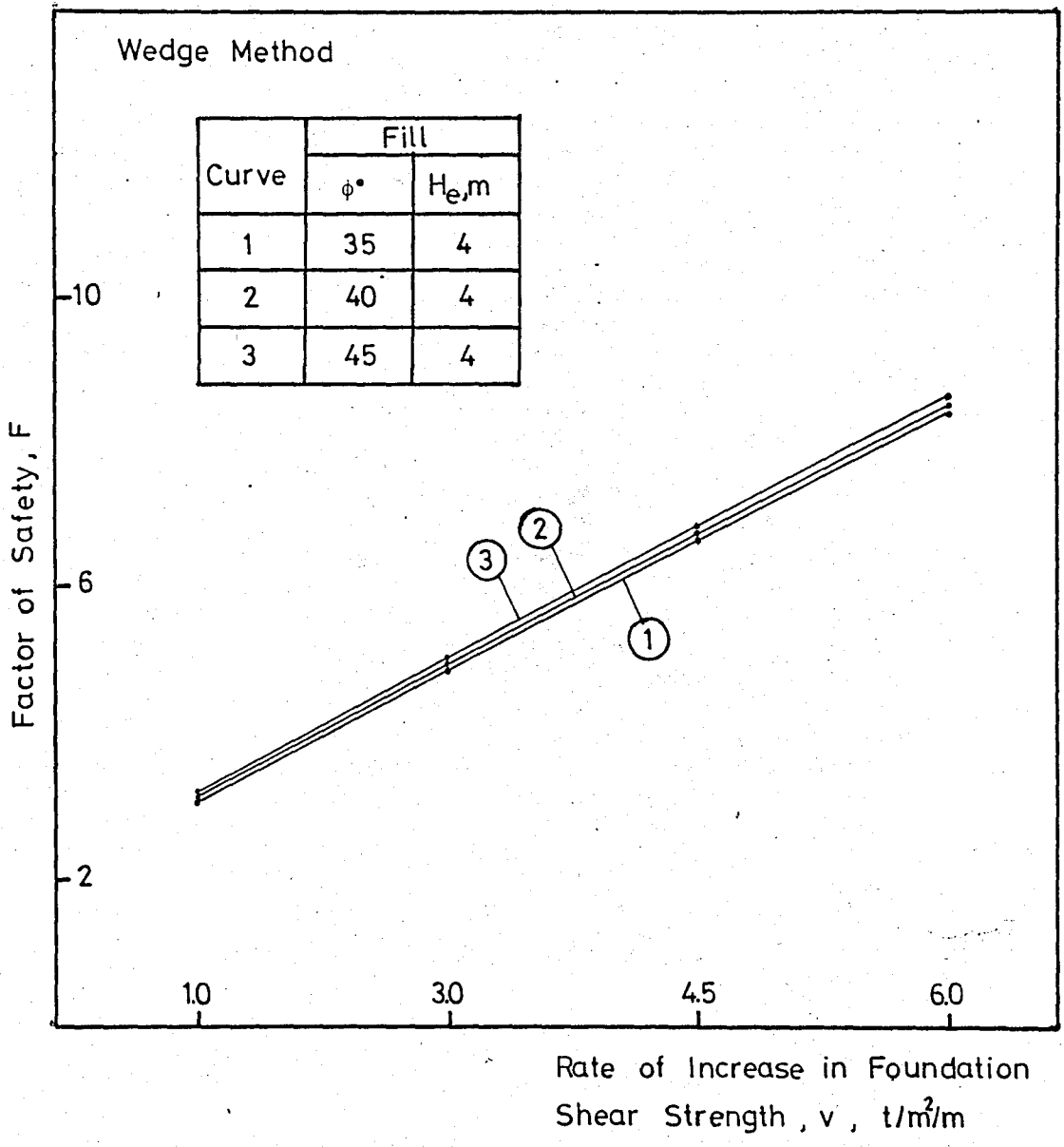

FIG.A.33 Effect of Rate of Increase in Foundation Shear Strength ,v, on Factor of Safety of the Typical Embankment Shown in Fig.5.10 by Wedge Method (for c=2 t/m²)

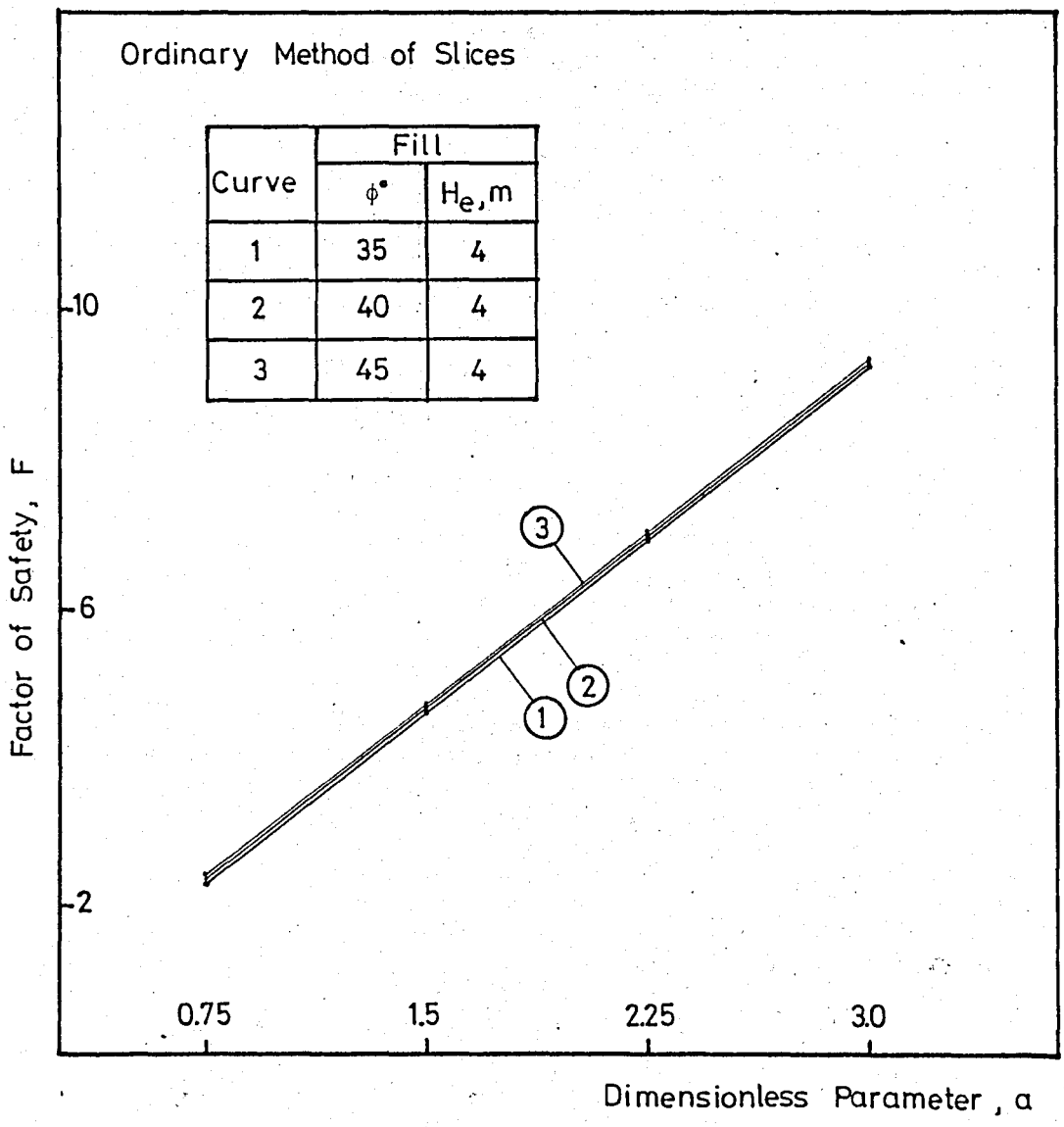

FIG.A.34 Effect of Dimensionless Parameter ,a, on Factor of Safety of the Typical Embankment Shown in Fig.5.10 by Ordinary Method of Slices

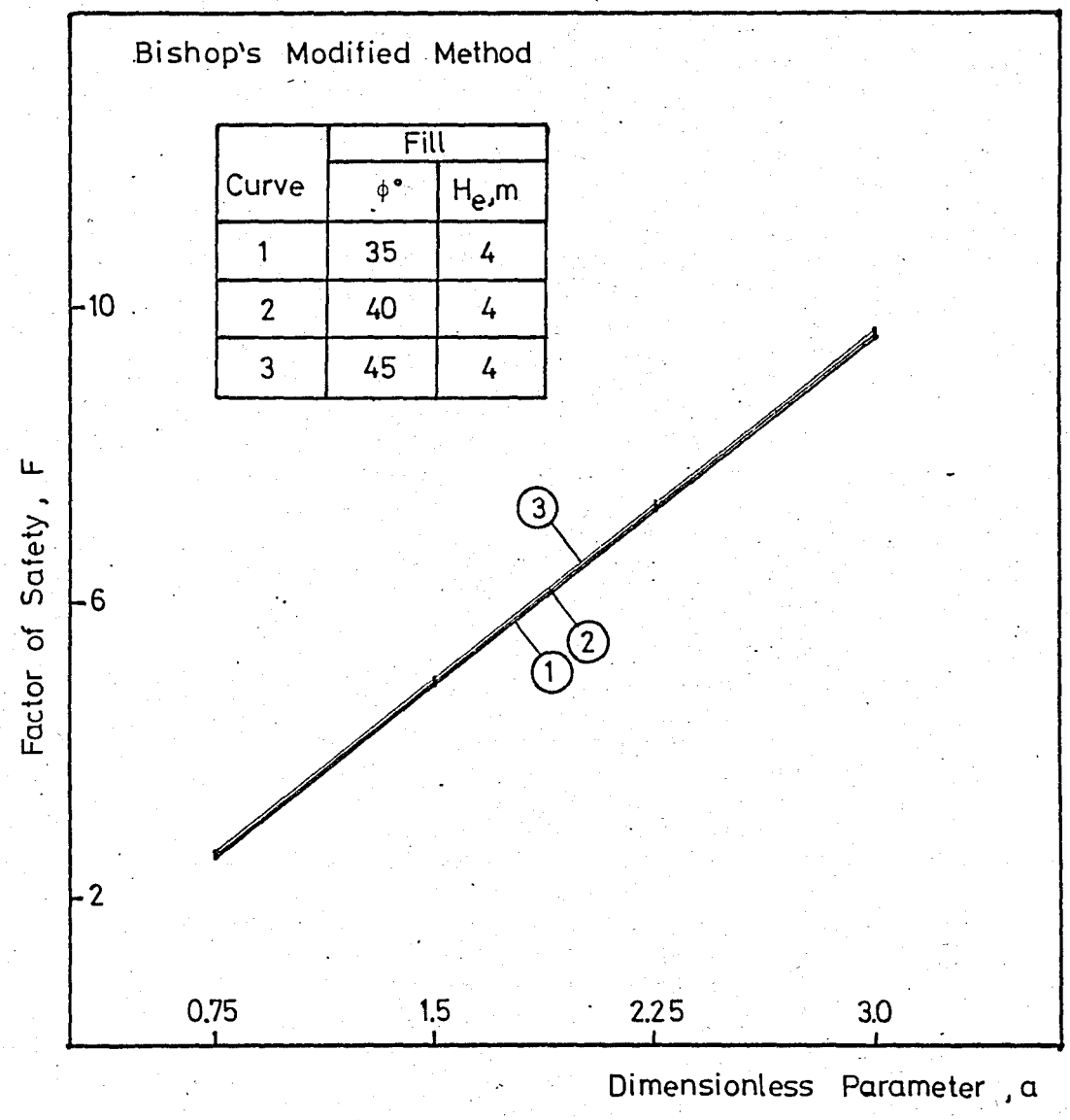

FIG.A.35 Effect of Dimensionless Parameter ,a, on Factor of Safety of the Typical Embankment Shown in Fig.5.10 by Bishop's Modified Method

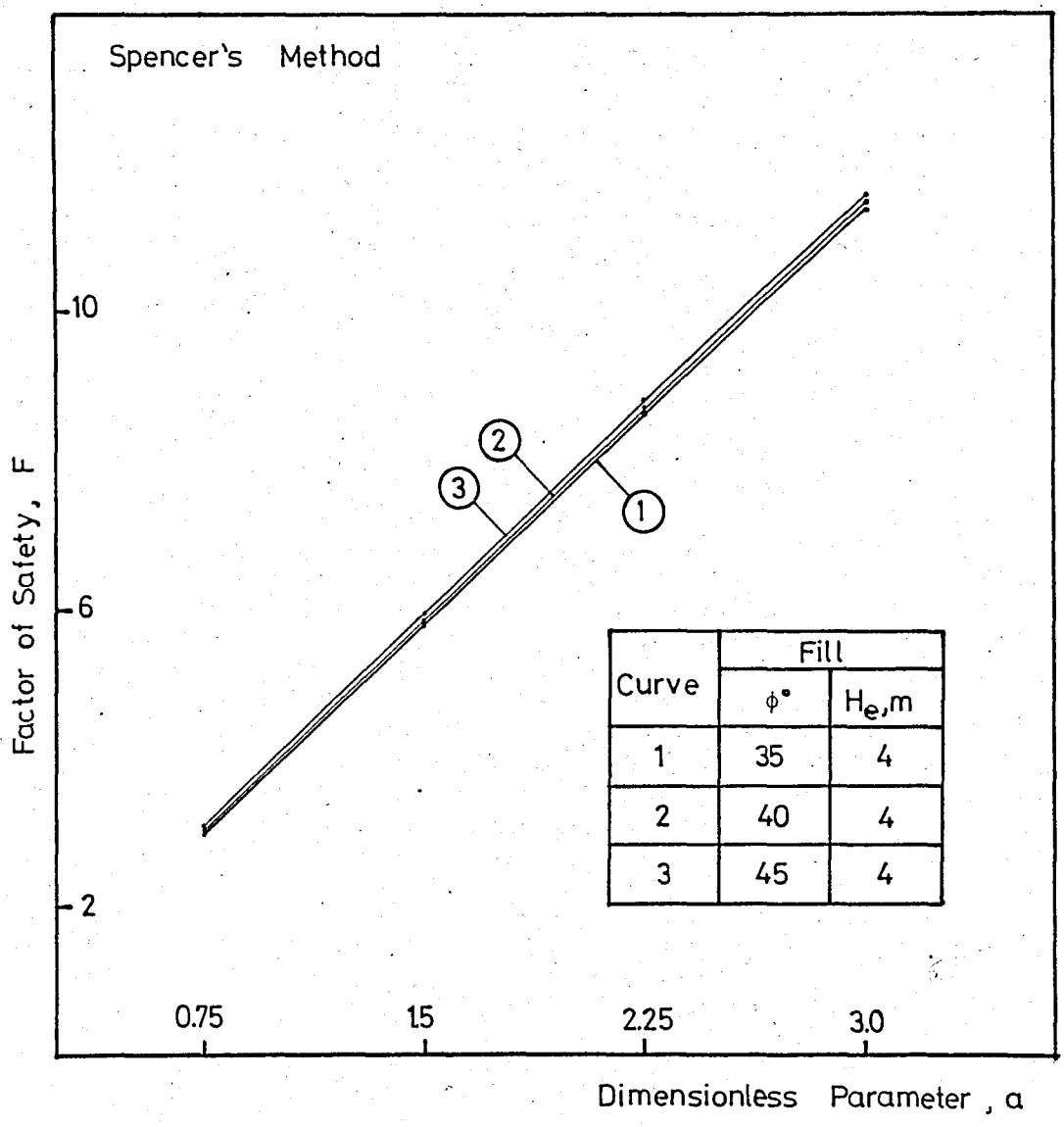

FIG.A.36 Effect of Dimensionless Parameter ,a, on Factor of Safety of the Typical Embankment Shown in Fig.5.10 by Spencer's Method

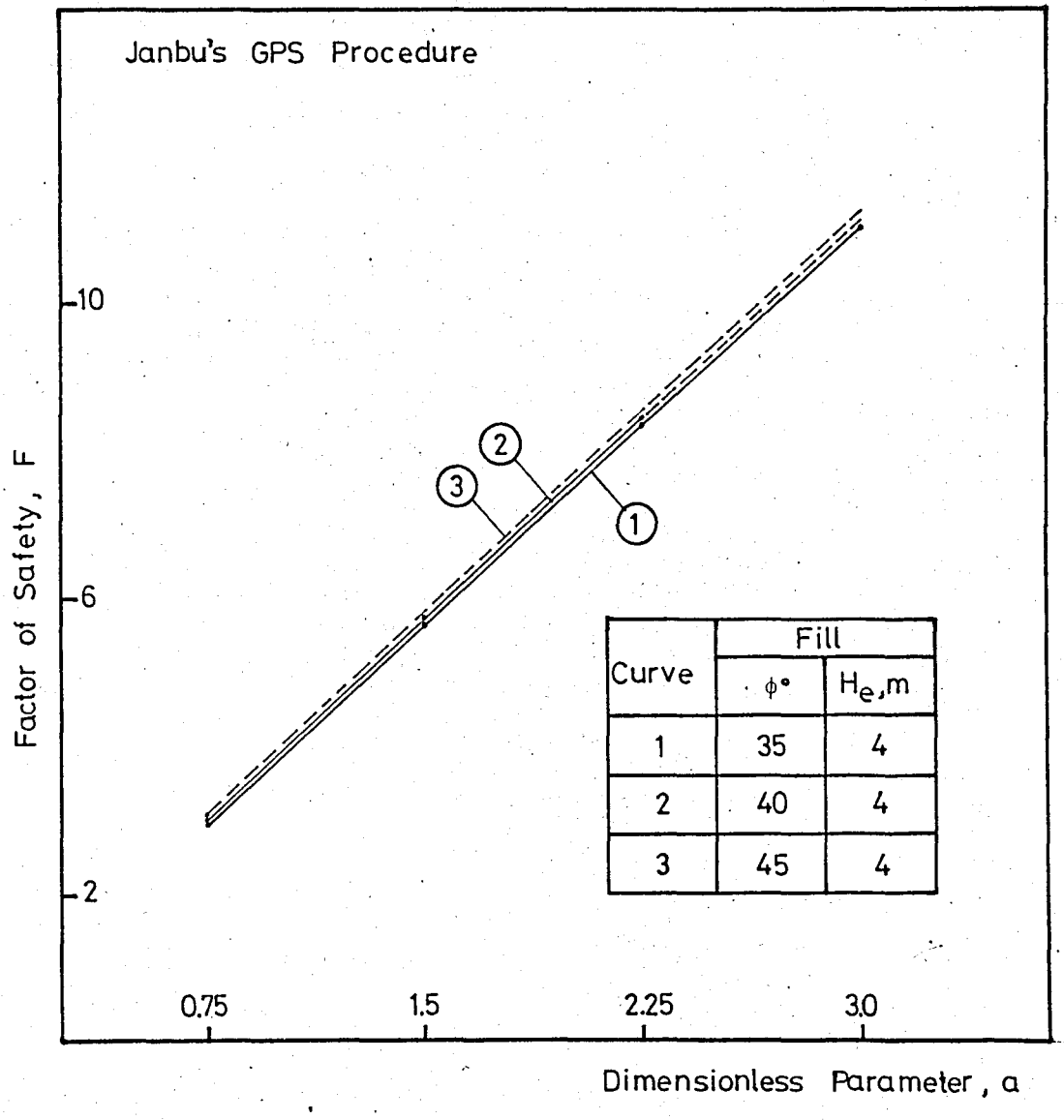

FIG.A.37 Effect of Dimensionless Parametr ,a, on Factor of Safety of the Typical Embankment Shown in Fig.5.10 by Janbu's Generalized Procedure of Slices

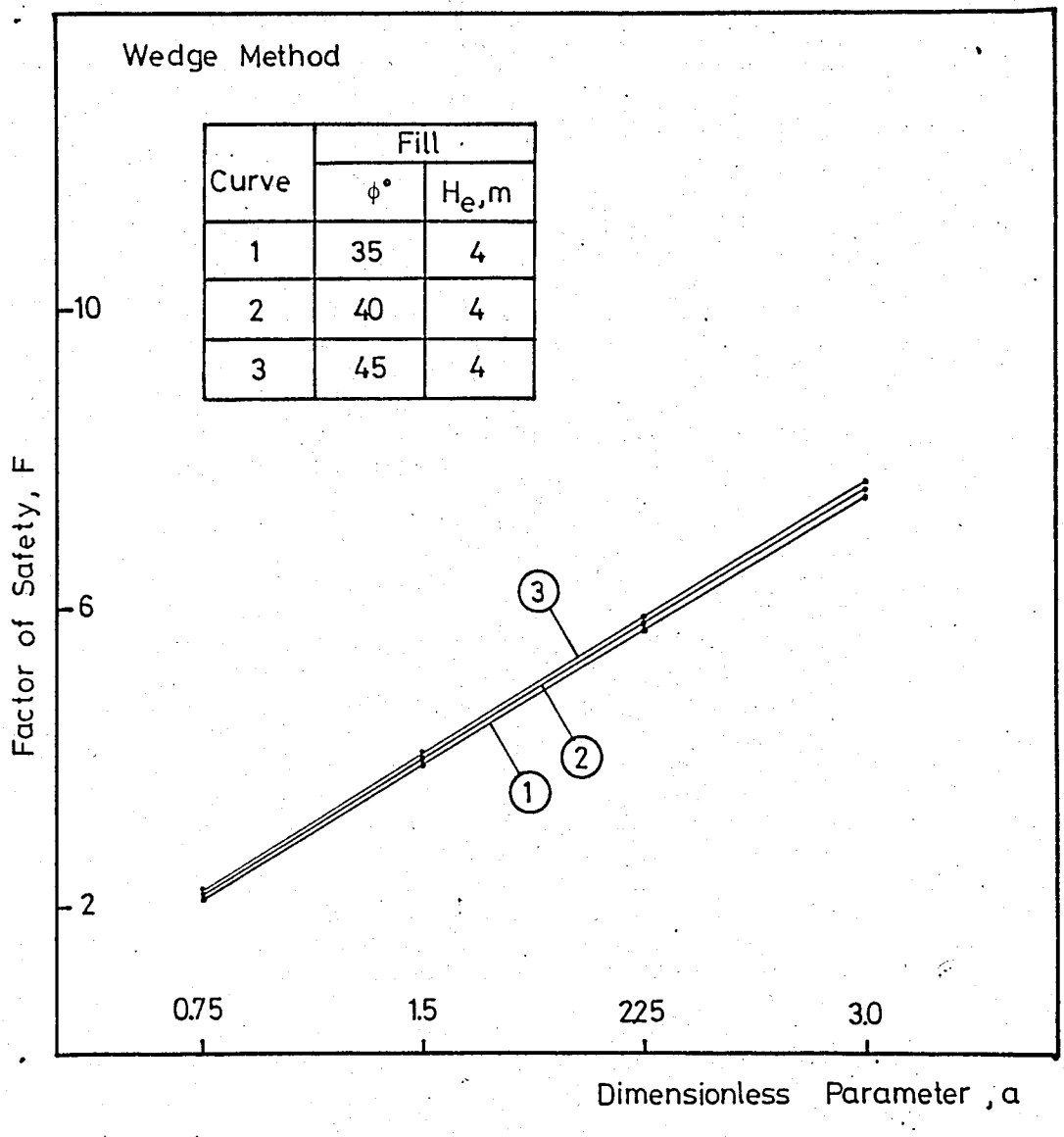

FIG.A.38 Effect of Dimensionless Parameter ,a, on Factor of Safety of the Typical Embankment Shown in Fig.5.10 by Wedge Method

APPENDIX B

TABLE B.1 Factors of Safety Calculated for Possible Critical Circles Shown in Fig.6.1

$H_e = H_f = 4m$, $\gamma = 1.9\ t/m^3$, $\phi = 35^0$

(for Constant Shear Strength of Foundation)

	Circle centers y(m)	Ordinate of Lowest Point on the Circle									
		y = 0		y = 1		y = 2		y = 3		Toe Circles	
		OMS	BM	OMS	BM	OMS	BM	OMS	BM	OMS	BM
x = 15 m	12	1.972	2.110	1.979	2.135	2.006	2.183	2.070	2.271	2.119	2.328
	11.5	1.959	2.100	1.961	2.121	1.980	2.164	2.034	2.245	2.075	2.295
	11	1.948	2.092	1.943	2.109	1.955	2.146	2.000	2.222	2.033	2.265
	10.5	1.938	2.087	1.928	2.099	1.932	2.131	1.968	2.202	1.993	2.238
	10	1.932	2.084	1.916	2.093	1.912	2.120	1.938	2.186	1.956	2.216
	9.5	1.930	2.085	1.908	2.090	1.896	2.114	1.912	2.177	1.924	2.201
	9	1.932	2.091	1.905	2.093	1.885	2.114	1.892	2.177	1.899	2.195
	8.5	1.941	2.102	1.908	2.103	1.882	2.122	1.883	2.191	1.886	2.201
	8	1.958	2.121	1.923	2.121	1.892	2.143	1.890	2.225	1.890	2.225

Ordinary Method of Slices, Minimum Factor of Safety = 1.882

Bishop's Modified Method, Minimum Factor of Safety = 2.084

TABLE B.2 Factors of Safety Calculated for Possible Critical Circles Shown in Fig.6.1

$H_e = H_f = 4m$, $\gamma = 2.0\ t/m^3$, $\phi = 40^0$

(for Constant Shear Strength of Foundation)

	Circle centers y(m)	Ordinate of Lowest Point on the Circle									
		y = 0		y = 1		y = 2		y = 3		Toe Circles	
		OMS	BM	OMS	BM	OMS	BM	OMS	BM	OMS	BM
x = 15 m	12	1.904	2.047	1.927	2.087	1.980	2.164	2.108	2.318	2.224	2.445
	11.5	1.890	2.036	1.906	2.072	1.952	2.142	2.069	2.289	2.169	2.401
	11	1.877	2.027	1.887	2.058	1.924	2.123	2.031	2.262	2.115	2.359
	10.5	1.867	2.020	1.870	2.047	1.899	2.106	1.994	2.239	2.062	2.321
	10	1.859	2.016	1.855	2.039	1.875	2.092	1.959	2.220	2.012	2.287
	9.5	1.854	2.015	1.844	2.034	1.856	2.083	1.928	2.207	1.966	2.260
	9	1.854	2.018	1.838	2.034	1.841	2.079	1.902	2.203	1.927	2.240
	8.5	1.860	2.027	1.838	2.040	1.833	2.084	1.886	2.212	1.898	2.233
	8	1.874	2.042	1.848	2.055	1.837	2.100	1.886	2.242	1.886	2.242

Ordinary Method of Slices, Minimum Factor of Safety = 1.833

Bishop's Modified Method, Minimum Factor of Safety = 2.015

TABLE B.3 Factors of Safety Calculated for Possible Critical Circles Shown in Fig.6.1

$H_e = H_f = 4m$, $\gamma = 2.1\ t/m^3$, $\phi = 45^0$

(for Constant Shear Strength of Foundation)

	Circle centers y(m)	Ordinate of Lowest Point on the Circle									
		y = 0		y = 1		y = 2		y = 3		Toe Circles	
		OMS	BM	OMS	BM	OMS	BM	OMS	BM	OMS	BM
x = 15 m	12	1.850	1.992	1.888	2.049	1.972	2.156	2.172	2.384	2.363	2.591
	11.5	1.834	1.980	1.866	2.032	1.941	2.132	2.128	2.351	2.294	2.534
	11	1.819	1.970	1.844	2.016	1.910	2.110	2.085	2.321	2.226	2.479
	10.5	1.807	1.962	1.825	2.003	1.881	2.090	2.043	2.293	2.159	2.427
	10	1.796	1.956	1.807	1.992	1.854	2.073	2.002	2.269	2.094	2.379
	9.5	1.789	1.952	1.793	1.985	1.830	2.061	1.965	2.252	2.033	2.337
	9	1.787	1.953	1.784	1.982	1.811	2.054	1.933	2.243	1.977	2.303
	8.5	1.790	1.959	1.780	1.985	1.798	2.054	1.909	2.247	1.931	2.279
	8	1.800	1.970	1.786	1.995	1.796	2.065	1.900	2.271	1.900	2.271

Ordinary Method of Slices, Minimum Factor of Safety = 1.780

Bishop's Modified Method, Minimum Factor of Safety = 1.952

TABLE B.4 Factors of Safety Calculated for Possible Critical Failure Surfaces Shown in Fig.6.2

$H_e = H_f = 4m$ (for Constant Shear Strength of Foundation)

Fill Properties	Ordinate of Lowest Point on the Failure Surface											
	y = 0			y = 1			y = 2			y = 3		
	SM	GPS	WM	SM	GPS	WM	SM	GPS	WM	SM	GPS	WM
$\gamma = 1.9\ t/m^3$ $\phi = 35^0$	1.745	2.271	1.764	1.695	NC	1.805	2.141	NC	1.867	2.347	2.285	1.975
$\gamma = 2.0\ t/m^3$ $\phi = 40^0$	2.183	2.211	1.726	1.976	NC	1.776	NC	2.150	1.855	2.164	2.309	1.994
$\gamma = 2.1\ t/m^3$ $\phi = 45^0$	1.379	2.162	1.690	1.918	NC	1.750	2.084	NC	1.846	2.376	NC	2.019

TABLE B.5 Factors of Safety Calculated for Possible Critical Circles Shown in Fig.6.4

$H_e = H_f = 4m$, $\gamma = 1.9\ t/m^3$, $\phi = 35^0$

(for Linear Variation of Foundation Shear Strength)

	Circle centers y(m)	Ordinate of Lowest Point on the Circle									
		y = 0		y = 1		y = 2		y = 3		Toe Circles	
		OMS	BM	OMS	BM	OMS	BM	OMS	BM	OMS	BM
x = 16 m	12	2.579	2.740	1.983	2.141	1.452	1.590	1.095	1.175	1.191	1.244
	11.5	2.564	2.729	1.965	2.128	1.430	1.574	1.069	1.156	1.139	1.194
	11	2.552	2.721	1.949	2.117	1.410	1.560	1.043	1.137	1.086	1.144
	10.5	2.543	2.716	1.935	2.109	1.390	1.548	1.017	1.119	1.033	1.095
	10	2.537	2.716	1.923	2.104	1.373	1.539	0.990	1.102	0.979	1.047
	9.5	2.537	2.720	1.916	2.103	1.359	1.534	0.963	1.087	0.927	1.002
	9	2.544	2.731	1.915	2.108	1.348	1.533	0.937	1.074	0.876	0.961
	8.5	2.559	2.751	1.921	2.120	1.343	1.539	0.914	1.066	0.829	0.928
	8	2.587	2.780	1.938	2.143	1.348	1.555	0.895	1.064	0.791	0.907

Ordinary Method of Slices, Minimum Factor of Safety = 0.791

Bishop's Modified Method, Minimum Factor of Safety = 0.907

TABLE B.6 Factors of Safety Calculated for Possible Critical Circles Shown in Fig.6.4

$H_e = H_f = 4m$, $\gamma = 2.0\ t/m^3$, $\phi = 40^0$

(for Linear Variation of Foundation Shear Strength)

	Circle centers y(m)	Ordinate of Lowest Point on the Circle									
		y = 0		y = 1		y = 2		y = 3		Toe Circles	
		OMS	BM	OMS	BM	OMS	BM	OMS	BM	OMS	BM
x = 16 m	12	2.481	2.653	1.931	2.094	1.455	1.589	1.186	1.250	1.407	1.464
	11.5	2.465	2.641	1.911	2.080	1.431	1.571	1.156	1.227	1.343	1.402
	11	2.452	2.632	1.893	2.067	1.408	1.555	1.125	1.204	1.278	1.339
	10.5	2.441	2.626	1.877	2.057	1.386	1.540	1.094	1.182	1.211	1.276
	10	2.434	2.624	1.863	2.050	1.365	1.529	1.062	1.160	1.145	1.213
	9.5	2.431	2.626	1.853	2.047	1.347	1.520	1.030	1.139	1.078	1.152
	9	2.435	2.635	1.848	2.049	1.332	1.516	0.997	1.121	1.012	1.095
	8.5	2.448	2.651	1.851	2.058	1.323	1.519	0.966	1.106	0.950	1.044
	8	2.472	2.676	1.863	2.077	1.322	1.530	0.940	1.098	0.895	1.005

Ordinary Method of Slices, Minimum Factor of Safety = 0.895

Bishop's Modified Method, Minimum Factor of Safety = 1.005

TABLE B.7 Factors of Safety Calculated for Possible Critical Circles Shown in Fig.6.4

$H_e = H_f = 4m$, $\gamma = 2.1\ t/m^3$, $\phi = 45^0$

(for Linear Variation of Foundation Shear Strength)

	Circle centers y(m)	Ordinate of Lowest Point on the Circle									
		y = 0		y = 1		y = 2		y = 3		Toe Circles	
		OMS	BM	OMS	BM	OMS	BM	OMS	BM	OMS	BM
x = 15	12	2.376	2.552	1.870	2.029	1.449	1.564	1.265	1.296	1.423	1.446
	11.5	2.358	2.538	1.846	2.011	1.421	1.542	1.229	1.265	1.358	1.383
	11	2.341	2.525	1.824	1.994	1.392	1.521	1.192	1.234	1.294	1.322
	10.5	2.326	2.516	1.804	1.980	1.365	1.501	1.155	1.204	1.230	1.264
	10	2.315	2.509	1.785	1.968	1.338	1.483	1.117	1.175	1.168	1.210
	9.5	2.308	2.506	1.770	1.959	1.313	1.467	1.079	1.149	1.109	1.163
	9	2.306	2.509	1.759	1.955	1.291	1.455	1.042	1.125	1.055	1.125
	8.5	2.312	2.517	1.753	1.955	1.272	1.447	1.007	1.105	1.008	1.100
	8	2.327	2.533	1.756	1.963	1.260	1.445	0.975	1.093	0.975	1.093

Ordinary Method of Slices, Minimum Factor of Safety = 0.975

Bishop's Modified Method, Minimum Factor of Safety = 1.093

TABLE B.8 Factors of Safety Calculated for Possible Critical Failure Surfaces Shown in Fig.6.2
$H_e = H_f = 4m$ (for Linear Variation of Foundation Shear Strength)

Fill Properties	Ordinate of Lowest Point on the Failure Surface											
	y = 0			y = 1			y = 2			y = 3		
	SM	GPS	WM	SM	GPS	WM	SM	GPS	WM	SM	GPS	WM
$\gamma = 1.9t/m^3$ $\phi = 35^0$	2.402	3.099	2.183	1.846	NC	1.805	1.657	NC	1.423	1.120	1.148	1.018
$\gamma = 2.0t/m^3$ $\phi = 40^0$	3.013	3.005	2.121	2.411	NC	1.776	1.821	1.714	1.416	1.223	1.151	1.033
$\gamma = 2.1t/m^3$ $\phi = 45^0$	2.275	2.950	2.087	1.993	NC	1.750	1.615	1.742	1.411	1.200	1.155	1.047